Final Report
Integrated Commercial Carbon Capture and Storage (CCS) Prefeasibility Study at Dry Fork Station, Wyoming

May 30, 2019

SUBMITTED UNDER FUNDING OPPORTUNITY ANNOUNCEMENT

DE-FE0029375

SUBMITTED BY
Center for Economic Geology Research
School of Energy Resources, University of Wyoming, Energy Innovation Center
1020 E. Lewis Street
Laramie, WY 82071

PRINCIPAL INVESTIGATORS
Scott Quillinan
(307) 766-6697
(307) 766-6078 (fax)
scottyq@uwyo.edu

Kipp Coddington, Esq.
(307) 766-6731
(307) 766-6078 (fax)
kcodding@uwyo.edu

BUSINESS POINT OF CONTACT
Cindy Ishkanian
(307) 766-6896
(307) 766-6078 (fax)
cishkani@uwyo.edu

SUBMITTED TO

U.S. Department of Energy
National Energy Technology Laboratory

Acknowledgment: This portion of the presentation is based upon work supported by the Department of Energy under Award Number DE-FE0029375.

EXECUTIVE SUMMARY

The study focuses on the Basin Electric Dry Fork Power Station (DFS), the newest coal-fired power plant operating in the lower 48 states. DFS began operation in 2011 and has an operating lifetime of approximately 80 years, is a 420 MW plant, and emits roughly 3.3 million metric tonnes (Mt) of CO_2 per annum. Adjacent to DFS is the Wyoming Integrated Test Center (ITC). The ITC provides space and access to DFS flue gas for researchers to test CO_2 utilization and CO_2 capture technologies.

The objective of this study is to identify saline storage opportunities proximal to DFS and the ITC in the Powder River Basin. The objectives of the prefeasibility study were as follows: (1) to establish a CCS coordination team capable of achieving a successful implementation of commercial scale CCS for the Dry Fork Power Station; (2) to develop site-specific business and execution strategies; and (3) to identify and describe promising saline storage sites capable of storing 50 million metric tons of CO_2.

Coordination team. The project team brings together: (1) leading academic and industry researchers with unparalleled expertise in saline storage assessments; (2) Wyoming governmental entities lending political support; and (3) private sector companies with major energy infrastructure commercialization and financing expertise. Led by the University of Wyoming's (UW) Center of Economic Geology Research and with the support of the Energy & Environmental Research Center (EERC), Advanced Resources International, Inc. (ARI), UW's Enhanced Oil Recovery Institute (EORI) and others, team members individually and collectively have participated in nearly every major geologic storage project in the United States. Partner Basin Electric Power Cooperative (BEPC), through its for-profit subsidiary Dakota Gasification Company, owns and operates the Great Plains Synfuels Plant, which supplies CO_2 to a large CO2-EOR project. Partner KKR is a leading global investment firm that manages approximately $10 billion in energy and infrastructure related assets, including Wyoming CO_2-EOR properties. To help address CO_2 long-term storage liability issues, the team partnered with the former Chief Climate Product Officer at Zurich Financial Services and the author of the first U.S. commercial geologic storage insurance policy. Also on the team are a UW economist who is an international expert on CO_2 pricing and an attorney who negotiated the multi-state acquisition of pore space rights in what remains one of the largest real estate transactions in the United States. The team enjoys the highest levels of Wyoming political backing, having received letters of support from the Governor of Wyoming, a key committee of the State of Wyoming Legislature, and the Wyoming Infrastructure Authority (WIA), which manages the ITC. The assembled team has the necessary expertise and Wyoming political support to take this uniquely favorable project site forward through storage site feasibility and future commercialization phases.

Site Specific business and execution strategies. The team estimates the capital (CAPEX) and annual operating (OPEX) costs of implementing the preferred scenario will be in the range of $768-$944 million and $58-$116 million, respectively, based upon the project's economic model. Subject to change as conditions unfold, these CAPEX and OPEX estimates assume: (1) an amine capture system sized for a 340-380 MW DFS-like source;

(2) saline storage site within a 5-mile radius of DFS that includes a 15-mile CO_2 pipeline for regional CO_2-EOR opportunities; (3) utilization of DFS' steam cycle; (4) purchase of power at wholesale prices; (5) 25% debt financing; (6) sale of CO_2 for EOR; (7) revenues from tradable CO_2 allowances; and (8) utilization of tax equity from §45Q and §48A tax credits. The recently enacted amendments to §45Q make the credit transferable, thereby facilitating tax equity deal structures.

Identification of promising saline storage targets. The team has identified four high-priority storage reservoirs as part of the storage complex for further feasibility study in Phase II. Each target formation is likely saline and lies at a depth sufficient to maintain supercritical CO2. Preliminary analysis of the target formations show the thickness, permeability, and porosity of the combined formations to satisfy the U.S. Department of Energy's volumetric saline storage requirements. The Minnelusa and Sundance are promising target formations to independently meet the volumetric saline storage requirements.. The target reservoirs have a unique depositional environment, petrology, and chemistry, allowing for scientific study of several reservoir types at the same location. Each reservoir is confined above and below by low permeable shales, including a 5,000+ foot shale to form the uppermost seal. This uppermost seal forms a major hydrogeologic divide between the lowest USDW and the strata below.

During the course of study it was determined that the prefeasibilty study successfully meets criteria and was ready for Phase II (Storage Complex Feasibility). In summary, the identified storage complex is immediately adjacent to Basin Electric Power Cooperative's (BEPC) coal-fired Dry Fork Station (DFS) in the Powder River Basin (PRB) near Gillette in Wyoming's northeast corner. The storage complex's location alone mitigates project risks and improves project economics -- from environmental impacts to the need for new carbon dioxide (CO_2) pipeline infrastructure. DFS also is the location of the Wyoming Integrated Test Center (ITC), a new carbon capture, utilization and storage (CCUS) test facility, which creates additional project synergies. Phase I pre-feasibility assessments confirm that the storage complex has the potential to safely, permanently and economically store at least 50+ million metric tons (Mt) of CO_2 in secure saline reservoirs. The storage complex also benefits from: (1) favorable Wyoming carbon capture & storage (CCS) laws; (2) existing CO_2 pipeline infrastructure; (3) a population that supports CCS; and (4) opportunities to improve economics through sales of CO_2 for enhanced oil recovery (CO_2-EOR) and low-carbon electricity to nearby states.

Table of Contents

EXECUTIVE SUMMARY *3*

Chapter I: Scenarios Generation *7*

Section 1.1: Initial Scoping **8**

Section 1.2: Source & Transport Components Generation **10**

Section 1.3: Storage Components Generation **11**

Section 1.4: Scenario Combination, Screening, & Prioritization: **12**

Chapter II: Regional and Stakeholder Analysis *17*

Section 2.1: Economic Assessment **17**

Section 2.2: Legal Assessment **32**

Section 2.3: Environmental Assessment **36**

Section 2.4: Community and Public Outreach Assessment **51**

Section 2.5: Regional Non-technical Suitability Briefs **55**

Chapter III: Geologic Evaluation *59*

Section 3.1: Development of Borehole Catalog and Risk Assessment **59**

Section 3.2: Subsurface Description **72**

Section 3.3: Hydrostratigraphy Description **83**

Section 3.4: Geophysical Description **86**

Chapter IV: Geologic Model Development and Simulation *128*

Section 4.1 Introduction **128**

Section 4.2 Model Construction **128**

Section 4.3 Volumetric Storage Resource Estimates **132**

Section 4.4 Numerical Simulation **136**

Section 4.5 AoR Determination **140**

Chapter IV Appendix A – Modeling and Simulation **145**

Chapter IV Appendix B – Characterization Well Designs and Cost Estimates **196**

Chapter V: NRAP Modeling and Validation *229*

Section 5.1 Executive Summary **229**

Section 5.1 Introduction **229**

Section 5.1 NRAP Tools **231**

Section 5.2 ROM Evaluation **237**

Section 5.3 Recommendations **246**

Chapter V Appendix A 249

Chapter VI: Identification of Future Characterization Activities 277

Section 6.1: Site Characterization 277

Section 6.2: Testing Plan 278

Chapter I: Scenarios Generation

Charles Nye
Research Scientist, Center for Economic Geology Research
School of Energy Resources, University of Wyoming
1020 E. Lewis Street, Energy Innovation Center
Laramie, WY 82071

Abstract

The scenarios generation task (herein Task 2) sought to identify sources, transport, and storage components into a system that could be capable of storing 50 million tonnes (5.0×10^{10}kg) of CO_2 in 25 years. These scenarios were down selected to the five most promising options and then ranked. The first results of Task 2 identified an area around Gillette Wyoming and listed possible CO_2 sources and storage nearby. At this point the study area was a 25-mile radius around Gillette. This area was later refined to a ~18-mile by ~30-mile rectangle (3 by 5 townships), which persisted for the rest of CarbonSAFE Phase I.

The result of this work is a primary scenario that would use emissions from Dry Fork Station, minimal pipeline transport of less than 5 miles, and sequential storage in the Permian Minnelusa formation, Jurassic Canyon Springs and Hullet, Cretaceous Lakota, Dakota, and Muddy reservoirs. The Canyon Springs and Hullet are collectively referred to as the Lower Sundance in this work, and likewise, the Lakota and Dakota are collectively referred to as the Dakota. This grouping simplifies work and reflects the claim that elsewhere in the Powder River Basin these units have a degree of connectivity (Brobst, 1961). The primary scenario is expected to be the focus of later phases of the Project.

A secondary scenario is also maintained, which uses emissions from one or more of the WyoDak cluster of five power stations and transport to an area between WyoDak and Dry Fork Station. This scenario is fault-tolerant due to its ability to adapt to many sources if anything were to happen to one source and also allows multiple routing options for pipelines. Over its target storage area, geology should be very similar to the primary scenario, which allows geologic knowledge from one to be cross applied to the other. To manage risk, the secondary scenario is expected to be maintained as a back-up in later phases of Project.

The sections of this chapter explain (1) the initial scoping of this project; (2) the generation of source and transport components; (3) the generation of storage components; (4) the combination and screening of these components; (5) the prioritization of the resulting scenarios; and (6) conclude with a deeper explanation for the resulting primary and secondary scenarios.

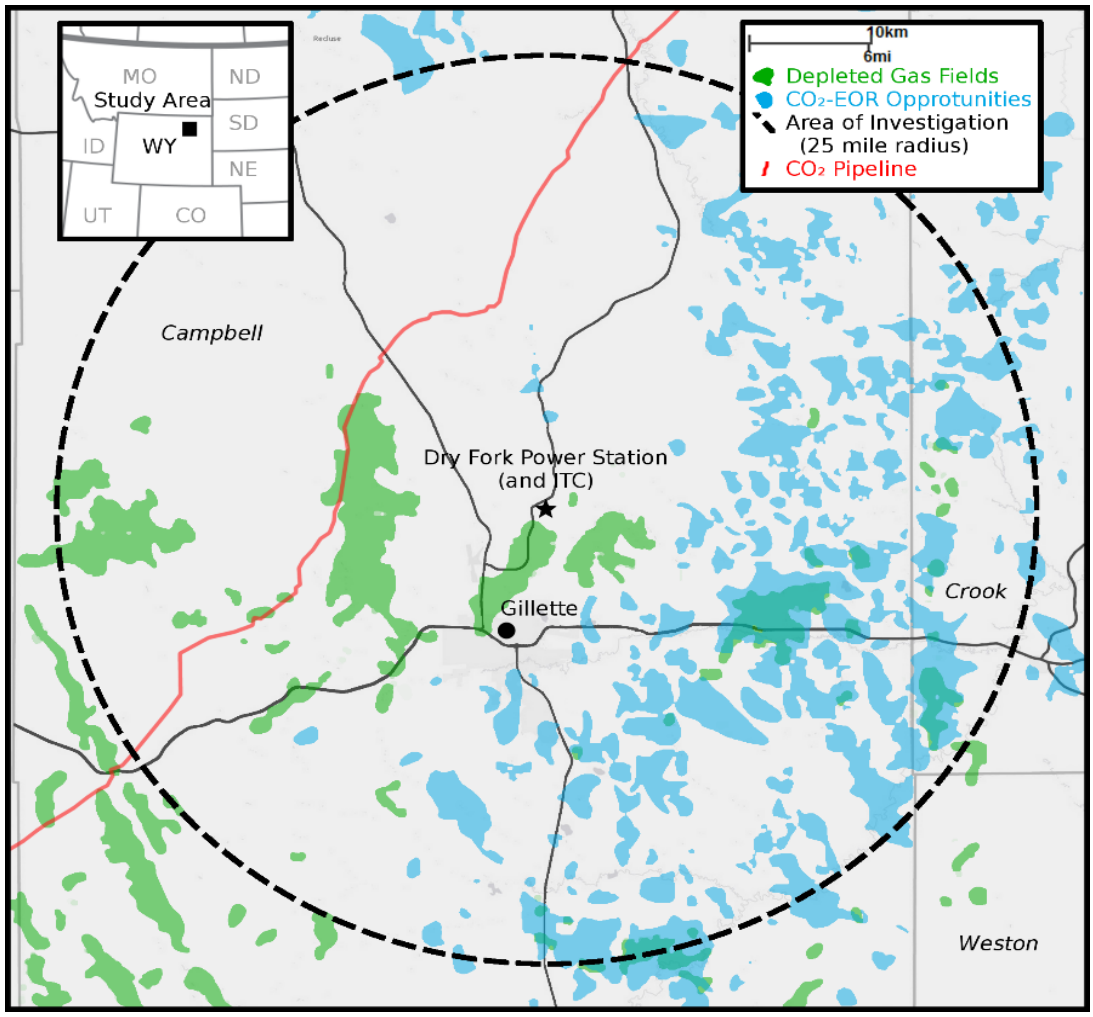

Figure 1.1 The earliest iteration of the Dry Fork Station Study Area

Section 1.1: Initial Scoping

Wyoming is an ideal location for CCS. Wyoming has abundant CO_2 sources and similarly abundant geologic locations to store that CO_2 (EPA, 2017). If one only wanted a middling CCS project, one could combine almost any major Wyoming power station, and almost any nearby sedimentary package occurring at a depth greater than 3,000 feet. Such an off-the-cuff proposal in Wyoming could rival deliberately crafted projects elsewhere in the United States. In recognition of Wyoming's advantages, the goal of this scoping work was not merely to identify a location that could achieve the goals of CarbonSAFE, but to identify the best location to achieve those goals.

Past CCS work in Wyoming had been performed in the state's southwest, first at the Moxa Arch (Campbell et al., 2011) and then on the Rock Springs Uplift (RSU) (Surdam, 2013). In order to maintain a geographically distinct project from that work this project considered northern and eastern Wyoming. In this initial scoping the area was crudely defined as either north of 42.5N Latitude or east of -106.5W Longitude. In this area, there are four coal-fired power stations that produce over 2 million metric tons per annum and

so might meet the CarbonSAFE goals as sole-source (Table 1.1.1, light blue). Further, there are seven other sources that annually produce over a quarter of the emissions needed for CarbonSAFE goals, and so might be categorized as auxiliary sources that could augment the main source if unforeseen circumstances reduced the amount of CO_2 it could contribute (Table 1.1.1).

Facility	Tonnes of CO_2	Purpose
Laramie River	11,203,246	Electricity
Dave Johnston	5,007,460	Electricity
Dry Fork Station	3,282,713	Electricity
Wyodak	3,066,540	Electricity
Wygen I	870,082	Electricity
Wygen II	852,783	Electricity
Wygen III	850,415	Electricity
HollyFrontier Cheyenne Refining	751,109	Petroleum Processing
Lost Cabin Gas Plant	732,717	Natural Gas Processing
Neil Simpson II	696,799	Electricity
Mountain Cement Plant	635,427	Cement

Table 1.1.1 Northeast Wyoming facilities that produce more than 0.5 million metric tonnes (Mt) of CO_2 per year. Those producing enough to be sole-source are highlighted in blue. This list considers Wyoming sources that are either north of 42.5N Latitude or east of -106.5W Longitude.

Of the 11 facilities identified, most are coal-fired power stations, which is ideal for CarbonSAFE' s programmatic mission. All such power stations on this list, except for Laramie River and Dave Johnston, are near Gillette, Wyoming. This assessment allowed scope to be narrowed to Gillette, as the two sole-source options and four auxiliary-source options reduce risk and provide high chances of securing CO_2 for injection. Figure 1.1 shows the scope after this initial narrowing.

The initial radius of 25 miles was chosen to ensure nearby secondary structures in the PRB could be considered - such as the Belle Fourche Arch (Rasmussen and Bean 1984) - and partly-drained hydrocarbon fields - such as the Mill-Gillette or Kitty fields. This radius also includes the 20" Greencore Pipeline (725 MMcf CO_2 per day), which follows a corridor of pre-approved pipeline network negotiated by the Wyoming Pipeline Authority (WPA) (Denbury, 2017). The Greencore Pipeline may be viewed as either a means of transport to a distant sink or from a distant source.

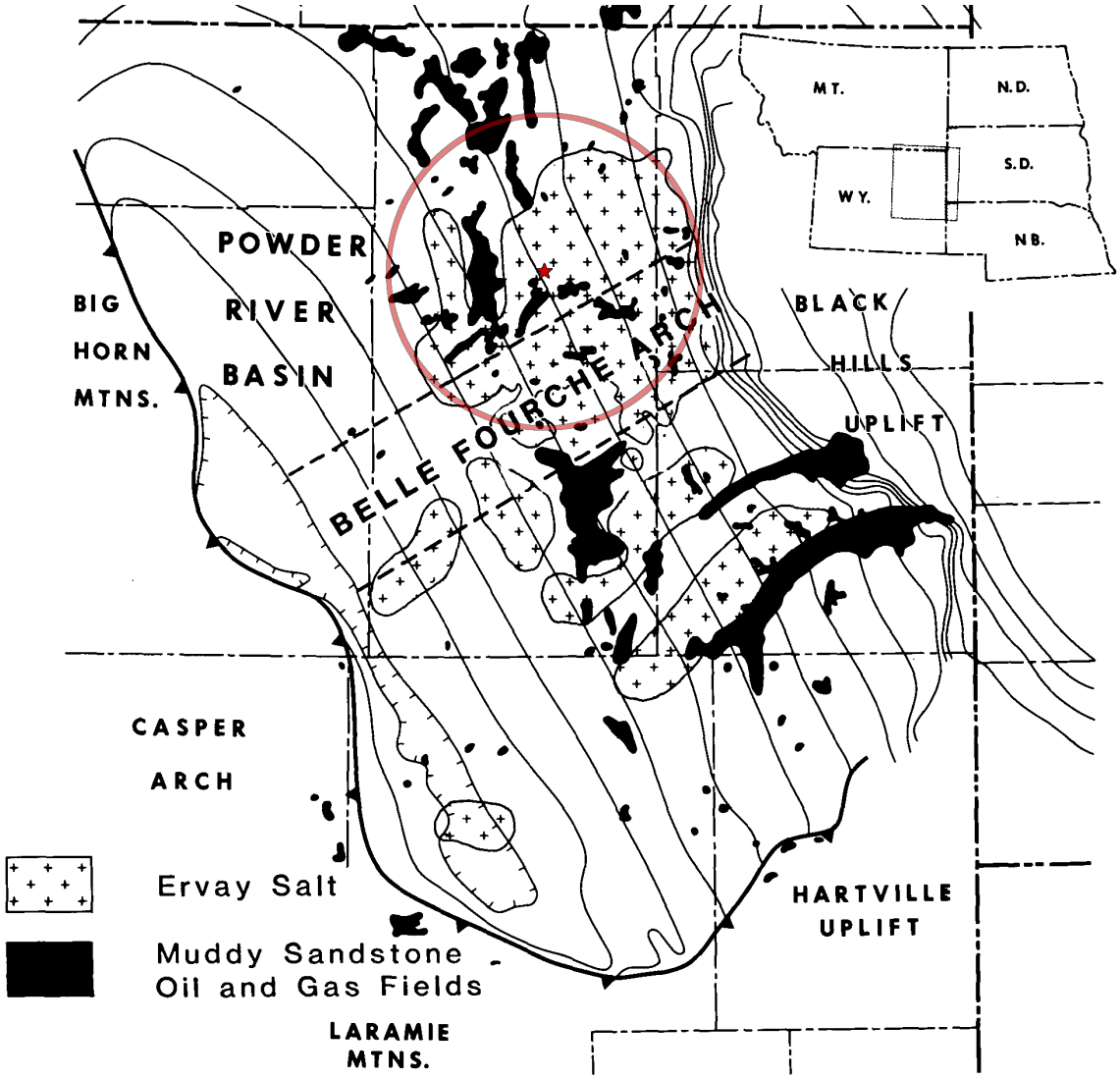

Figure 1.1.1 The original study area (highlighted in red) includes a significant area of the Belle Fourche Arch. Rasmussen and Bean 1984 describe the thickening of all superior sedimentary units as dissolution of the Ervay Salt leads to collapse on the arch's margins, and observe that Muddy Formation oil and gas fields tend to occur in areas where the Ervay Salt is not present. Figure modified from Rasmussen and Bean 1984.

Section 1.2: Source & Transport Components Generation

As described above, the six large coal-fired power stations in northeast Wyoming contributed to the choice of a 25-mile radius around Gillette for scope. These six sources simultaneously became the Source components to be considered for the Project.

The six sources were partitioned into two groups each of which could serve as a source component. Dry Fork Station on its own was considered a source component because it is geographically distant from the other five power stations and can qualify as a sole-source of CO_2 with a modest 61% capture efficiency. The second source component was the Wyodak cluster of five plants, which could meet target CO_2 volumes even if their capture plant(s) had a poor average efficiency of only 32%. More likely, either a subset of these five plants would be outfitted with capture, or CO_2 in excess of the 32% needed for the

Project could be sold to offset costs. In the early stages of the Project, the Wyodak plant was occasionally considered as a standalone third source component to reflect its ability to serve as sole source with 65% capture efficiency. However, Wyodak as a standalone source is merely a variation in the details of how capture from the full cluster of five plants might be performed. In recognition of that, only DFS and the full Wyodak cluster were considered further for simplicity's sake.

Transport components were not explicitly generated until there was some understanding of storage components. The implicit transport component at this time was a pipeline of less than 20 miles. This understanding was based on the work of McCoy (2009) who showed that transport in excess of ~20 miles would carry significant risk of needing re-compression stations, and those such stations would greatly increase cost. Estimates detailed in the economic assessment showed the cost of re-compressing could be almost 10% of the total project costs, and that such increases would greatly damage the project's feasibility. In addition to this awareness of the need for a short pipeline, the team was aware that Dry Fork Station would have a simpler transport component, because its surroundings include fewer highways and a lower population density. This is why there was an early focus on DFS in this project, even as the Wyodak cluster was duly investigated.

Section 1.3: Storage Components Generation

Over most of the study area, the stratigraphic units are similar. Accordingly, storage focused on the same six saline storage units but included appreciation of the depth they occur at and the facies changes laterally within their strata. These six units are the: Muddy, Dakota, Lakota, Hulett, Canyon Springs, and Minnelusa (A-B-C-D sands) as mentioned at the start of this chapter, Dakota and Lakota were considered together, as were the Hulett and Canyon Springs. For more information on the facies and formation, specific considerations see Chapter III.

The most significant feature that varies over the study area is depth to a given strata. While shallower units result in savings on well construction costs, shallow strata are also more likely to have a fluid salinity of under 10,000 mg/L. A TDS of 10,000 mg/L or less can allow a reservoir to qualify as an Underground Source of Drinking Water (USDW), which precludes its use to store CO_2. While some uncertainty exists (see Chapter III hydrostratigraphy), every reservoir becomes fresher closer to the basin margins and more saline towards the basin axis.

Within the study area, all considered storage components were well below the 800 meters (2,600 feet) critical depth, which is the depth CO_2 generally, enters a supercritical phase (NETL, 2019). This depth is commonly rounded to 1km and 3,000 feet to add a margin of safety. The ultimate regional seal, the Upper Cretaceous shale package, and all target storage formations are below this critical depth and safety margin. As a result, these storage components reduce project risk.

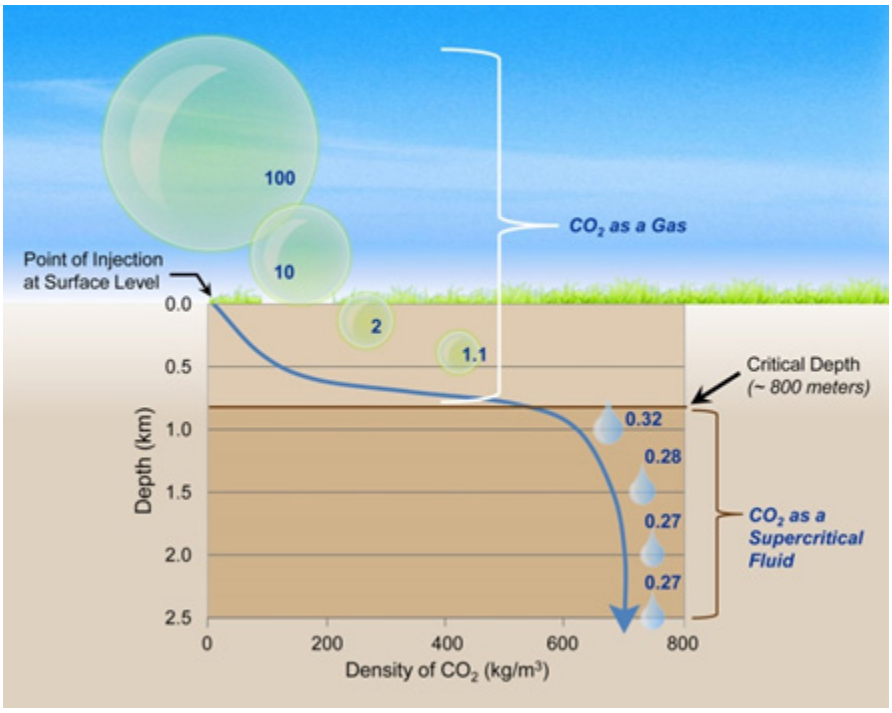

Figure 1.3.1 Illustration of Pressure Effects on CO_2 (based upon image from CO_2CRC). The blue numbers show the volume of CO_2 at each depth compared to a volume of 100 at the surface. Image from NETL, 2019.

Although enhanced oil recovery or gas recovery and other CCUS techniques would not fulfill the CarbonSAFE programmatic mission, the opportunity to use those might augment revenue streams. Accordingly, storage components, including semi-depleted oil and gas fields, were considered, including the Mill-Gillette field, Kitty field, and Minnelusa fairway.

Section 1.4: Scenario Combination, Screening, & Prioritization:

The source, transport, and storage components were combined into five unique scenarios. These were ranked and re-ranked as work on the project revealed new discoveries. While many variables affected the ranking below, the storage area's distance from the most favorable source, DFS, proved most important to the ranking, as had been originally expected.

Scenario #1 On Site:

The primary scenario could use reclaimed mine land around the site to minimize the potential for surface disturbance during construction. Proximity also makes transport costs lowest.

CO_2 Source: Dry Fork Station (DFS) (3.2 Mt/year)
CO_2 Transport: From DFS to four injectors sited on reclaimed land less than 5 miles away
CO_2 Storage: Minnelusa Formation, or/and Lower Sundance Formation, which are expected to store 31Mt and 20Mt respectively under the P50 case, with an area of review

of ~200 mi^2 (details in Chapter IV). The stored volume can be significantly increased by operating at a higher bottom hole pressure, or adding more wells. Such changes would trade acceptable risk for improved performance. These could allow a single formation to meet the project goal of 50 Mt in 25 years with a smaller Area of Review. Stacked storage allows the area of review to shrink considerably as described in Chapter IV.

Scenario #2 Between DFS and Wyodak Cluster:
This secondary scenario is designed as a backup if unforeseen events require a change in source, transport, or storage components. While inferior to #1 On Site, it is a good secondary scenario, because any one problem that invalidated #1 On Site can be accommodated.
CO_2 Source: DFS, the Wyodak Cluster, or both (3.2, 6.1, or 9.3 Mt/year respectively)
CO_2 Transport: From one or both sources to one or more state-owned sections between the plants such as T51N-R72W-Sec36, T50N-R71W-Sec8, or T50N-R71W-Sec16.
CO_2 Storage: Minnelusa Formation or/and Sundance Formation, with expected behavior similar to #1 On Site, as these locations are geologically in strike with each other.

Scenario #3 East (T51N-R70W):
If many more than eight injection wells were required, this scenario could become favorable through partial offset of transport with shallower storage. The work in Chapter IV determined that such an event was unlikely. #3 East is slightly further from DFS than #4 West but ranks higher because the shallower storage units under #3 East would almost certainly reduce construction costs more than the slightly shorter transport saves. While #3 East has merit, it is clearly inferior to both the primary and secondary scenarios and will not be advanced for further consideration.
CO_2 Source: DFS or the Wyodak Cluster (3.2 or 6.1 Mt/year respectively)
CO_2 Transport: From one or both sources to T51N-R70W, with the DFS pipeline over 7 miles long, and the Wyodak Cluster pipeline over 10 miles long. Pipelines that meet in a "Y" junction are possible but introduce more complexity.
CO_2 Storage: Minnelusa Formation, or/and Sundance Formation

Scenario #4 West (T51N-R73W):
If policy and social factors become dominant considerations, this scenario could become favorable due to its extreme distance from USDWs, and its proximity to an interstate CO_2 pipeline. However, at this time, policy and social risks seem small, and good community buy-in has been achieved for all scenarios. Additionally #4 West requires transport down-dip so well construction cost increases as transport cost also increases, rather than having an offsetting relationship like in #3 East. As a result of all of the above, #4 West will not be advanced for further consideration.
CO_2 Source: DFS (3.2 Mt/year)
CO_2 Transport: From DFS to T51N-R73W
CO_2 Storage: Minnelusa Formation, or/and Sundance Formation

Scenario #5 County Line (T52N-R69W):
If the Ervay salt dampens seismic signatures too much, this scenario could become favorable due to pre-existing 3D seismic and shallower salt units, which are easier to penetrate. The geophysical team is cautiously optimistic that a well-designed 3D seismic acquisition can penetrate the Ervay salt in the other parts of the study area, so #5 County Line will not be advanced for further consideration. The scenario also suffers from large transport costs and interference with oil and gas mineral estates, which are a disadvantage because EOR is not allowed as a project goal.
CO_2 Source: DFS (3.2 MM tonnes/year)
CO_2 Transport: From DFS to T52N-R69W
CO_2 Storage: Minnelusa Formation or/and Sundance Formation

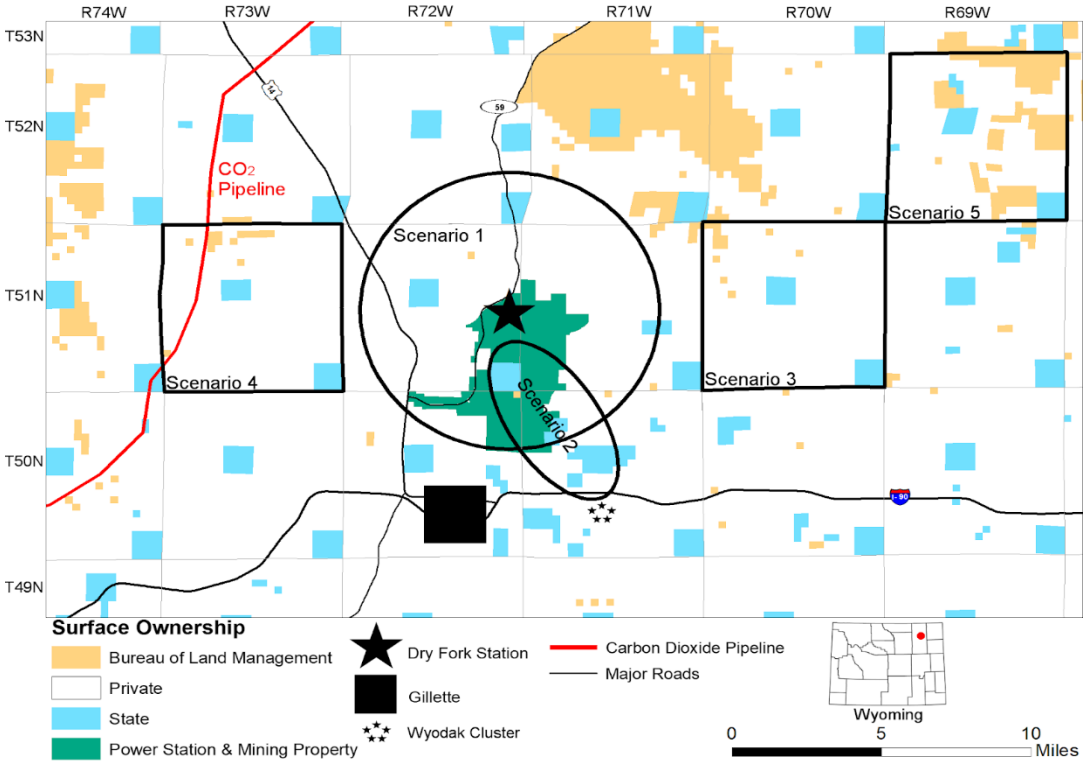

Figure 1.4.1 Project Land Ownership and CCS Scenarios.

Conclusion

At the conclusion of Phase I of this work, the two preferred scenarios were #1 On Site and #2 Between DFS and Wyodak Cluster. Each appearing to be capable of meeting project goals at low risk to social, environmental, and economic concerns.

Scenario #1 On Site is located within 5 miles of DFS, and minimizes environmental, community, and infrastructure risks. Section 2.3 of this report details many of those reduced risks. This scenario is expected to use CO_2 saline storage, ordered by expected significance, in the Minnelusa Formation, the lower Sundance Formation. If salinity and reservoir quality are high enough, the Lakota/Fall River Group and the Muddy Sandstone could also accept CO_2 in saline storage.

Located a little further south of DFS, scenario #2 Between DFS and Wyodak Cluster uses the same saline formations while potentially making additional use of the five coal-fired power plants in the "Wyodak Cluster": PacifiCorp's Wyodak Plant; and Black Hills Energy's Wygen I, Wygen II, Wygen III, and Neil Simpson II plants. For Phase II, the team will further investigate the top-ranked scenario #1 On Site, with scenario #2 Between DFS and Wyodak Cluster as a backup. Both scenarios are ready for feasibility assessments.

This work showed that multiple suitable sources and storage locations exist in the Gillette area. It also showed that these sources could be connected by pipeline transport, but that it is economically expedient to transport as little as possible. Preliminary estimates of ~five injection wells plus associated monitoring wells, indicate that transport (if necessary) should prefer the eastern areas to western areas. However, because the dip of the units in this area is very gentle, transport to shallower areas will almost certainly not recoup the costs of transporting a greater distance. These findings are reflected in maintaining the #1 On Site as the primary scenario for investigation in later CarbonSAFE work.

Chapter I References

Brobst, D.A. 1961 https://doi.org/10.3133/b1063B

Campbell, Erin, Ranie Lynds, Carol Frost, Thomas P.Becker, and Bridget Diem."The Wyoming carbon underground storage project: Geologic characterization of the Moxa Arch and Rock Springs Uplift". Energy Procedia, 4 (2011), pp. 4656-4663 DOI: https://doi.org/10.1016/j.egypro.2011.02.426

Sean T Mccoy 2008 "The Economics of CO2 Transport by Pipeline and Storage in Saline Aquifers and Oil Reservoirs" Thesis for Carnegie Mellon University. April 2009.

EPA, 2017 Facility Level Information on Greenhouse Gases Tool (FLIGHT) https://ghgdata.epa.gov/ghgp/main.do

Surdam RC (2013) Geological CO_2 storage characterization: the key to deploying clean fossil energy technology. Springer, New York. https://doi.org/10.1007/978-1-4614-5788-6

NETL (2019) Carbon Storage FAQs. https://www.netl.doe.gov/coal/carbon-storage/faqs/carbon-storage-faqs

Rasmussen, Donald L. and Daniel W. Bean. (1984) *Dissolution Of Permian Salt And Mesozoic Syndepositional Trends, Central Powder River Basin, Wyoming*. Thirty-Fifth Annual Field Conference -- 1984, Wyoming Geological Association Guidebook. Available at: http://archives.datapages.com/data/wga/data/041/041001/pdfs/281.pdf

Denbury (2017) *Greencore Pipeline Project.* Available at: https://www.denbury.com/default.aspx?SectionId=0fd5e3fd-08bc-480b-ac91-ece9dd20240b

Chapter II: Regional and Stakeholder Analysis

Section 2.1: Economic Assessment

Ben Cook
Assistant Professor of Economics, College of Business/Enhanced Oil Recovery Institute
University of Wyoming
1000 E. University Ave, Dept. 3985
Laramie, WY 82071

MODEL OVERVIEW

A. Techno-Economic Basis

The economic modeling and assessment for the Dry Fork Station study area consists of four principal components:

(1) the capital and operating costs of constructing an amine capture system sized for a flue gas stream of 340-380 MWs;
(2) a geologic saline storage site within a 1-mile radius of the plant, which includes a 15-mile carbon dioxide (CO_2) pipeline for CO_2 enhanced oil recovery (CO_2-EOR) opportunities in the region[1];
(3) a revenue and equity-sizing module incorporating options for CO_2 sales, premiums on sales of "green electrons" (e.g., electricity sales to carbon-constrained jurisdictions, such as the State of California), monetization of carbon offsets/credits, and the earning of tax credits; and
(4) a trust account module for accumulating sufficient funds for post-injection site care (PISC) and long-term liability (LTL).

While new and more cost effective technologies may emerge in the future, at this time the most deployed technology for large-scale industrial capture at power plants is amine capture.

The techno-economic aspects of the amine system and storage site are largely based on the documentation for the Integrated Environmental Control Model (IECM 9.5, 2017), developed by Carnegie Mellon/NETL, and the FE/NETL CO_2 Saline Storage Cost Model (NETL 2017).

While capital costs (CAPEX) have been calibrated so that the model can roughly duplicate the NRG W.A. Parish Petro Nova facilities (Armpriester 2017), the maintenance and operating (OPEX) expenses are largely linked to consumable pricing and the ratio of non-fuel OPEX to CAPEX in IECM 9.5. Power and fuel usage volumes are paid with pricing paths for electricity, natural gas, and coal to allow for dynamic scenario modeling of these commodities.

[1] This 1-mile distance reflects the scenario currently favored by the Project. Other scenarios exist at distances up to 25 miles, and analysis of those is as simple as changing this distance-value in the model. The 15-mile distance is enough to access the major CO_2-EOR-ready fields under each considered scenario.

Due to the differences in geography and weather conditions from existing facilities, the model largely ignores cost reductions from economies of scale or learning, with CAPEX and OPEX expressed in terms of 2016 averages.

B. Scenario Modules

The Excel-based modeling approach taken allows for both discrete and stochastic scenario analysis, along with adjustments to the various equipment requirements of the facility.

The model dynamically scales to the sizing of the capture stream and allows the user to modify significant inputs, such as CAPEX for the major components, the fuel usage and consumables of the various processes, pricing for both consumables and revenue sources, and other meaningful scenario options.

Carbon Capture System

The "Carbon Capture System Block" is composed of six major components:

- The amine system itself (quencher, absorber, regenerator).
- The low-pressure steam source (choice of either a co-gen facility for power plus steam, a natural gas auxiliary boiler, or integration into the plant's coal-based steam system).
- The compression and dehydration equipment to condition the CO_2 for pipeline transportation based on the 5-stage compression outlined in McCollum et al. (2006).
- An optional cooling tower.
- An optional water treatment/demineralization plant with CAPEX calibrated to the Petra Nova project and operating parameters calibrated to Loganathan (2014, Appendix A).
- The flue-gas tie-in and control system.

A detailed Front End Engineering Design (FEED) study will be needed to precisely design the facilities at Dry Fork Station, but in Phase I of this study it is assumed that both the cooling tower and water treatment components will be required. Unless otherwise noted, the operating parameters and costs for each of these components is based on information available for the Petra Nova project and the IECM 9.5.

CO_2 Transport Pipelines

The "Pipeline System Block" is mostly composed of internal calculations, but does allow the user to set the length and OPEX assumptions for two pipelines, one to the geologic storage site and another for CO_2 sales. Also included are calculations for the number of CO_2 meters/gauges, and any required pressure boosting stations in the case of long-distance transportation.

The pipeline construction and meter costs are based on the model described in Cook (2012) with updates for inflation.[2] The horsepower rating of the booster stations is based on the algorithm in FE/NETL (2017), with the cost calibrated to the IECM. In the scenario illustrated below, no booster station was needed, but this option was maintained to facilitate application of this tool by other researchers.

Saline Storage Injection Site & Post-Injection Site Care

The "Storage Site Block" includes three main elements: (1) pre-injection site characterization; (2) the operating phase; and (3) the PISC plan.

- Pre-Injection Site Characterization includes some permitting costs, 2-D and 3-D seismic for the area of review (AoR, approximately 10 mi^2 for Dry Fork Station or about double the estimated areal surface of the plume), drilling, and VSP tools and analysis for test wells (1-well per 25 mi^2 of AoR). Permitting costs and test well spacing were drawn from IECM 9.5. The cost of seismic runs, drilling, and test-well analysis are based on discussion with Advanced Resources International (ARI), WellDog Inc., and EIA (2016).
- The Operating Phase includes the drilling and completion of injection wells (based on estimated injection rates and contingency for well interruptions) and a number of wells for the monitoring plan based on information from IECM and FE/NETL. Periodic seismic surveys and well analyses are conducted each of the first two years of injection, again in year five, and then every five years during the 25 years of injection operations.
- PISC includes costs to plug and abandon wells, basic site observation and contingency, and periodic seismic or other tests every seven years during the default 50-year PISC period. These costs are accounted for by setting aside the necessary funds in a trust account during the operating phase to be drawn down over the PISC term.

Tax Equity, CO_2 Sales, and Other Revenues

The "Capital & Revenue Block" contains assumptions related to the pricing of CO_2 sales to CO_2-EOR customers, investment tax credits, and potential tax credits, such as those of

[2] The model underlying Cook (2012) includes provisions for inflation and industry changes based on the WTI oil price, the Nelson-Farrar Labor index, the PPI Index for O&G manufacturing, and the Consumer Price Index (CPI-U-LFE).

the 45Q "Future Act," and the option to earn either marketable carbon offsets/credits or to sell "Green Electrons" at a premium to normal electricity.

- The user can set either what percentage of captured CO_2 is used for sales as constant for all years, or can specify a sales schedule for each year of operations.
- CO_2 Sales for EOR are typically tied to the WTI oil price along with a fixed charge for transportation. Based on prevailing information, longer-term contracts would amount to roughly $0.50 plus 2% of WTI for each Mcf of CO_2. For example, oil that sells for $60 barrel, such a contract would price CO_2 at $33 per metric ton, or $1.70 per mcf. For the Petra Nova project, vertically integrating with an EOR project was seen as a way to solve the project economics. An additional barrel of oil over the life of an EOR flood requires around 7 mcfs of purchased CO_2. With CO_2 prices tied to WTI oil, the contract described above amounts to $13.10 per barrel, which is similar to having a 20% non-working royalty interest in the CO_2-EOR project itself.
- An important consideration for CO_2-EOR sales is the trade-off between EOR revenues, and how those CO_2 volumes are treated for tax credits, carbon offsets, or "green electrons." One option would be to attempt to negotiate a minimum price in CO_2-EOR contracts in order to offset some of these opportunity costs.
- Tax Credits, such as the Investment Tax Credit (ITC) under section 48A and the 45Q "Future Act" Tax Credits, have the potential to serve as a major source of equity capital through the Tax Equity Market. Tax Credits directly offset liability, and pre-selling these tax credits at a discount to investors with adequate tax liability to utilize these credits essentially serves as a capital channel. Tax-equity investors typically require returns of 10% to 18% annualized.
- "Green Electron" sales allow the model to sell the generated electricity associated with the captured carbon at a premium; the idea was outlined in Farhat et al (2013), comparing electricity rate differences in California and Wyoming, with retail prices differing substantially across the two regions. The model distinguishes between EOR and saline storage by placing a 50% discount on EOR, similar to the 45Q provision.
- Tradeable Offsets or Allowances would principally be another mechanism for receiving a premium on carbon-free electrons but with different mechanics than wheeling electricity. The model imputes offsets at a 50% lower rate for EOR, again in line with 45Q. The 2018 minimum reserve price for carbon allowances in the California Cap-and-Trade Program is $14.68 per ton.[3] At some point in the future, it is conceivable that CO_2 capture at existing pulverized coal plants would generate tradable allowances or offsets, thus serving as another source of revenue for the project.

[3] https://www.arb.ca.gov/cc/capandtrade/auction/auction.htm#auctionreserveprice

Energy & Commodity Price Paths

The “Pricing Path Block” allows the user to customize the future annual price path of WTI Crude Oil, PRB Coal, Henry Hub Gas, Commercial and Industrial Gas, as well as Industrial and Wholesale Electricity rates.

Depending on the plant configuration chosen, these different consumable prices factor differently into the model results. WTI oil price is used to calculate the CO_2 price for EOR sales when the contract is tied to oil prices. The natural gas and PRB coal prices are applied to the user options for the regenerator steam source; natural gas is used in the case of an auxiliary boiler or co-gen plant, and coal is used if the steam is sourced from the parent plant.

The electricity pricing enters the model in two ways as the capture process itself consumes electricity, but the user has the option to sell “green electrons” at a premium, or to sell any excess power if the user elects a co-gen plant in the facility design.

Price path options for scenario analysis include constant prices, constant growth rate, linear trend, stochastic pricing for Monte Carlo analysis, and placeholders for user defined scenarios.

Capital Structure

The “Capital Structure Block” allows the user to set the various parameters associated with the mix and costs of debt and equity. Debt is assumed to be a single syndicated loan with terms specified by the user, and equity is assumed to come from both traditional project-finance equity as well as tax-equity.

The two major constraints that are used to ensure project viability are the debt terms, such that the minimum debt-service coverage ratio (DSCR) is not violated and simultaneously ensuring that there is sufficient equity available to fund the balance of the project. Changing the required rate of return on tax equity can improve the tax-equity available, but this also decreases the probability that capital markets will actually supply sufficient tax-equity capital.

Insurance, Trust Accounts & Long-Term Liability

The "Insurance and Trust Account Block" contains assumptions related to general liability coverage for the carbon capture and storage facilities, along with settings for the management of two trust accounts – the PISC account and the LTL accounts.

- The general liability coverage assumptions include a basic underwriting fee, an annual premium based on the non-owner's share of CAPEX, and the fee itself can be escalated at inflation or another user defined rate. Based on discussion with industry, these charges can vary from 1% up to 3-4% for comprehensive casualty, liability, and business interruption coverage.
- The PISC trust fund assumptions are merely the estimated annual return on invested funds, and a provision for contingency. The model then uses these assumptions to calculate how much needs to be set aside each year at the project inception to have sufficient funds to disperse during the 50 years of PISC.
- The LTL assumptions allow the user to specify the maximum possible loss in current dollars, apply various contingency and probabilities, set the estimated return on the trust account, and arrive at an estimate for the required annual "tipping fee" to be deposited into the LTL trust account so that the maximum "probable" loss value can be accumulated in the fund by the end of the PISC period (time value of money and inflation are also accounted for).

Hypothetically speaking—if the maximum possible loss were equal to the replacement cost of the Dry Fork Station—roughly $1.5 billion with 20% contingency, with a 6% return on the account (very long-term account with higher equity allocation), and with an extremely pessimistic 40% chance of occurrence, this fee would be about $0.94 per ton of CO_2 each year (comparable to Dooley et al (2009)). With a chance of occurrence of only 1%, this "tipping fee" would only be 2-cents per ton.

RESULTS

A. Key Outputs

The principal outputs of the model are CAPEX and OPEX for the CCS facilities and the associated sizing of debt and equity. Scenario analysis can then be used to assess the likelihood of an economically viable project from the perspective of capital markets.

In the event that the model indicates short-fall in capital funding, these costs would have to be covered in some other way in order for the modeled project to go forward. Other options for funding might include absorbing the costs into the capital base of the utility and

passing costs on to rate-payers (which is only likely in the event of carbon regulation that affects coal plants), or with the aid of "make-up capital" in the form of direct government assistance (as opposed to indirect in the form of tax-credits).

B. Project Cost Scenarios

It is assumed in Table 2.1.1 that each scenario includes a 380 MW flue-gas stream, an amine capture system, a cooling tower and water treatment, compression and dehydration, CO_2 pipelines and the storage site, general industrial insurance, trust payments for PISC and LTL, miscellaneous owner's costs, and a debt and working capital reserve. It is also assumed that each project is financed 30% by debt; however, this assumption will in fact depend on revenues and tax credits.

The remaining assumptions about the source of process steam, and the rates at which electric power and natural gas must be purchased, then drive the variations in system costs.

Ignoring inflation or any variation in fuel and power purchases, the CAPEX of the system are expected to be between $746 and $944 million, with annual OPEX between $58 and $116 million.

Table 2.1.1

Basic Assumptions	Steam Source	Power & Fuel Rates	CAPEX	Year-One OPEX	Total OPEX	All-In Costs	All-In Costs per Ton
380 MW Flu-Gas Stream (50-58 MtCO2 over 25 years) <u>Included Components:</u> - Amine System - Cooling Tower - Water Treatment - Compression - Pipelines - Storage Site - PISC/LTL Trust Payments - Insurance - Owner's Costs - Debt Reserve (one-half payment) - Working Capital (30% year-one OPEX)	Co-Gen, Steam plus Power	No Power Purchased Gas at Henry Hub ($3/Mcf)	$936 M	$68 M	$1,607 M	$2,543 M	$43.74
		No Power Purchased Gas at Industrial ($4.3/Mcf)	$939 M	$76 M	$1,816 M	$2,755 M	$47.38
		No Power Purchased Gas at Commercial ($7/Mcf)	$944 M	$93 M	$2,251 M	$3,195 M	$54.94
	Natural Gas Axillary Boiler	Power at Wholesale ($25/MWh) Gas at Henry Hub ($3/Mcf)	$746 M	$71 M	$1,693 M	$2,439 M	$41.94
		Power at Wholesale ($25/MWh) Gas at Industrial ($4.3/Mcf)	$748 M	$79 M	$1,900 M	$2,648 M	$45.55
		Power at Wholesale ($25/MWh) Gas at Commercial ($7/Mcf)	$754 M	$97 M	$2,330 M	$3,084 M	$53.04
		Power at Industrial ($70/MWh) Gas at Henry Hub ($3/Mcf)	$752 M	$91 M	$2,187 M	$2,939 M	$50.55
		Power at Industrial ($70/MWh) Gas at Industrial ($4.3/Mcf)	$754 M	$99 M	$2,395 M	$3,149 M	$54.16
		Power at Industrial ($70/MWh) Gas at Commercial ($7/Mcf)	$760 M	$116 M	$2,825 M	$3,585 M	$61.61

– 30% Debt Funded	Coal Plant Steam Cycle Integration	Power at Wholesale ($25/MWh) PRB Coal ($12.50/short-ton)	$786 M	$58 M	$1,374 M	$2,160 M	$37.14
		Power at Industrial ($70/MWh) PRB Coal ($12.50/short-ton)	$792 M	$78 M	$1,869 M	$2,660 M	$45.76

C. Breakdown of Costs

The lowest all-in cost would be realized utilizing the coal-based steam cycle assuming that needed electricity can be purchased at wholesale (CAPEX of $786 million, OPEX of $58 million). A breakdown of costs are shown in Table 2.1.2 and illustrated in Figure 2.1.1 and Figure 2.1.2.

A detailed FEED study would need to be conducted to ensure the accurate design and more appropriate pricing of various plant components. In particular, the feasibility of integrating with the plant steam cycle, as well as the need for and sizing of a cooling tower and water treatment plant must be determined. Eliminating the need for a water treatment and demineralization system can remove around $4.00/ton from the capture cost.

Because the system shown in Table 2.1.2 requires 65,000+ KWs of power to operate (nearly 60% for compression), the price that must be paid for this power is a critical component of controlling costs. Every $10/MWh of electricity cost adds around $4.4 million annual to the OPEX of the system.

Table 2.1.2

COMPONENT	CAPEX	Year-One OPEX	Total OPEX	ALL-IN	per TON
Amine Capture & Tie-In	$381 M	$18.65 M	$415 M	$796 M	$13.70
Aux Steam or Boiler Integration	$53 M	$6.29 M	$157 M	$211 M	$3.62
Cooling Tower	$28 M	$2.26 M	$56 M	$85 M	$1.46
Water Treatment	$52 M	$6.07 M	$152 M	$204 M	$3.50
Compression	$96 M	$9.23 M	$231 M	$326 M	$5.61
Storage Site Pipeline	$2 M	$0.01 M	$0 M	$2 M	$0.04
EOR Sales Pipeline	$10 M	$0.03 M	$1 M	$10 M	$0.18
Pipeline Meters/Boosters	$1 M	$0.00 M	$0 M	$1 M	$0.01
Storage Site	$36 M	$2.98 M	$39 M	$75 M	$1.29
Owner's Costs, Reserve & WC	$127 M	$0.00 M	$0 M	$127 M	$2.19
Total Trust Payments	$0 M	$3.01 M	$75 M	$75 M	$1.29
Industrial Insurance	$0 M	$9.88 M	$247 M	$247 M	$4.25
Total	**$786 M**	**$58 M**	**$1,374 M**	**$2,160 M**	**$37.14**

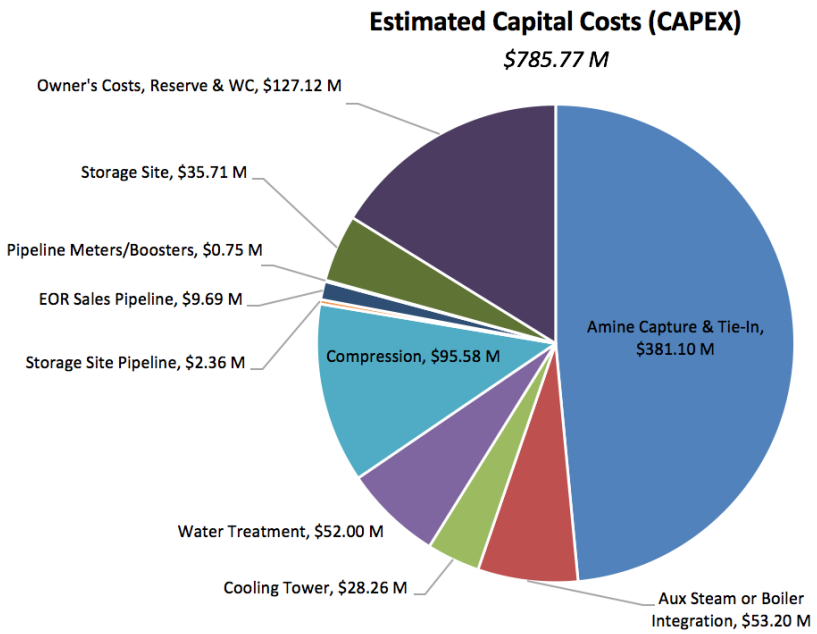

Figure 2.1.1

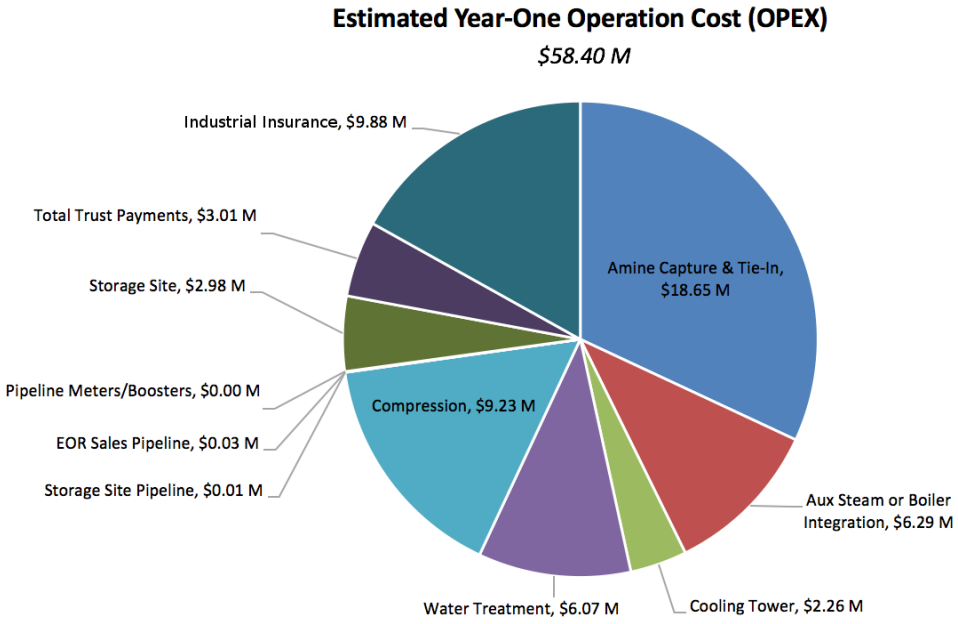

Figure 2.1.2

D. Revenues & Capital Structure

Ignoring revenues and/or tax credits, the entire cost of the storage system would have to be carried by either the ratepayers' purchasing power from Dry Fork Station, direct government assistance, or both.

However, several possibilities exist for revenues streams. Although modifications to 45Q were not included in the recently enacted tax legislation, any successor to the 45Q "Future Act" would serve as a basis for private tax-equity capital.

The most obvious source of revenue would be CO_2 sales for EOR purposes; this CO_2 is ultimately trapped in the associated oil reservoirs. Assuming the current oil price around $60/barrel, selling 90% of the captured CO_2 would yield revenues around $68 million annually.

Another source of revenue could be the sale of "green electrons" at a premium rate, or comparatively, the ability to sell tradable CO_2 credits or offsets for the de-carbonized electricity. Currently, European CO_2 allowances sell for around $7 per ton, and offsets in the California Cap-and-Trade program have a settlement price around $15 per ton. Should these "green electrons" qualify for consideration in a cap-and-trade market (EOR sales being credited at only 50%), this would supply another $9 to $19 million in annual revenues to the project.

Assuming the project qualifies for the Investment Tax Credit under Section 48A, as well as for the Carbon Tax Credits being considered in the "Future Act" legislation, these policies would be able to attract significant tax-equity to the project. Because of the project complexity and risk, companies would likely assign a fairly high discount rate to purchasing these tax credits, perhaps as much as 15%-20%. At a discount rate of 17%, such tax credits could bring over $500 million in potential tax equity.

Taken together, the 90% of CO_2 sold to EOR, $5-$10 per ton for Tradable Offsets, and over $500 million in tax-equity would likely be sufficient to finance the lowest-cost project with only 25% debt (refer to Table 2.1.3).

Table 2.1.3

Capital Structure	Value
Share of Debt (%)	25.0%
Min Debt (%) Based on Equity Sizing	21.3%
Cost of Debt (rd, %)	6.0%
Share of Equity (%)	75.0%
Cost of Equity (re, %)	16.3%
Corporate Tax Rate (%)	21.0%
Debt-to-Equity (fraction)	0.3
Post-Tax WACC (%)	13.4%
Loan Terms & Covenants	**Value**
Loan/Bond Tenor (years)	20
Cost of Debt (rd, %)	6.0%
Debt Payment ($MM)	$16.51
Syndicated Loan Min. 10yr DSCR	1.25
Average 10yr DSCR	1.45
Avg. DSCR First 3yrs	1.35
Min DSCR Over Loan	1.25
Funding Feasibility	**Value**
Total Debt	$196.03
Total Equity	$588.09
Expected Return on Tax Equity/ITC	17.0%
Expected Return on FCFE	12.0%
Equity Value of ITC	*$81.70*
Equity Value of Tax Credits	*$436.17*
Equity Value of Cashflow	***$78.06***
Total Equity Potential	*$595.93*
Capital Excess (Shortfall)	*$7.84*

Conclusion

Constructing and operating a carbon capture system that is integrated into the operation of an existing facility requires careful planning and engineering to reduce the risks inherent in large complex projects. The recent on-budget successful completion of NRG's Petra Nova capture project at the W.A. Parish Generating Station demonstrates that successful execution on such projects is indeed possible and can strengthen confidence in potential partners and capital markets for future endeavors.

The primary techno-economic baseline for evaluating the financial prospects of an amine capture system on a 380 MW flue-gas stream from Basin's Dry Fork Station was built

utilizing the IECM 9.5 and FE/NETL Saline Storage models. Costs were calibrated to match discussion with industry and the realizations at the Petra Nova project. The model also incorporates various opportunities for revenue recognition, and accounts for PISC and LTL, utilizing payments into trust accounts during the 25-year operating period.

The major design decisions will include the source of steam for the amine process and evaluating the need for a cooling tower and water treatment plant. Two major sources of OPEX are tied to the price at which the facility is charged for electricity and the cost of natural gas in the case of a gas-fired steam source.

The lowest cost option considered would involve utilizing the coal fired steam cycle of the host plant and requires power purchased at wholesale rates. Under such a scenario, the facilities would cost an estimated $768 million, with around $58 million in annual OPEX. Financing such a project could include up to 25% debt but would require 90% of CO_2 to be sold for EOR, earnings from tradable CO_2 allowances, and the significant tax equity from section 45Q and 48A tax credits.

Section 2.1 References

Integrated Environmental Control Model, Current Public Version 9.5 (2017), Carnegie Mellon University, Department of Engineering & Public Policy. Available at: https://www.cmu.edu/epp/iecm/

National Energy Technology Laboratory, (2017). "FE/NETL CO2 Saline Storage Cost Model. U.S. Department of Energy." Last Update: Sep 2017 (Version 3) https://www.netl.doe.gov/research/energy-analysis/searchpublications/vuedetails?id=2403

Armpriester, Anthony, (2017). "W.A. Parish Post Combustion CO_2 Capture and Sequestration Project Final Public Design Report." United States. Retrieved from http://www.osti.gov/scitech/servlets/purl/1344080

U.S. Department of Energy, National Energy Technology Laboratory. (2014). "Acquisition and Development of Selected Cost Data for Saline Storage and Enhanced Oil Recovery (EOR) Operations." Prepared by Advanced Resources International. DOE/NETL-2014/1658. http://www.netl.doe.gov/File%20Library/Research/Energy%20Analysis/Publications/saline-and-eor-operation-cost-estimation-recommendations-ari-final-7-2.pdf

McCollum, David L. and Joan M. Ogden, (2006). "Techno-Economic Models for Carbon Dioxide Compression, Transport, and Storage & Correlations for Estimating Carbon Dioxide Density and Viscosity." Institute of Transportation Studies, University of California, Davis, Research Report UCD-ITS-RR-06-14.

Farhat K., Koplin J., Lewis D., Peterlin S., Simms R., (2013). "Financial Assessment of CO2 Capture and Storage with Electricity trading in the U.S.: Role of Interim Storage and Enhanced Oil Recovery." Energy Procedia 37 (2013) 7512-7525.

Cook, Benjamin R. (2012). "Wyoming's Miscible CO2 Enhanced Oil Recovery Potential in Main Pay Zones: An Economic Scoping Study." University of Wyoming Enhanced Oil Recovery Institute.

Loganathan, Kavithaa (2014). "Water Management through Water Treatment Technologies." IETP Final Report prepared by Canadian Natural Resources Limited for the Government of Alberta's Innovative Energy Technology Program (IETP). Accessed online, November 2017 at http://www.energy.alberta.ca/4229.asp.

U.S. Energy Information Administration (EIA 2016). "Trends in U.S. Oil and Natural Gas Upstream Costs." Independent Statistics & Analysis, report prepared by EIA and IHS Global Inc. https://www.eia.gov/analysis/studies/drilling/pdf/upstream.pdf

Dooley, James J., Chiara Trabucchi, Lindene Patton (2009). "Tipping Fees Can't Save us from the Tipping Point: The Need to Create Rational Approaches to Risk Management that Motivate Geologic CO2 Storage Best Practices." Energy Procedia, Volume 1, Issue 1, 2009, Pages 4583-4590.

Section 2.2: Legal Assessment

Tara Righetti
Associate Professor of Law, University of Wyoming College of Law
Director, Academic Program in Professional Land Management
School of Energy Resources, University of Wyoming
1000 E. University Ave, Dept. 3035
Laramie, WY 82071

Pore Space Ownership and Obtaining Injection Rights

Each of the proposed injection scenarios for the Integrated Commercial Carbon Capture and Storage Project at Dry Fork Station is located in eastern Wyoming's Powder River Basin. Unlike the majority of Wyoming, and many other western states, surface land in the Powder River Basin is primarily privately owned. This landowner's pattern is significant to the project, because private ownership significantly streamlines the process for obtaining injection rights relative to federal lands. There is no leasing program or established guidance on obtaining injection rights for CCUS into federal pore space at this time, and accordingly, it is unclear whether such rights could be obtained, and if so, how long it would take. Therefore, choosing an injection area made up of primarily privately owned surface lands would avoid potential bureaucratic entanglements inherent in leasing federally owned pore space, such as delays in the development of a guidance, environmental analysis, and potential legal challenges.

Wyoming Statute 34-1-152 statutorily vests ownership of the pore space in the owner(s) of the surface. This clarification largely resolves any ambiguity regarding which party can grant injection rights. However, Wyoming law permits the severance and separate conveyance of pore space rights, and as a result, a full title analysis will be required prior to obtaining injection rights.

The privately owned portions of the project area may include split estate configurations where the owner of the surface is different from the owner of the underlying minerals. In Wyoming, the mineral estate is dominant over the surface estate—including the pore space—meaning that surface uses are subordinate to use of the land as is necessary for mineral extraction. Although Wyoming requires mineral developers to make reasonable accommodation of existing surface uses, the surface owner may not use pore space in a way that damages, interferes with, or otherwise diminishes the mineral estate. These constraints may limit potential development sites within the project area and subject the project to legal challenge from mineral owners regarding potential impacts to hydrocarbons or federal and private coal assets. The project can mitigate these risks by contracting with mineral owners and developing injection plans in a way to minimize potential interference. A large portion of the privately owned land in the project area is owned by entities with which the project shares a strong working partnership, and accordingly, objections from severed mineral owners are not anticipated to be a significant hurdle.

Transportation

Any pipelines constructed for transportation of CO_2 to or from the site will require right-of-ways (ROW). Right of ways may be across either private or federal land. BLM has authority to issue ROW for CO_2 pipelines pursuant to the Mineral Leasing Act (MLA). Pipeline developers receiving a ROW pursuant to the MLA are required to operate the pipeline as a common carrier, meaning that they must offer non-discriminatory access to the pipeline infrastructure at reasonable published rates. Significant existing CO_2 pipeline infrastructure already exists in the region. Where such pipelines are required to operate as common carriers, the project may be able to access this infrastructure providing access to additional markets for CO_2-EOR. Should the project need to construct new pipelines across federal land, a ROW from BLM will be needed and the pipeline will be required to operate as a common carrier.

The siting, permitting, construction, and transportation of CO_2 pipelines across private land in Wyoming is regulated according to state law. There is no state permitting requirement. Further, Wyoming's Eminent Domain Act provides pipeline companies with broad condemnation authority. However, state law prohibits use of eminent domain for carbon capture and sequestration projects; although, it is unclear whether this prohibition would apply to a pipeline transporting CO_2 for both sequestration and utilization. Wyoming's pipeline corridor initiative has promoted and advanced the acquisition of right of way specifically for the construction of CO_2 pipelines. These existing ROW resources may be available to the project.

Safety of CO2 pipelines is regulated by the Department of Transportation's Pipeline and Hazardous Materials Safety Administration (PHMSA) pursuant to the Hazardous Liquid Pipeline Safety Act of 1979 (HLPSA). Wyoming has accepted responsibility for enforcement of HLPSA requirements and has obtained Certification pursuant to Section 60105(a). In addition to HLPSA requirements, Wyoming's Department of Transportation mandates specific casing and siting requirements for hazardous liquid pipelines facilities within the state highway system right-of-way.

Section 404 of the Clean Water Act requires a permit for any "utility line" crossing requiring discharge of dredge or fill material into waters of the United States. CO_2 pipelines are considered a utility line. Accordingly, if the proposed pipelines require water crossings, either the project must obtain a general (nationwide) or individual permit prior to construction of new pipeline infrastructure.

Although unlikely, a release of CO_2 during transport could result in fines as well as civil and criminal liability pursuant to Wyoming Statute §35-11-201 and §35-11-901 as well as federal environmental laws.

Injection

Prior to injection, project proponents must obtain a Class VI permit from EPA and the creation of an injection unit by the Wyoming Oil and Gas Conservation Commission. EPA regulations categorize facilities that inject carbon dioxide for long-term storage purposes as Class VI wells under the Underground Injection Control program. Presently, no state has primacy to administer the EPA Class VI injection program; however, the Wyoming Department of Environmental Quality anticipates that Wyoming will have primacy to

administer the program before the proposed project implementation. The project will be obligated to comply with all regulations for Class VI wells, including reporting.

The Wyoming Oil and Gas Conservation Commission has authority to create injection units for CCUS pursuant to Wyoming Statute §35-11-315. Unitization plans approved by the Commission will not become effective until the unitization plans has been signed or ratified in writing by the owners representing no less than eighty percent (80%) of the total unit capacity as per Wyoming Statute §35-11-316(c). A review of surface land and pore space ownership within the proposed project areas indicates that the project will be able to reach the 80% approval hurdle. There are no unaffiliated owners within the proposed project area controlling more than 20% of the land area, and thus, no one party has the ability to veto the project. In the event that injected CO_2 migrates outside approved unit boundaries, Wyoming's unitization statute provides an avenue for inclusion of those owners within the unit and sharing of project benefits with such owners. Although the statute's provisions for inclusion do not eliminate the possibility of liability for migration of CO_2 into subjacent parcels, it may significantly limit the potential tort exposure of the project

During injection there is a low probability of a potential catastrophic risk of events with impacts to air, water, earth, public health, and soil, either with or without a seismic event. These could result in liability under a number of federal and state laws or expose the project to tort liability under theories of trespass, nuisance, negligence, and strict liability.

Storage

Although Wyoming has authority to establish a "special revenue account" for the "measurement, monitoring and verification of geologic sequestration sites following site closure," it has not waived its immunity from suit or assumed liability for "geologic sequestration sites or the carbon dioxide and associated constituents injected into those sites." Ownership and operation of a CO_2 storage facility presents long-term liability for adverse impacts to property, environment, or human health resulting from either transboundary migration outside the injection unit and surface releases of CO_2. The project will address long-term liability issues through one or more vehicles: (1) commercial insurance; (2) negotiations with project participants; and/or (3) negotiations with the State of Wyoming Legislature.

General Laws Applicable to the Project

The National Environmental Policy Act (NEPA). NEPA requires an environmental impact statement (EIS) to be prepared whenever a project proposal, "involves a major federal action that will significantly affect the quality of the human environment." An Environmental Impact Statement or Environmental Assessment may be required if federal lands or permits are necessary to the project. The NEPA process can be lengthy and expensive, and subject to legal challenge.

Clean Air Act. Carbon dioxide and other greenhouse gases are included under the Clean Air Act's definition of "pollutant." Accordingly, a mass release of carbon dioxide during the project could subject project proponents to administrative, civil, and criminal penalties, or require permitting revisions for capture facilities.

Clean Water Act. The project will require adherence to all rules and regulations related to Class VI wells, discussed *supra*, including permitting, geological site characterization, and financial responsibility, well construction, mechanical integrity testing and monitoring, well plugging, post injection site care, and site closure.

Resource Conservation and Recovery Act. Carbon dioxide streams that are injected in Class VI wells are conditionally excluded from classification as hazardous wastes under the U.S. Resource Conservations & Recovery Act.

National Historic Preservation Act. The NHPA requires federal agencies to consult with the Advisory Council to limit impacts to historic properties. Any such impacts will need to be considered in project siting. An onsite assessment of cultural and archeological resources will be a necessary component in identifying the final injection site and scenario.

Species Conservation and Habitat Mitigation. Wyoming has proactively addressed concerns regarding the declining population of the Greater Sage Grouse with a multi-agency Sage Grouse Conservation Strategy. This strategy limits surface disturbances within core habitat and requires habitat mitigation, both of which may affect surface facilities and project timing and costs. In addition to Sage Grouse Conservation measures, the project must consider and comply with the Endangered Species Act and other species conservation acts.

Section 2.3: Environmental Assessment

Tom Moore
Research Scientist, Center of Economic Geology Research
School of Energy Resources, University of Wyoming
1000 E. University Ave, Dept. 3012
Laramie, WY 82071

Project background: This study seeks to identify saline storage opportunities proximal to the Dry Fork Power Station in the Powder River Basin (**Figure 2.3.1**). The objectives of the proposed work are as follows: (1) to establish a CCS coordination team capable of achieving a successful commercial scale CCS for the Dry Fork Power Station; (2) to develop site-specific business and execution strategies; and (3) to identify and describe promising saline storage sites capable of storing 50 million tonnes of CO_2.

The goal of the environmental assessment is to evaluate environmentally sensitive areas and potential impacts in the region. This assessment includes the major biome and inorganic environmental concerns with regard to the suggested source, transport, and storage components for a Phase 1 Pre-Feasibility study, including an overview of protected species and their habitat, surface water, ground water, air quality, protected areas, cultural resources, and population centers as described in the National Energy Technology Laboratory (NETL) Best Management Practices (BMP) manual (NETL, 2013). In addition, topography and animal migration corridors have also been evaluated to identify scenarios that could portend mitigation.

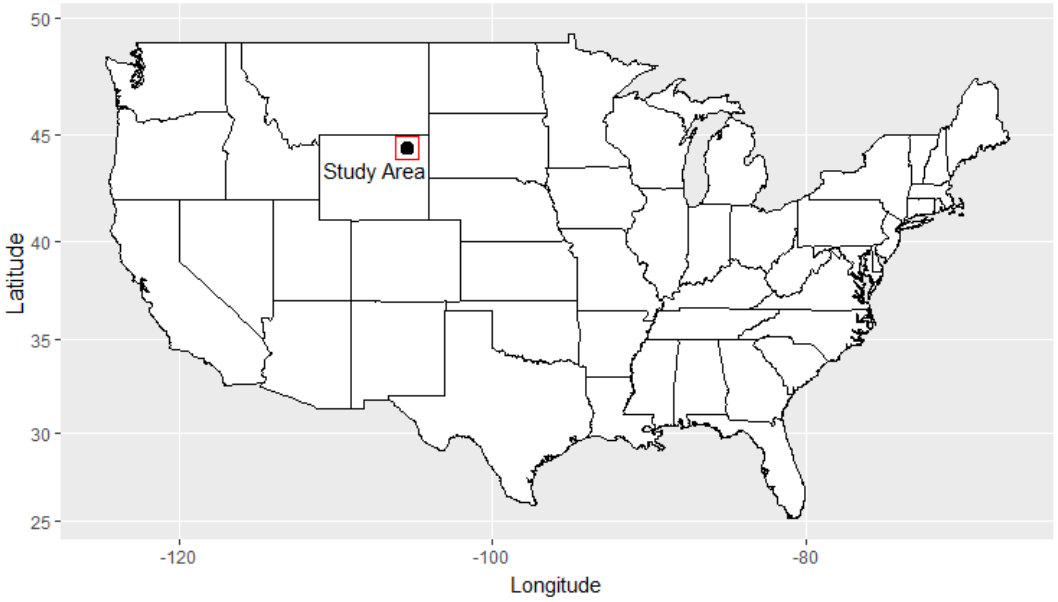

Figure 2.3.1 Map of the United States, showing where the study area lies in the northeast corner of Wyoming.

Scenarios. We discuss environmental considerations in relation to five proposed source-transport and storage scenarios proposed under Task 2 of this project. The five scenarios include: 1) On Site, 2) Between DFS and Wyodak Cluster, 3) East (T51N-R70W), 4) West (T51N-R73W), and 5) County Line (T52N-R69W) (**Figure 2.3.2**). The Area of Review (AOR) discussed in this assessment pertains to the land surface encompassed in all five scenarios.

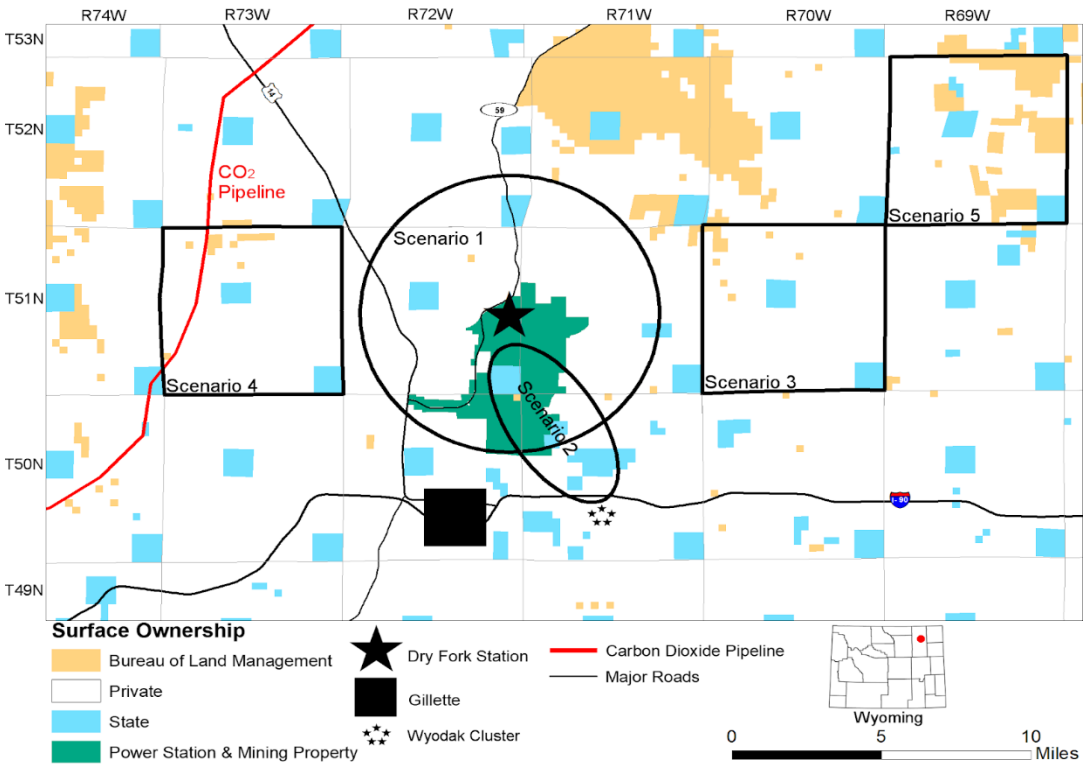

Figure 2.3.2 Project Land Ownership and CCS/CCUS Scenarios.

Protected Species. The U.S. Fish and Wildlife Service (USFWS) official species list (USFWS, 2017), compiled in fulfillment of the USFWS Endangered Species Act of 1973 (ESA) section7(c), identifies 26 protected species within the AOR. No critical habitat (defined as essential to the species) of any protected species are identified in the AOR of this study. However, there are two threatened species with potential habitat (defined as habitat that could support species) in the AOR. The species include the Northern Long-eared bat (*Myotis septentrionalis*) and the Ute ladies-tresses *(Spiranthes diluvialis*), an orchid. The Northern Long-eared bat roost underneath bark or in crevices of both live and dead trees; they have also been known to roost in caves. This habitat generally follows riparian and wetland areas where cottonwood species are dominant and their food source, insects, are found (ECOS, 2017). The Ute ladies-tresses is an orchid that prefers moist

soil found proximal to wetland and riparian areas (ECOS, 2017). Potential habitat for both species follow wetland and riparian corridors (**Figure 2.3.3**).

Scenario 4 to the West of DFS has the least potential habitat for both species and a state plot that has no potential habitat. Scenarios 1, 2, and 5 are largely covered by potential habitat, although sections exist with none. Scenario 3 is almost completely covered; however, potential habitat does not yet support either species, meaning each scenario will likely not be affected by either protected species.

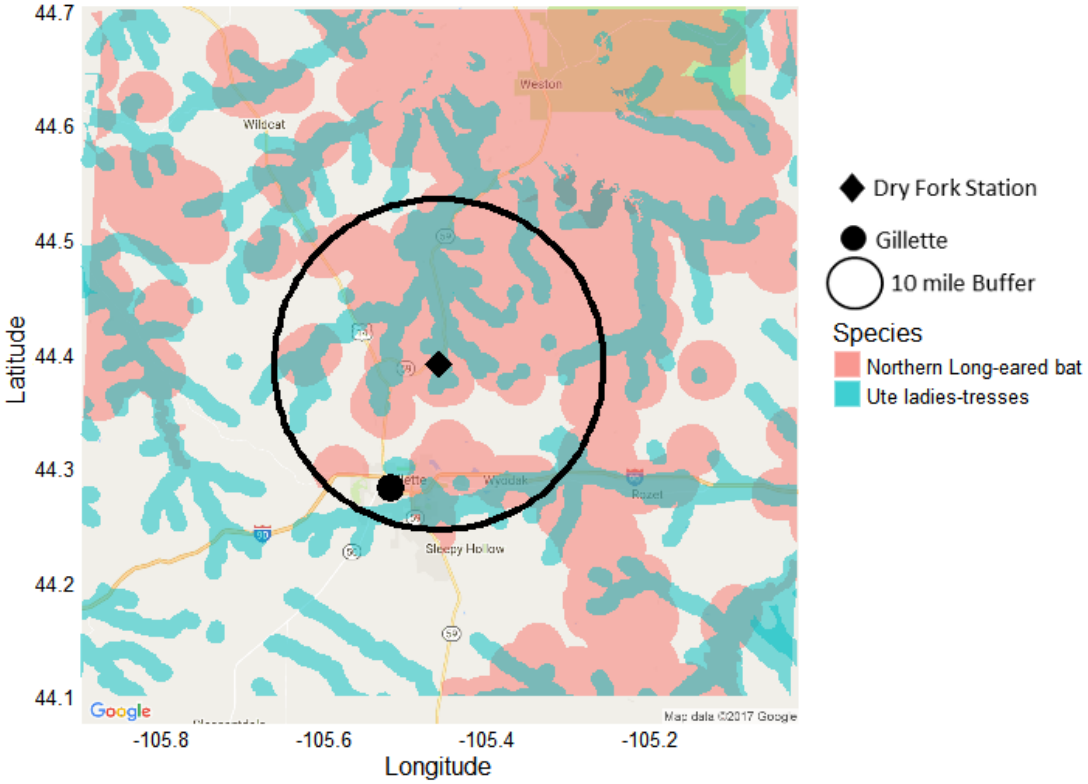

Figure 2.3.3 Potential habitat of the Ute ladies-tresses (ULT) and Northern Long-eared bat (NLEB) surrounding Dry Fork Station (USFWS, 2012; 2016).

The Migratory Bird Treaty Act and the Bald and Golden Eagle Protection Act protect bird species native to the AOR. Twenty-four migratory birds of conservation concern have been observed within the AOR. Six species reside in the AOR year round, one species uses the AOR as winter habitat, and the remaining fourteen species use the AOR during migration and breeding periods (**Table 2.3.1**). Three of these birds, the Golden eagle, Bald eagle, and Prairie falcon are raptors, which prefer sparse grassland habitat with trees to perch on (**Figure 2.3.4**). Scenario 2 has the least potential to impact raptors, followed by scenarios 4, 3, 1, and 5. A raptor nest survey will be required in later phases of this project. The project will also be required to consider the fourteen species that migrate and breed in the AOR to mitigate impacts from construction during these

sensitive periods. The majority of these birds are sparse grassland species. Scenarios 1 and 2 have the least potential to impact this habitat, followed by scenario 3, 4, and 5. There are two wetland and four riparian species; although, the Bald eagle, Curlew, Mountain plover, and Sandpiper also frequent wetland and riparian habitat. Scenario 4 is the least impactful to wetland birds, followed by 1, 2 & 3, and 5. Riparian bird habitat is least impacted by scenario 2, and then similar for the remaining scenarios. Areas for site selection and CO_2 pipe routing that avoid high impact areas will be preferentially selected (**Figures 2.3.4**). These concerns can be mitigated by strategically timing construction during breeding and migration periods (**Table 2.3.1**) and by avoiding sensitive areas. The Greater sage grouse (*Centrocercus urophasianus*) is a candidate species for ESA protection, and core habitat (defined as habitat designated by the state) is located approximately 9 miles north of Dry Fork Station. No project scenario suggested by Task 2 is predicted to disturb the surface proximal to this core habitat. Overall, scenario 2 looks the least impactful to protected bird species, followed by scenarios 1, 4, 3, and 5.

Table 2.3.1 Protected bird species habitat and periods of sensitivity compiled from Cornell 2017.

Habitat	**Species**	**Use**	**Timing**
Riparian	Lewis's woodpecker	Breeding	May-Aug
	Willow flycatcher	Migration/Breeding	June-Jul
Wetland	American bittern	Breeding	Apr-Jul
	Western grebe	Breeding	June-Aug
Sparse Grassland	Black Rosy Finch	Winter	-
	Brewers sparrow	Breeding	June-Jul
	Burrowing owl	Breeding	Mar-Aug
	Dickcissel	Breeding	Mar-Jul
	Ferruginous hawk	Breeding	Apr-Jul
	Grasshopper sparrow	Breeding	June-Jul
	Greater Sage grouse	Year-round	Mar-Aug
	Loggerhead shrike	Breeding	Mar-Jun
	Long billed curlew	Breeding	Apr-Jul
	McCown's Longspur	Breeding	May-Jul
	Mountain plover	Breeding	Apr-Aug
	Pinyon Jay	Year-round	Feb-Jul

	Red-headed woodpecker	Breeding	May-Aug
	Sage thrasher	Breeding	May-Jul
	Short-eared owl	Year-round	Apr-May
	Swainson's hawk	Breeding	Apr-Jun
	Upland Sandpiper	Breeding	May-Jun
Raptor	Bald eagle	Year-round	Apr-Aug
	Golden eagle	Year-round	Apr-Aug
	Prairie falcon	Year-round	Apr-Jun

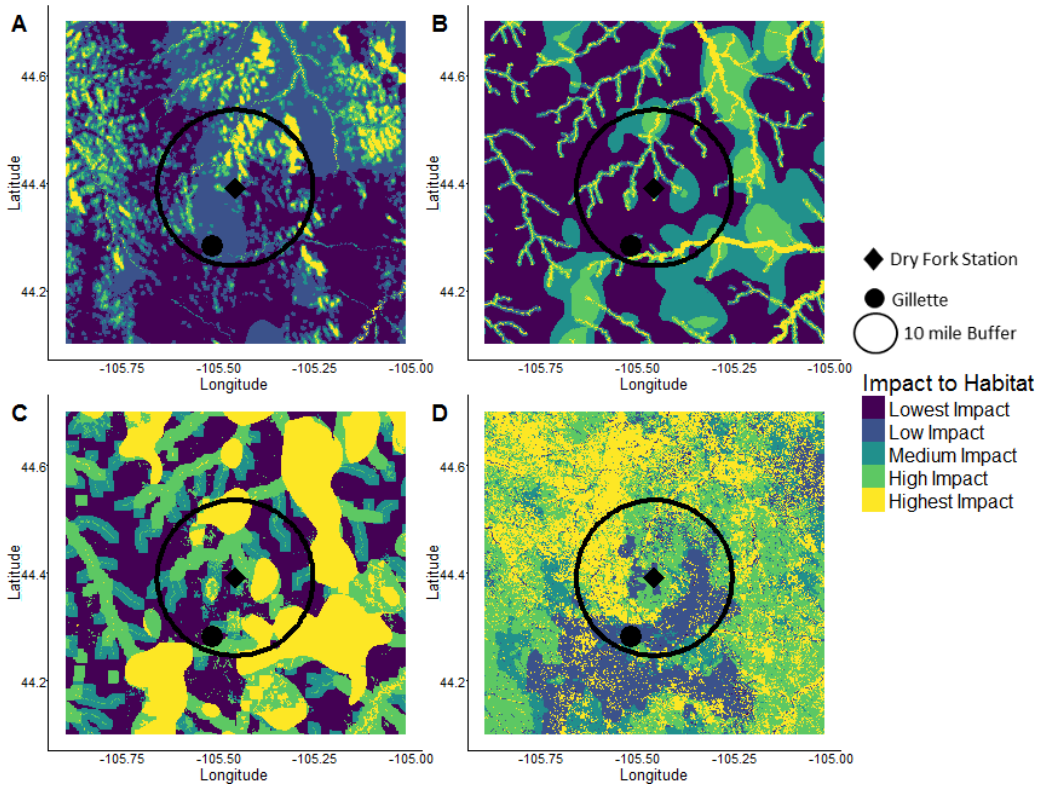

Figure 2.3.4 A map displaying the importance of habitat to A) raptors, B) riparian bird species, C) wetland bird species, D) grassland bird species, and the potential impact developing the area may have (pulled from: Pocewicz et al., 2013).

Wetlands & Streams. Two federal acts protect waterbodies, the USEPA Safe Drinking Water Act (SDWA) and the Clean Water Act (CWA). Wetlands are protected by section 404 of the CWA, which regulates discharge of dredged and fill material into streams and wetlands (EPA, 2002). Construction of new roads, CO_2 pipeline, and well pads could potentially fall under the prevue of section 404 of the CWA. Additionally, wetlands affected by construction may need to be replaced at a 1:1 or 2:1 ratio (USEPA, 2002). All project scenarios have the potential to cross and affect wetlands, streams, and riparian

areas. A map was created to guide site selection and CO_2 piping to minimize negative impacts of the project (**Figure 2.3.5**). Scenario 1 will minimize piping and has the greatest opportunity to avoid ephemeral drainages and streams. Scenarios 3 and 4 have a similar potential. However, they will require more piping that is likely to cross more drainages. Scenario 5 requires the most piping, and scenario 2 drains into Donkey Creek, which has a Total Daily Maximum Load (TMDL) and is impaired from *E. coli.*

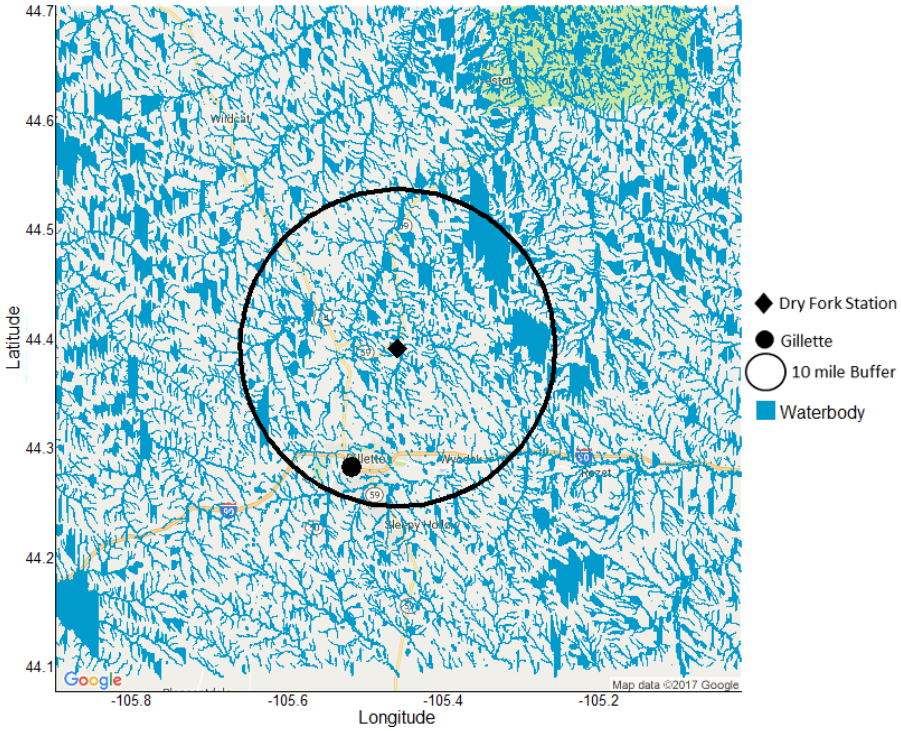

Figure 2.3.5 Surveyed riparian and wetland areas in the area of study surrounding Dry Fork Station (USFWS, 2009).

Groundwater. Groundwater is protected by the SDWA, which regulates water by its designated uses defined by the USEPA. The storage reservoirs selected for this study either a) have a salinity exceeding 10,000 ppm total dissolved solids (TDS) or, b) further salinity data needs to be collected to determine the groundwater salinity. Salinity distribution maps were created from the USGS National Produced Waters Geochemical Database v2.2 (Blondes et al., 2016) for potential reservoirs. Groundwater resources lie above the reservoirs targeted under this study and are hydrologically separated from drinking water aquifers by thick laterally continuous confining units. There are no sole-source aquifers as defined by the EPA in the AOR or in northeastern Wyoming. However, this region has experienced extensive deep oil and gas exploration; thus, we consider areas where these deep wells may create a conduit across the confining units. The location of wells that penetrate the reservoir seals are shown in **Figure 2.3.6**. Scenario 4 has the fewest number of wells penetrating the shallowest seal, the Lewis. Scenario 5 is the second best option, followed by scenario 3, and finally, scenarios 2 and 4.

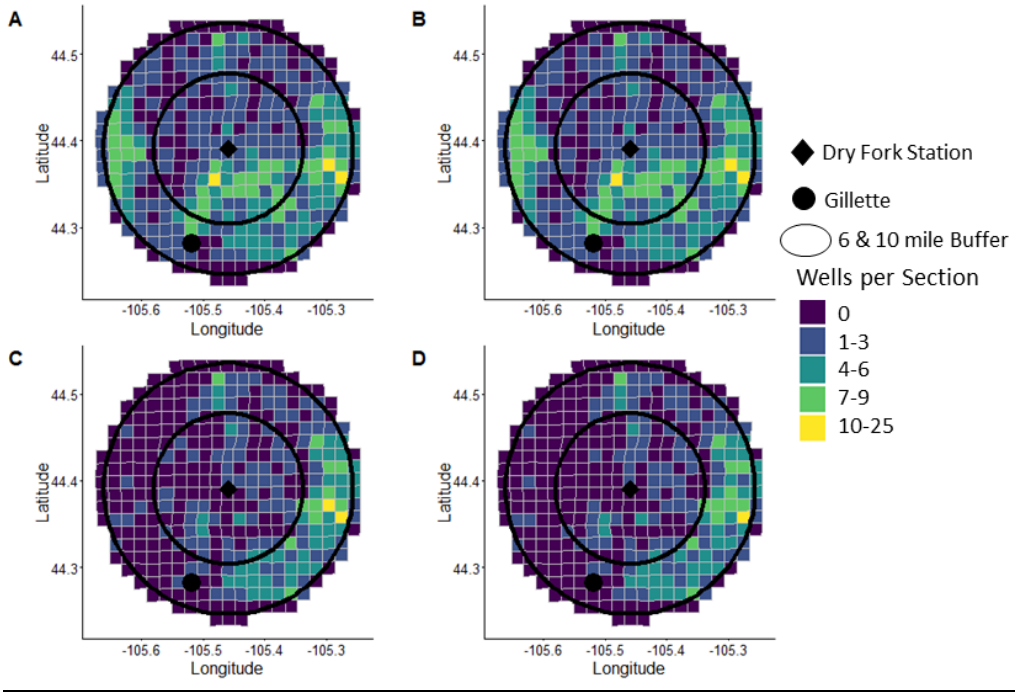

Figure 2.3.6 The density of wells per township section (1 mile x 1 mile) that penetrate the A) Lewis, B) Mowry, C) Morrison, and D) Opeche confining layers surrounding Dry Fork Station near Gillette, WY.

For each seal, an isopach map was created showing the unit thickness interpolated from well logs (**Figure 2.3.7**). Each seal is present for each scenario, and therefore, not considered in ranking. The seals protect underground safe drinking water, which is drawn from wells. Three Domestic wells penetrate the Lewis seal (**Figure 2.3.8**). Two of these wells were exploratory oil and gas wells and were plugged above the Lewis seal where water is now drawn and pose the same risk that was analyzed in the penetration analysis. One Domestic well draws water beneath the Lewis and could be a direct conduit for CO_2 to migrate through the Lewis. No wells permitted for irrigation or stock water penetrate the Lewis.

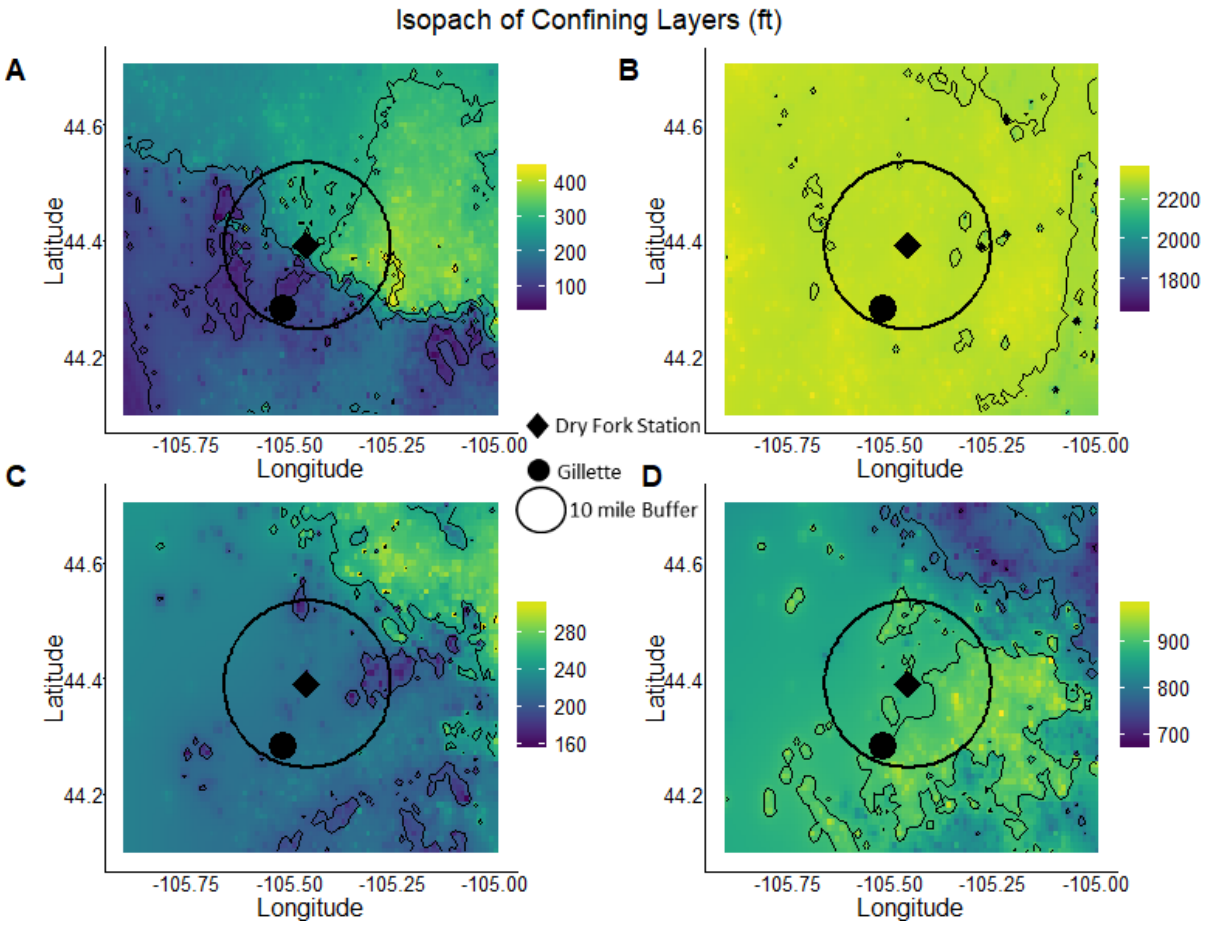

Figure 2.3.7 An isopach map estimating the thickness of the A) Lewis, B) Mowry-Niobrara, C) Morrison, and D) Opeche formations acting as seals for the underlying reservoirs. Interpolated (IDW) from well logs (GDI, 2000).

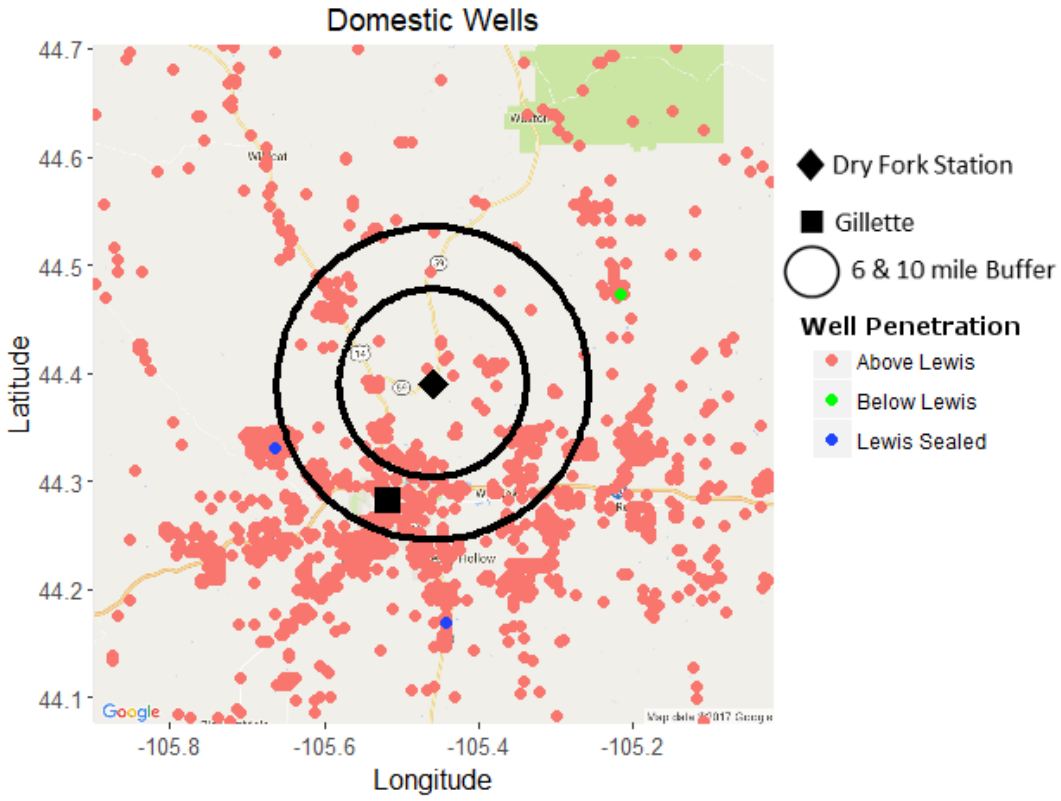

Figure 2.3.8 Location of wells permitted for domestic use, including wells that do not penetrate the shallowest Lewis seal, wells that penetrate the Lewis, and wells that were drilled through the Lewis, but are now sealed above the Lewis and draw water from more shallow formations.

Air Quality. Data has been compiled from the EPA Facility Level Information on GreenHouse gasses Tool (FLIGHT) and Wyoming Department of Environmental Quality (WDEQ) inventories to summarize emissions from DFS. DFS's yearly emissions have averaged 3.2 million tonnes CO_2, 51 tonnes CH_4, and 230 tonnes N_2O from 2012-2015 (USEPA, 2017). The WDEQ has reported the 2011-2013 average regulated emissions from DFS (**Table 2.3.2**) (WDEQ, 2017). The short-term construction process affects air quality due to generators, vehicle emissions, and increased particulates; however, the long-term effects will decrease greenhouse gas emissions. Scenario 1 would minimize construction and piping by being on-site and is therefore treated as the least impactful in this analysis.

Table 2.3.2 Average concentration (Tonnes/year) of regulated emissions from the DFS (WDEQ 2017).

Pollutant	CO	NO_X	SO_2	CH_2O	C_6H_6	Pb	Hg	HF	HCl	PM-10	PM-25	VOC
Tonnes/year	521	450	544	0.29	0.000002	0.001	0.029	0.56	1.14	129.34	2.54	0.44

Protected Areas. Protected areas include national parks, wildlife refuges, state parks, and national monuments, all of which lie outside the locations being considered for this project.

Cultural Resources. The Natural Resource and Energy eXplorer (NREX) was used to map published surveys of cultural artifacts and sites found within the AOI. The number and location of these sites and artifacts does not appear to significantly affect any proposed scenario, although continued awareness and slight mitigation will be needed. A large portion of scenario 1 has already been surveyed, which will benefit scenario 1. The remaining scenarios have less inventoried cultural resources due to less surveys; however, no one areas seems better than another to avoid cultural resources. Communication has been maintained with the Wyoming State Historic Preservation Office throughout the course of this assessment. A survey of these sites is recommended during later project development under the advisement of the Wyoming State Historic Preservation Office (SHPO).

Population Centers. Though the study area is sparsely populated to the north, there are several population centers south of DFS. The largest is Gillette, with a population of 32,398, located 8 miles south of DFS (USCB, 2016). Small unincorporated towns include Antelope Valley-Crestview (1,658 people), and Sleepy Hollow (1,308 people), which are 5 miles southeast of Gillette. Scenario 5 is located the furthest from a population center (19 miles), while scenario 1, 3, and 4 are between 2 and 9 miles away. Scenario 1 and 2 are the closest to Gillette at around 2 miles.

Topography. Although damaging landslides in the study area are rare, the topography surrounding DFS should be understood to avoid potential hazards. The soil type is identified as relatively erosive using data from the NRCS SSURGO database (USDA-NRCS, 2016). A slope map was generated and includes areas of mass movement. On the basis of this information, the slopes directly surrounding DFS are between 0 to 5 degrees. Higher slopes are generally associated with drainages. Slopes above 15 degrees should be avoided for site selection and are correlated with mass movement events (**Figure 2.3.9**) in the study area. Any increase in distance for CO_2 transport is more likely to cross-areas with slopes over 15 degrees. While all scenarios can put the well in a flat location, scenario 1 will have the least transport of CO_2, which will cross steeper areas. Scenario 2 is the second closest, and the rest of the scenarios will have similar problems associated with slope and the challenges of transport.

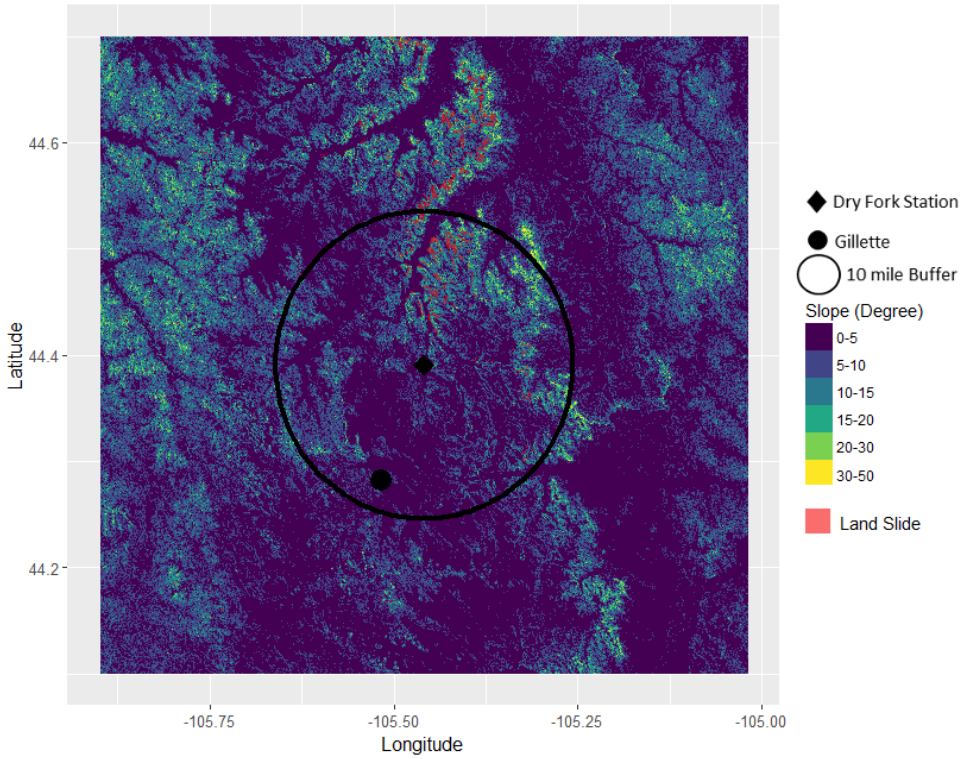

Figure 2.3.9 Slope steepness in the area of study surrounding Dry Fork Station processed from a USGS 10 meter digital elevation map (USGS, 2009) and the surveyed extents of historic mass movement events (WRDS 2009).

Migration Corridors. Big game migration corridors and critical habitat have been considered with respect to scenario selection. There is no critical habitat in the AOI. However several Pronghorn (*Antilocapra Americana*) migration corridors have been identified. The closest migration corridor is 7 miles north of DFS. None of the corridors are within 6 miles of DFS; however, the corridors should be considered in site selection to avoid impacts by construction and operation of a project site. While no scenario is predicted to affect a migration corridor, scenario 1 will minimize transport and any potential to impact future or unknown corridors.

Conclusion: This environmental assessment has found Scenario 1 to be the least impactful due to environmental considerations (**Table 2.3.3**). A large part of this is due to the proximal location to DFS, which will minimize construction of pipeline and new roads. However, it should be noted that while some scenarios will have a larger impact to the environment than others that each scenario is manageable and can be used for CCUS. No environmental parameter was given an increased weight in this analysis. However the considerations to protect groundwater may take precedence over surface parameters. Sub-surface models and other consideration within each scenario will affect this decision. For example, within scenario 1, CCUS may occur in any one of 4 reservoirs or a combination of them. In all cases, the deepest reservoir would pose the lowest risk to groundwater resources. The location with the lowest risk in regards to scenarios and groundwater shift with depth. The surface parameters may also change in the course of this study. New

surveys will be required as site selection is narrowed down, which could change any of the results presented above.

While the NETL documentation, specifically the NETL BMP manual, provided significant instruction and guidance to this environmental assessment, there are improvements that can be made to make future assessments more clear. The environmental assessment was required as part of subtask 3.1 for the project; however, the NETL BMP manual never specifies what this should include. Instead, section 3.0 site screening provides a sweep of topics that should be considered. Some of these considerations fall under different subtasks that are clearly not part of the environmental assessment. The BMP document does specify that research of local considerations must be completed to better guide each project's specific considerations. Local NEPA documents are the most comprehensive way to access this information. It would be beneficial for a more powerful search tool on the DOE to find similar NEPA documents. This includes NEPA document near the AOR and documents related to CCUS project throughout the US. The more comprehensive the database was, including more departments, the better. To clarify these recommendations, a more specific section to the environmental assessment in the BMP manual as well as a comprehensive database with NEPA documents and a powerful search tool would be beneficial to future projects.

Table 2.3.3 Final rankings of an environmental assessment for surrounding Dry Fork Station near Gillette, WY. Lower numbers represent a higher rank or less of an environmental impact for each consideration.

Scenarios	**1**	**2**	**3**	**4**	**5**
Threatened Species	1	2	3	2	2
Migratory Birds	2	1	3	2	4
Wetlands & Streams	1	4	2	2	3
Groundwater	3	4	5	1	2
Air Quality	1	2	2	2	2
Protected Areas	1	1	1	1	1
Cultural Resources	1	2	2	2	2
Population Centers	2	3	2	2	1
Topography	1	2	3	3	3
Migration Corridors	1	2	2	2	2
Total	**14**	**22**	**23**	**18**	**21**

Section 2.3 References

Blondes, M.S. Gans, KD. Rowan, E.L. Thordsen, J.J. Reidy, M.E. Engle, M.A. Kharaka, Y.K. Thomas, B. (2016). U.S. Geological Survey national produced waters geochemical database. https://energy.usgs.gov/EnvironmentalAspects/EnvironmentalAspectsofEnergyProductionandUse/ProducedWaters.aspx#3822349-data. Accessed: 8/1/2017.

Cornell (2017). The Cornell lab of ornithology.

http://www.birds.cornell.edu/Page.aspx?pid=1478. Accessed: 8/1/2017.

ECOS (2017). Environmental conservation online system. https://ecos.fws.gov/ecp/.

Accessed: 8/1/2017.

GDI (2000). Powder River Basin Geological Framework.

Pocewicz, A. W.A. Estes Zumpf, M.D. Andersen, H.E. Copeland, D.A. Keinath, H.R. Griscom (2013). Modeling the distribution of migratory bird stopovers to inform landscape-scale siting of wind development. PLoS ONE 8 (10): e75363

NETL (2013). Site screening, selection, and initial characterization for storage of CO_2 in deep geologic formations. https://www.netl.doe.gov/File%20Library/Research/Carbon-Storage/Project-Portfolio/BPM-SiteScreening.pdf. Accessed: 5/23/2017.

USCB (2016). United States Census Bureau quick facts. https://www.census.gov/quickfacts. Accesses: 8/08/2017.

USDA-NRCS (2016). Soil Survey Geographic (SSURGO) for Wyoming.

USEPA (2017). Facility level information on greenhouse gasses tool (FLIGHT). https://ghgdata.epa.gov. Accessed: 8/01/2017.

USEPA (2002). Federal Water Pollution Control Act. https://www.epw.senate.gov/water.pdf. Accessed: 5/23/2017.

USFWS (2017a). Species List, consultation code: 06E13000-2017-SLI-0268.

USFWS (2017b). Big game. https://wgfd.wyo.gov/Wildlife-in-Wyoming/Geospatial-Data/Big-Game-GIS-Data. Accessed: 8/1//2017.

USFWS (2016). FWS critical habitat for threatened and endangered species dataset. https://catalog.data.gov/dataset/fws-critical-habitat-for-threatened-and-endangered-species-datasetf6b00. Accessed: 8/1/2017.

USFWS (2012). Area of influence ranges for 18 critical species in Wyoming. http://www.fws.gov/Wyominges/Pages/WYES_GISdata.html. Accessed: 8/1//2017.

USFWS (2009). A system for mapping riparian areas in the western United States. http://www.fws.gov/wetlands/data/Data-Download. Accessed: 8/1//2017.

USGS (2009). Digital elevation model for Wyoming 10 meter. http://viewer.nationalmap.gov/viewer. Accessed: 8/1//2017.

WDEQ (2017). Wise view and oil and gas production (OGER) database. http://qrywiz.wyo.gov/. Accessed: 8/1//2017.

WOGCC (2017). Wyoming oil and gas commission database. http://wogcc.state.wy.us/legacywogcce.cfm. Accessed: 8/1//2017.

WRDS (2009). Landslides per county basis for Wyoming. http://www.wrds.uwyo.edu/wrds/wsgs/hazards/landslides/county/county.html. Accessed: 8/1//2017.

Section 2.4: Community and Public Outreach Assessment

Steve Carpenter[1], Wesley Peck[2], Dan Daly[2], and Scott Quillinan[3]
[1]Enhanced Oil Recovery Institute, Casper WY
[2]Environmental & Energy Research Center, Grand Forks, ND
[3]Center for Economic Geology Research, University of Wyoming, Laramie, WY

Abstract
This document lays out a plan for developing and implementing public engagement associated with the development of a major long-term CO_2 storage project from coal-based power facilities in Campbell County, Wyoming. The multi-step plan includes formation of a strategy based on the region's societal profile, geographic scale, outreach audiences, and resources to provide outreach for future CCS investigations and projects. The project team in collaboration with an outreach advisory group will execute the plan. Outreach activities under Phase I of CarbonSAFE will focus on laying the foundation for active public engagement.

Introduction
Public and project stakeholders have diverse perspectives and have varying levels of influence and control with respect to project success. Understanding the nuances of stakeholder opinion, power, and perspective is necessary for the development of a stakeholder engagement strategy that can reduce program/project risk, while creating buy-in and understanding about program/project objectives. Lack of attention to stakeholder engagement can increase project risk and create an environment in which public action can be at cross-purposes with project goals. To ensure the long-term success of the Dry Fork Station CarbonSAFE project, a strong stakeholder engagement plan will be implemented.

Approach
The approach will be to develop a plan informed by publicly available information on demographics, economics and social character, interviews with select stakeholders, and the experience embodied in the project outreach team and the project coordination team and by drawing on the resources available from the broader CCS/CCUS outreach community. The focus of outreach plan will be engagement with audiences primarily in the Campbell county area, but the plan will be crafted to ensure engagement with key audience segments at the State level.

The plan begins with designating a formal outreach team and an outreach advisory group. The outreach advisory group is comprised of representatives from key project partners and is intended to provide guidance and feedback to the project outreach team. The next step is to establish the goal and vision for the outreach effort. Once a goal has been determined, a strategy will be developed to meet that goal. The strategy will reflect the setting, project considerations, audience character, and methods (e.g., open houses, fact sheets, web content). Next, the strategy is implemented and the methods applied. Lastly,

feedback from the stakeholders is assessed and adjustments to the strategy are made if necessary.

The steps of the plan are as follows:

1) Form the project outreach team and the outreach advisory group.
2) Determine the goal of the outreach efforts.
3) Form a strategy to meet the goal.
4) Implement strategy.
5) Evaluate feedback and refine strategy.

Plan Outline

Step 1: Form Outreach Team and Advisory Group

The Advisory Board shall be made up of the seven members listed in the table below. The Advisory Board shall provide oversight and set the strategic direction for the Coordination Team.

Table 2.4.1

Entity	**Suggested Professionals**	**Core Outreach Team**	**Project Coordination Team**	**Outreach Advisory Board**
Center for Economic Geology Research	Scott Quillinan and Kipp Coddington	**X**	**X**	**X**
Basin Electric Power Cooperative	TBD		**X**	**X**
Enhanced Oil Recovery Institute	Steve Carpenter	**X**	**X**	**X**
UW Center for Energy & Environmental Public Policy	Kipp Coddington	**X**	**X**	**X**
Wyoming Infrastructure Authority	Brian Jefferies		**X**	**X**
Wyoming Governor's Office	Matt Fry		**X**	**X**
Wyoming ENDOW	Jeremiah Reiman		**X**	**X**
Advanced Resources Institute	George Koperna	**X**	**X**	

Energy & Environmental Research Center	Nick Bosshart, Wes Peck, Charlie Gorecki, Dan Daly	**X**	**X**	
Kohlberg Kravis Roberts & Co.	TBD		**X**	
Locality Representative	TBD		**X**	
University of Wyoming, College of Law	TBD		**X**	

Step 2: Determine Goal

This step includes identifying and defining the goals and objectives of the stakeholder engagement process along with determining the methods and tools to be used to collect data from stakeholders.

Step 3: Form Strategy

This step includes social characterization based on available information sources as well as the initiation of a group workshop with the project team and any other key participants who can provide insights into potential stakeholders. The workshop will include several exercises designed to define stakeholder groups, discuss stakeholder concerns and/or ideas, rank stakeholders by influence and importance, and gather input and ideas from the project team about stakeholder strategies. As part of the workshop, a SWOT (Strengths, Weaknesses, Opportunities, Threats) assessment will be conducted which will help to identity gaps in both identification of stakeholders and any relationships that may exist.

Subsequent to this workshop, a communication plan will be developed for the project that will contain a central narrative and methods (e.g., open houses, fact sheets, web content) matched to audiences.

Specific activities to be completed may include:

- Facilitate workshop with project team
- Determine potential stakeholders
- Discuss potential stakeholder issues, opportunities, and challenges
- Conduct pre-feasibility SWOT
- Select methods for data dissemination and collection
- Create feedback and data collection systems
- Define what handout materials and electronic media are needed
- Determine gaps and recommendations

Step 4: Implement

This step is the actual implementation of the public outreach and stakeholder engagement strategy. Specific implementation methods will be defined in the previous step 3. A tracking capability will be implemented that will cover actions such as media releases and articles, contact with stakeholders, attendance at activities, inquiries, and materials distribution as a basis for assessing level of information distribution and stakeholder coverage and response. Specific activities may include:

- Hold town hall event(s)
- Conduct observations at events, meetings, and workshops
- Conduct focus groups and surveys

Step 5: Evaluate Feedback and Refine:

As the project is implemented, events will provide information about the project, including the suitability of it goals, objectives, and methods. Feedback may be enhanced through use of focus groups and interviews with stakeholders. It is expected that the data will allow for the further understanding and development of both the stakeholders engagement and refinement of the strategy to ensure project success. The process will also allow for an evaluation of existing relationships and reveal if groups are being overlooked. This task includes analysis of data collected from participants (e.g., issues, risk management, financial mechanisms, public policy needs, knowledge sharing needs, etc.). This task will also evaluate the stakeholder inputs, the outreach strategy, and effectiveness. Specific activities may include:

- Plot stakeholders influence against level of engagement
- Create stakeholder maps (type and location)
- Analyze SWOT compared to project objectives

Evaluation of the overall feedback will determine if any refinements to the strategy or additional data collection needs exist. This is the iterative aspect of the process and may occur as necessary.

Section 2.5: Regional Non-technical Suitability Briefs

Kipp Coddington
Director, Energy Policy & Economics
Center for Economic Geology Research
School of Energy Resources, University of Wyoming
1020 E. Lewis Street, Energy Innovation Center
Laramie, WY 82071

POLITICAL SUITABILITY BRIEF

Project team members cannot speak for any third party, to include any politician, politician's staff or political body. This brief is thus based on the Project's team observations and views, supported where indicated by materials or statements in the public domain.

Wyoming's federal delegation – specifically the two U.S. Senators, John Barrasso (R-WY) and Mike Enzi (R-WY) – support CCS. Indeed, earlier this year, Sen. Barrasso co-sponsored the FUTURE ACT, a bipartisan bill to encourage technological innovation in CCS. Over the past year and at the invitation of Sen. Barrasso, several individuals from Wyoming, including Kipp Coddington, a co-PI here, testified on various related matters before the U.S. Senate Committee on Environment & Public Works, which Sen. Barrasso chairs.

Project team members have met with many of the Wyoming-based representatives of the federal delegation, all of who have signaled general support for CCS and specific support for the CarbonSAFE program.

At the state level, the Project enjoys general and broad support from the legislative and executive branches of the Wyoming government. With respect to the legislative branch, about a decade ago the Wyoming State Legislature enacted a suite of laws related to CCS and CCS-related projects. Specifically, Wyoming law:

- ✓ Specifies who owns the pore space (Wyo. Stat. § 34-1-152 (2016));
- ✓ Establishes permitting procedures and requirements for CCS sites, including permits for time-limited research (Wyo. Stat. § 35-11-313);
- ✓ Provides a mechanism for post-closure MRV via a trust fund approach (Wyo. Stat. § 35-11-318);
- ✓ Provides a mechanism for unitization of storage interests (Wyo. Stat. § 35-11-315);
- ✓ Specifies that the injector, not the owner of pore space, is generally liable (Wyo. Stat. § 34-1-513);

- ✓ Clarifies that vis-à-vis storage rights, production rights are dominant but cannot interfere with storage (Wyo. Stat. § 30-5-501); and

- ✓ Provides a certification procedure for CO_2 incidentally stored during EOR (Wyo. Stat. § 30-5-502).

On June 29, 2017, the Joint Minerals, Business and Economic Development Interim Committee of the Wyoming State Legislature provided the Project team with a letter of support for its continued participation in the CarbonSAFE program.[4]

A couple of months ago, representatives of the Project team met informally with several state representatives and senators who represent the Gillette area. That meeting was positive.

With respect to the executive branch, the Project team has received letters of support from the Office of Governor Mead and the Wyoming Department of Environmental Quality. Last year, the team also met informally with staff of the Wyoming Public Service Commission.

The Project team has not yet other met with local politicians or citizens in the Gillette area, to include Campbell County. We anticipate local support for various anecdotal reasons, but that thesis will only be tested when the outreach plan is officially implemented during Phase 2.

[4] http://www.wyoleg.gov/InterimCommittee/2017/09-0629APPENDIXF-2.pdf.

SOCIAL SUITABILITY BRIEF

Politically, as discussed above, the State of Wyoming could be fairly described as broadly in favor of CCS and CCS-related projects. This sentiment is also shared by several major industries operating within the state, to include the coal industry. Coal companies such as Peabody Energy and Cloud Peak Energy, for example, have issued public statements in support of CCS over the years. Nationally, it is fair to conclude that the coal industry has taken the position that CCS is necessary to manage its GHG impacts – a sentiment that long ago trickled down into and took root in Wyoming, too.

A regional NGO is opposed to CCS on various technical and policy grounds.[5]

Though the Project area is sparsely populated to the north, there are several population centers south of DFS. The largest is Gillette, with a population of 32,398, located 8 miles south of DFS (USCB, 2016). Gillette is also the county seat of Campbell County. Small unincorporated towns include Antelope Valley-Crestview (1,658 people), and Sleepy Hollow (1,308 people), which are 5 miles southeast of Gillette. Scenario 5 is located the furthest from a population center (19 miles), while scenarios 1, 3, and 4 are between 2 and 9 miles away. Scenario 1 and 2 are the closest to Gillette at around 2 miles.

Calling itself the "Energy Capital of the Nation," Gillette is centrally located in the PRB, which produces vast quantities of American coal and oil. As of 2000, the median income for a household in the city was $69,581, and the median income for a family was $78,377. Males had a median income of $41,131 versus $22,717 for females. The per capita income for the city was $18,749. About 5.7% of families and 7.9% of the population were below the poverty line, including 6.2% of those under age 18 and 14.1% of those age 65 and over.[6]

A 1Q 2018 City of Gillette Development Summary prepared by the City of Gillette Planning Division reflects general stabilized economic conditions.[7] In recent years, Gillette has weathered adverse economic conditions, mirroring in part recent challenges facing the coal industry. It is likely that local economic developers may view the Project as leading to potential economic activity down the road; again, however, this thesis remains untested.

Updated as of 4Q 2017, the following table indicates the major industry segments providing employment in Campbell County. The table confirms that the area is home to a talented workforce for projects of this type, and that the citizenry generally are acquainted with energy production activities.[8]

---

[5] http://www.worc.org/media/Too_Good_to_Be_True_Report.pdf.

[6] https://en.wikipedia.org/wiki/Gillette,_Wyoming.

[7] https://www.gillettewy.gov/home/showdocument?id=38395.

[8] https://www.wyomingatwork.com/vosnet/lmi/profiles/profileDetails.aspx?enc=Elzv7W1H4bwmL+k+/LJ5/fdexwlKhtyEFubTiyvqsXDmUKob5BM0i+eO5GozGAGHfC70uvcdLMfRKUYTY/ke2VqYZpfcexUKzD6s6LrscKU=.

Table 2.5.1

Rank	Industry Sector	Number of Establishments	Number of Employees
1	Mining	173	6,032
2	Retail Trade	161	2,302
3	Health Care and Social Assistance	174	2,231
4	Accommodation and Food Services	121	2,179
5	Construction	227	1,851
6	Public Administration	32	1,432
7	Wholesale Trade	136	1,394
8	Transportation and Warehousing	86	856
9	Other Services, Ex. Public Admin	143	834
10	Administrative and Waste Services	86	786

Chapter III: Geologic Evaluation

Section 3.1: Development of Borehole Catalog and Risk Assessment

Tom Moore[a], Charles Nye[a], Scott Quillinan[a], and Sitian Xiong[a&b]

[a] *Center for Economic Geology Research, School of Energy Resources, University of Wyoming*

[b] *Geographic Information Science for Development and Environment, Clark University*

Abstract

Wyoming's Powder River Basin (PRB) has experienced over a century of oil and gas exploration. Currently the Powder River Basin is under investigation for geologic storage of commercial quantities (50+ million tonnes) of carbon dioxide (CO_2). With this study, we evaluate the risk associated with geologic storage of anthropogenic CO_2 posed by existing oil and gas wells in this well-explored geologic basin.

Previously drilled wells that penetrate confining lithology introduce risk to CO_2 geologic storage projects. For this study, we modified an existing methodology (Nelson, 2013) to determine the risk these wells pose to a Carbon Capture, Utilization and Storage (CCUS) project in the pre-feasibility phase. Factors of risk considered independently in this study include well density, age, permanent plug and abandonment (P&A) date, and topography. The P&A date and topography are then combined to identify wells and geographic areas with elevated risk.

This risk assessment results in a five part risk assessment, which is used to compare the location of carbon storage and the potential risk wells pose in the area. The results of this project leverage data to help to inform CCUS site selection and minimize the risk of CO_2 migration out of the target reservoir.

Introduction

There is growing political and social pressure to reduce CO_2 emissions. The global average atmospheric CO_2 concentration has grown to 402.9 ±0.1 ppm from ~315 ppm in 1958 (Blunden and Arndt, 2017), the highest in recorded history. To reduce CO_2 concentrations, a multi-faceted solution spanning multiple disciplines will be needed. One such solution is Carbon Capture Utilization and Storage (CCUS) (Edenhofer, 2011). CCUS captures and compresses anthropogenic CO_2 from industrial sources, such as coal-fired power plants, and then injects the supercritical CO_2 into deep saline formations for permanent storage. Successful CCUS projects have injected up to 1 Mt CO_2/year for a total of 20 Mt of CO_2 as of 2008 (Michael et al., 2010). More recently, 15 large-scale CCUS projects have been implemented worldwide, with a capture capacity of 30 Mt/year (Global C.C.S., 2016). The International Energy Agency (2014), estimated CCUS could provide 14% of the needed reductions in global CO_2 emissions by 2050 for the estimated threshold to hold the global temperature rise below 2° C compared to pre-industrial levels.

Reservoirs considered for CCUS must be well understood to manage the risks of CO_2 escaping the target reservoir (USEPA, 2010). EPA regulations ensure that every reservoir legally selected for CCUS is either proven saline (>10,000 ppm TDS) or exempt after consideration of other factors by the EPA. While these regulations ensure the target reservoir is not suitable for drinking water or another beneficial use, the potential remains for migration of the CO_2 out of the target reservoir affecting other geologic reservoirs or the land-surface (Loizzo et al., 2011; Choi et al., 2013; Nelson, 2013). Migration of the CO_2 plume out of the target reservoir(s) is prevented by layers of rock with low permeability called confining layers (seals). CCUS projects must consider any natural or anthropogenic weakness of the seals where CO_2 could migrate (USEPA, 2010). Migration may occur through natural paths in the confining strata, diffusion, or as considered here, through wellbores.

Variables including the density of penetrating wells, age of wells, date the wells were permanently plugged and abandoned (P&A), and topography surrounding the well have been linked with an increased risk of leakage (Loizzo et al., 2011; Watson et al., 2009). Well density is considered for two reasons: 1) cross flow between nearby wells has been linked to CO_2 leakage and 2) areas with more wells are more likely to have a leak because more wells are present (Watson et al., 2009; Getzlaf et al., 2013). Well age is considered on the basis that older wells were drilled with less advanced techniques; however, the direct effect of this on risk has not been demonstrated due to a lack of data (Watson et al., 2009). The P&A date of wells has been associated with an increase in risk due to common practices of different time periods (Watson et al., 2009). Over time the regulations and common practices of plugging wells has improved. Most significantly, cement, and the quality of the techniques to lay the cement, have improved, providing more competent seals (Choi et al., 2013). Surface topography affects the hydrostatic pressure near the land surface, thus increasing the risk (Watson et al., 2009). The severity of this risk is compounded if the denser than air CO_2 reaches the surface and pools in a topographic depressions (Chow et al., 2009). Chow et al. (2009) showed that atmospheric mixing is inadequate in depressions with a slope greater than 10 degrees, and wells within 100 meters of such depressions can accumulate CO_2 if failure occurs. Such failures are rare but should be considered due to their high consequences. Comparing the location of wells with older P&A dates and wells confined by a topographic depression can be used to further identify wells of greater risk (Nelson, 2013).

We have selected the Powder River Basin (PRB) with an estimated 196 GT of storage capacity to further investigate the potential for a large scale CCUS project (NETL, 2010). In this area, we define four variables that describe the risk pre-existing wells pose to a CCUS project: 1) well density, 2) age, 3) P&A date, and 4) topography. We then combine two of these variables, the P&A date and the topography, for a practical assessment and discussion of at risk wells in the area of review (AOR).

Methods

Area of Review. We first selected the AOR based on the Dry Fork Power Station (DFS), which emits approximately 3 million tonnes of CO_2 per year (USEPA, 2017) and is the largest CO_2 source in the PRB **(Figure 3.1.1)**. Analysis was completed in a ten-mile radius surrounding DFS, and a six-mile radius was included as a reference, representing the maximum pressure plume expected in a homogeneous sandstone. Previous studies

have identified the Mesa-Verde, Muddy, Sundance, and Minnelusa formations as potential reservoirs for CCUS (Craddock et al., 2012). We focus on the seals overlying each of these formations: the Lewis (2,484-5,060 feet below land surface (fbs)), Mowry (6,295-8,978 fbs), Morrison (6,905-9,070 fbs), and Opeche (8,135-10,268 fbs) confining layers, respectively, and the wells that penetrate them.

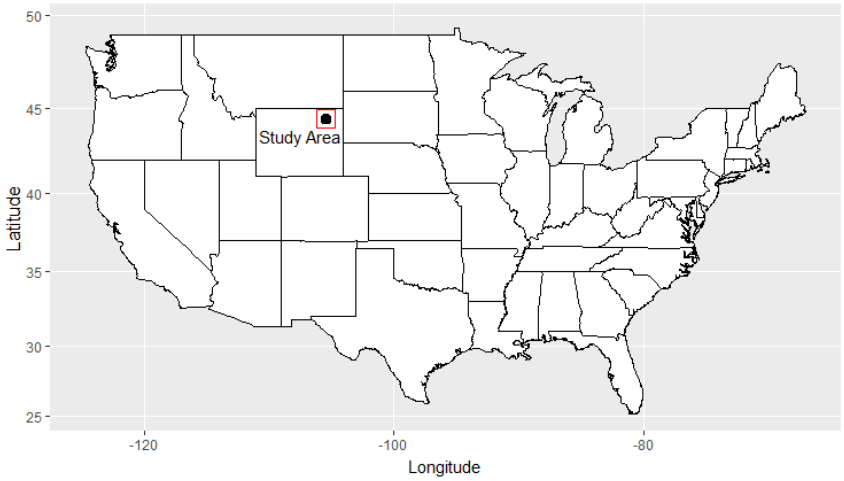

Figure 3.1.1 Map of the United States, showing where the study area lies in the northeast corner of Wyoming.

Well Analysis. All queries, summary statistics, and spatial analysis were run on the dataset using R (R Core Team, 2016) and the packages ggplot2, ggmap, and rgdal (Wickham, 2009; Kahle and Wickham, 2013; Bivand et al., 2017). The first step, to catalog wells in the AOR, was completed by downloading well data (coordinates, spud date, P&A date, depth (ft), and bottom formation) from the Wyoming Oil and Gas Commission (WOGCC) legacy database and querying wells within a ten mile radius of DFS (WOGCC, 2017). These data were further queried to select wells that penetrate the Lewis, Mowry, Morrison, and Opeche confining layers. Analysis of these wells was performed in four groups, one for each confining layer. Each group contained wells that penetrated that layer.

These data were first used to create density maps per township section (1 mile x 1 mile) identifying the number of wells penetrating the confining layers. Next, the well age and P&A dates were compared on the basis of the frequency of wells through time. The P&A date was further analyzed on the basis of pre-existing methodology to define each well's "leakage risk" with respect to regulatory rules of Nelson, 2013. Nelson, 2013 defined the risk of P&A practices and regulations through an in-depth study in Wyoming (**Table 3.1.1**). Regulations governing the drilling, completion, and closure of wells have become more rigorous over time; therefore, years that are more recent are given a lower leakage risk. Active and shut-in wells are actively monitored for potential leaks, and therefore given a "Leakage Risk" value of "0".

Table 3.1.1 Risk levels assigned to the different regulatory requirements for oil and gas plugging in Wyoming (from: Nelson, 2013).

Dates Abandoned	Responsible regulatory body in Wyoming	Written rule?	Cement used?	Cementing standards	Leakage Risk
1883-1933	No regulatory oversight	No	Unknown	● No written cementing standard. ● Stumps, logs, and animal carcasses sometimes used to plug holes. ● Mud laden fluid used for plugging	6
1934-1951	State Mineral Supervisor	Yes	Most state agencies require cement plugs	Plug placement and length not defined, but operators required to report location and depth of plugs in the Subsequent Report of Abandonment	5
1952-1962	WOGCC	No	Probably, however, no regulation to prohibit plugging by other materials	American Petroleum Institute published cementing standards and classes of cementing	5
1963-1976	WOGCC	Yes	Likely, regulation states that no other materials other than those normally involved in plugging may be used	Cementing circulation method for plugging in widespread use	4
1977-1982	WOGCC	Yes	Yes	● Plugged in a manner to protect drinking water sources. ● Displacement method of cementing common practice, which is still used today. ● Cementing records from third party must be kept and transmitted to Supervisor.	3
1983-1998	WOGCC	Yes	Yes	Specific well plugging instructions including length and intervals	2
1999-Present	WOGCC	Yes	Yes	Job log and cement verification report required from plugging contractor	1

Topography was also used to define risk based on methodology from Nelson, 2013. The methodology was slightly modified to simplify the risk assessment from "7" levels to "6." This removed the unused super-category, which defined all topographically confined wells that were further categorized by the percent of area in a 100-meter buffer. Wells were either classified as not affected by a depression "unconfined," directly in a depression, or within 100 meters of a depression, both of which are "confined." A low point surrounded by at least two slopes greater than 10 degrees (Chow et al., 2009) defined depressions. Wells were assigned a "Risk" of "1" to "6," based on the percent of area in the 100-meter buffer surrounding the well that was part of a depression and then compared to each other **(Table 3.1.2)**. Finally, the risks defined by the regulatory period and topography were combined into a single map to visualize both (combined) risks side-by-side.

Table 3.1.2 Risk associated with wells based on whether the wells are in or near a topographic depression with a slope greater than 10° and the percent of a 100 meter buffer (potential CO_2 plume) surrounding the well that is in or near a depression.

Well In Depression		Wells Near Depression	
Area in buffer (%)	Risk	Area in buffer (%)	Risk
>75%	6	>75%	5
50-75%	5	50-75%	4
25-50%	4	25-50%	3
0-25%	2	0-25%	2
unconfined	1	unconfined	1

Results

Density. The well density in the AOR is highest in the shallowest confining layer, the Lewis shale. The density analysis found 69% of the sections have less than four wells penetrating the Lewis; however, three sections exist with 10-25 wells penetrating the Lewis (**Figure 3.1.2**). Two of these wells are outside the six-mile buffer. Each subsequent seal has a lower density of wells per section penetrating it, indicating less risk with increased depth (**Figure 3.1.2**). This trend is most significant to the west, where few wells penetrate the Opeche seal. The density analysis shows 58% of sections have no wells penetrating the Opeche, and 85% of sections have less than four wells per section. Only one section contains more than ten wells that penetrate the Opeche. This section is located on the border of the ten-mile buffer to the east. For each seal, the highest concentrations of wells exist outside of the six-mile buffer.

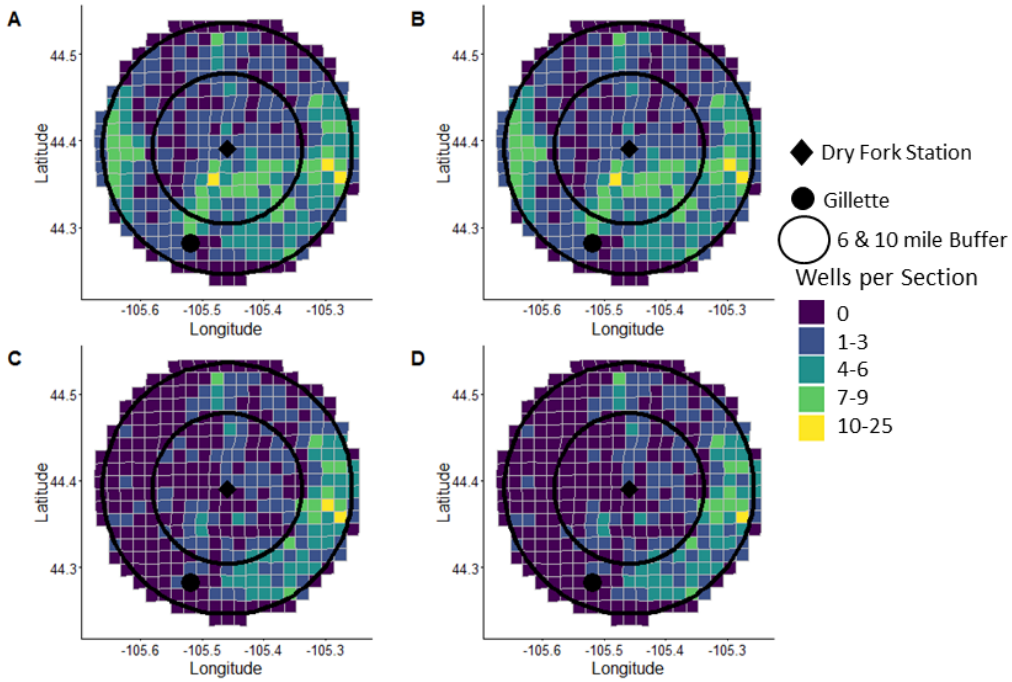

Figure 3.1.2 The density of wells per township section (1 mile x 1 mile) that penetrate the A) Lewis, B) Mowry, C) Morrison, and D) Opeche confining layers surrounding Dry Fork Station near Gillette, WY.

Well Age and Plug Date. Well development surrounding DFS began circa 1937 but rapidly developed in the 1970's, drilling of wells (n=909) that penetrate the Lewis shale (**Figure 3.1.3**). There are twenty wells with unknown ages, which pose an unknown risk. Thus, they are treated as pre-1933 wells as a precaution. Well development penetrating the Morrison and Mowry began later than the Lewis and Mowry, peaking in the 1980's as opposed to the 1970's.

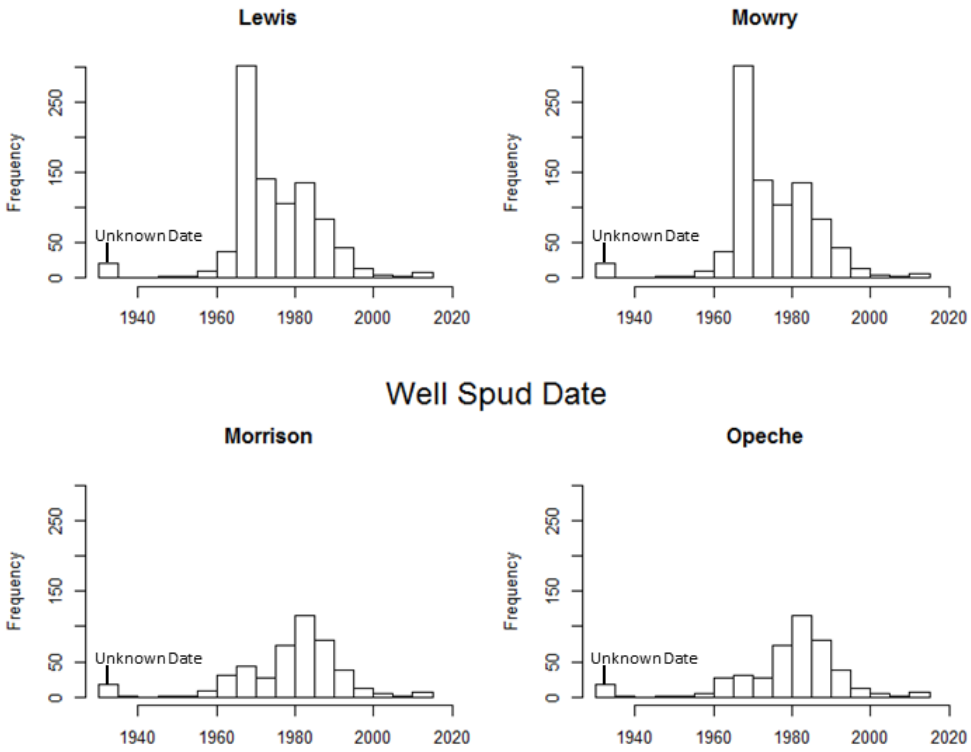

Figure 3.1.3 Distribution of well age, in five-year intervals, surrounding Dry Fork Station, including wells with no known spud date. Unknown spud dates are treated as pre-1933 wells.

Figure 4 illustrates the frequency of P&A dates in different regulatory climates for each seal. A number of wells (n=767) have been P&A in the AOR. Four wells were plugged between 1883 and 1933 when there was no regulatory oversight. However, 98% of wells (n=748) were plugged and abandoned after 1962 when cement was widely used. The time periods when wells were plugged does not shift between the confining layers; however, fewer abandoned wells exist with each subsequent seal at depth. Wells with higher risk levels should be prioritized for further assessment.

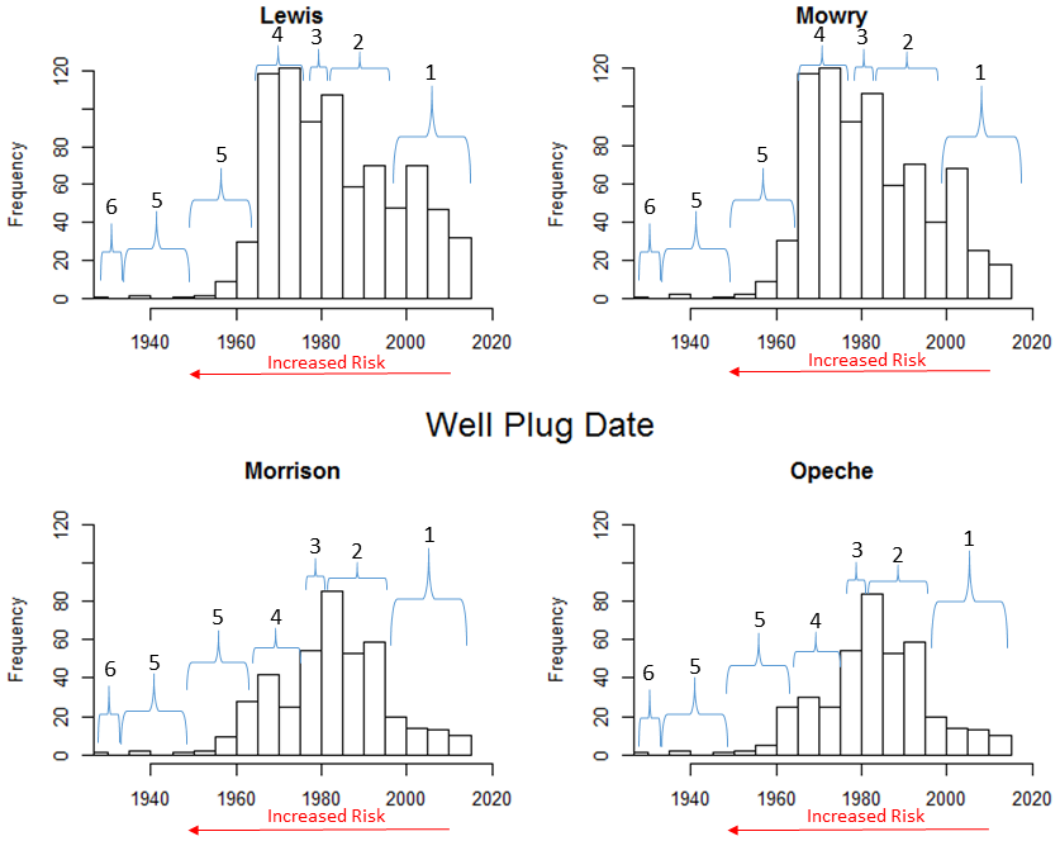

Figure 3.1.4 Histogram of the date wells were plugged and abandoned for each seal being studied and the risk associated with different regulatory periods (**Table 1**).

Topography. About half (n=472), or 52%, of the wells are topographically unconfined, and were given the lowest risk value of "1." The remainder of the wells (n=381) are within a 100 meter radius of a depression, and fifty-six wells are directly in a depression. A single well was defined with the highest risk value "6," and twenty-one wells were classified as having a risk of a "5" **(Table 3.1.3)**. Each subsequent risk value, representing less risk, has more wells in its category. When reviewing the topographically confined wells, 65% (n=282) were defined the lowest risk value "2." Higher risk wells should be prioritized for further assessment.

Table 3.1.3 Number of wells and "associated risk" (Nelson, 2013) on the basis of local topography.

Well In Depression			Wells Near Depression		
Area in buffer (%)	**Risk**	**# Wells**	**Area in buffer (%)**	**Risk**	**# Wells**
>75%	6	1	**>75%**	5	1
50-75%	5	20	**50-75%**	4	28

25-50%	4	24	**25-50%**	3	81
0-25%	2	11	**0-25%**	2	271
Total Confined Wells:	56		**Total Confined Wells:**	381	

Combining Risk Factors. Figure 5 displays the location of P&A wells attributed with topographic risk (**Table 3.1.3**) and plugging regulations (**Table 3.1.1**). The single well with a topographic risk of "6" was plugged in 1976, Leakage Risk "4", and is approximately eight miles northeast of DFS. Nine wells with a topographic risk of "5" were plugged between 1962 and 1976; the closest is located one mile northeast of DFS. Four wells were plugged between 1933 and 1951 and were assigned a topographic risk of "4." One is located approximately seven miles west of DFS, and the other three are nine miles west of DFS. This information can be further queried to better understand the risks and the needed well plug tests associated with CCUS surrounding DFS.

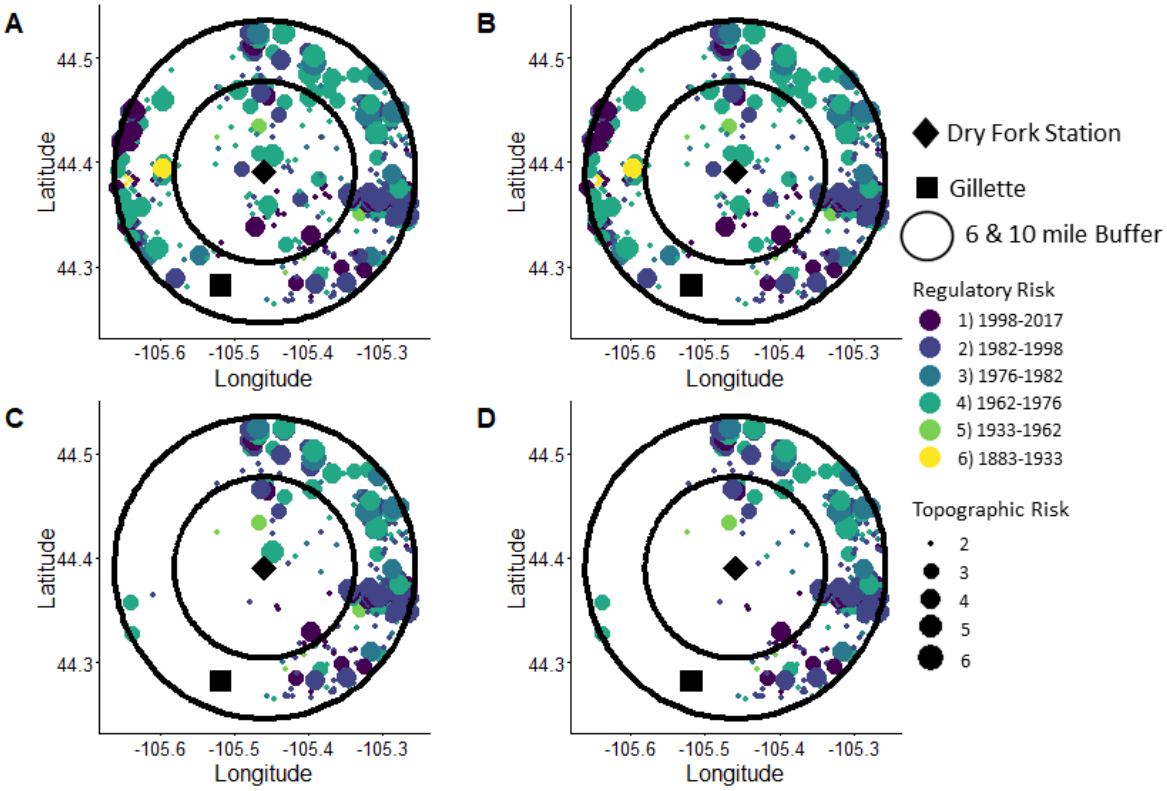

Figure 3.1.5 The risk associated with each plugged and abandoned well within ten miles of Dry Fork Station. The size of the point indicates the risk associated with topographic depressions, "6" being the riskiest. The color indicates the plug regulations of the time period, with yellow having the highest risk. (**Table 3.1.1**).

Discussion

The PRB has the potential to store an estimated 196 GT of CO_2 (NETL, 2010). The project considered here aims to store an estimated 50 million tonnes of CO_2 in a 25-year timeframe; however, the risks of CCUS must be fully understood before any storage can occur (USEPA, 2010). To facilitate a better understanding of this risk, the present study has examined the density of wells, the age of wells, the P&A date, and near-well topography (USEPA, 2010; Nelson, 2013). By defining these variables in the area surrounding DFS, we can examine risk in terms of the spatial extent surrounding DFS and in regards to four confining layers. By defining these variables, project managers will have a better understanding of a) the risks these wells pose, b) how risk changes across the landscape, and c) how risk changes with the depth of the reservoir. Finally, recommendations are made for how this research can be applied and for future research that can better define this risk.

To examine risk, we first consider the Lewis seal for a conservative estimate. The Lewis, being the shallowest seal, includes every well in this analysis, because a well penetrating a deeper formation must first penetrate the Lewis. This is important when interpreting the results of this study, because when a formation is discussed in terms of risk that risk also applies to the confining layer above it. It would be advantageous to select an area with a low well density to minimize both risk and the costs of monitoring and testing wells within the pressure plume extent. In a scenario with a pressure plume under a one-mile radius, there are several sections close to DFS with no wells present, particularly to the west. However, when considering lager plumes, the area to the northwest of DFS has the largest area of sections with 0-3 wells. To better quantify risk to the west of DFS, the P&A date and topography can be examined. Looking once again at the Lewis for conservative estimates, the area to the west has less P&A wells, particularly to the southwest. However, active wells do exist there at a high density. The area to the west of DFS also has high-risk wells with P&A dates between 1833 and 1933. The closest of these wells, about seven miles west of DFS, also has a topographic risk of "4." Despite these wells, the lower density of wells in this area are appealing to a CCUS project.

Risk also depends on the confining layer that has been penetrated. This study only considers wells to determine risk, and based on this assumption, we found less risk associated with deeper formations. Not only are there fewer wells penetrating the deeper formations (Morrison and Opeche), but these wells are less dense, the spud dates are on average more recent, the P&A dates are more recent, and the topographic risks are lower. Given this information, more locations are available for a low risk CCUS site below the Morrison and Opeche seals. The area directly west of DFS is mostly composed of sections with zero wells, and the highest P&A risk wells do not penetrate deeper than the Mowry, making this area appealing. However, the area in the six-mile buffer surrounding DFS only has four sections with 4-6 wells, and any site within this area would be manageable.

While this risk assessment has been used to guide site selection for a CCUS project, the same method can be used to prioritize monitoring of at risk wells and required integrity tests (NETL, 2013; Choi et al., 2013). Air quality tests can be used to detect emissions and possible well leakage (Field et al., 2015), which can be followed by more specific tests of soil surrounding wells (Boothroyd et al., 2016). These leakage tests can be used

to ensure a safe CCUS project, to better understand variables that affect the risk of leakage, and can be applied to monitoring methane leaks in natural gas plays. Among the tasks for future studies is to ground-truth the coordinates of the wells to ensure the reported coordinates are correct (Nelson, 2013). These tasks could also include an investigation of the company (licensee) who drilled the well, surface-casing depth, total depth, well deviation, well type, oil price, and low cement top or exposed casings to fully understand the risk each well presents (Watson et al., 2009).

Conclusion

This study examined the density of wells, age of wells, age of well plug, and topography to better understand the risk pre-existing wells pose to a CCUS project in the Powder River Basin. In doing so, this study has provided a way for researchers and managers to: 1) guide site selection in Phase II of the CCUS project; 2) systematically examine and test wells that pose a risk to a CCUS project; 3) better understand the condition of wells in the PRB; and 4) help establish a methodology to better examine the risk wells pose to CCUS project. Finally, this project offers the following guidance for further development of the project in the site-specific study:

- Well density is lowest northwest of DFS for the Lewis and Mowry and directly to the west for the Morrison and Opeche.
- Wells drilled into the deeper confining layers, the Morrison and Opeche, were drilled more recently and pose less risk.
- The most at risk wells, based on the P&A date, do not penetrate to the Morrison or Opeche.
- The area encompassed by the six miles buffer has a low topographic risk. This risk is lowest to the west of DFS when related to the Morrison and Opeche confining units.
- The least risk appears to be west of DFS within the six-mile buffer and below the Morrison or Opeche confining layers.

Section 3.1 References

Blunden, J., Arndt, D. S., 2017. State of the climate in 2016. Bull. Amer. Meteor. Soc., 98 (8), Si–S277, doi:10.1175/2017

Bivand, R., Keitt, T., Rowlingson, B., 2017. rgdal: Bindings for the geospatial data abstraction library. R package version 1.2-8. https://CRAN.R-project.org/package=rgdal

Boothroyd, I. M., Almond, S., Qassim, S. M., Worrall, F., Davies, R. J., 2016. Fugitive emissions of methane from abandoned, decommissioned oil and gas wells. Science of the Total Environment 547, 461-469.

Choi, Y.-S., Young, D., Nešić, S., Gray, L.G.S., 2013. Wellbore integrity and corrosion of carbonsteel in CO2 geologic storage environments: A literature review. International Journal of
Greenhouse Gas Control.

Chow, F.K., Granvold, P.W., Oldenburg, C.M., 2009. Modeling the effects of topography and wind on atmospheric dispersion of CO2 surface leakage at geologic carbon sequestration sites. Energy Procedia 1, 1925-1932.

Craddock, W.H., Drake R.M., Mars J.C., Merrill M.D., Warwick P.D., Blondes M.S., Gosai M.S., Freeman P.A., Cahan S.M., DeVera C.A., Lohr C.D., 2012. Geologic framework for the national assessment of Carbon dioxide storage resources- powder river basin, Wyoming, Montana, South Dakota, and Nebraska. US Department of the Interior, US Geological Survey.

Edenhofer, O., Pichs-Madruga, R., Sokona, Y., Seyboth, K., Matschoss, P., Kadner, S., Von Stechow, C., 2011. IPCC special report on renewable energy sources and climate change mitigation. Prepared By Working Group III of the Intergovernmental Panel on Climate Change, Cambridge University Press, Cambridge, UK.

Field, R.A., Soltis, J., McCarthy, M.C., Murphy, S., Montague, D.C., 2014. Influence of oil and gas field operations on spatial and temporal distributions of atmospheric non-methane hydrocarbons and their effect on ozone formation in winter. Atmospheric Chemistry and Physics.

Global, C. C. S., 2016. Institute. (2016, October). The global status of CCS.

Kahle, D., Wickham, H., 2013. ggmap: Spatial Visualization with ggplot2. The R. Journal 5(1), 144-161.

Lesti, M., Tiemeyer, C., Plank, J., 2013. CO2 stability of Portland cement based well cementing systems for use on carbon capture & storage (CCS) wells. Cement and Concrete Research 45, 45-54.

Loizzo, M., Akemu, O. A., Jammes, L., Desroches, J., Lombardi, S., Annunziatellis, A., 2011. Quantifying the risk of CO2 leakage through wellbores. SPE Drilling & Completion 26(3), 324-331.

Michael, K., Golab, A., Shulakova, V., Ennis-King, J., Allinson, G., Sharma, S., Aiken, T., 2010.
Geological storage of CO2 in saline aquifers—A review of the experience from existing storage operations. International Journal of Greenhouse Gas Control 4, 659-667.

Nelson, J. D. 2013., Assessment Tools for Assigning Leakage Risk to Individual Wells at a Geologic Sequestration Site in Wyoming. University of Wyoming.

NETL., 2010. Carbon Sequestration Atlas of the United States and Canada. Third Edition. https://www.netl.doe.gov/KMD/CDs/atlasIII/2010atlasIII.pdf Accessed: 10/2/2017.

USEPA., 2010. Federal requirements under the underground injection control (UIC) program for Carbon Dioxide (CO2) geologic sequestration (GS) wells; Final Rule, 40 CFR Parts 124,
144, 145, et al. Environmental Protection Agency

USEPA., 2017. Facility level information on greenhouse gasses tool (FLIGHT). https://ghgdata.epa.gov. Accessed: 8/01/2017.

Watson, T. L., Bachu, S., 2009. Evaluation of the potential for gas and CO2 leakage along wellbores. SPE Drilling & Completion 24(01), 115-126.

Wickham, H., 2009. ggplot2: Elegant Graphics for Data Analysis. Springer-Verlag, New York.

WOGCC., 2017. Wyoming oil and gas commission database. http://wogcc.state.wy.us/legacywogcce.cfm. Accessed: 8/

Section 3.2: Subsurface Description

Scott Quillinan, Yuriy Ganshin, Erin H.W. Phillips Tom Moore J. Fred McLaughlin, Zunsheng Jiao, Heng Wang, Davin Bagdonas, Matthew Johnson and Charles Nye
Center of Economic Geology Research
School of Energy Resources, University of Wyoming
1000 E. University Ave, Dept. 3012
Laramie, WY 82071

HIGH-LEVEL TECHNICAL SUB-BASINAL EVALUATION

Storage Reservoirs. The team has identified four high-priority storage reservoirs as part of the storage complex for further feasibility study in Phase II (Figure 3.2.1). Each target formation is saline, lies at a depth sufficient to maintain supercritical CO_2, and has adequate thickness, permeability, and porosity to satisfy the U.S. Department of Energy's volumetric saline storage requirements. These reservoirs are described in further detail below.

Minnelusa Formation. The Minnelusa in the northern PRB was deposited as near-shore dunes and shoreline sands, which graded westerly into a continental sabkha and easterly into a shallow evaporitic sea (Anna, 2009). It is divided into Lower, Middle, and Upper Members bound by unconformities. In the northern PRB, the Lower and Middle Members consist of shale and carbonate layers. The Upper Member consists of sandstone with minor carbonate layers and is a prolific hydrocarbon reservoir with dispersed fields across the eastern margin of the PRB, having produced 600+ million barrels of oil (Anna, 2009). These fields commonly have a limited water drive, indicative of confinement.

The Upper Minnelusa in the project's study area is thick, porous, permeable, and saline. Located at approximately 9,450 ft. below land surface, the Minnelusa is approximately 150 ft. thick (Figure 3.2.2). Porosity and permeability measured during Phase I from core within 6.2 miles of DFS had an average porosity of 9% and permeability values as high as 169 milliDarcies (mD; n=6; Figure 3.2.3). Characterization of well logs surrounding the study area suggest that the Minnelusa and its overlying seal are laterally continuous. Data from the USGS Produced Waters database report a salinity of 33,500 parts per million (ppm) total dissolved solids (TDS) proximal to DFS.

Lower Sundance Formation. The Hulett and Canyon Springs members are the two primary reservoirs located in the lower Sundance (Ahlbrandt and Fox, 1997). They were deposited in prograding shoreface and foreshore parasequences prior to inundation of the Jurassic Sundance Sea (Ahlbrandt and Fox, 1997). The Hulett and underlying Canyon Springs Members were deposited in a barrier island complex during regression of the Sundance seaway (Rautman, 1978; DeCelles, 2004). The Hulett is a trough-crossbedded, silty sandstone with shale interbeds (Rautman, 1978). The Canyon Springs Member consists of fine-grain sands of incised valley fill and eolian/sabkha sand deposits (Ahlbrandt and Fox, 1997). Sundance reservoirs are considered to be "exceptional reservoirs" with a high potential for confinement (Ahlbrandt and Fox, 1997), though they are not typically hydrocarbon-bearing.

In the project's study area, the basal sands of the Sundance lie at a depth of 8,410 to 8,550 ft. below land surface and have a combined thickness of 110 ft. During Phase I, log porosity (Figure 3.2.4) was used to estimate porosity ranges from 2-18% and permeability ranges from 0.1 to 1000 mD (with an average of 6.26 mD). To supplement these well log data, eight samples collected from outcrop from the Hulett and Canyon Springs members had measured porosity from 18 to 24% and permeability ranging from 38.86 to 1083 mD. Logfacies profiles indicate that the Sundance is characterized by good lateral continuity and is a promising reservoir in terms of thickness and uniformity (Figures 3.2.2 and 3.2.5). Because of variability between legacy data and Phase I findings, coupled with the possibility of a 30 ft.-thick interval within the Hulett sandstone with superior reservoir properties, the Phase II feasibility study will investigate this reservoir(s) in detail. Water quality data for these intervals are also limited, including only one measurement of salinity (33,000 ppm) reported roughly 5 miles up-dip from the study area. Generally, formation salinity in the PRB increases with depth and distance from recharge (Quillinan and Frost, 2012); thus, the team assumes that in the study area the Sundance reservoirs are of equal or greater salinity than the up-dip measurement.

Lakota/Fall River Group. The Lakota sandstones were deposited on an alluvial plain in a large, north-trending fluvial system in incised valleys across multiple, unconformable surfaces (Meyers et al., 1992). They include conglomerate, siltstone, mudstone, and coarse sandstone. Across the region, porosity measurements of up to 25% are reported by Dolton and Fox (1996), and permeability ranges from 0.1 to 450 mD (Craddock et al., 2012; Nehring and Associates, Inc, 2010). Proximal core samples were not available during Phase I for site-specific reservoir quality estimates; however, log porosities allow the team to predict an average porosity of 15%. The Fall River (also called Dakota) sandstones were deposited as a broad deltaic system that included valley and distributary fill, delta plain facies, and delta front facies. Average reservoir porosity in the PRB ranges from 8 to 23% (Dolton and Fox, 1996), permeability ranges from a few hundred to several thousand mD, and total reservoir thickness varies from 50 to 80 ft. (Bolyard and McGregor, 1966).

In the study area, Lakota/Fall River reservoirs represent roughly 60 ft. of reservoir quality thickness that occur at depths 7,650 to 7,790 ft. below land surface. Formation salinity is the largest unknown variable associated with these reservoirs. Water quality measurements for these reservoir intervals have not been reported in the public domain, and as such, salinity measurements within these formations during the Phase II feasibility study will be a significant contribution to understanding the storage feasibility of Lakota/Fall River. Though water quality data are not available, salinity estimates from resistivity logs in the area suggest a salinity value greater than 20,000 ppm.

Muddy Sandstone. The Muddy lies at a depth of 7,400 to 7,450 ft. and consists of fluvial and marine lithologies. These include channel and bar sands, over-bank deposits, splays, deltas, incised valleys, and nearshore sands. This prolific hydrocarbon reservoir is found across the Rocky Mountains. In the PRB, most of the Muddy production comes from thickened sands associated with incised valley and transgressive channel fill deposits. As

such, the Muddy can locally vary in thickness and reservoir characteristics. Porosity of reservoir lithologies can range from 4 to over 20% with permeability ranging from <0.01 to over 1000 mD (Anna, 2009). From core collected within 4 miles of DFS, the permeability ranges from 0.0002-0.21 mD and porosity averages 9.4% (n=8; Figure 3.2.3). The Muddy's reservoir thickness in the eastern PRB averages between 10 and 25 feet (Anna, 2009), and in the immediate area of DFS, is as thin as 0 to 4 ft. in total reservoir thickness. The non-reservoir lithologies have significantly lower porosity and permeability and can be 50 ft. thick in the study area. TDS of Muddy brines exceeds 67,000 ppm in the study area. The Muddy is sealed above by thick and regionally continuous Upper Cretaceous marine deposits of the Mowry Shale and below by the Skull Creek Shale (Figure 3.2.2).

Confining Systems

Opeche Formation (Opeche). The Opeche seals the Minnelusa. In the eastern PRB, and within the study area, the Opeche and Minnekahta become formations distinct from the overlying Goose Egg Formation. The Opeche is a redbed shale with some fine-grained siltstones and minor evaporite deposits occurring throughout the shale section. The Opeche is overlain by the Minnekahta, which in turn is overlain by the Goose Egg and then Spearfish Formations with a combined thickness of 950 ft. (Figure 3.2.5). This confining system of Opeche through Spearfish is a proven seal in Minnelusa hydrocarbon fields (Anna, 2009). Mercury injection capillary pressure (MICP) measurements of three Opeche samples from core within 7 miles of DFS show entry pressures of 691, 4789, and 1596 psia, with pore throat sizes indicative of excellent seal characteristics (Figure 3.2.6).

Upper Sundance/Morrison Formations (Sundance/Morrison). The sandstone units of the lower Sundance are sealed by thick shales of the upper Sundance and the overlying Morrison (Figure 3.2.2). The Redwater Shale Member of the Sundance/Morrison is the primary seal of the basal sands. This seal was deposited in a westerly transgressing sea and is continuous across much of Wyoming (Ahlbrandt and Fox, 1997). In the study area, the sealing lithology of the Sundance/Morrison is approximately 125 ft. thick (Figure 3.2.2).

Skull Creek Shale/Upper Cretaceous (Skull Creek/Cretaceous). The Skull Creek is the primary seal of the Lakota/Fall River. Both Lakota/Fall River and Muddy are capped with a thick section of marine shales, including the Mowry, Belle Fourche, Carlile, Niobrara, and Pierre (also called Lewis). In the study area, the total stratigraphic section of these regionally continuous seals is 3,990 ft. in total thickness. This makes the Skull Creek/Cretaceous the ultimate seal for all reservoirs below. Near DFS, the top of the Skull Creek/Cretaceous ultimate seal is slightly more than 6,000 ft. below land surface. MICP measurement of a Mowry sample from core ~4 miles southwest of DFS yielded an entry pressure of 194 psia and a median pore throat radius of 0.0140 mm (Figure 3.2.6). Legacy MICP analyses from elsewhere in the PRB indicate closure pressures as high as 11,461 psia (USGS Core Research Center (CRC) well #T322 and D636) for the Mowry, indicating superior seal qualities at the bottom of the ultimate seal. This high closure

pressure combined with the Skull Creek/Cretaceous seal's thickness offer exceptional stratigraphic confinement.

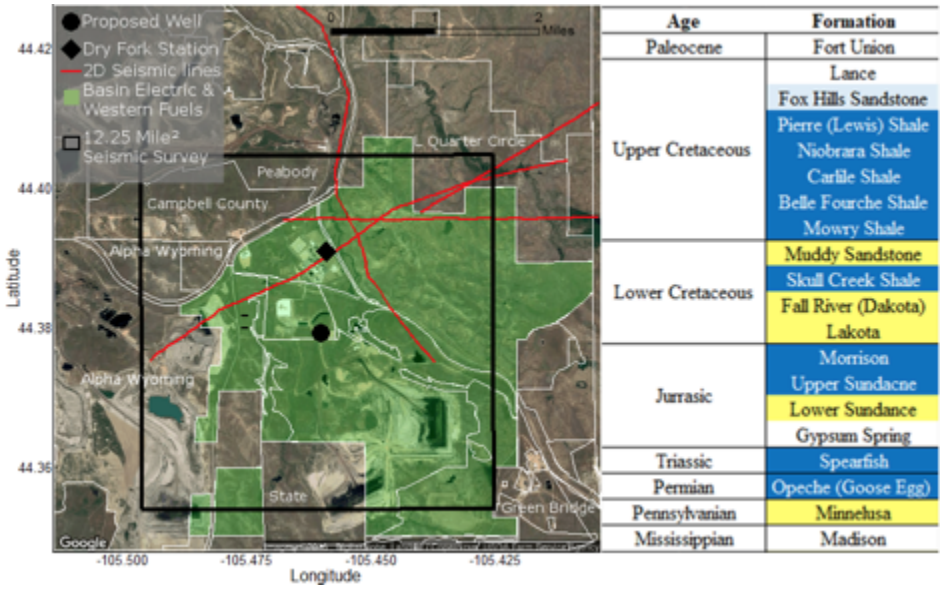

Age	Formation
Paleocene	Fort Union
Upper Cretaceous	Lance
	Fox Hills Sandstone
	Pierre (Lewis) Shale
	Niobrara Shale
	Carlile Shale
	Belle Fourche Shale
	Mowry Shale
Lower Cretaceous	Muddy Sandstone
	Skull Creek Shale
	Fall River (Dakota)
	Lakota
Jurrasic	Morrison
	Upper Sundacne
	Lower Sundance
	Gypsum Spring
Triassic	Spearfish
Permian	Opeche (Goose Egg)
Pennsylvanian	Minnelusa
Mississippian	Madison

Figure 3.2.1 Study Area for the Phase II feasibility study and key elements: (1) location of the proposed stratigraphic test well and storage complex; (2) area of coverage for the proposed new 3-D seismic survey; (3) 2-D seismic lines (to be purchased); (4) land ownership; and (5) storage units within the storage complex with reservoirs (yellow) and seals (blue) indicated. The continuous Upper Cretaceous shale package is ~3990 ft. thick and a proven regional seal across the PRB, greatly reducing risk of communication with the overlying Underground Source of Drinking Water (USDW), the Fox Hills Sandstone (light blue).

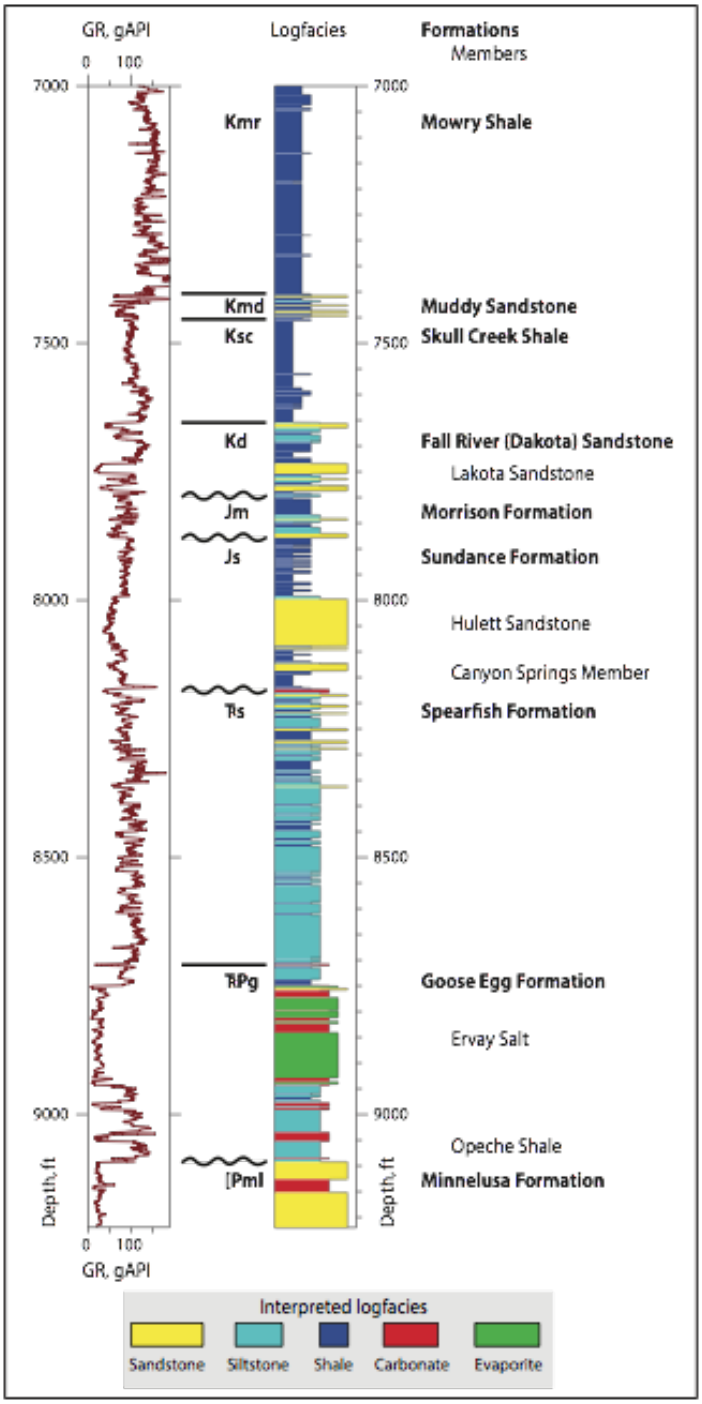

Figure 3.2.2 Wireline log (left) from Callaway 15-5 well (API 562532), approximately 4 miles from DFS, and color-coded logfacies profile (right) obtained from log cluster analysis. This analysis is able to discriminate sandstone reservoir units from non-reservoir shale-siltstone.

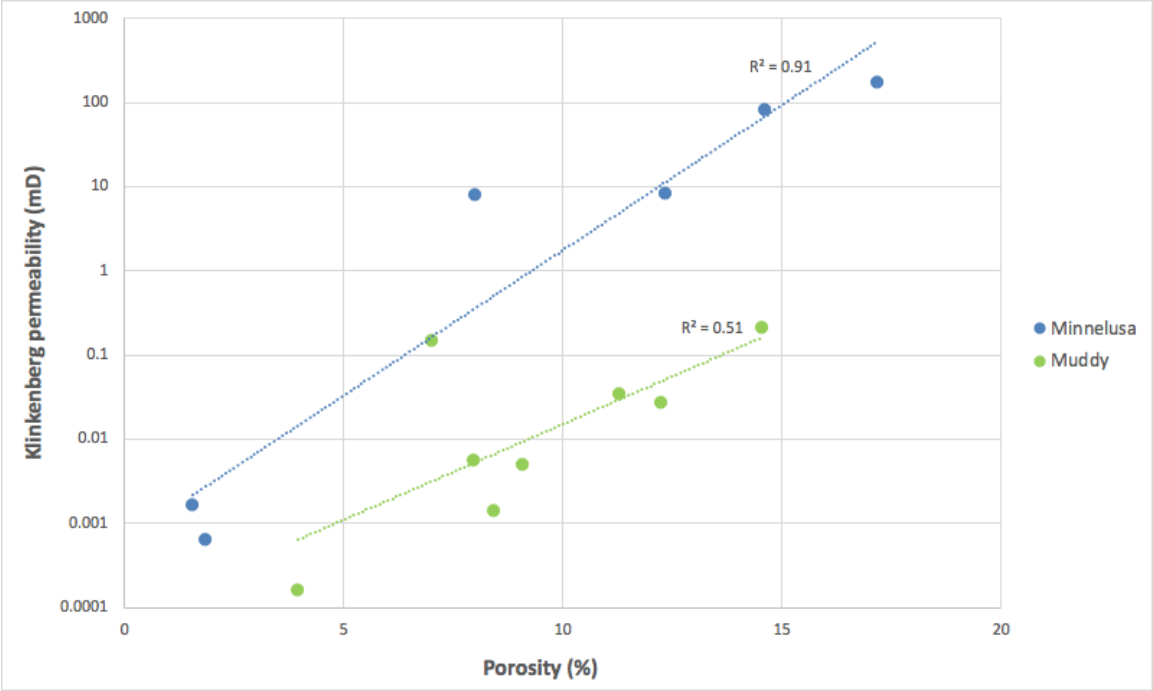

Figure 3.2.3 Semi-log plot of porosity versus Klinkenberg permeability at reservoir pressures for the Minnelusa (USGS CRC #B070(4), D379, B649) and Muddy (USGS CRC #T123(4), A606, D780, A110, A650) for samples analyzed by routine core analysis in this pre-feasibility study. Exponential trend lines are shown for each geologic unit.

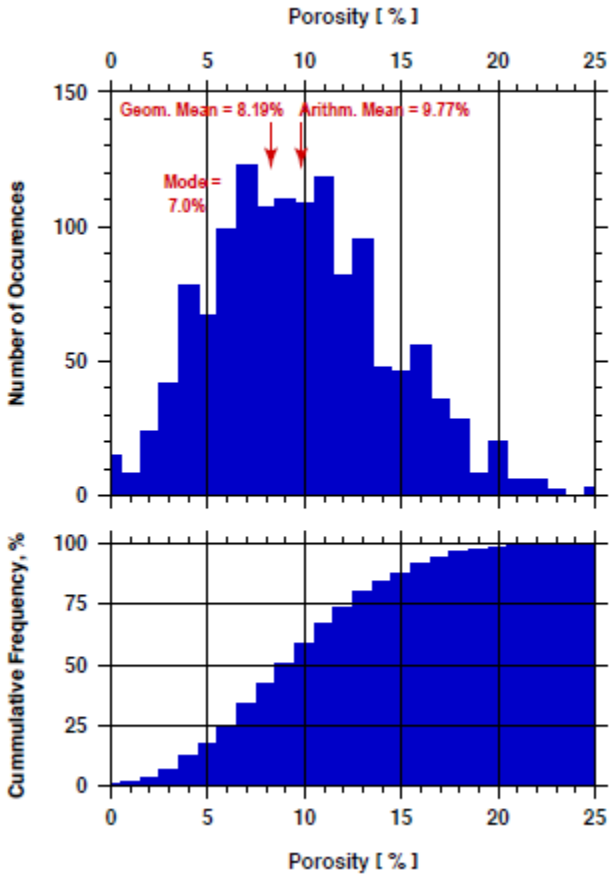

Figure 3.2.4 Ordinary (top panel) and cumulative (bottom panel) histograms of log-derived porosity interpreted for the Hulett-Canyon Spring Sandstones of the lower Sundance Formation based on log measurements in six wells in the project's study area.

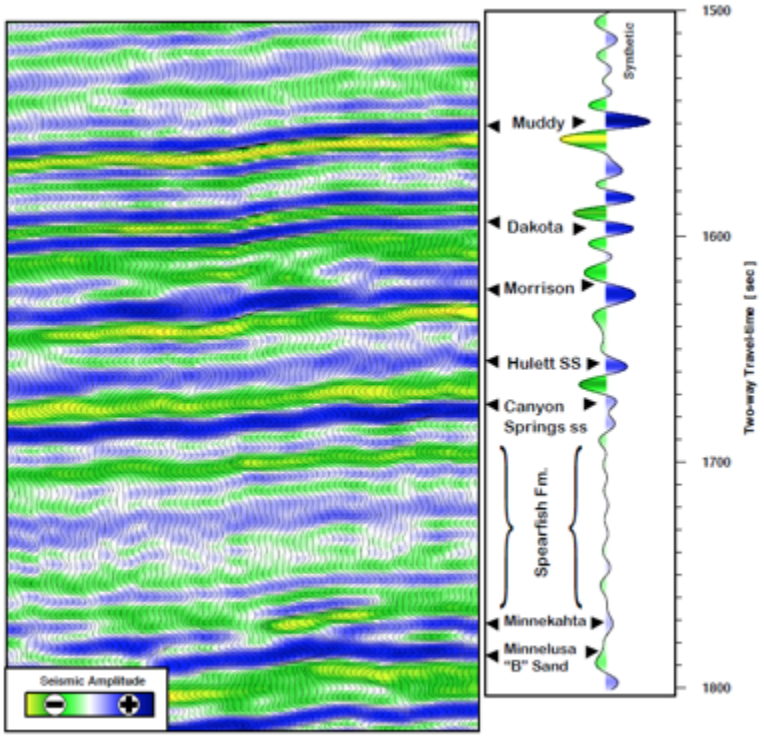

Figure 3.2.5 Segment of a seismic amplitude section from a 3-D survey located 12 miles northeast of the DFS storage complex. Note the thick lateral continuity of the Spearfish sealing lithologies.

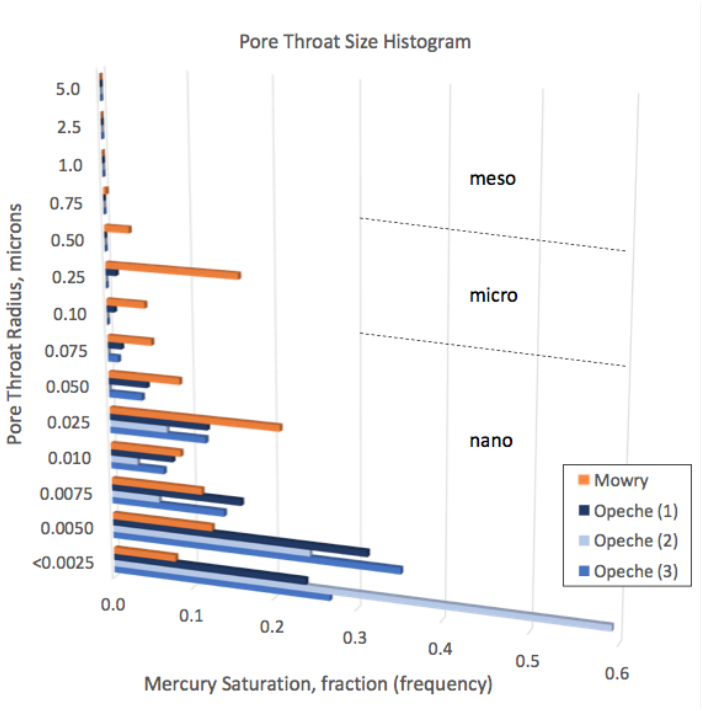

Figure 3.2.6 Pore throat size histogram for three Opeche samples (USGS CRC #D106(2) and B070) and one Mowry sample (USGS CRC #B200) from MICP analysis.

Section 3.2 References

Ahlbrandt T.S. and Fox J.E. (1997) Middle Jurassic incised valley fill (eolian/estuarine) and nearshore marine petroleum reservoirs, Powder River basin. *Mountain Geologist*, **34(3)**.

Anna O.L. (2009) Geologic assessment of undiscovered oil and gas in the Powder River Basin province, Wyoming and Montana. US Geological Survey Digital Data Series DDS-69-U.

Bolyard D.W. and McGregor A.A. (1966) Stratigraphy and Petroleum of Lower Cretaceous Inyan Kara Group in Northeastern Wyoming, Southeastern Montana, and Western South Dakota. *Bulletin of the American Association of Petroleum Geologists*, **50**, pp. 2221-2244.

Craddock W.H., Drake R.M., Mars J.C., Merrill M.D., Warwick P.D., Blondes M.S., Gosai M.S., Freeman P.A., Cahan S.M., DeVera C.A., and Lohr C.D. (2012) Geologic Framework for the National Assessment of Carbon Dioxide Storage Resources - Powder River Basin, Wyoming, Montana, South Dakota, and Nebraska. US Department of the Interior, US Geological Survey Open-File Report 2012-1024-B.

DeCelles P.G. (2004) Late Jurassic to Eocene evolution of the Cordilleran thrust belt and foreland basin system, western USA. *American Journal of Science*, **304(2)**, pp. 105-168.

Dolton G. L. and Fox J.E. (1996) Powder River Basin Province. In: Gautier D.L., Dolton G.L., Takahashi K.I., and Varnes K.L. (eds), 1995 National Assessment of United States Oil and Gas Resources -- Results, Methodology, and Supporting Data, U.S. Geological Survey Digital Data Series DDS-30, Release 2 [CD-ROM].

Meyers J.H., Suttner L.J., Furer L.C., May M.T., and Soreghan M.J. (1992) Intrabasinal tectonic control on fluvial sandstone bodies in the Cloverly Formation (Early Cretaceous), west-central Wyoming, USA. *Basin Research*, **4**, pp. 315–334.

Nehring Associates, Inc. (2010) The significant oil and gas fields of the United States. Database available from Nehring Associates, Inc., P.O. Box 1655, Colorado Springs, CO 80901, U.S.A. [data current as of December 2008].

Quillinan S.A. and Frost C.D. (2012) Spatial variability of coalbed natural gas produced water quality, Powder River Basin, Wyoming: Implications for future development. Wyoming State Geological Survey Report of Investigation No. 64-2012 56p.

Rautman C.A. (1978) Sedimentology of Late Jurassic Barrier-Island Complex--Lower Sundance Formation of Black Hills. *AAPG Bulletin*, **62(11)**, pp. 2275-2289.

Section 3.3: Hydrostratigraphy Description

Tom Moore
Research Scientist, Center of Economic Geology Research
School of Energy Resources, University of Wyoming
1000 E. University Ave, Dept. 3012
Laramie, WY 82071

The Powder River Basin (PRB) is an asymmetric syncline bound by the Black Hills uplift to the west and the Bighorn mountains to the east. The target reservoirs are exposed to meteoric recharge at the basin margin. Each formations salinity increases with depth as the formations gain distance from the basin margins where the formations are exposed to meteoric recharge (Figure 3.3.1).

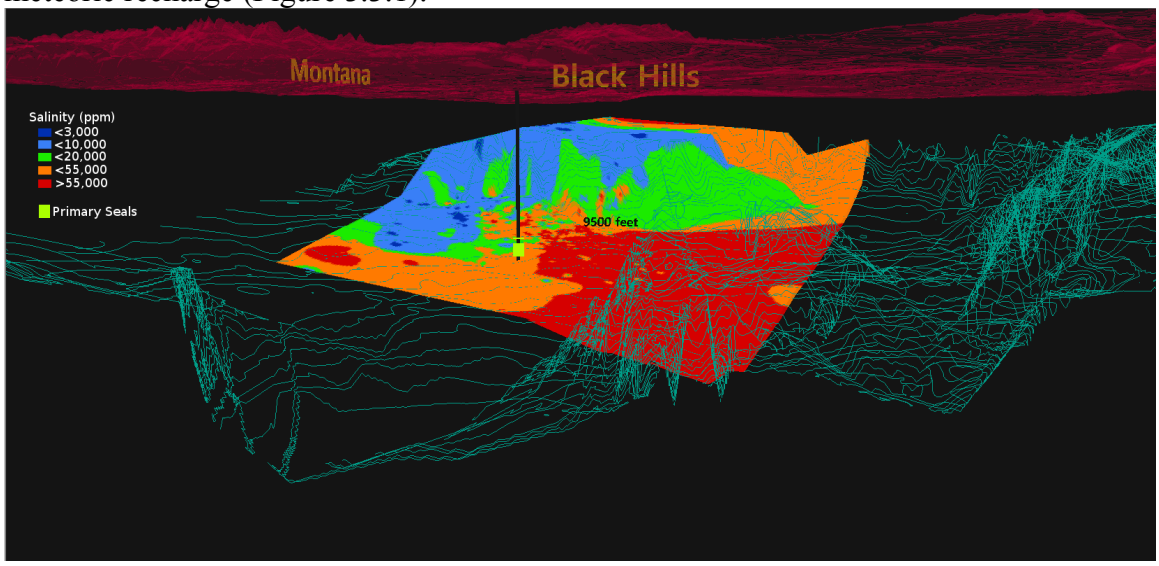

Figure 3.3.1 A 3D rendering of the Powder River Basin showing salinity increasing with depth. (Vertical exaggeration 5x).

For a formation to be considered for saline storage, the formation must have a salinity exceeding 10,000 parts per million (ppm). Salinity is measured and reported as total dissolved solids (TDS). Multiple methods were used to predict formation salinity of the four target reservoirs, including kriging and inverse distance weighting (IDW) and using resistivity measurements from geophysical well logs, which is further explained in chapter 3.4.

For the Muddy and Minnelusa formations, we used the USGS National Produced Waters Geochemical Database v2.2 (See Chapter 3.1: Blondes et al., 2016) to estimate salinity for the location of the test well (-105.459,44.379). The first method considered all of the data available for the PRB and used IDW from the R gstat package (TDS~1, maxdist=7000, omax=8) to interpolate the salinity at the test well. Using this method, the Muddy was predicted to have a TDS of 11,237 ppm and the Minnelusa was predicted at 37,465 ppm (Figure 3.3.2).

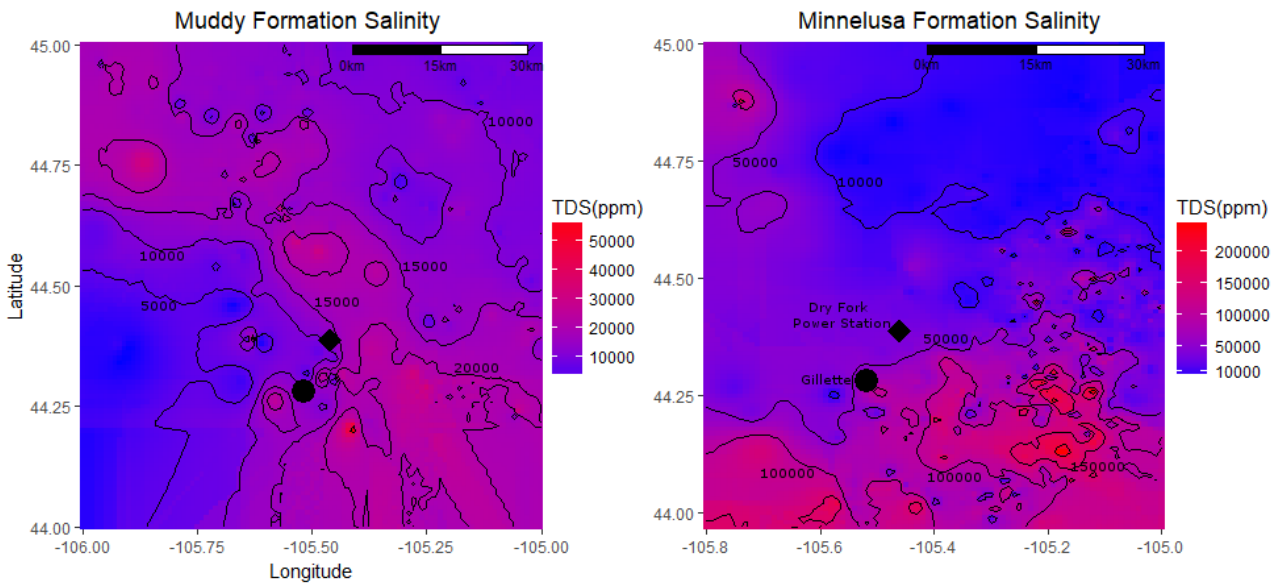

Figure 3.3.2 Salinity map of the Muddy and Minnelusa Formation predicted using inverse distance weighting.

Estimates were also predicted by kriging a subset of the full dataset, using the autoKrige tool from the automap R package, where TDS ~1 (Figure 3.3.3). First, the data was clipped to include only data points that lie within 15 miles of the test well location. Data with a charge balance greater than 15% was not considered, unless the charge balance was bad due to missing a major cation or anion. In the case that a missing anion or cation would balance the measurement, the datum point was included. Salinity was estimated to be 16,710 ppm with a standard error of 10,416 for the Muddy Formation and 63,537 ppm with a standard error of 56,946 for the Minnelusa formation.

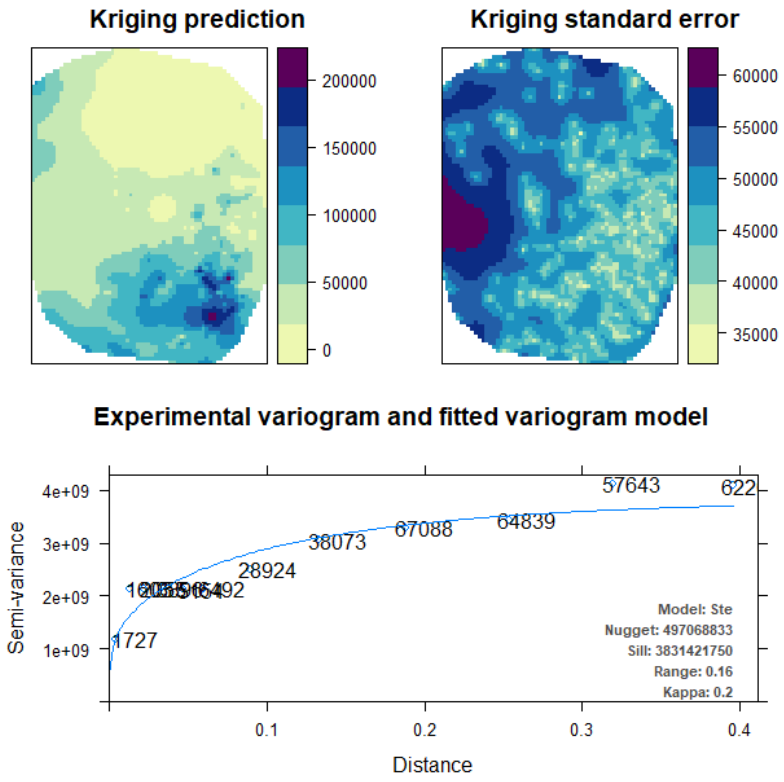

Figure 3.3.3 Output of the autokrige package from R run on Minnelusa salinity data.

The Lakota/Dakota and Sundance formations did not have enough data to use either interpolation method to predict the formation salinity through statistical approaches. Instead, the closest sample was used. The closest Lakota/Dakota sample, 9.5 miles to the northeast, has a TDS of 17,256 ppm. The closest Sundance sample, 6 miles to the north, had a TDS of 33,661 ppm. As both of these samples are updip of the site, the salinity would be expected to increase, providing evidence that both samples are above 10,000 ppm. Chapter 3.4 uses nearby well logs to model the salinity of the Sundance and Muddy formations. Using this methodology, the Muddy TDS estimate does not exceed 10,000 ppm and the Sundance does.

Caution should be used when interpreting the above results to state formation salinity. The interpolated results had standard errors of 10,416 and 56,946 ppm for the Muddy and Minnelusa formations respectively. Such a large error shows the uncertainty of the analysis. The Muddy formation was also predicted to be under 10,000 ppm in chapter 3.4. The Lakota/Dakota formation was predicted from a single sample. Other nearby samples have TDS values lower than 10,000 ppm, and while the nearest sample does exceed 10,000 ppm it should not be overstated. The Sundance formation estimate is also from a single sample, but no other sample can inform the quality of the sample. For these reasons, further sampling should take place in Phase II of this study to ensure the target reservoirs are saline (>10,000 ppm).

Section 3.4: Geophysical Description

Yuriy Ganshin
Senior Research Scientist, Center of Economic Geology Research
School of Energy Resources, University of Wyoming
1020 E. Lewis Street, Energy Innovation Center
Laramie, WY 82071

Abstract

We estimated the permeability in an approximately 110-ft-thick sandstone interval within the lower Sundance formation in the study area with the objective of increasing the accuracy of our CO_2 flow simulation program. We used core data collected in outcrops to identify the porosity-permeability relationship for this stratigraphic interval. On the basis of this relationship and well log data, we constructed several continuous vertical permeability profiles. The resulting statistical estimators of the permeability distribution led us to classify the Jurassic Hulett and the Canyon Springs sandstones as relatively poor quality reservoirs with a high degree of heterogeneity. However, there is a chance of about 30-foot-thick interval occurrence within the Hulett sandstone with a better reservoir property. 3D high-resolution seismic will be a good tool to delineate this "sweet spot." Logfacies and synthetic seismogram modeling indicate that the study area is characterized by a good lateral continuity of the Sundance/Morrison and the Minnelusa/Goose Egg reservoir/seal pairs. Synthetic seismic response within the Mesozoic section indicates that 3D seismic data should be able to determine reservoir extent away from existing wells. We propose that dense seismic velocity analysis can be used in the study area for lithology identification (in vertical sections) and porosity mapping (in horizon slices), and hence, can be used to characterize the reservoir quality. After the test well is drilled and logged, and 3D seismic acquired, we propose a two-step process of integrating stratigraphy, petrophysical, and geophysical data into a subsurface reservoir model. It will focus on utilizing geostatistical 3D seismic inversion to predict facies and reservoir/geomechanical properties.

Geophysical data available in study area.

An analysis of available geophysical data in the Dry Fork Station (DFS) area of west central Powder River Basin has been made. The available geophysical information is the following: 2D and 3D seismic surveys, seismic images, and well-log data.

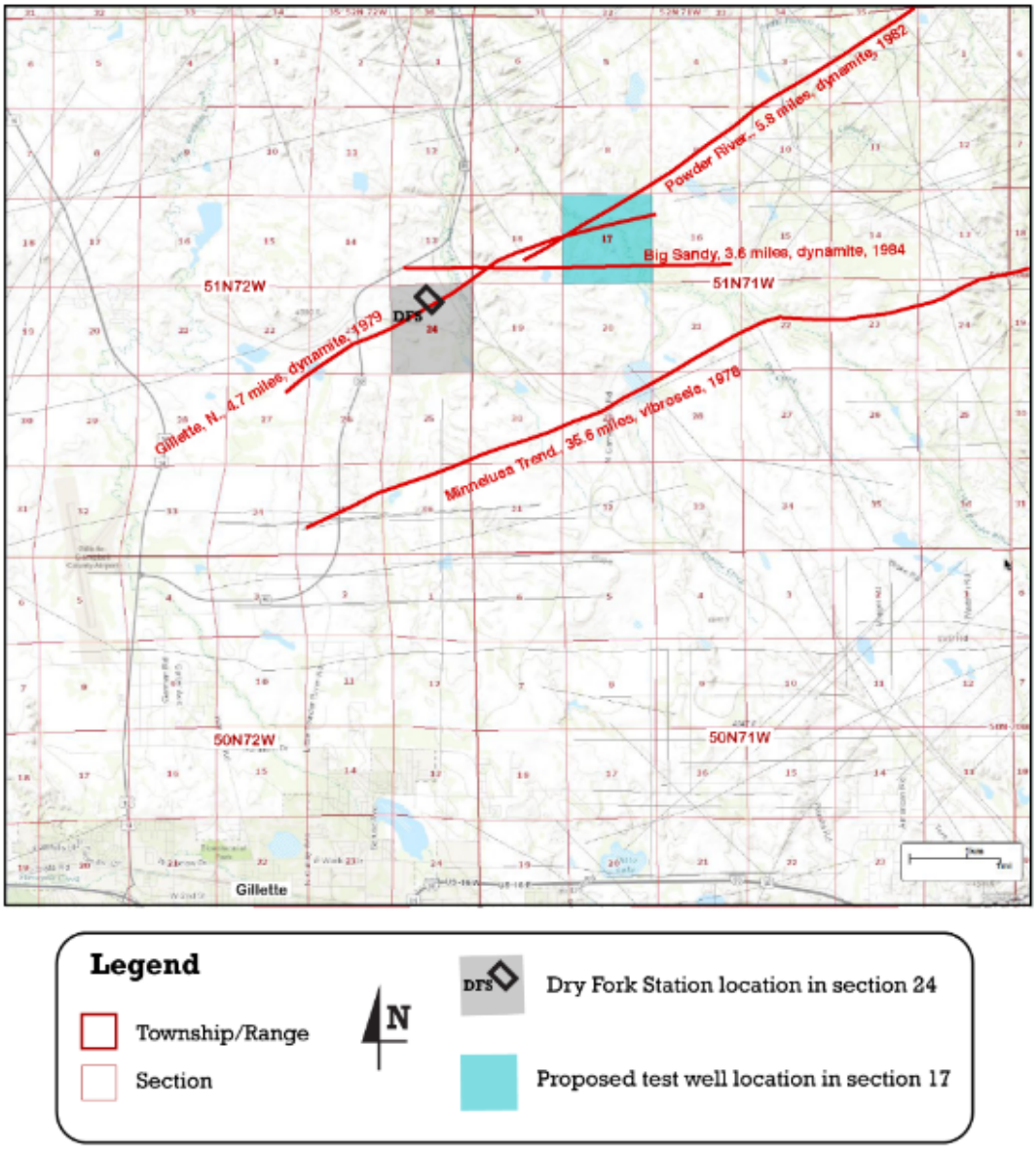

Figure 3.4.1 shows 2D seismic lines from the Seismic Exchange library (http://gis.seismicexchange.com/1). The lines highlighted in red pass across the Dry Fork Station location in section 24 and/or across the proposed test well location in section 17 of township 51N-71W. These are relatively short lines (about 5-miles long) shot with dynamite in the 1980s. A regional scale 2D line (35.6-miles long) is located just south of the DFS location. The lines are oriented from northeast to southwest and correspond to a general dip direction of the subsurface strata.

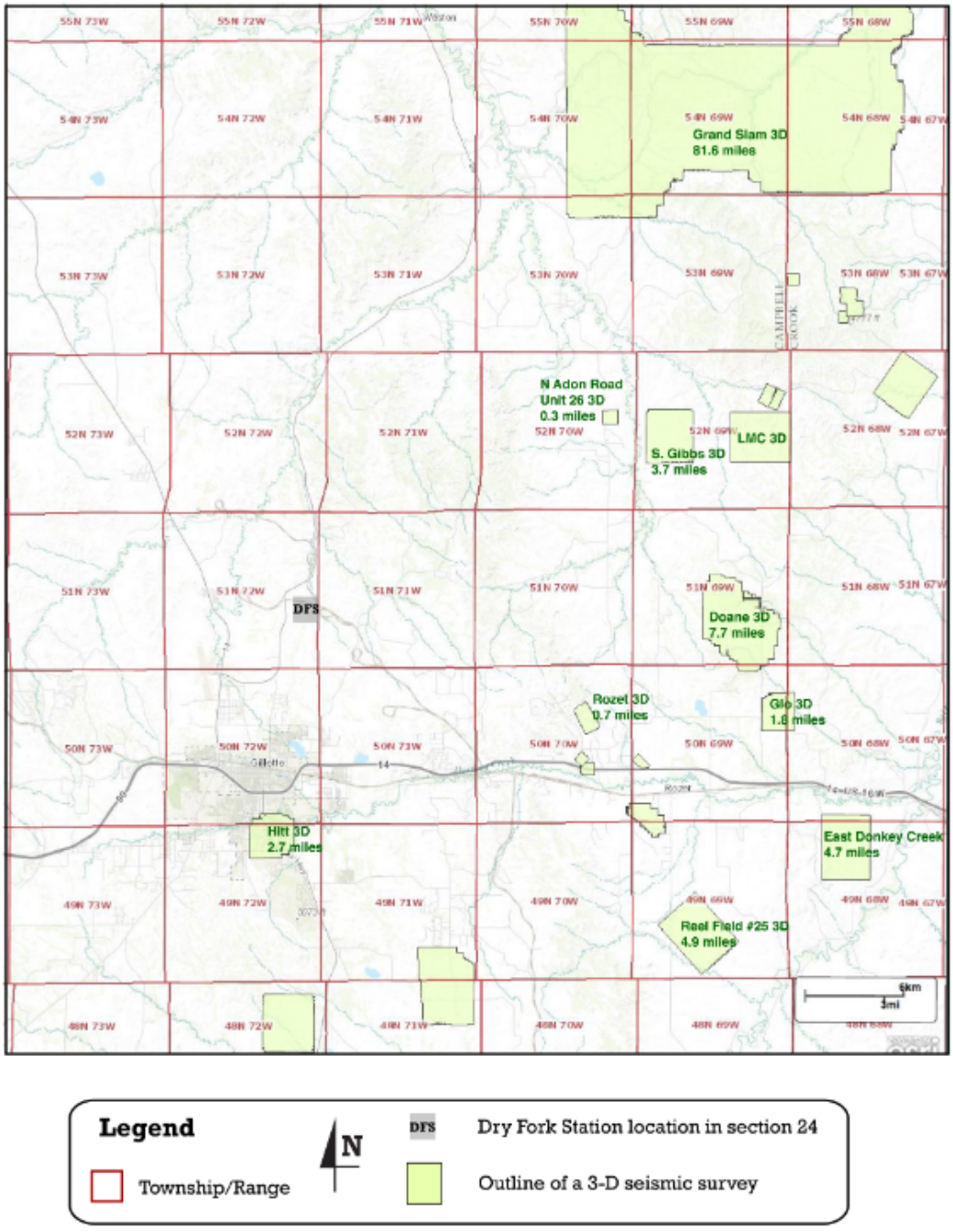

Figure 3.4.2 shows 3D seismic surveys from the Seismic Exchange library. There is no 3D seismic data neighboring the DFS study area; most of the surveys are located west and northwest of DFS, the areas of the Upper Minnelusa oil fields concentration. Correspondingly, the 3D seismic data were acquired to aid in the understanding of the Upper Minnelusa sandstone reservoir distribution and performance.

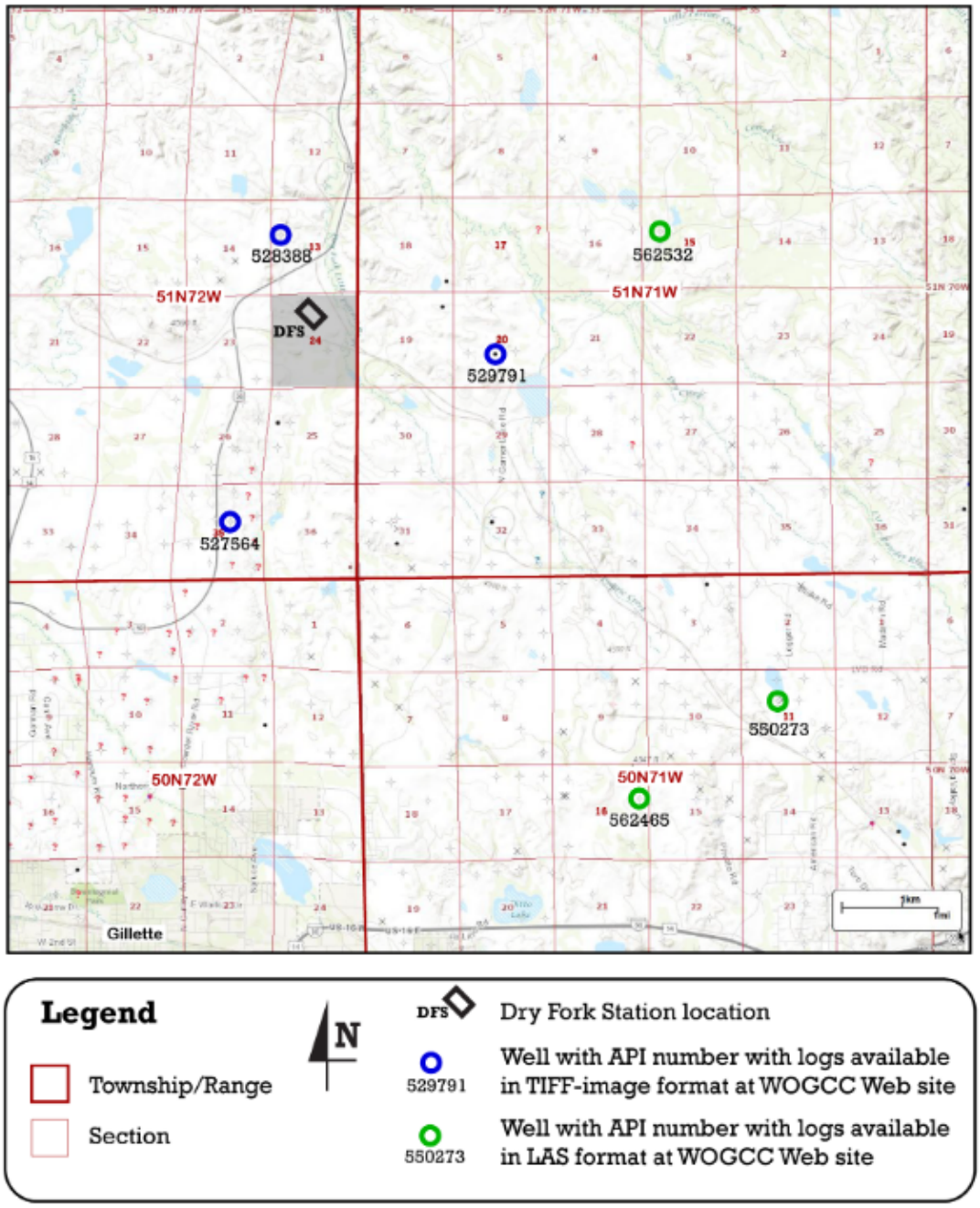

Figure 3.4.3 Map showing well locations (blue and green circles) used for analysis of Dry Fork study area (Powder River Basin).

Figure 3.4.3 shows wells drilled within the DFS study area according to the WOGCC database (http://wogcc.state.wy.us/). Producing wells are shown with solid dots, while the abandoned ones are shown with crossed out circles. Most of hydrocarbon production in the area comes from the Lower Cretaceous Muddy Sandstone, and therefore, there are only a few wells penetrating stratigraphically lower horizons. There are only six wells that were drilled and logged through the Mesozoic sedimentary section

up to the Upper Minnelusa sandstones. Some of these wells have logs available in TIFF-image format and were digitized manually (large blue circles in **Figure 3.4.3**), and there are only three wells with logs recorded in LAS digital format (green circles in **Figure 3.4.3**). These last three wells possess the most complete suite of logs acquired with modern tools in 2003 and 2014. We used digital data for log-based facies analysis, petrophysical analysis and physical rock properties computation, lithological interpretation, and estimation of the concentration of total dissolved solids (TDS) in formation fluid. We used gamma ray (GR) log to pick the top of the Muddy Sandstone throughout the area and to build the structure contour map shown in **Figure 3.4.4.**

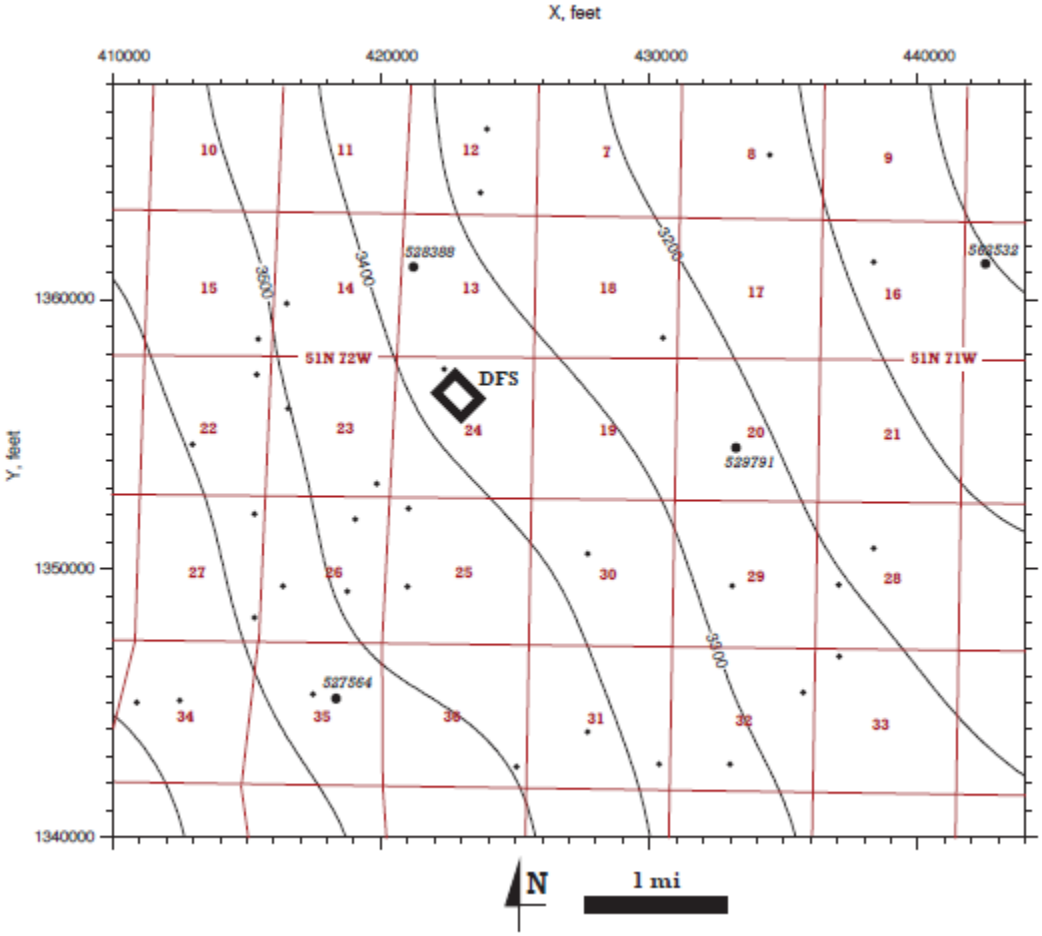

Figure 3.4.4 Map showing structure contours on top of the Muddy Sandstone, Dry Fork study area (Powder River Basin). Contour interval is 100 feet with labels indicating depth below mean sea level. Dark red lines are PLSS section boundaries. State Plane coordinates (Wyoming East zone 4901) outline the northern and western edges. Black dots show well locations used for structural mapping. Bigger dots with API numbers show wells that were logged up to the Upper Minnelusa Formation. (DFS = Dry Fork Station.) Note that for Cretaceous strata, a general south-westerly dip prevails with an average dip value of 1 degree.

Methodology.

This study focuses on utilizing petrography, lithology, petrophysics, and geophysics to predict reservoir/seal properties of the subsurface proximal to the Dry Fork Power Station. This is a multi-disciplinary, collaborative project incorporating scientists and engineers from different organizations that may follow different approaches of data analysis, interpretation, and modeling. Therefore, it seems reasonable to develop a unified integrated approach that will guide all the team members in our ongoing and future research. This will allow for reducing economic risk, facilitating improved and faster decision-making, and enabling more efficient and effective well(s) placement for successful injection and storage of commercial amounts of anthropogenic CO_2.

At the current stage of our prefeasibility study, abundant information is available from multiple disciplines and at different scales of investigation, from microscopic thin sections to seismic-scale Minnelusa sands models. Analysis of formation tops, wireline logs, core data, and production information provides a global context to understanding the big picture of the reservoir(s); however, only dense and high-resolution 3D seismic datasets provide a wealth of both quantitative and qualitative subsurface information away from wells, in terms of seismic attributes that correlate directly to observations at the well bore.

The important calibration information obtained and extracted from the 3D seismic data are the "*elastic properties*": namely P-velocity, S-velocity, and Density which link directly to the same elastic properties obtained from the wireline data as measured in the well bore. These two independent measurements of elastic properties, from two different primary sources, calibrate with each other and provide a mechanism for lithofacies and reservoir rock property relationships to be established. Essentially, elastic properties bridge the well centric world with the seismic centric world to significantly increase our understanding of the subsurface, so more intelligent decisions can be made. Therefore, acquiring dense and high-resolution 3D seismic adjoin to the test well location is a necessary condition for our next phase preparation. This will enable us to generate a 3D seismically constrained subsurface geomodel with predicted lithofacies and reservoir properties away from known control points provided by well and core data.

After the test well is drilled and logged, and 3D seismic acquired, we propose the following two-step process of integrating stratigraphy, petrophysical, and geophysical data into a subsurface reservoir model. It will focus on utilizing geostatistical 3D seismic inversion to predict facies and reservoir/geomechanical properties. The first step involves the discrimination of a number of distinct lithofacies from core upscaled to corresponding logfacies discernable from wireline logs. These facies are correlated to acoustic/elastic parameters and upscaled to generate seismic facies. The second step will transform 3D seismic partial stacks into reservoir rock property volumes by a simultaneous geostatistical inversion. Each of the core, log, and seismic facies are to be correlated to each other in an integrated model. This seismically constrained geomodeling approach will enable optimum identification of fluid migration pathways for injection/production wells placement.

The first step of proposed methodology requires petrophysics and rock physics modeling of wireline logs. Fundamental properties of rocks are usually understood by

their detailed description in the field (*lithofacies* analysis) and laboratory (*petrofacies* analysis). The facies (lithofacies and petrofacies) determination in most subsurface studies is impractical, due to lack of cores and cuttings. In such situations, where the wireline logs are the only data available, the *logfacies* are determined instead. Below we present preliminary logfacies analysis for the initial two wells. For the next phase, we are planning to extend this analysis with an additional 4-5 wells across the entire region of interest to come up with a unified log facies model.

Logfacies Analysis

Petrophysical properties commonly vary by facies, and thus, facies modeling becomes essential for the determination of reservoir versus non-reservoir quality units within a geologic formation. Typically, many lithofacies can be distinguished in the field, but different lithofacies can have similar petrophysical properties, and therefore, are' grouped into petrofacies based on similar ranges of measured parameters (e.g. porosity and permeability). Following this logic, logfacies can be considered as petrofacies upscaled from core measurements to well-log scale.

Using multivariate cluster analysis, in this study we practiced the logfacies determination on the stratigraphic section from the Minnelusa to the Mowry Formation by programming new software built on a very popular k-means algorithm (MacQueen, 1967). An interactive program 'CLUSTERS' was developed at CMI and is available for free download from http://www.uwyo.edu/cmi/dgl-software/. The software is adapted to input multi-curve data stored as plain text files.

It is critical for cluster analysis that log-derived facies represent only rock composition and texture. Therefore, we first used a cross-plotting technique to visualize the calibration of wireline measurements with petrofacies, and thus, to identify input logs for cluster analysis. Gamma ray intensity, photoelectric factor, density, and neutron porosity were particularly good at discriminating sandstone from carbonate and shale facies (**Figures 3.4.5 and 3.4.6**). Overall, if a well log did not relate closely with petrofacies classes, as assessed in the cross-plots, then it was not selected for input. The final selection of input logs was density, neutron porosity, photoelectric factor, gamma ray, true resistivity, spontaneous potential, and caliper. Actually, this selection corresponds to a standard wireline log suite for the wells drilled after 2003 (green circles in **Fig. 3.4.3**).

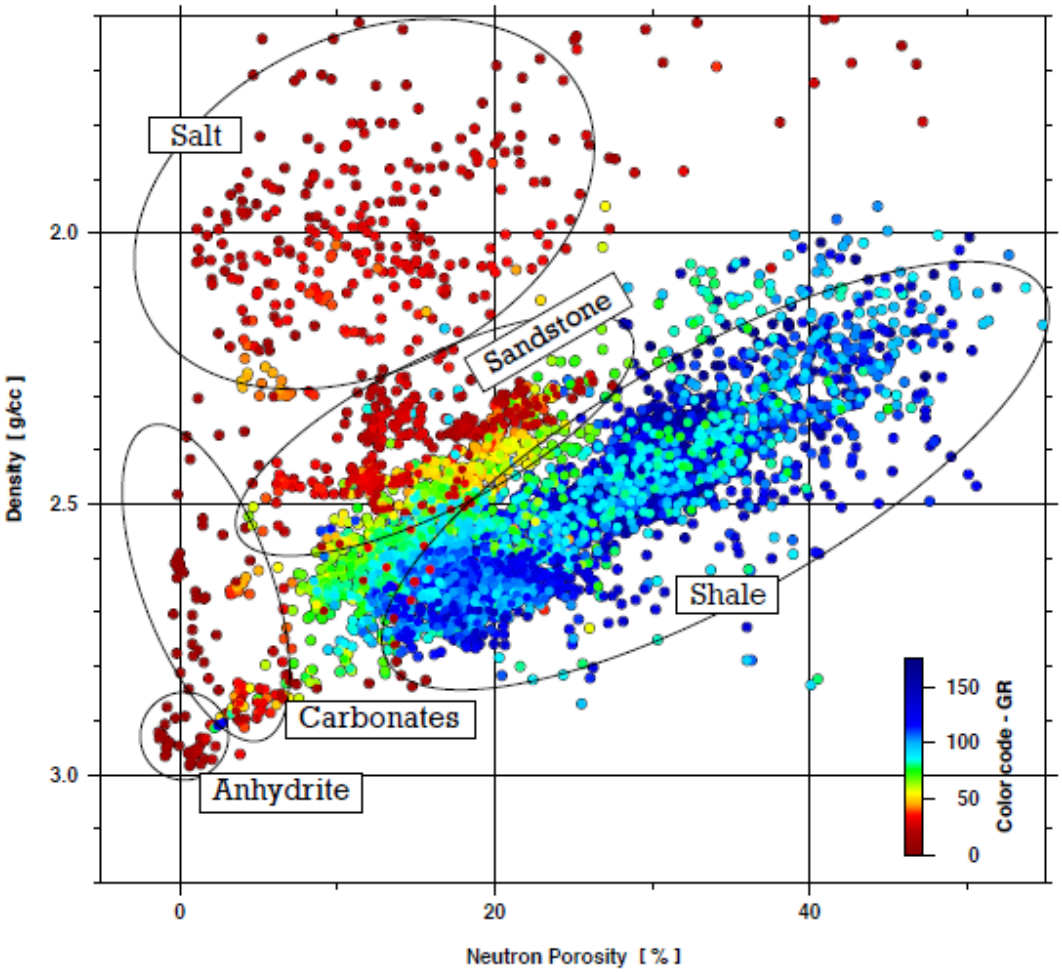

Figure 3.4.5 Logfacies interpreted from Density versus Neutron Porosity cross-plot. The color code is gamma-ray intensity. The measurements are from the Callaway 15-5 well (API 562532; 7,000 - 9,220 feet depth interval), Powder River Basin, Wyoming.

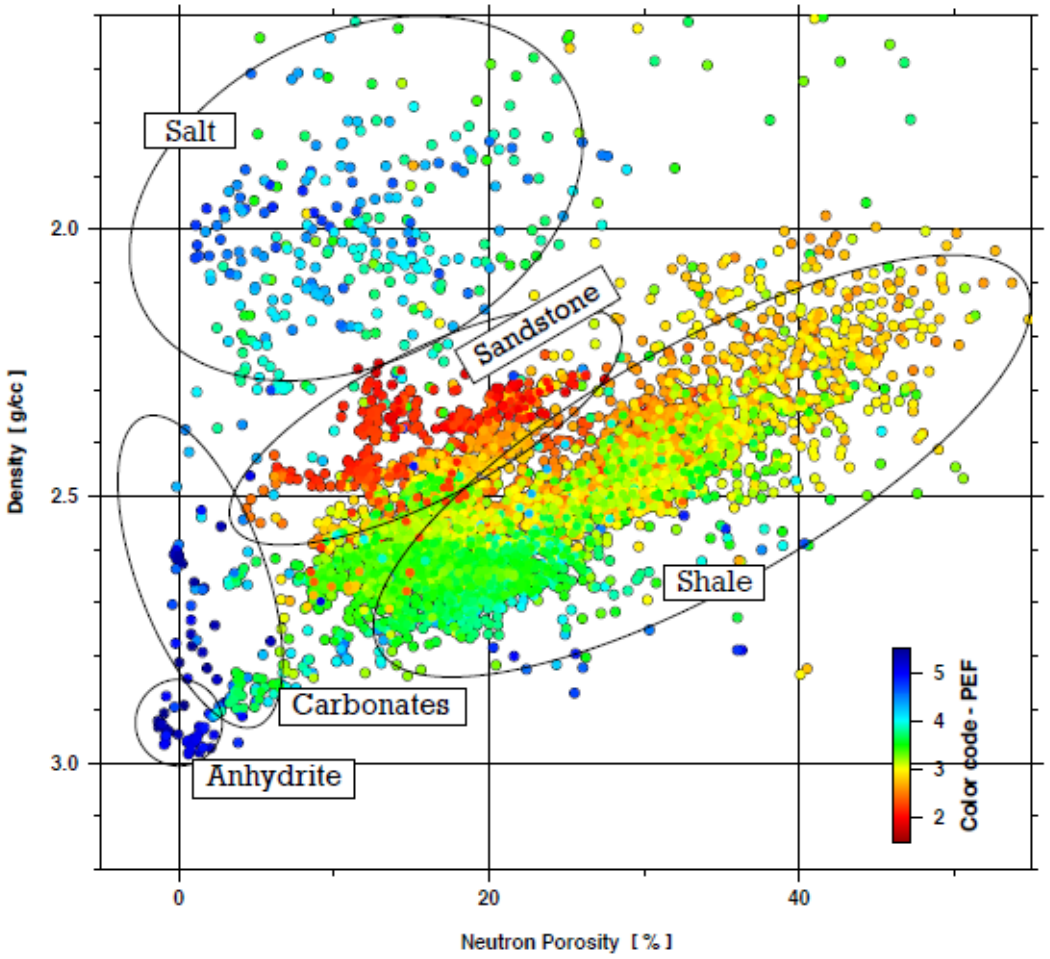

Figure 3.4.6 Logfacies interpreted from Density versus Neutron Porosity cross-plot. The color code is photo-electric factor. The measurements are from the Callaway 15-5 well (API 562532; 7,000 - 9,220 feet depth interval), Powder River Basin, Wyoming.

For the Callaway 15-5 well (API 562532) the cluster analysis resulted in seven logfacies: sandstone, siltstone, carbonates, evaporates, and three shale facies. For convenience, we named these preliminary shale facies as calcareous, competent, and simple shale. Clustering results were colored and scaled by logfacies and displayed next to the log data in the style of a lithology column (**Fig. 3.4.7**). The logfacies profile clearly discriminates sandstone reservoir units versus non-reservoir shale-siltstone sequences. Among the storage components considered in this study, the Hulett sandstone member shows superior characteristics in sense of its thickness and uniformity (**Fig. 3.4.7**). The deepest part of logged section for the Callaway 15-5 well, the upper Minnelusa Formation, also demonstrates two distinct sandstone units with uniform properties. Unfortunately, this well did not penetrate the whole stack of Minnelusa sands, so nothing can be said about their aggregate thickness.

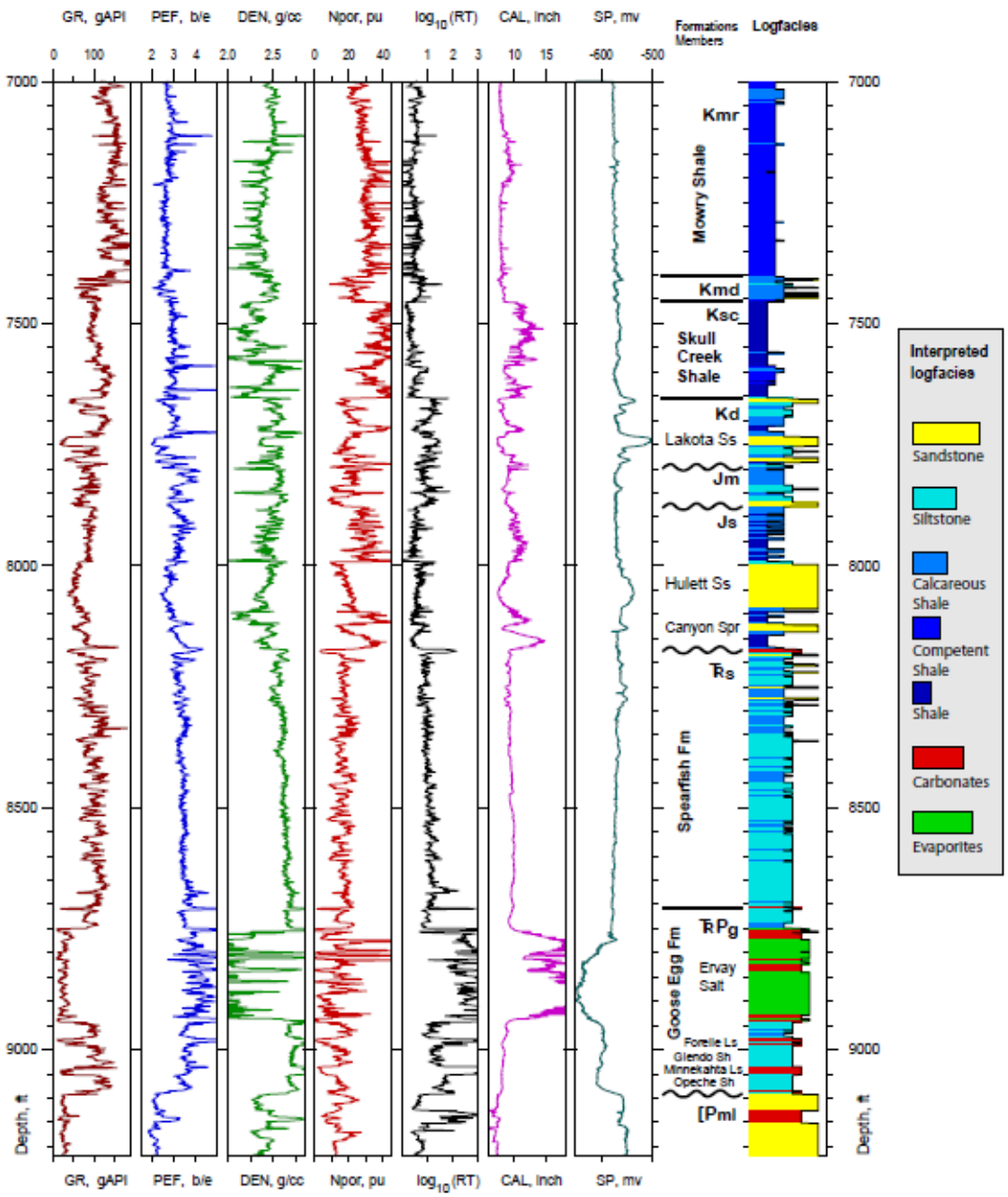

Figure 3.4.7 Wireline logs from the Callaway 15-5 well (API 562532, PRB Wyoming) and color coded logfacies profile (the rightmost panel) obtained from the logs cluster analysis.

Cluster analysis with the same amount of pre-specified facies (seven) was carried out for the DW STATE #22-11well (API 550273), located about 5 miles south of the Callaway 15-5 well (**Fig. 3.4.3**). And again, we observe a relative superiority of reservoir parameters (thickness and uniformity) for the Hulett sandstone over other potential storage units, such as the Muddy and Lakota sandstones (**Fig. 3.4.8**). It is important to note the overall strong correlation between logfacies modeled for the two wells having 5-

miles separation between them. It indicates that the study area is characterized by a good lateral continuity of the Sundance/Morrison and the Minnelusa/Goose Egg reservoir/seal pairs. On the contrary, the Muddy/Dakota/Lakota sandstones demonstrate a high degree of heterogeneity, vary in thickness, and are thinly interlayered with shale beds.

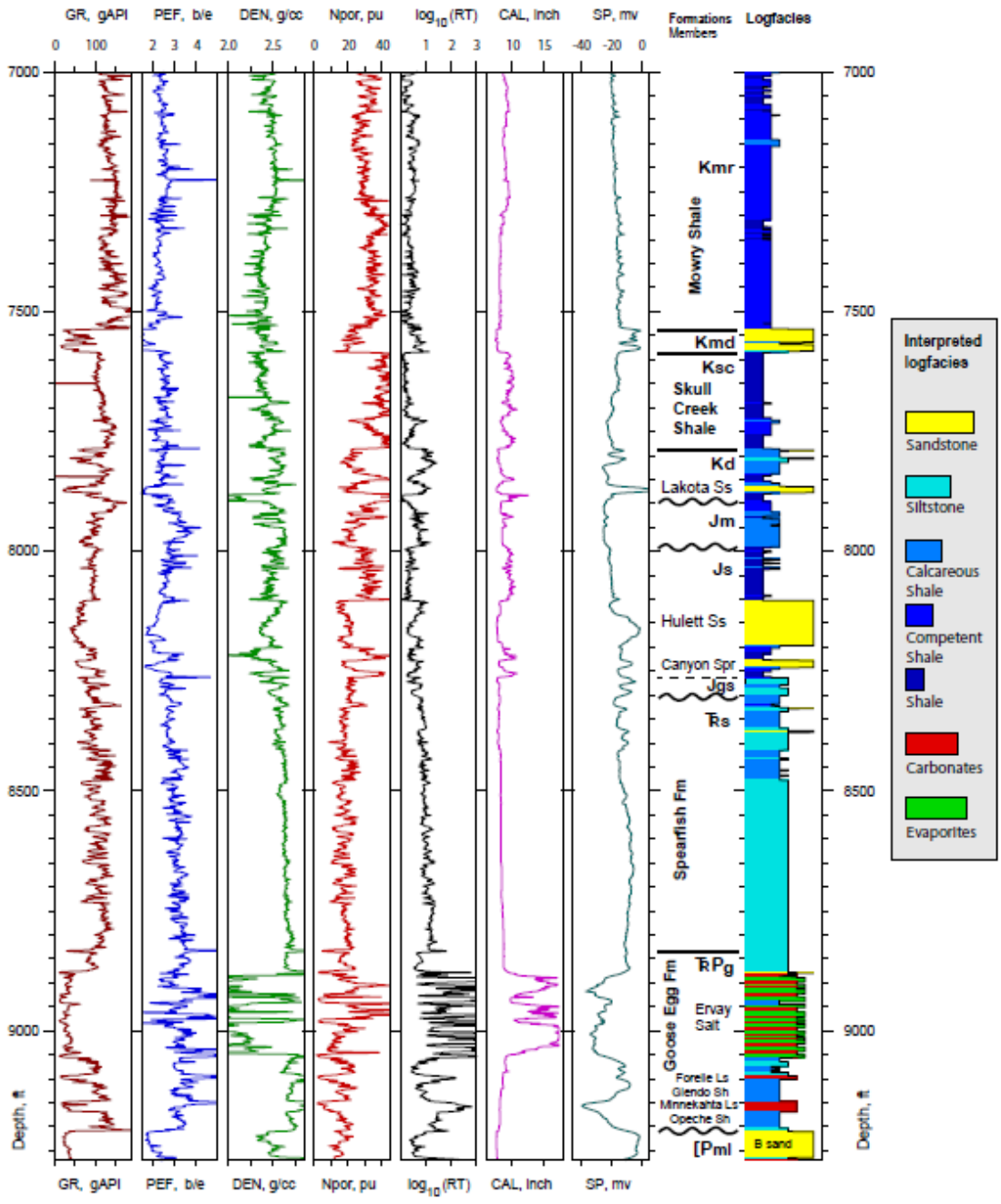

Figure 3.4.8 Wireline logs from the DW STATE #22-11 well (API 550273, PRB, Wyoming) and color coded logfacies profile (the rightmost panel) obtained from the logs cluster analysis.

Synthetic seismogram modeling

Synthetic seismogram, commonly called synthetic, allows predicting seismic response of the Earth by means of forward modeling. Convolving the reflectivity function, derived from digitized sonic velocity and density logs, with the wavelet derived from seismic data, generates the synthetic. A synthetic seismogram is the fundamental link between well data and seismic data, and it is the main tool (along with a vertical seismic profile, if available) that allows geological markers to be associated with reflections in the seismic data. By comparing formation tops picked on well logs with major reflections on the seismic section, interpretations of the data can be improved. Besides, forward modeling can elucidate the potential utility of seismic technique prior to acquisition of field seismic data. Modeling prior to acquisition gives a good indication whether we will be able to resolve the geologic objective and to ensure that appropriate field acquisition parameters are used. We will probably be able to identify our geologic objective on real seismic data if its seismic image is visible on synthetic seismogram.

To generate synthetic seismogram, we used digitized sonic velocity and density logs from the Globe-Federal 12-13 well that is located just one mile north of the Dry Fork Station (API 528388 in **Figure 3.4.3**). First, a reflectivity series was derived from the log data. The reflectivity series was then convolved with a Ricker wavelet of 125-foot-long wavelength to produce a synthetic seismogram in depth domain. The corresponding depth-to-time transformed synthetic version was filtered with the 20 – 70 Hz bandwidth to match the real seismic data. The depth-domain version of synthetic seismogram is shown in **Figure 3.4.9** together with wireline logs and interpreted lithology column. The synthetic spans rocks ranging from Permian to Cretaceous age.

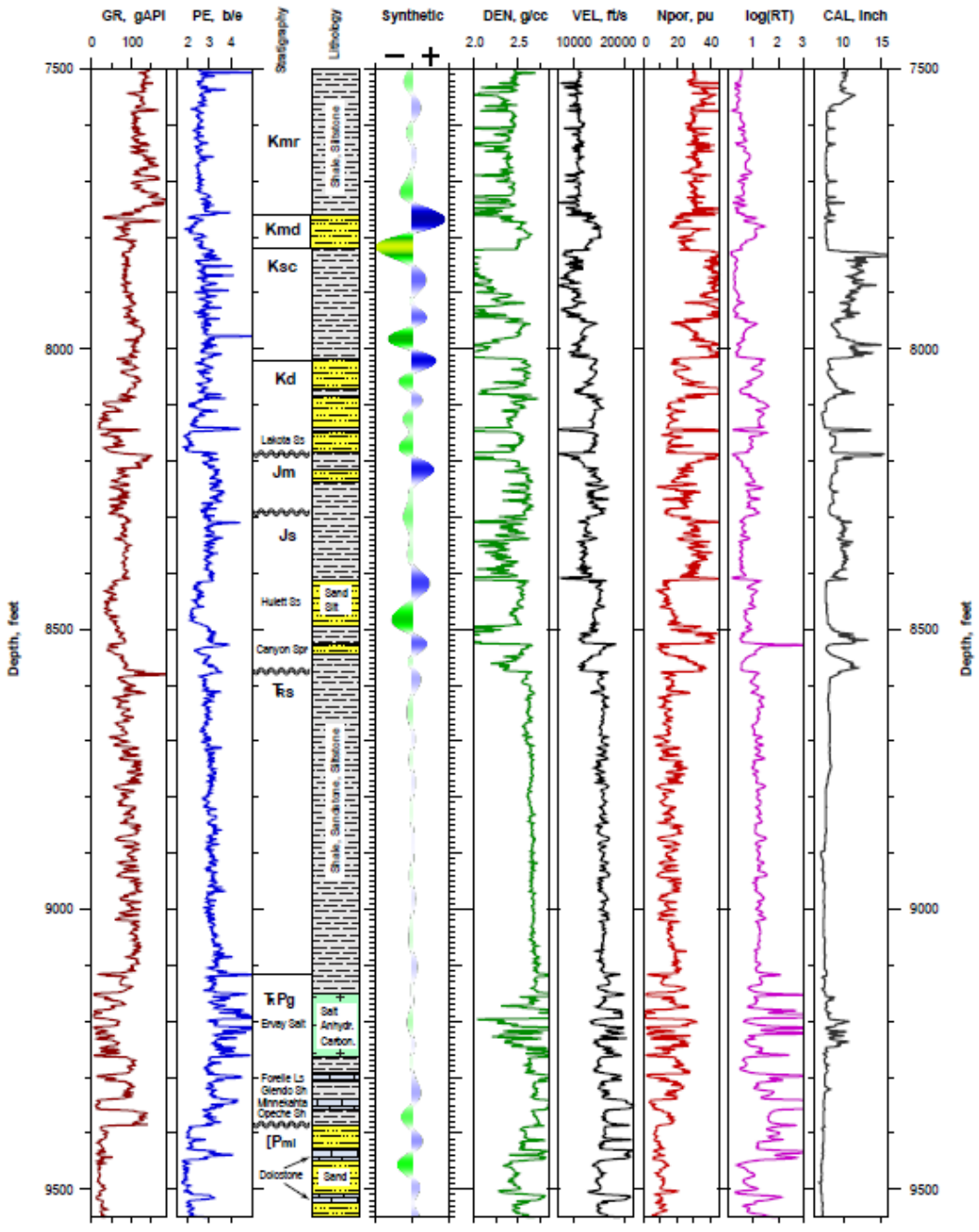

Figure 3.4.9 Interpreted wireline logs from the Globe-Federal 12-13 well (API 528388, PRB, Wyoming) with synthetic trace inserted next to the lithology column.

Synthetic seismic response within the Mesozoic section indicates that 3D seismic data should be able to determine reservoir sand extent seen in logs at the DFS study site. Indeed, the tops of the major sandstone bodies (the Muddy, Dakota, and Hulett) correlate with seismic peaks (positive amplitude) in the produced synthetic (**Figure 3.4.9**). Rocks within the Spearfish Formation appear to be seismically transparent, since they are

relatively uniform as seen in velocity/density log profiles; we should not expect any significant seismic reflections within this interval. The Minnelusa sands show up in synthetic with relatively low increase in reflectivity (**Figure 3.4.9**). A possible reason for low-amplitude Minnelusa event is thin-bed tuning that is referred to as the modulation of seismic amplitudes due to constructive and destructive interference. Furthermore, the presence of high-velocity carbonate layers within and above the Minnelusa sands contributes to loss of seismic amplitude due to additional destructive interference. Note that variations in shale, dolomite, and sand thicknesses affect seismic amplitude and make it difficult for seismic data to delineate the Minnelusa sands, especially when their thickness is less than quarter wavelength.

We tried to match the synthetic seismogram obtained at the DFS site to a segment of real seismic data acquired several miles away from the site. To do this, we first transformed the synthetic into time domain, and then filtered it with the bandwidth (20-70 Hz) of seismic section. The results of comparison, presented at the same time scale and similar in amplitude color, are shown in **Figure 3.4.10**. There is a relatively strong correlation between synthetic and seismic data, especially within the time interval corresponding to the Mesozoic-age strata. This is an encouraging result indicating (1) the possibility to image sandstone reservoirs in seismic reflected wavefield, and (2) a significant extent and lateral continuity of the Mesozoic reservoir/seal pairs in the study area.

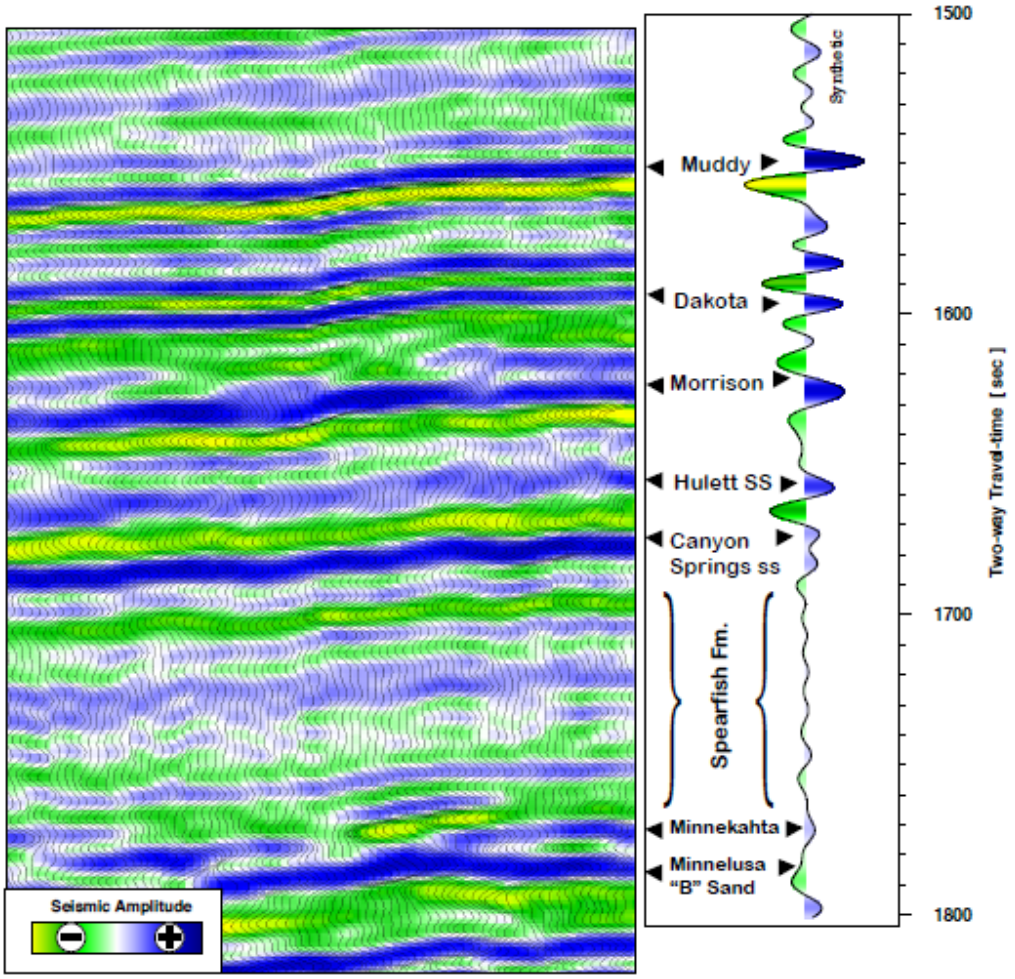

Figure 3.4.10 Segment of a seismic amplitude section from a 3-D survey located northeast of the GLOBE-FEDERAL 12-13 well location (API 528388). The right-hand panel shows formation tops with synthetic seismic trace obtained at the well from sonic and density logs (time-transformed, 125-foot-long Ricker wavelet filtered with 20-70 Hz band-pass filter).

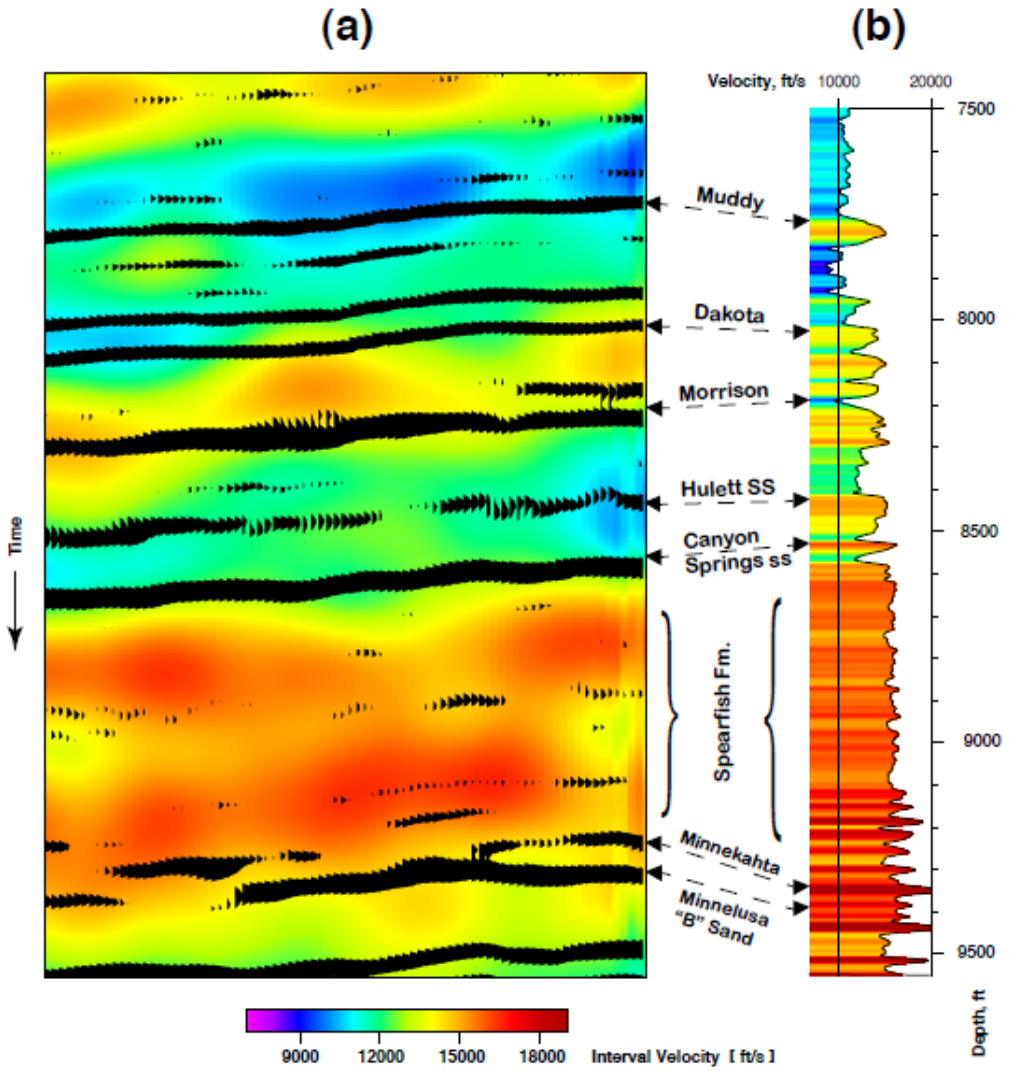

Figure 3.4.11 Correlation between seismically derived interval velocities and sonic-log velocities. (a) Segment of a seismic interval velocity section from a 3-D survey located northeast of the GLOBE-FEDERAL 12-13 well location (API 528388). (b) Interpreted sonic velocity profile for the GLOBE-FEDERAL 12-13 well. Note the same color scheme for both panels.

Figure 3.4.11 shows another way to calibrate seismic data with well-log information. Here we present the same section as in **Figure 3.4.10** but overlain with seismically derived interval velocities, and compare it to sonic-log velocities from the Globe-Federal 12-13 well. Both velocity profiles demonstrate highly variable Cretaceous- and Jurassic-age part of the section. This is due to interlayering of contrasting in physical properties of sandstone and shale layers. There is an abrupt increase in velocity for the underlying rocks of the Spearfish Formation that is equally visible both in the sonic velocity profile and seismic section (**Figure 3.4.11**). As the result of the above observations, we propose that dense seismic velocity analysis can be used in the study area for lithology identification in vertical sections. In case of horizon-based analysis (assuming negligible lithology variations along them), interval velocity maps can be

interpreted in terms of porosity variations, and hence, can be used to characterize the reservoir quality.

Predicting Permeability in Sundance sandstones

Porosity-Permeability Relation. The most obvious control on permeability is porosity. However, permeability also depends upon the interconnectivity of the pores, and that in turn depends on the size and shape of grains, the grain size distribution, and such other factors as wetting properties of the rock and diagenetic history. For sandstone reservoirs of the Sundance Formation, some generalizations can be made:

- The smaller the grains, the smaller the pores and pore throats, and the lower the permeability.
- Secondary porosity is negligible; thus, the bulk permeability is controlled solely by matrix (primary) porosity.

Under these assumptions and based on empirical knowledge (e.g., Archie 1950, Nelson 1994, Nelson 2004), permeability can be estimated from the relationship

$$log\ (k)\ = a\varphi + b. \qquad (3.4.1)$$

Almost invariably for a consolidated sandstone, a plot of permeability (k) on a logarithmic scale against porosity (φ) results in a clear trend with a degree of scatter associated with the other influences determining the permeability. **Figure 3.4.12** shows a $log\ log\ (k)$ -vs.-φ plot for the rock samples from the Hulett and the Canyon Springs sandstone members (the rock samples were collected by Davin Bagdonas and later measured at Piri Technologies, LLC). There is a strong linear correlation (R^2=0.80) between $log\ log\ (k)$ and φ with a relatively steep trend that is characteristic of "tight gas sands" (Nelson 1994). Clearly, permeability can be predicted from porosity in such an environment.

With insertion of the regression coefficients into **Eq. 3.4.1**, the corresponding power-law equation for the Sundance sandstones permeability will be:

$$k = 10^{(0.243\varphi - 3.098)}. \qquad (3.4.2)$$

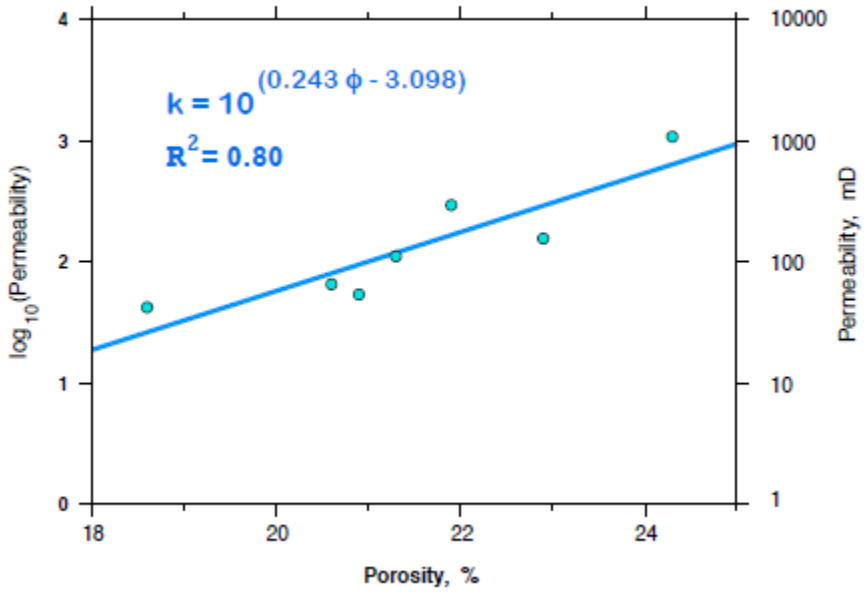

Figure 3.4.12 Semilog plot of permeability vs. porosity measurements for the rock samples from the Sundance Formation, Dry Fork study area, Wyoming. The line of best fit, its equation, and coefficient are shown in blue color.

Porosity-Permeability Estimation. We used six logged wells designated in Figure 4.4.3 for porosity-permeability estimation within the sandstone members of the Sundance Formation. We used **Equation 3.4.2** to calculate continuous permeability profiles for the lower part of the Sundance Formation, while the density log was used to calculate porosity in all six wells. Density porosities were derived assuming a mono-component mineral composition (sandstone with matrix density $\mathbf{r}_{ma}$= 2.65 g/cc) for the whole depth interval containing sand bodies (about 200 feet). We also assumed the pore fluid density $\mathbf{r}_f$= 1 g/cc, and then the final formula for porosity estimation is:

$$\varphi = 100*(\mathbf{r}_{ma} - \mathbf{r}_b)/\mathbf{r}_{ma} \qquad (3.4.2)$$

Where $\mathbf{r}_b$ is bulk density as measured by the logging tool, and φ is measured in percent.

The calculated porosity profiles built for the lower part of the Sundance Formation are shown in **Figures 3.4.13** through **3.4.18**. In all these Figures, the calculated porosity curves (green color) overlay the measured neutron porosity readings (orange bar graphs). Although the neutron porosity tool was set-up in all cases to give the true porosity in water filled sandstone, a significant mismatch between the density porosity and the neutron porosity exist in all six **Figures** (**3.4.13-3.4.18**). This mismatch within the sandy intervals may indicate (1) incorrectness of our mono-component matrix composition assumption, and (2) that neutron porosity tool actually measures hydrogen content but not porosity. It is a well-established fact that elevated neutron porosity readings within the shales are due to clay minerals that have a high ability to bond with

water molecules. Combining the neutron and density responses has for a long time been one of the principal and standard ways of deriving porosity. The rationale is simple; two readings combined are better than just one. Even so, we prefer to use the density log alone, because the density response is more consistent and has better vertical resolution than most neutron tools.

The permeability profiles shown in **Figures 3.4.13** through **3.4.18** (the rightmost curve) are characterized by significant variability (about three orders of magnitude) even within the sandstone bodies of the same well. Most of permeability estimates for the Hulett-Canyon Spring Sandstones of the Sundance Formation lie between 0.001 and 100 millidarcies. Although there are few depth intervals within the Sundance stratigraphic interval where permeability has values above 1.0 mD, overall the Sundance sandstones in the study area can be classified as tight reservoirs.

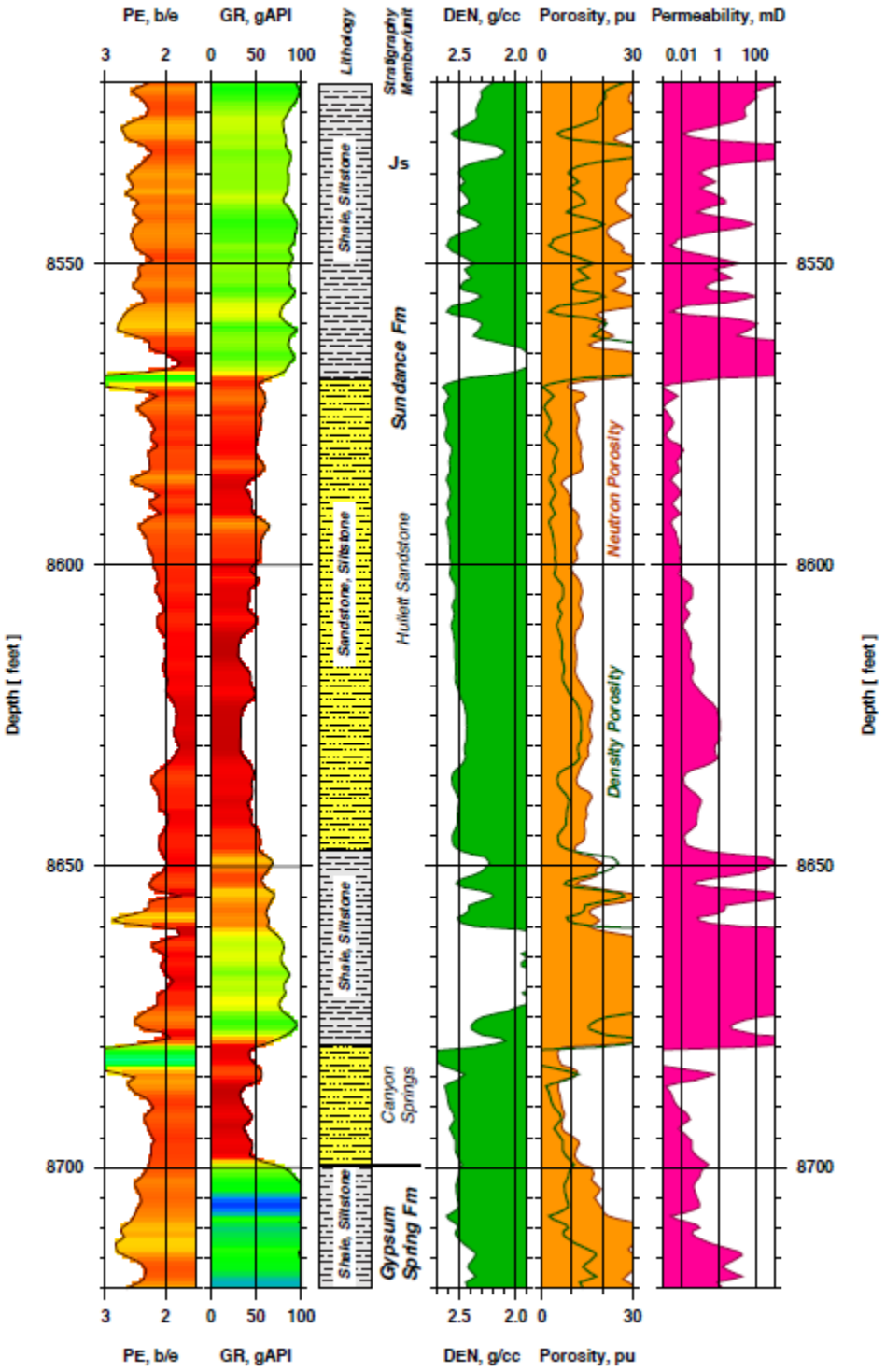

Figure 3.4.13 Interpreted logs from the WESTWIND 1 well (API 527564) for the lower Sundance stratigraphic interval, Dry Fork study area. Tracks from left to right are (PE) photo electric.

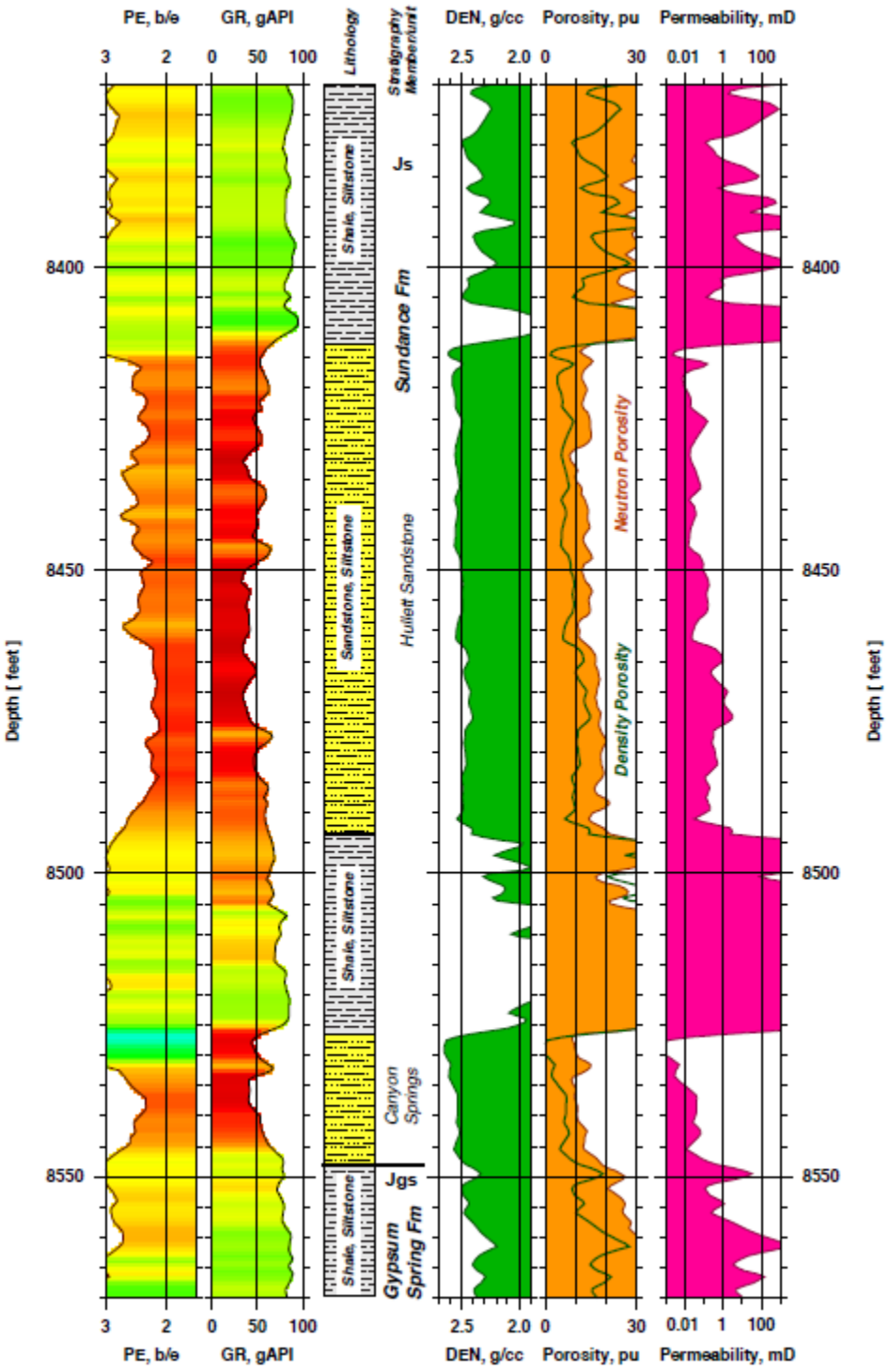

Figure 3.4.14 Interpreted logs from the Globe-Federal 12-13 well (API 528388) for the lower Sundance stratigraphic interval, Dry Fork study area. Tracks from left to right are (PE) photoelectric section, (GR) gamma ray, lithological interpretation, (DEN) formation density, Neutron (orange), and Density Porosity (grenn curve), and modeled Permeability.

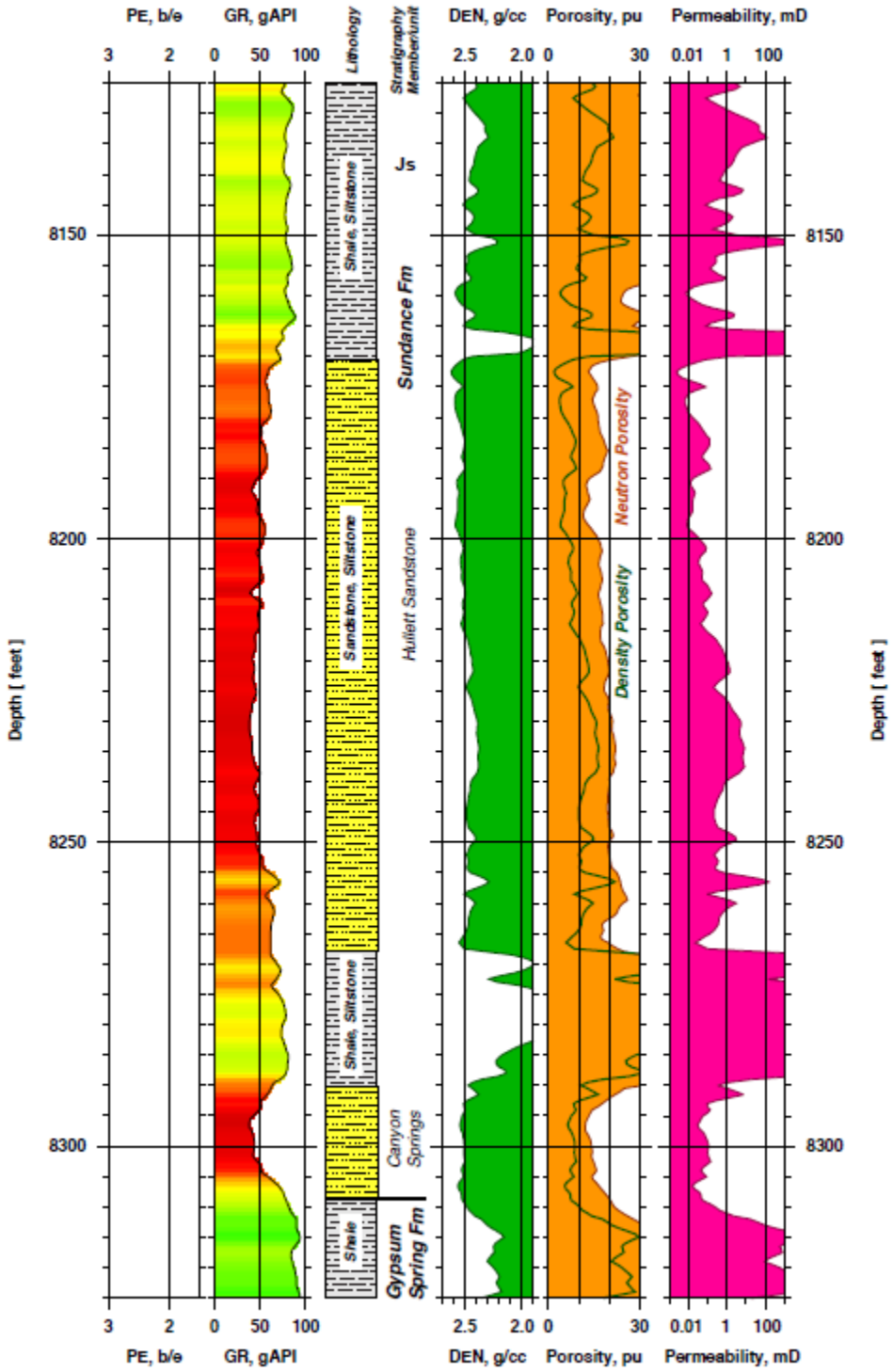

Figure 3.4.15 Interpreted logs from the FEDERAL 23-20 well (API 529791) for the lower Sundance stratigraphic interval, Dry Fork study area. Tracks from left to right are (PE) photoelectric section, (GR) gamma ray, lithological interpretation, (DEN) formation density, Neutron (orange), and Density Porosit (green curve), and modeled Permeability.

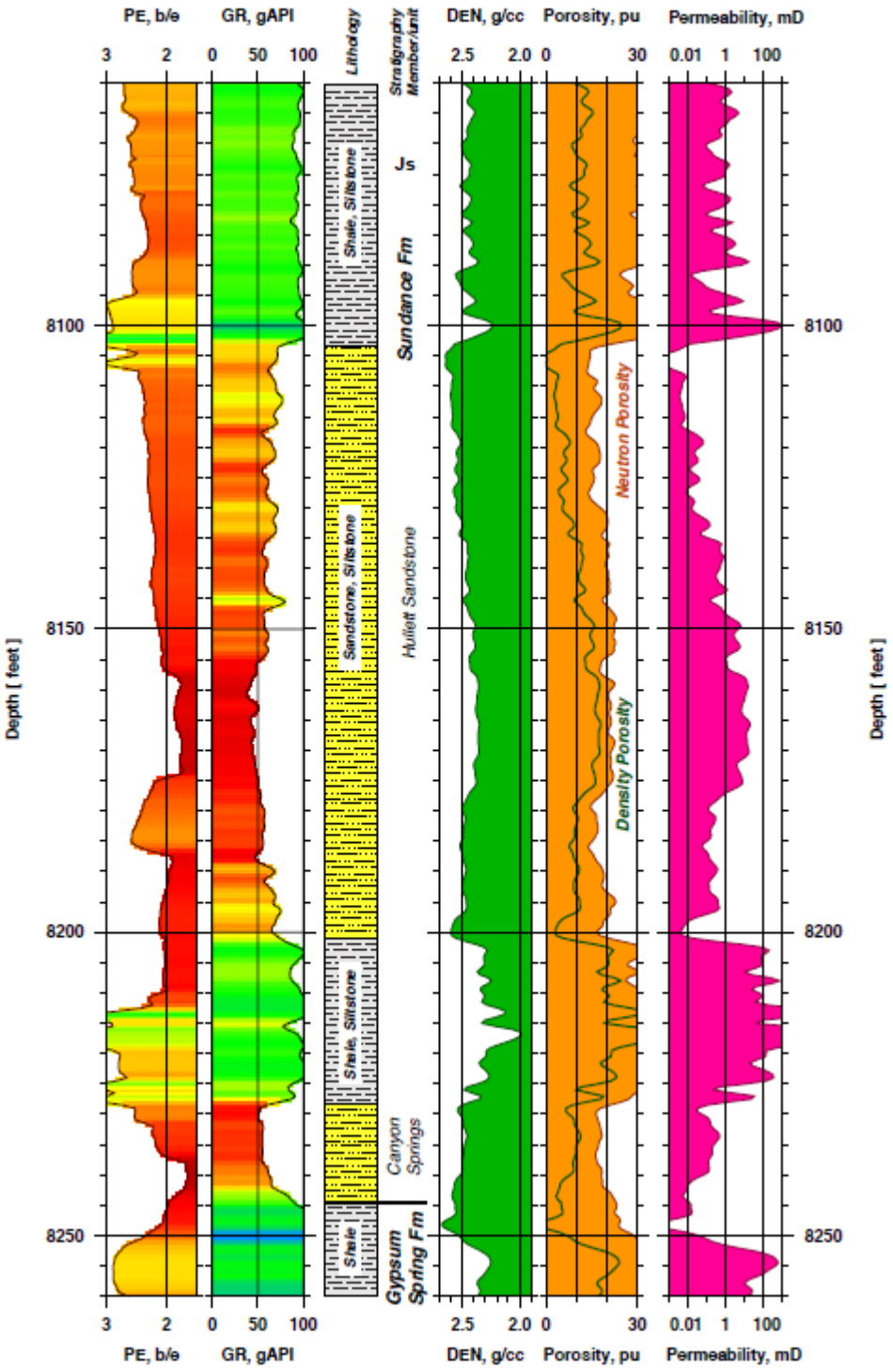

Figure

Figure 3.4.16 Interpreted logs from the STATE 22-11 well (API 562532) for the lower Sundance stratigraphic interval, Dry Fork study area. Tracks from left to right are (PE) photoelectric section, (GR) gamma ray, lithological interpretation, (DEN) formation density, Neutron (orange), and Density Porosity (green curve), and modeled Permeability.

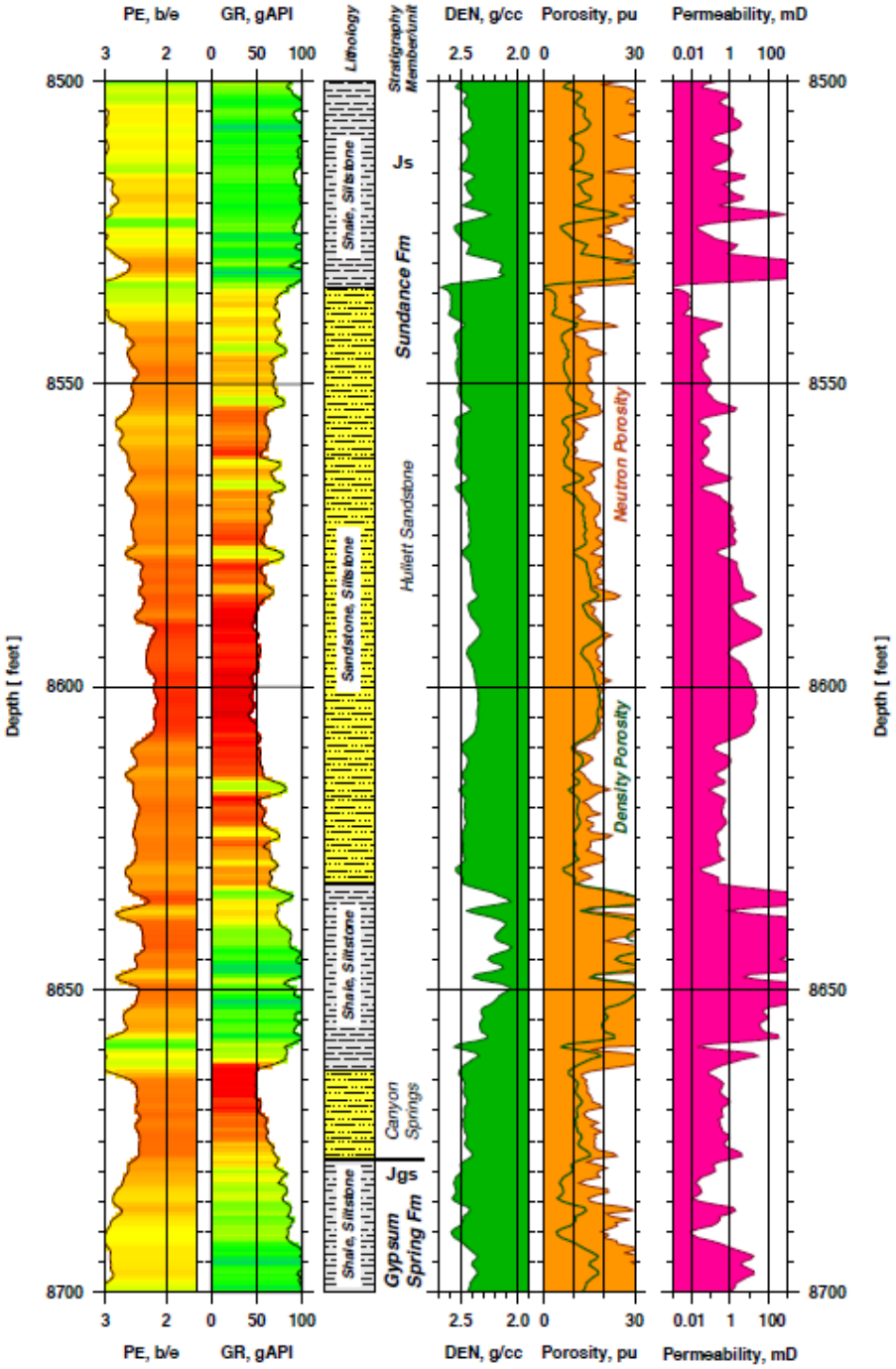

Figure 3.4.17 Interpreted logs from the State 44-16-5071 well (API 562465) for the Sundance stratigraphic interval, Dry Fork study area. Tracks from left to right are (PE) photoelectric section, (GR) gamma ray, lithological interpretation, (DEN) formation density, Neutron (orange), and Density Porosity (green curve), and modeled Permeability.

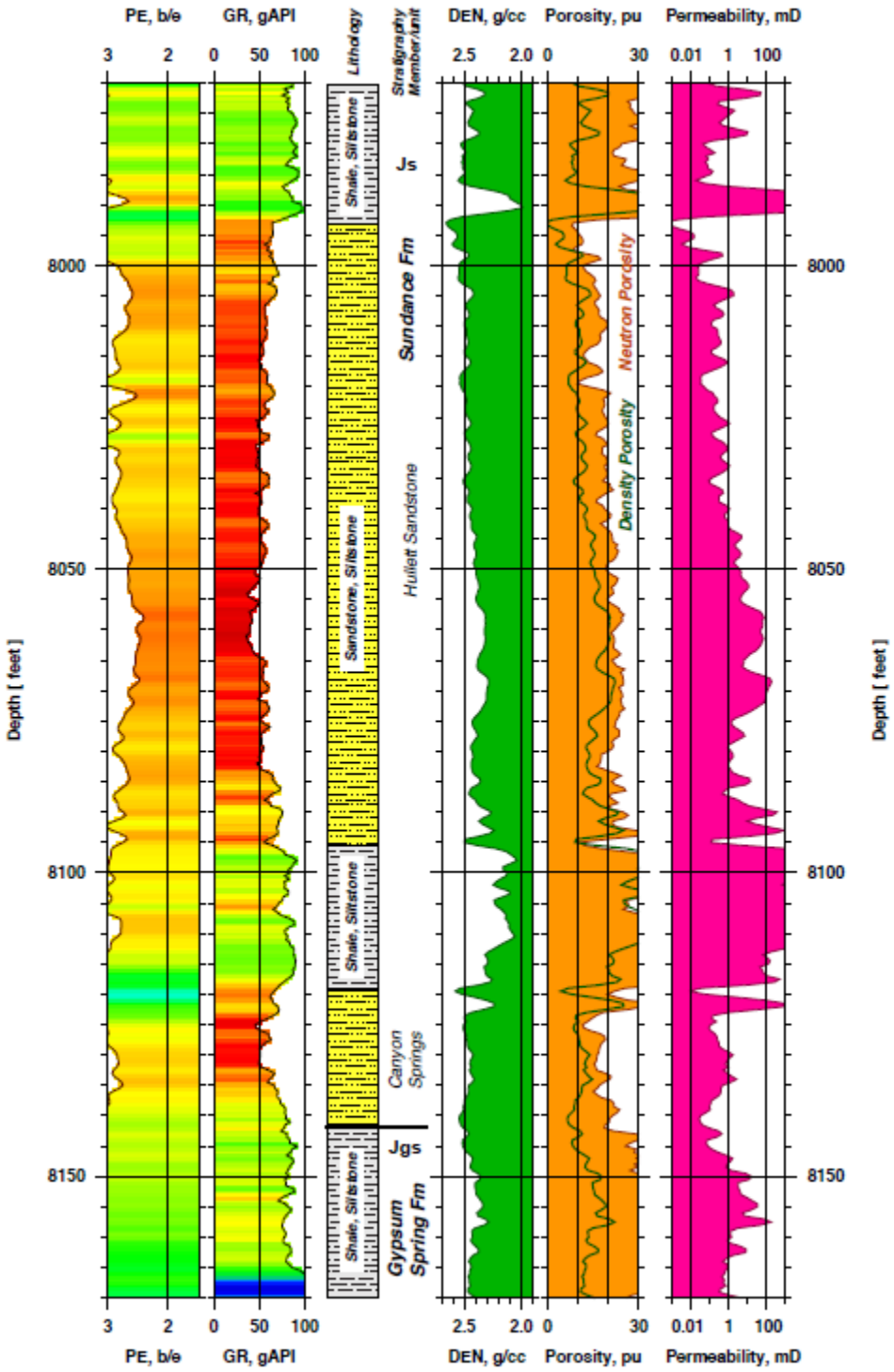

Figure 3.4.18 Interpreted logs from the Callaway 15-5 well (API 562532) for the lower Sundance stratigraphic interval, Dry Fork study area. Tracks from left to right are (PE) photoelectric section, (GR) gamma ray, lithological interpretation, (DEN) formation density, Neutron (orange), and Density Porosity (green curve), and modeled Permeability.

Statistical Descriptors of Porosity and Permeability. Plots of petrophysical data vs. depth, like those in **Figures** (**3.4.13-3.4.18**), can be used to distinguish and separate geologic units. However, many modern flow simulation routines require a general quantitative reservoir descriptor obtained from data samples that are treated as random variables and are not attributed to a specific location. Both the probability and cumulative distribution functions (histograms) are common statistical tools that can be used to derive such a generalized descriptor of a formation. We have combined the modeled permeability profiles for the interpreted sand intervals in **Figures** (**3.4.13-3.4.18**) into a single profile characterizing an average Sundance sandstone reservoir within the study area. Our interpretation estimates the total thickness of this averaged sandstone reservoir within the Sundance Formation to be 110 feet. We suggest using this value for geologic model development and simulation to be accomplished in the subsequent Tasks 5 and 6.

Figure 3.4.19 shows histograms of the porosity distribution within the Jurassic Hulett and Canyon Springs Sandstones, based on density log and sandstone matrix = 2.65 g/cc. To get the distribution and statistical averages, we used a total of 1336 data samples from the 110-ft-thick interval corresponding to a mean sandstone thickness within the Sundance Formation. The porosity distribution (**Fig. 3.4.19** top panel) appear to be slightly asymmetrical in shape with relatively close values of different averaging estimators: the arithmetic mean = 9.77%, the geometric mean = 8.19%, the median = 9.46%, and the mode = 7%. We suggest using **9.5%** as the best porosity descriptor of sandstone facies found within the Sundance Formation in the study area.

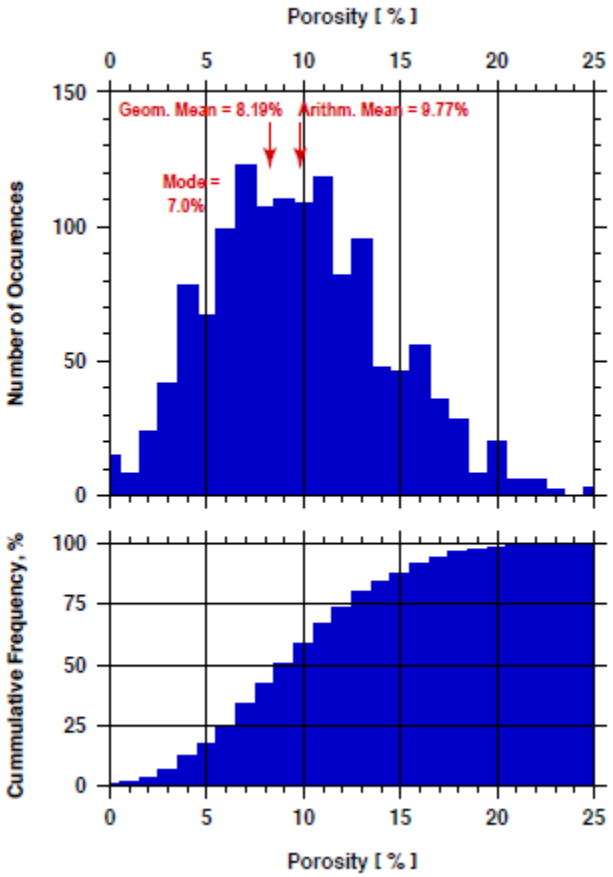

Figure 3.4.19 Ordinary (top panel) and cumulative (bottom panel) histograms of log-derived porosity interpreted for the the Jurassic Hullett-Canyon Spring Sandstones of the Sundance Formation based on log measurements in six wells with API's 527564, 528388, 529791, 562532, 550273, and 562465 in the Dry Fork Study area, PRB, Wyoming. Matrix density assumed for porosity calculations = 2.65 g/cc (siliceous sandstones).

The corresponding permeability distribution, modeled with Eq. 4.4.2, is shown in **Figure 3.4.20**. Plotted on a logarithmic scale, the permeability is characterized by a multi-peak, slightly right-skewed distribution. Unlike a symmetrical distribution, the skewed one has different averages produced by different estimators. In our case, we have the following results: the arithmetic mean = 6.26 mD, the geometric mean = 0.19 mD, the median = 0.16 mD, and the mode = 0.04 mD. Mean is what most people commonly refer to as an average. However, in this case, the arithmetic mean is 6.26 mD, which is much greater than the median value, 0.16 mD. Now, how well do these estimators represent the permeability population? According to Jensen et al. (2000), the geometric mean should produce a better estimate for a log-normal distribution. The permeability distribution of the Sundance sandstone facies has close to a log-normal shape (only slightly skewed); therefore, we might use the geometric mean (0.19 mD) as a statistical permeability estimate for all sandstone units within the Sundance Formation. The median (0.16 mD)

value is very close to the geometric mean; hence, we conclude that ***0.20 mD*** (here, the rounded average of the geometric mean and the median) would be the best permeability descriptor for sandstones of the Sundance Formation.

The cumulative histogram can be used to determine the number of permeability values within a given range that have occurred (interval probabilities). As can be seen in **Fig. 3.4.20** (lower panel), 50% of the data (samples) have a permeability value ($k_{0.50}$) of about 0.16 mD or less; that is the median value. 75% of modeled data have permeability estimates of 1.0 mD or less (**Fig. 3.4.20**), and hence, can be classified as tight gas sands. Only 25% of cumulative sandstone thickness of the Sundance Formation can be considered as relatively good quality reservoirs; that is cumulative reservoir thicknesses of the Sundance storage units do not exceed **30 feet** within the study area.

The Dykstra-Parsons coefficient (V_{DP}) is commonly used in the petroleum industry as a measure of permeability variation or reservoir heterogeneity (Jensen et al. 2000). It is defined as

$$V_{DP} = \frac{k_{0.50} - k_{0.16}}{k_{0.50}}, \tag{5.6}$$

where $k_{0.50}$ is the median permeability and $k_{0.16}$ is the permeability one standard deviation below the median on a log-probability plot. V_{DP} ranges between zero (0.0) for absolutely homogeneous reservoirs and one (1.0) for "infinitely" heterogeneous reservoirs. With a V_{DP} of **0.95** and average permeability of **0.2** mD, the Jurassic Hulett and Canyon Springs sandstones can be considered as poor quality reservoirs with a high degree of heterogeneity. However, there is a chance of about 30-foot-thick interval occurrence within the Hulett sandstone with better reservoir properties. 3D high-resolution seismic will be a good tool to delineate this "sweet spot."

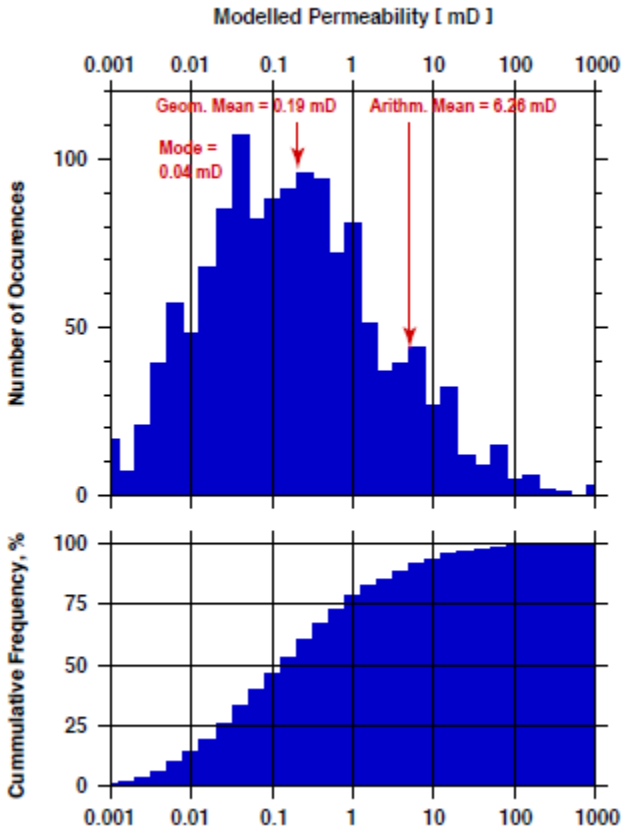

Figure 3.4.20 Permeability distribution within the Jurassic Hullett-Canyon Spring Sandstones of the Sundance Formation based on log data from wells with API's 527564, 528388, 529791, 562532, 550273, and 562465 in the Dry Fork Study area, PRB, Wyoming. Ordinary histogram (top); cumulative histogram (bottom).

Nugget vs. Hulett: reservoir properties comparison

The Jurassic Nugget Sandstone in the Rock Springs Uplift (RSU) can be considered as the counterpart of the Jurassic Hulett and Canyon Springs sandstones in the Powder River Basin (PRB). Based on the core and log data analysis performed at the RSU #1 site (McLaughlin et al., 2013) and adjacent wells, an average porosity value for the Nugget is about 13% and the corresponding permeability is 20 mD. Based on these parameters, the Nugget possesses much better reservoir characteristics compared to the Sundance sandstones in the PRB. So, what causes this big difference in reservoir properties? We used well-log data from the two sites and petrophysical analysis in order to answer this question. **Figure 3.4.21** shows composition-porosity interpretation on a neutron-density crossplot done for the Nugget Sandstone at the RSU #1 site. Almost all data points cluster along the clean (quartz) sandstone line that indicates dependence of both density and

neutron porosity on total porosity variations. Hence, quartz minerals dominate the Nugget Sandstone formation. Only a small amount of data points deviate from the sandstone line towards the lower density values. These points are also characterized with increased gamma ray readings (green color) indicating appearance of clay minerals. **Figure 3.4.22** shows exactly the same kind of crossplot done for the wells in the DFS study area (PRB). All of the data points in this plot are shifted downwards relative to the clean sandstone line. It indicates elevated shale fraction presence in the Hulett and the Canyon Springs sandstones compared to the Nugget. The abundance of clay minerals makes sandstone formations more tightly compacted with poor interconnectivity of the pores due to clay cement development. Besides, the smaller grain size and platy shape of clay minerals also declines permeability and worsens reservoir properties.

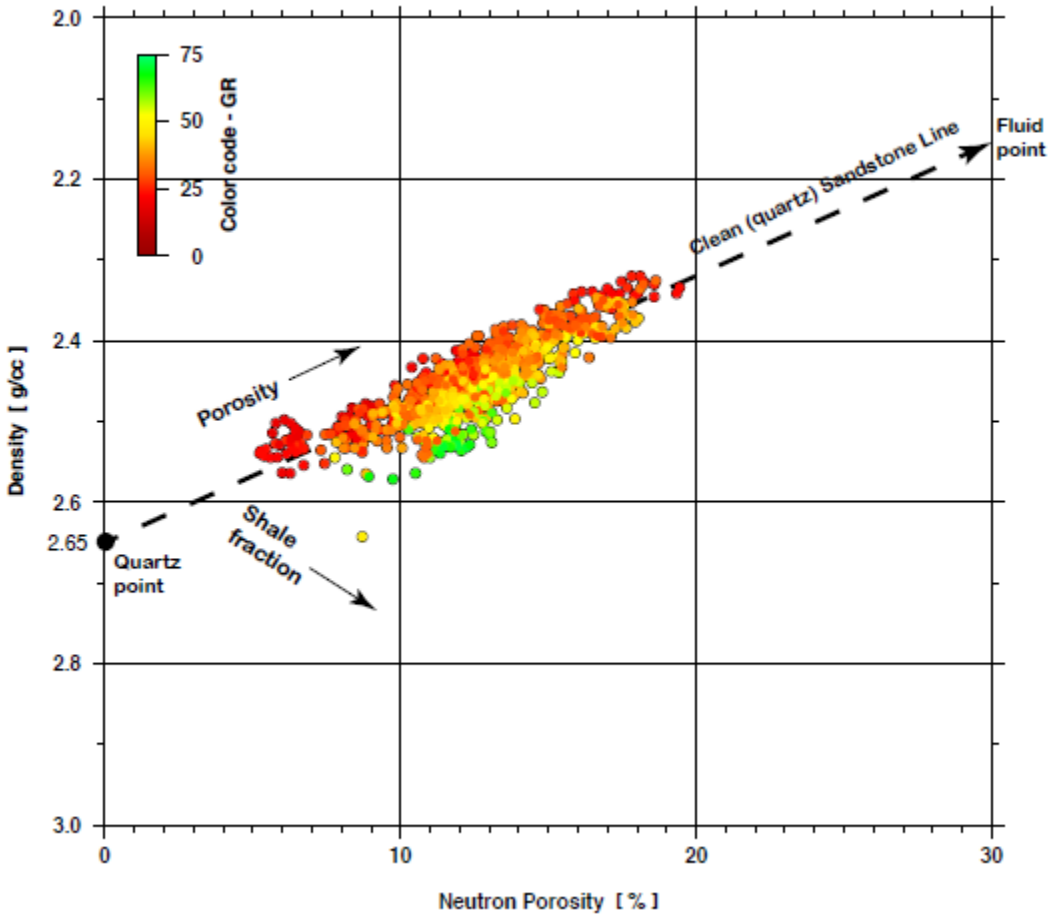

Figure 3.4.21 Composition-porosity interpretation on a neutron-density crossplot of log data for the Nugget Sandstone (9,216 - 9.660 ft. depth intervak), RSU #1 well, Rock Springs Uplift, Wyoming. The color code is gamma-ray intensity. Note that neutron tool was set up to read the true porosity in water bearing sandstones (with a matrix density of 2.65 g/cc). Note also that true formation porosity increases from left to right along the "clean sandstone" trend-line, and the shale content increases towards the bottom right corner of the crossplot.

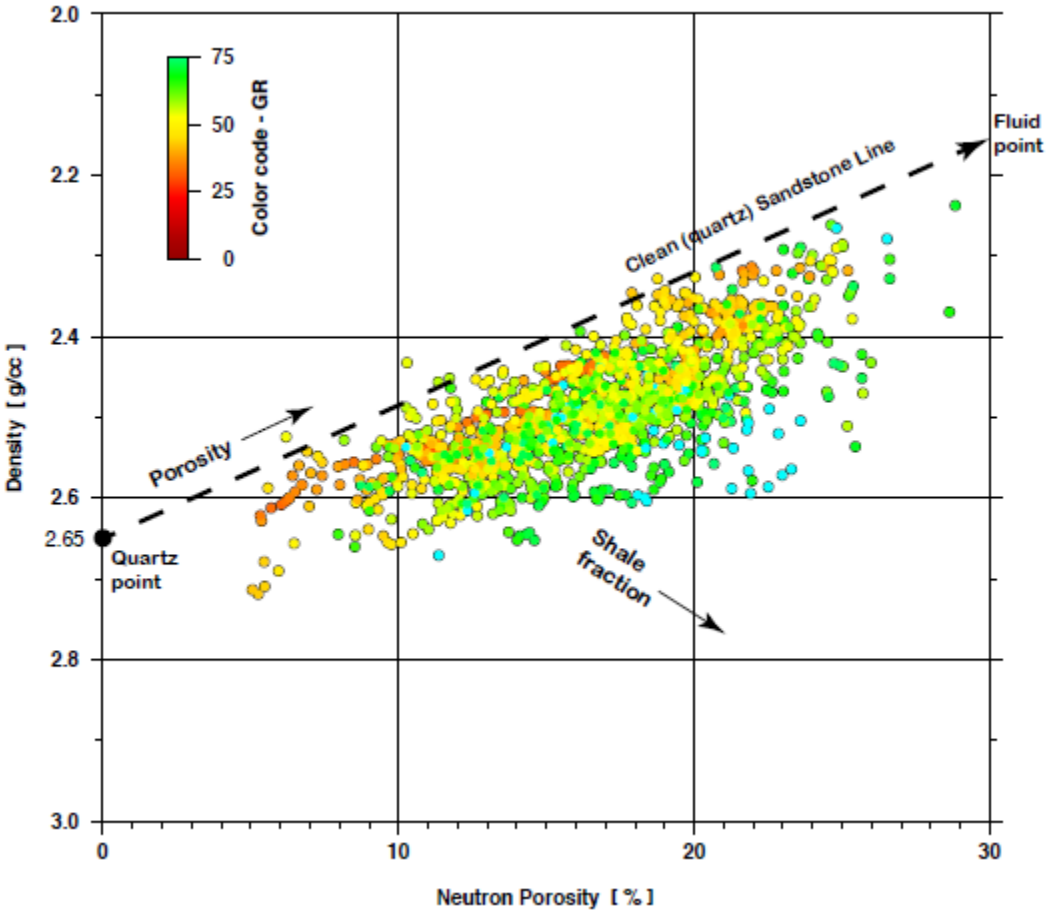

Figure 3.4.22 Composition-porosity interpretation on a neutron-density crossplot of log data from six wells with API's 527564, 528388, 529791, 562532, 550273, and 562465 in the Dry Fork Study area, PRB, Wyoming. The color code is gamma-ray intensity. For all six wells, the measured depth interval corresponds to the Jurassic Hullett-Canyon Spring Sandstones of the Sundance Formation. Only those measurements were considered that fall within the interpreted sandstone intervals. Note that neutron tool was set up to read the true porosity in water bearing sandstones (with a matrix density of 2.65 g/cc). Note also that true formation porosity increases from left to right along the "clean sandstone" trend-line, and the shale content increases towards the bottom right corner of the crossplot.

Utility of dense seismic velocity analysis technique for assessing deep sequestration targets in the Powder River Basin, Wyoming: Minnelusa Sandstone

The upper Minnelusa sandstones have yielded significant reserves in Wyoming's Powder River Basin (PRB). However, geologic complexities have made these sandstones an elusive target. This report briefly describes the utility of seismic velocity analysis technique, which can decrease uncertainty in the exploration of Minnelusa sandstones. The methodology proposed in this study is based on an enormous velocity contrast between different lithologies constituting the Upper Minnelusa. Multiple sonic logs available in the area clearly indicate the difference in compressional wave velocities

between the Permian-age rocks of different mineral composition. The range of sonic-velocity readings in the study area generally agree with the laboratory measurements presented in the following table.

Table 3.4.1. Typical sonic P-wave velocities:
(The Geological Interpretation of Well Logs, M. Rider and M. Kennedy, 2011)

Lithology	Porosity Range	Vp (ft./s)
SHALE	0% - 20%	18,000 - 8,000
SANDSTONE	5% - 20%	16,500 - 11,500
LIMESTONE	5% - 20%	18,000 - 13,000
DOLOSTONE	0% - 20%	23,000 - 15,000

Seismic velocity analysis scheme proposed in this study assumes anisotropic earth model (possibly multilayered) with sub-horizontal beds that produce only primary reflections. The algorithm seeks to create instantaneous velocity and anisotropic parameter from semblance estimates. Our objectives are twofold, (1) to estimate porosity by inverting effective velocity into the interval one, and (2) to obtain sandstone vs. dolostone and sandstone vs. shale distributions from velocity and anisotropy parameters. To extract these parameters from a seismic survey, automated nonhyperbolic velocity analysis routine was recently designed and tested. The DGL "vest" freeware (http://www.uwyo.edu/cmi/dgl-software/) enables a simultaneous estimate of parameters affecting reflection traveltime, $\boldsymbol{V}$nmo, and anisotropy $\boldsymbol{\eta}$. The anisotropy parameter $\boldsymbol{\eta}$ allows to discriminate shales from the massive rock formations, such as sandstones and dolostones, and $\boldsymbol{V}$nmo can be converted to interval velocity, for example, with the DGL's "dix" utility. As a result, dense volumes of both interval velocity and anisotropy attributes can be calculated for every data sample of a seismic survey.

Seismic velocity anomalies associated with thick Minnelusa sandstone lenses: a case study. The Minnelusa Formation in the PRB can be divided informally into lower, middle, and upper members. The lower and middle members are Pennsylvanian in age and the upper unit is Permian. In the eastern part of the PRB, the upper member of the Minnelusa, based on oil company terminology, is divided into five successions or cycles— A, B, C, D, and E, with E being the oldest cycle. Generally, each depositional cycle consists of dolomite, evaporitic succession, and overlying sandstone. Lateral variation of the carbonate-sand cycle is common and can make correlation difficult. The sandstones in the lower D and E zones are seldom penetrated because all production to date is from the upper Minnelusa A, B, or C zones. The A, B, and C zones are a complex succession of dolomite, evaporite, and sandstone. Of the three, the C zone is the most continuous, extending over the entire basin, exhibits the best lateral and vertical continuity, and has the best porosity and permeability. Sea-level fall at the close of Minnelusa time exposed the Minnelusa surface to various amounts of erosion by fluvial processes, leaving isolated to partly isolated remnants of the A zone and B zones and, in places, incised into the C zone. The surface was covered with a saline pan system of

bedded anhydrite and halite, red mudstone, siltstone, and thin sandy layers of the Opeche Shale.

Figure 3.4.23 shows a map of seismically derived interval velocity distribution along the Minnelusa reflection horizon. The accuracy of seismic horizon picking and sonic-to-seismic tie was validated with two synthetic seismograms generated at well locations numbered 508 and 435 (**Fig. 3.4.23**). Relative correlation strength between synthetic trace and seismic data can be examined in **Figure 3.4.24**. It is characterized by Pearson's correlation coefficient **r** = 0.67 over time window of about 500 msec. This result indicates a high degree of confidence in the interpreted sonic-seismic tie. A good continuity of seismic reflections observed in **Figure 3.4.24** made it possible to auto-track the Minnelusa horizon throughout the whole data volume. Only minor corrections were made after manual examination of the tracked horizon. The velocity distribution map shown in **Figure 3.4.23** is characterized by a big degree of lateral heterogeneity with overall velocity variations from 12,500 ft./s to 16,500 ft./s. This result may seem to be suspicious for a lithologically uniform stratigraphic unit. There are two important things that must be considered before making interpretation. First, the Upper Minnelusa Member within the study area represents a stack of silica-carbonate intercalated deposits with extremely contrasting P-wave velocities, and second, seismically derived interval velocities possess a limited vertical resolution. The last statement means that the time (or depth) interval for seismic velocity estimation cannot be infinitely small due to the seismic method limitations. In our study, the vertical resolution limit do not exceed 100-feet interval. This means that interval velocities presented in **Figure 3.4.23** represent, at best, an averaged rock velocity within a 100-feet interval. At locations with increased seismic noise, the averaging interval becomes bigger, which deteriorates the resolution power of seismically derived velocities.

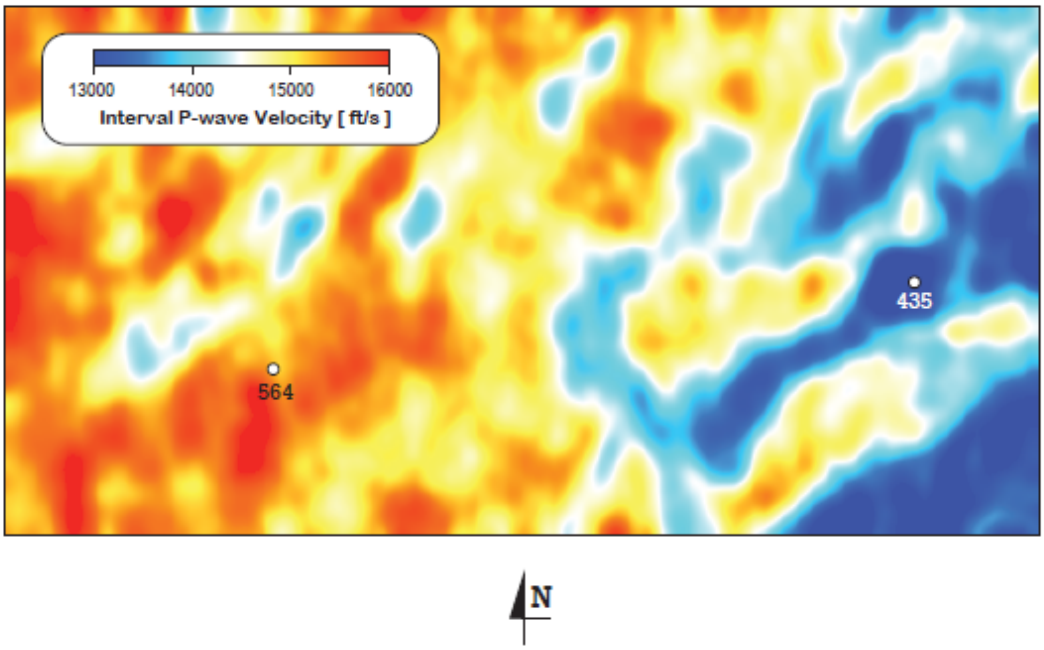

Figure 3.4.23 Seismic interval velocity map calculated along the Minnelusa stratigraphic interval, Powder River Basin, Wyoming. The enumerated white circles represent well locations with secured API numbers that were used for seismic data calibration.

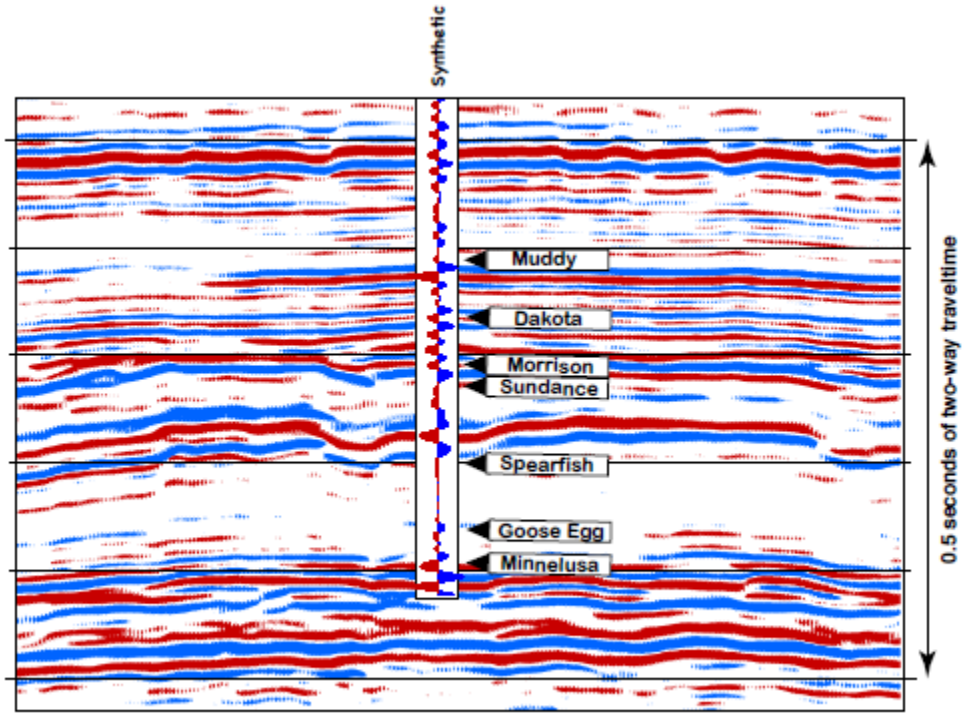

Figure 3.4. 24 Interpreted seismic profile with inserted synthetic trace generated from sonic and density logs from well with API 435.

In examining the sonic logs (**Fig. 3.4.25**), it was observed that the A, B, and C zones within the productive upper Minnelusa are very closely spaced. In the study area, the section from the top of Opeche shale to the top of the 'B' dolomite is about 100 ft. thick. Thus, any seismic reflection from this interval is likely a composite one, and correspondingly, seismically derived velocities characterize a mixture of different lithologies rather then a velocity within a lithologically uniform layer. Further examination of the two wells shown in **Figure 3.4.25** did show a marked velocity contrast between porous sandy Minnelusa and the tight dolomitic Minnelusa. This pronounced velocity difference (60-80%) provides an explanation of big discrepancies in seismic interval velocity map (**Fig. 3.4.23**) and gave us sufficient encouragement to correlate sonic and seismic observations. Seismic interval velocity map (**Fig. 3.4.23**) correlates with sonic velocities averaged over the upper Minnelusa (A, B, and C zones) stratigraphic interval, and thus, represents a distribution (ratio) of high-velocity, carbonate-rich rocks to low-velocity, silica-rich rocks within the investigated interval (~100-feet thick). Thus, high-velocity areas in **Figure 3.4.23** are interpreted to represent tight dolomitic sections (red colors), whereas low-velocity areas should include thicker porous sandy Minnelusa, and possibly, some of the Opeche Shale interval. The overall southwest-northeast orientation of low-velocity areas in **Figure 3.4.23** do correlate with prevailing depositional patterns in the PRB and may serve as a structural control on the reservoir rock location. We have been able to establish, in a systematic way, that Minnelusa sandstone buildups in the PRB can be detected with dense seismic velocity analysis. If the method presented here can be verified, then it should significantly aid in future mapping of the Upper Minnelusa sand extent. We also believe that the method can be used to establish and define seismic anomalies associated with other sand buildups in the Powder River basin and elsewhere, because the procedure described here, involving a combined geologic and geophysical investigation, should be widely applicable to seismic exploration for stratigraphic oil and gas traps.

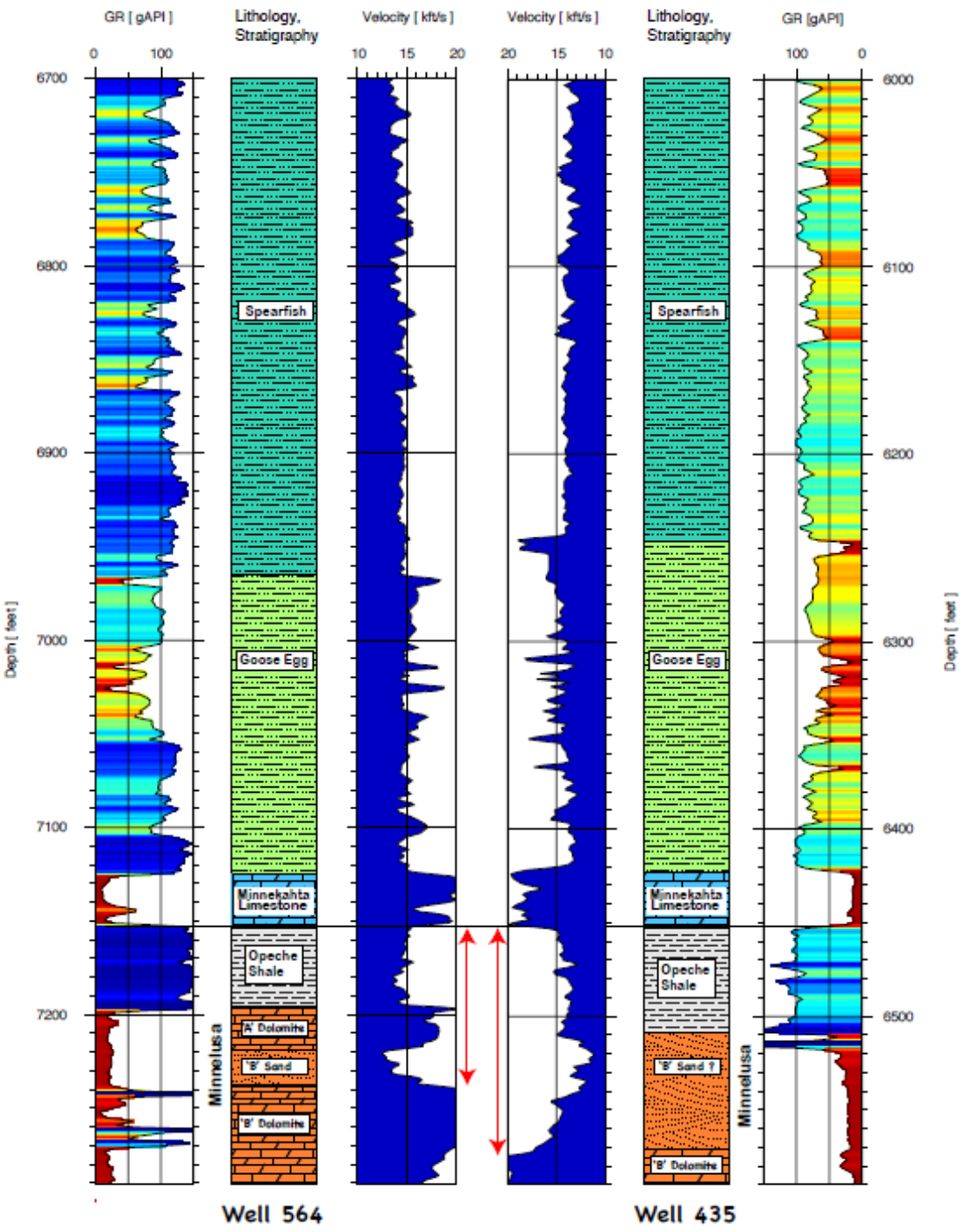

Figure 3.4.25 Interpreted wireline logs from wells 564 (left three panels) and 435 (right three panels), Powder River Basin, Wyoming. The logs are leveled at top of the Opeche Shale. Note a relative change in thickness of low-velocity interval below the Minnekahta Limestone (approximated with the double-headed arrows).

Determination of TDS in deep sedimentary formations by well-log analysis

Deep saline formations considered as CO_2 storage reservoirs in this study occur at a depth greater than 5,000 feet, the depth at which CO_2 in hydrostatic equilibrium is well above its critical pressure, and therefore, may be suitable for CO_2 injection. However, in the United States, for regulatory permitting of certain classes of underground injection wells, aquifers containing water with TDS of less than 10,000 mg/L are defined as underground sources of drinking water that are not appropriate for CO_2 injection. Therefore, an estimate of the chemistry of the pore-fluid within a potential reservoir is required to establish the possible environmental impact, which might develop during CO_2 injection.

While a detailed analysis of the chemical composition of a pore fluid can be obtained from a water sample only, an estimate of the total dissolved solids (TDS) in equivalent sodium chloride (NaCl) concentration can be obtained from well logs. Depending on the theoretical approach, various combinations of well logs can be used for TDS calculation: (1) spontaneous potential log; (2) deep- and shallow-reading resistivity logs; and (3) resistivity and porosity logs. The depth-temperature profile is additionally required for all the methods. The accuracy of TDS modeling strongly depends on assumptions underlying each method. In each particular study, the verification of TDS models becomes a difficult task because of the sparsity of both reliable logs and reliable analyses of water samples. In our study, we used high quality digital log data (LAS format) from wells produced by Schlumberger in 2014. These wells are Callaway 15-5 (15-51N-71W, API 562532) and State 44-16-5071 (16-50N-71W, API 562465). Both wells are logged up to the Minnelusa Formation with the location shown in **Figure 3.4.3**.

The TDS computational methods used in our study require (1) finding water resistivity (R_w) and (2) TDS estimation from a nomograph for NaCl water solutions (Log Interpretation Charts, Gen-6, Schlumberger, 2009 Edition). Knowing water resistivity and temperature, TDS in ppm of NaCl equivalents at 75˚F can be found. Alternatively, the Schlumberger nomograph can be fitted by the following equation (Dresser Atlas: Log Interpretation Charts, 1980):

$$\mathbf{NaCl_{75} = 10^{x}} \qquad (3.7)$$

where

$$\mathbf{x = (3.562 - \log(R_w(T+6.77)/(75 + 6.77) - 0.0123))/0.955}$$

and **T** is temperature in degrees Fahrenheit.

In our study, the above formula was introduced into a computer code enabling a continuous computation of TDS profiles from well-log data.

The most direct way of finding water resistivity is to obtain a sample of formation water and measure its resistivity. Practically, this is seldom possible, as formation water samples are usually contaminated by mud filtrate. Therefore, Rw is often determined by analytical methods.

Archie equation method

The method is based on the Archie (1942) equation:

$$\mathbf{R_t = F\, R_w} \qquad (3.8)$$

where $\mathbf{R_t}$ is the resistivity of 100% water-saturated formation (when all the pores were filled with brine), **F** is the formation resistivity factor, and $\mathbf{R_w}$ is the resistivity of the formation water. The equation states that the resistivity of rock is proportional to the resistivity of water (brine) it contains. The formation resistivity factor varies, among other properties, with the porosity and permeability of the reservoir rock. Roughly speaking, **F** increases as porosity decreases, and the following empirical relationship was established (Archie, 1942):

$$\mathbf{F = 1 / \varphi^m} \qquad (3.9)$$

where **F** is the porosity (decimal fraction). The exponent **m** in (3.9) has been found to range between 1.8 and 2.0 for consolidated sandstones. Combining equations (3.8) and (3.9), and assuming **m** = 2, we obtain the final formula for $\mathbf{R_w}$ estimation:

$$\mathbf{R_w = \varphi^2\, R_t} \qquad (3.10)$$

The data that are required for R_w estimate from eq. (3.10) include R_t from deep-reading resistivity tools, such as deep induction (ILD) or deep laterolog (LLD) and porosity log. It is assumed that there are no clay or conductive minerals in the analyzed water-bearing zone, and that the mud invasion is shallow enough for resistivity tools to be affected by it. The method may show unreliable results in highly fractured or vuggy reservoirs.

Resistivity ratio method

The method is also based on the Archie equation (eq. 2) but uses two types of resistivity readings, in invaded (fully flushed) and uninvaded zones. In the case of the fully flushed zone, the equation for formation resistivity factor **F** can be written as:

$$\mathbf{R_{xo}} = \mathbf{F}\,\mathbf{R_{mf}} \qquad (3.11)$$

where $\mathbf{R_{xo}}$ is the resistivity of the flushed zone, and $\mathbf{R_{mf}}$ is the resistivity of the mud filtrate. Combining equations (3.8) and (3.11), we obtain:

$$\mathbf{R_w} = (\,\mathbf{R_t} / \mathbf{R_{xo}}\,)\,\mathbf{R_{mf}} \qquad (3.12)$$

Values of $\mathbf{R_w}$, $\mathbf{R_t}$, and $\mathbf{R_{xo}}$ are assumed to be at the temperature of the formation.

In this method, $\mathbf{R_t}$ and $\mathbf{R_{xo}}$ are obtained from deep and shallow resistivity logs, and $\mathbf{R_{mf}}$ is obtained either from the log headers or from the resistivity of mud readings (Log Interpretation Charts, Gen-3, Schlumberger, 2009 Edition). The drawback of this method is that it requires a reliable measurement of $\mathbf{R_{xo}}$.

TDS modeling results

Because of bigger uncertainties associated with the Ratio Method, we used the Archie Equation Method to model concentration of total dissolved solids within the Sundance sandstone formations and the Muddy Sandstone. **Figures 3.4.26** and **3.4.27** show TDS profiles estimated for the Sundance sandstone intervals penetrated by the wells with API numbers 562532 and 562465 correspondingly. Both of these profiles show concentration of total dissolved solids well in excess of 10,000 ppm, indicating that the Sundance sandstone units can be classified as saline reservoirs. On the contrary, similar TDS modeling performed for the Muddy sandstones do not allow classifying this reservoir as suitable for CO_2 sequestration (**Figures 3.4.28**).

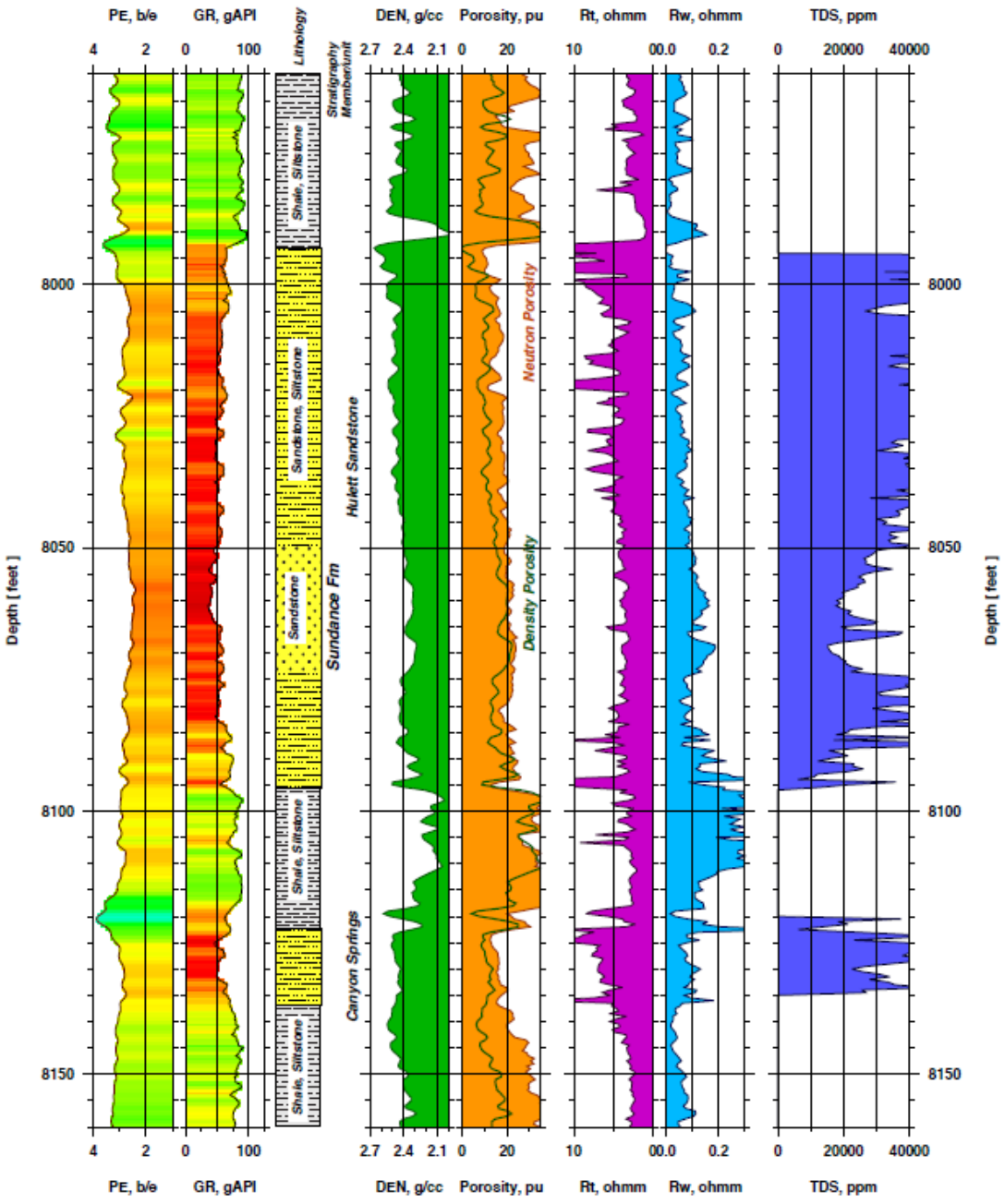

Figure 3.4.26 Interpreted logs from the Callaway 15-5 well (API 562532) for the Sundance stratigraphic interval, Dry Fork study area. Tracks from left to right are (PE) photo electric section, (GR) gamma ray, (DEN) formation density, Neutron (orange) and Density Porosity (green curve), (Rt) true, uninvaded formation resistivity, (Rw) formation water resistivity, and (TDS) concentration of total dissolved solids. The Rw and TDS logs were computed assuming that geothermal reservoirs are100% water saturated and no clay or other conductive minerals are present in the water-bearing zone.

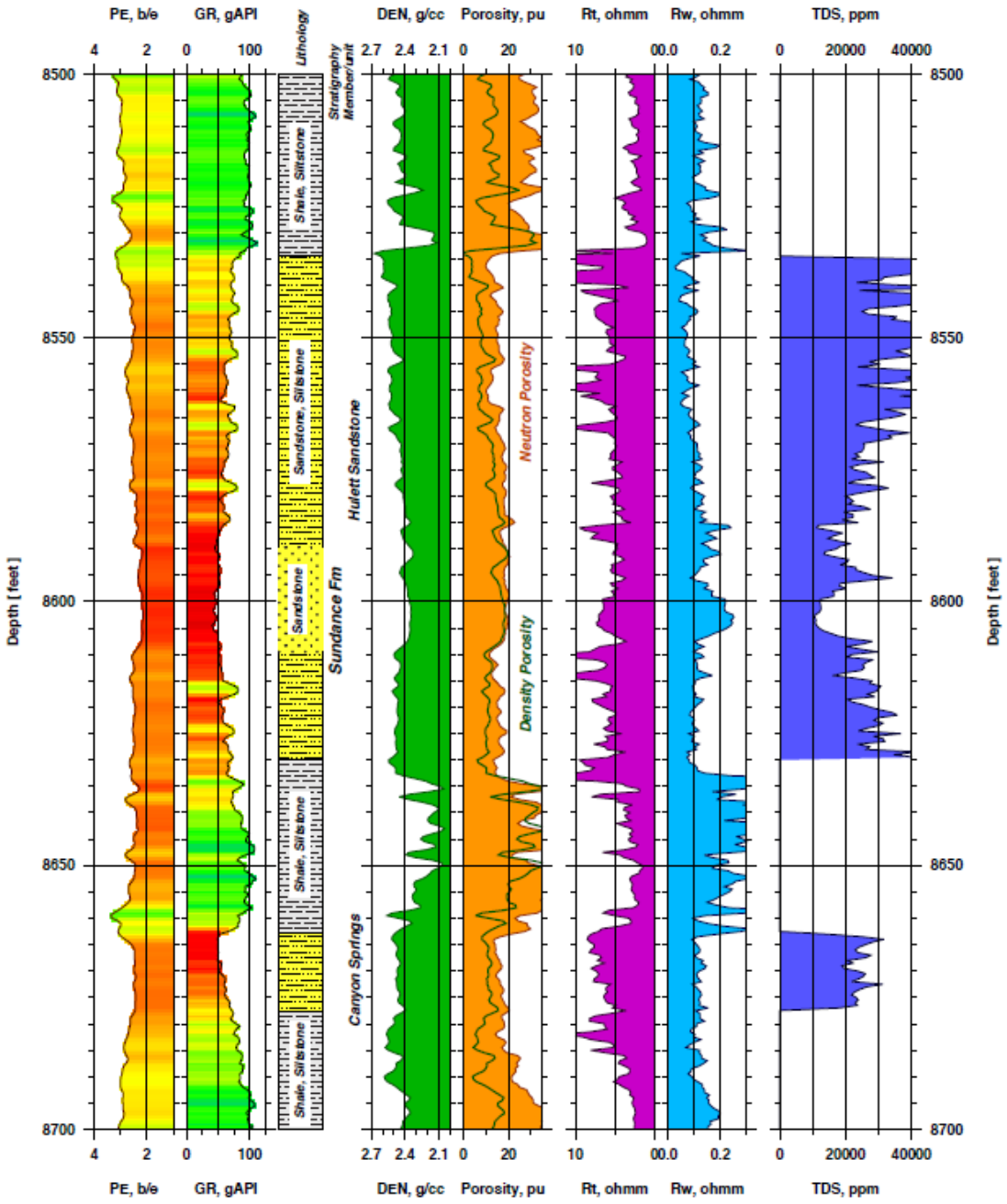

Figure 3.4.27 Interpreted logs from the State 44-16-5071 well (API 562465) for the Sundance stratigraphic interval, Dry Fork study area. Tracks from left to right are (PE) photo electric section, (GR) gamma ray, (DEN) formation density, Neutron (orange) and Density Porosity (green curve), (Rt) true, uninvaded formation resistivity, (Rw) formation water resistivity, and (TDS) concentration of total dissolved solids. The Rw and TDS logs were computed assuming that geothermal reservoirs are 100% water saturated and no clay or other conductive minerals are present in the water-bearing zone.

Section 3.4 References

Archie, G.E. 1942, "The electrical resistivity log as an aid in determining some reservoir characteristics", American Institute of Mining and Metallurgical Engineers Transaction, v. 146, pp. 54-62.

Archie G.E. 1950, "Introduction to petrophysics of reservoir rocks", American Association of Petroleum Geologists Bulletin 34(5): 943–961

Ganshin Yuri and Surdam Ronald, 2013, Utility of 3-D Seismic Attribute Analysis and VSP for Assessing Potential Carbon Sequestration Targets on the Rock Springs Uplift, Southwest Wyoming: in Ronald C. Surdam editor, Geological CO2 Storage Characterization, Chapter 7, pp. 97-150, Springer

Fomel Sergey, 2004, On anelliptic approximation for qP velocities in VTI media. Geophys. Prosp., 52: pp. 247-259.

Jensen JL, Lake LW, Corbett PWM, Goggin DJ (2000) Statistics for petroleum engineers and geoscientists, 2nd edn. Handbook of petroleum exploration and production, 2. Elsevier, Amsterdam

McLaughlin Fred, Bentley Ramsey, and Quillinan Scott, 2013, Regional Geologic History, CO_2 Source Inventory, and Groundwater Risk Assessment of a Potential CO_2 Sequestration Site on the Rock Spring Uplify in Southwest Wyoming: in Ronald C. Surdam editor, Geological CO2 Storage Characterization, Chapter 5, pp. 33-54, Springer

MacQueen, J. (1967). Some methods for classification and analysis of multivariate observations. Proceedings of the Fifth Berkeley Symposium on Mathematical Statistics and Probability, Volume 1: Statistics, 281--297, University of California Press, Berkeley, Calif.

Nelson PH (1994) Permeability-porosity data sets for sandstones. The Leading Edge (23): 1143–1144

Nelson, PH (2004) Permeability-porosity relationships in sedimentary rocks. The Log Analyst May–June:38–62

Chapter IV: Geologic Model Development and Simulation

Nicholas W. Bosshart, Benjamin S. Oster, Jun Ge, Matthew E. Burton-Kelly, Ian K. Feole, Lonny L. Jacobson, Augustinus Zandy, Wesley D. Peck, and Charles D. Gorecki

Energy & Environmental Research Center
University of North Dakota
15 North 23rd Street, Stop 9018
Grand Forks, ND 58202-9018
Phone (701) 777-5334; Fax (701) 777-5181
nbosshart@undeerc.org

Section 4.1 Introduction

This final report details actions and conclusions related to the pre-feasibility study conducted and centered around Basin Electric Power Cooperative's (BEPC) Dry Fork Station in Gillette, Wyoming. The goals of this pre-feasibility study included 1) establish a fully capable and experienced carbon capture and storage (CCS) coordination team; 2) follow an integrated approach to project development, which would result in a successful pre-feasibility assessment of the potential for a commercial-scale CO_2 storage project, including sourcing, transport, and long-term storage needs on both a technical and nontechnical basis; 3) conduct an extensive technical evaluation of the regional geology and CO_2 source that will provide a final scenario for CCS project completion; and 4) support a long-term goal of developing a certified (permitted) geologic storage opportunity with potential to receive 50+ million tonnes of CO_2 in a 25-year time frame.

Dry Fork Station, completed in 2011, is a coal-based electricity generation facility that emits 3.3 million tonnes of CO_2 annually. This project was led by the University of Wyoming's Center for Economic Geology Research (CEGR, formerly the Carbon Management Institute [CMI]), and partners in this work included BEPC; the Energy & Environmental Research Center (EERC); the University of Wyoming's Enhanced Oil Recovery Institute (EORI), College of Business, and College of Law; Carbon GeoCycle Incorporated; Advanced Resources International (ARI); and Schlumberger Carbon Services (Schlumberger).

Section 4.2 Model Construction

Geologic models were constructed and used for dynamic reservoir simulation to determine the suitability of each selected formation for storage of 50 million tonnes of CO_2 over 25 years. The models developed in this task were digital representations of each potential storage formation, including the Muddy, Fall River/Lakota, Sundance, and Minnelusa Formations, within the Dry Fork Station study area. The following section provides discussion of pertinent results from modeling activities, with full details provided in Appendix A.

Structural Model

Geocellular models of each formation were built with Schlumberger's Petrel E&P software platform (Schlumberger, 2016) using both public and private data. Each model encompassed a 766-mi^2 (18.2 mi × 42.2 mi) area around Dry Fork Station (Figure 4.1). Publicly available data used in model development were mainly acquired from the Wyoming Oil and Gas Conservation Commission (WOGCC), including well locations, well datum values (i.e., kelly bushing [KB]), well logs, formation top depths, and core sample descriptions and analyses.

Formation top depths recorded in existing wells were quality-checked using well logs and standards from literature and then interpolated across the study area, creating the structural framework for each formations of interest. Average depth and thickness of each formation throughout the study area, along with expected depth and thickness at Dry Fork Station, are found in Table 4.1.

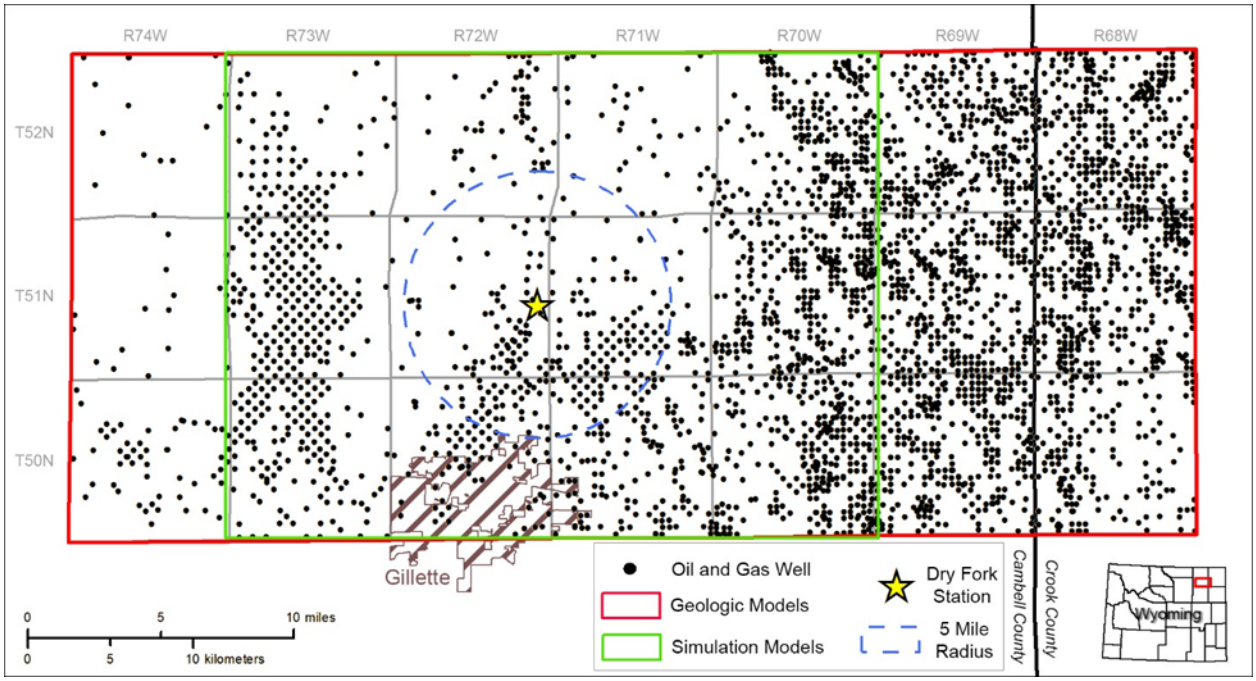

Figure 4.1 Map of the geologic (766 mi^2) and simulation (444 mi^2) model extents.

Table 4.1 Depth and Thickness of Formations of Interest

	Model Area		Dry Fork Station	
Formation	**Average Measured Depth, Ft**	**Average Thickness, ft.**	**Expected Depth, ft.**	**Expected Thickness, ft.**
Muddy	7870	55	7640	60
Fall River/Lakota	8150	130	7910	110
Hulett	8500	180	8260	170
Minnelusa	9560	250	9280	250

Facies Modeling

Muddy Formation

Muddy Formation lithologies were determined based on well log characteristics along with core descriptions. The Muddy Formation was divided into three lithofacies: sandstone, silty sandstone, and shale. Lithology logs were built using core descriptions or calculated from well logs using gamma ray log cutoffs that were chosen by comparing core descriptions with gamma ray logs in wells that had both data sets. "Porous" sandstone and gross sandstone isopach maps were digitized and used as probability trends for the sandstone distributions.

Fall River/Lakota Formations

The Fall River and Lakota Formations, along with the Fuson Shale, make up the Inyan Kara Group of the Powder River Basin (PRB). The facies model of the Fall River and Lakota Formations consisted of three lithologies: sandstone, silty sandstone, and shale. Lithofacies were assigned by using gamma ray log cutoffs and then distributed throughout the model to best represent the depositional environment of each formation.

Sundance Formation

The lower Sundance Formation consists of two reservoir sandstone intervals: the lower Canyon Springs member and the Hulett Sandstone. The Canyon Springs member and Hulett Sandstone are separated by the shale/siltstone of the Stockade Beaver Shale. Gamma ray logs through the Lower Sundance interval were normalized and used to assign sandstone, silty sandstone, and shale facies to the Lower Sundance Formation. Structural surfaces of the top and bottom of the Canyon Springs and Hulett Sandstone were used to constrain the sandstone facies distributions.

Minnelusa Formation

Four sandstone/dolostone intervals (A–D) were modeled throughout the study area. These units represent four cycles during Upper Minnelusa deposition. The sandstone intervals represent times of relatively stable sea level when dunes developed in an eolian environment across the study area. During times of relative sea level rise, marine carbonates (later dolomitized) were deposited on top of the previously developed eolian dunes. Using well log interpretations, top and bottom structural surfaces were created for each sandstone interval and used to constrain sandstone facies distributions. All other cells within the Minnelusa Formation model were given properties of a dolostone lithofacies.

Petrophysical Modeling

Petrophysical properties for each formation of interest (Table 4.2) were derived from legacy core data collected from cored wells. Additionally, core analysis was performed by CEGR, in which new porosity and permeability measurements were generated for the Muddy (five cored wells) and Minnelusa Formations (four cored wells) within the Dry Fork study area. Model porosity and permeability distributions were achieved using a variogram-based geostatistical method with conditioning to the previously developed facies model for each formation. Variogram parameters used in these distributions were adapted from generalized variogram ranges based on the depositional environment described by Deutsch (2008). The core-derived porosity-permeability crossplots used in petrophysical modeling can be found in Appendix A.

Table 4.2 Petrophysical Property Statistics for All Model Reservoir Lithofacies

	Porosity, %		Permeability, mD	
Unit	**Range**	**Mean**	**Range**	**Geometric Mean**
Muddy Sandstone	6.4–26.8	16.9	1.0–1085	16.53
Fall River/Lakota Sandstone	2.6–16.1	9.79	0.02–60	0.82
Lower Sundance Sandstone	2.6–27.3	13.8	0.01–1745	2.73
Upper Minnelusa Sandstone	0.1–29.1	10.7	0.003–1700	5.35

Petrophysical Uncertainty

Multiple property distributions were developed for each model to address petrophysical property uncertainty. Petrophysical properties were distributed, which represented P10, P50, and P90 cases within each previously developed facies model. The P10 distribution represented a generally conservative case, with a 10% chance that the actual values were lower. The P50 distribution represented a median value, and the P90 distribution

represented a more optimistic case, with a 10% chance that the values were higher. Petrophysical property values used in P10, P50, and P90 distributions can be found in Appendix A.

Other Reservoir Properties

Drillstem test results and temperature measurements within the study area were used to estimate pressure and temperature of each formation of interest to aid in numerical simulation efforts. Pressure and temperature gradients used for each formation are shown in Table 4.3. Interestingly, three of the four target formations showed evidence of underpressured conditions in comparison to hydrostatic pore pressure gradient (0.433 psi/ft. for fresh water). No further action was taken to investigate the cause.

Table 4.3 Pressure and Temperature Gradients for Each Formation of Interest

Formation	Pressure Gradient, psi/ft.	Temperature Gradient, °F/ft.
Muddy	0.31	0.013
Fall River/Lakota	0.44	0.014
Lower Sundance	0.39	0.014
Minnelusa	0.39	0.014

Section 4.3 Volumetric Storage Resource Estimates

The models developed in this work, discussed in the previous sections, were used to estimate the static, volumetric CO_2 storage resource potential. The U.S. Department of Energy (DOE) National Energy Technology Laboratory (NETL) has developed multiple methods of such estimations (DOE NETL, 2010). One such method was specifically developed to estimate the CO_2 storage resource potential of a saline formation using the following equation:

$$G_{CO2} = A_t h_g \varphi_{tot} \rho E_{saline} \quad \text{[Eq. 1]}$$

Where A_t is the total area in consideration, h_g is the gross formation thickness, φ_{tot} is the total porosity (effective and ineffective porosity together), ρ is the expected CO_2 density at the end of injection (after reaching maximum reservoir pressure constraints), and E_{saline}

is the efficiency factor describing the fraction of the pore volume that will be occupied by the injected CO_2.

Storage resource potential estimates were determined using the workflow created by Peck and others (2014), which expanded upon the DOE methodology reported in the Carbon Sequestration Atlas III (DOE NETL, 2010). The footprints of existing oil and gas operations within the study area were excluded from the final storage potential estimates to avoid potential negative interaction between CO_2 storage and other subsurface activities. The study area used in the equation for each formation was 766 mi^2. Isopach maps were built to describe formation thickness. Porosity was derived from formation-specific core analysis data collected from wells within the PRB. CO_2 density was calculated using the method of Wang and others (2015) using pressure calculated from a gradient of 0.6 psi/ft., a constraint placed on simulated injection wells in avoidance of fracturing the rock. Saline storage efficiency (E_{saline}) values from Peck and others (2014) were used in these calculations. As described in Peck and others (2014), different E_{saline} values were used for each selected formation, because different amounts of data were available. For example, the greatest amount of information was known about the Muddy Formation; therefore, the highest efficiency values were used; in comparison, much less data were available for the lower Sundance Formation, thus the use of lower efficiency values. For each formation, storage resource potential was calculated using P10 (conservative), P50 (median), and P90 (optimistic) E_{saline} values and the other values used in Table 4.4. Figure 4.2 shows the CO_2 storage potential map calculated using the methods described above for the Muddy Formation. CO_2 storage potential maps for the other formations of interest are included in Appendix A.

Table 4.4 Parameters Used to Calculate CO_2 Storage Resource Potential

	Porosity, %	**Average Thickness, ft.**	**Average CO_2 Density, lb/ft^3**	**P10 E_{saline}, %**	**P50 E_{saline}, %**	**P90 E_{saline}, %**
Muddy	16.9	11	50.74	7.40	14.00	24.00
Fall River/Lakota	7.1	128	50.75	1.62	4.41	9.53
Lower Sundance	13.8	162	50.76	1.62	4.41	9.53
Upper Minnelusa	10.7	165	50.78	7.40	14.00	24.00

The Muddy, Lakota/Fall River, and Minnelusa Formations all produce oil in the study area. A future potential CO_2 storage operation would be planned in such a way to avoid any potential detrimental impact on hydrocarbon resources, thus areas where oil fields exist were eliminated from the storage potential estimates of these formations. The Lower Sundance does not produce hydrocarbons in the study area and, therefore, needed no such adjustment. Table 4.5 represents the storage resource estimates with the oil fields removed. Maps of the P50 CO_2 storage resource estimates for each formation with oil fields removed from the calculations, as well as a combined CO_2 storage resource potential map (all formations), can be found in Figures 4.2–4.6.

Table 4.5 P10, P50, and P90 CO_2 Storage Resource Estimates with Oil Fields Eliminated

	P10		P50		P90	
Unit	**Sum, Mt**	**Mt/mi²**	**Sum, Mt**	**Mt/mi²**	**Sum, Mt**	**Mt/mi²**
Muddy	98	0.13	180	0.24	320	0.41
Fall River/Lakota	70	0.10	190	0.25	410	0.54
Lower Sundance	180	0.23	480	0.63	1000	1.40
Upper Minnelusa	500	0.66	950	1.20	1600	2.10
Combined	848	1.12	1800	2.32	3330	4.45

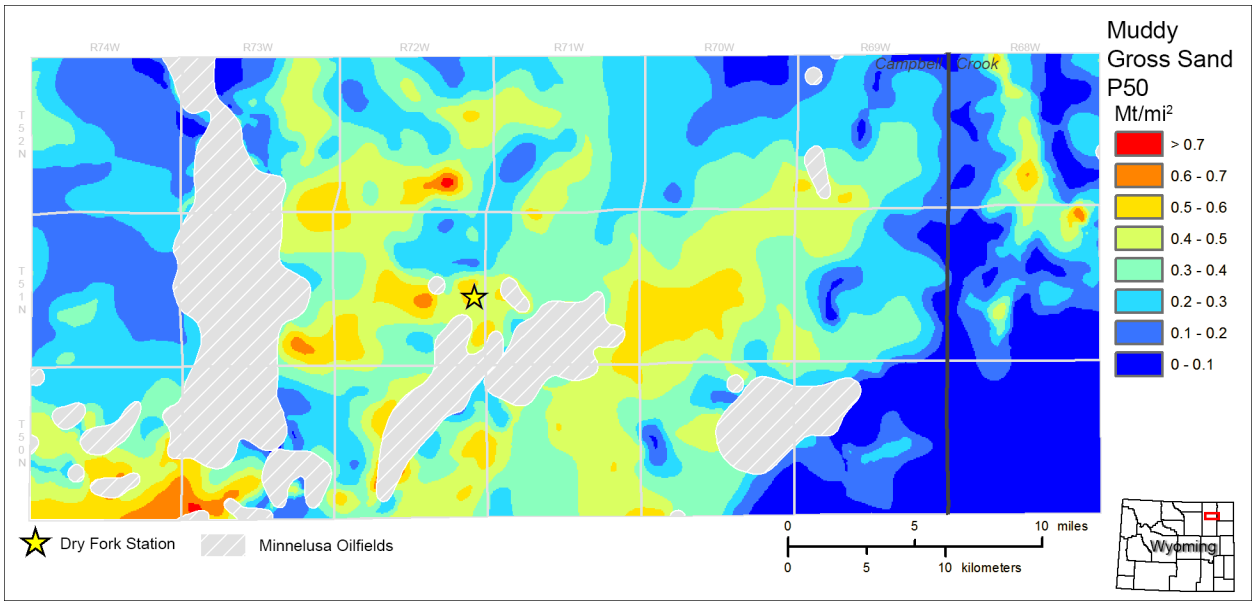

Figure 4.2 Map of the Muddy Formation estimated P50 CO_2 storage resource potential (million tonnes/mi²) with oil fields removed.

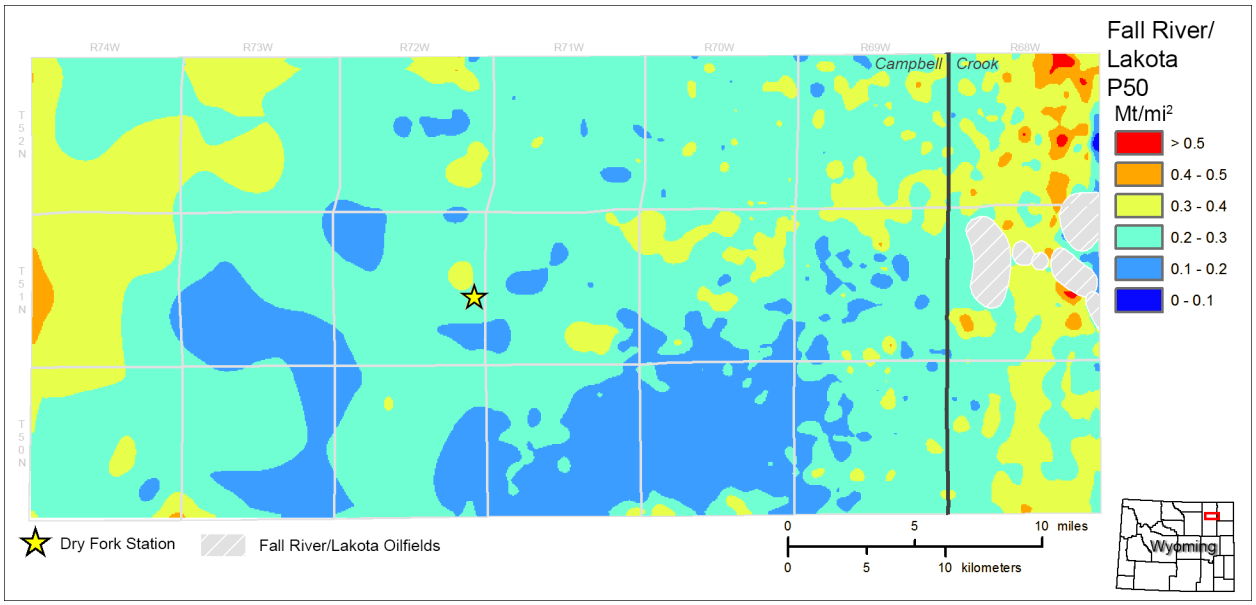

Figure 4.3 Map of the Fall River and Lakota Formations' estimated P50 CO_2 storage potential (million tonnes/mi^2) with oil fields eliminated.

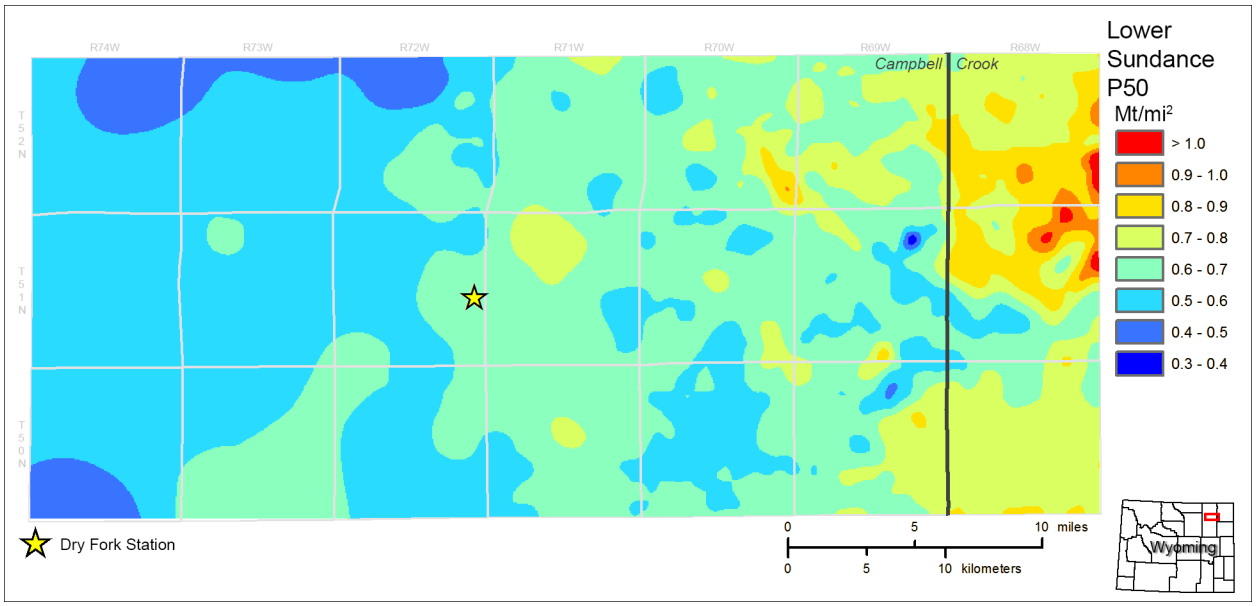

Figure 4.4 Map of the Lower Sundance Formation estimated P50 CO_2 storage potential (million tonnes/mi^2). No areas have been removed, because no oil is produced from the Lower Sundance in the study area.

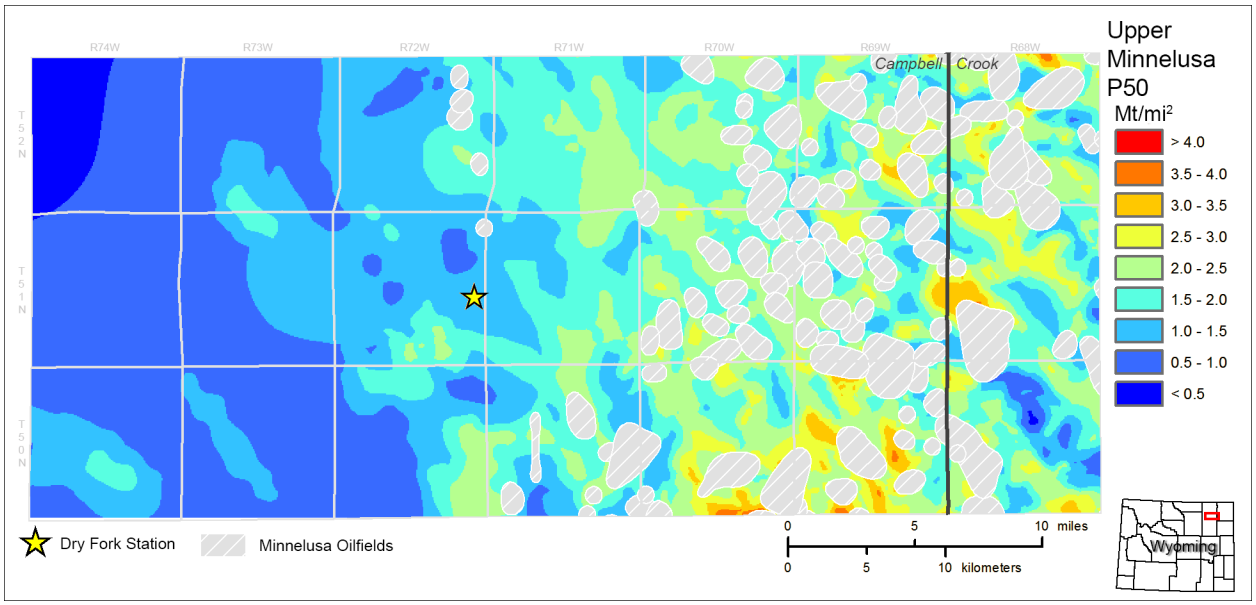

Figure 4.5 Map of Upper Minnelusa Formation P50 estimated storage potential (million tonnes/mi^2) with oil fields eliminated.

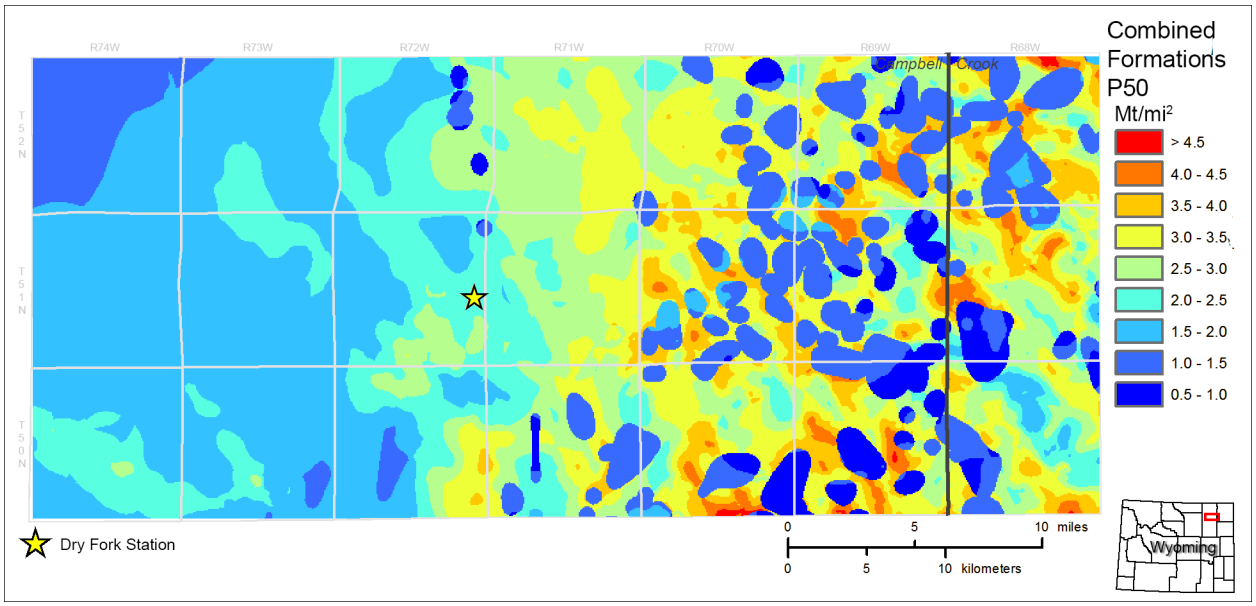

Figure 4.6 Map of combined P50 estimated storage potential (million tonnes/mi^2) with oil fields eliminated.

Section 4.4 Numerical Simulation

Numerical simulation of CO_2 injection was conducted using the models described in the previous sections. These simulations were run to test formation responses to injection and the probability of successful storage. Simulations were performed using Computer Modelling Group Ltd.'s (CMG's) GEM software (CMG, 2017). The intent of each simulation was to assess the potential of storing 50 million tonnes of CO_2 over a 25-year

time frame. The following sections include salient details of scenario designs, results, and area of review (AoR) determination. Further discussion is included in Appendix A.

Scenario Design

With the exception of Muddy and Fall River/Lakota cases, simulated wells were placed to maximize pore space use on BEPC, Western Fuels, and Wyoming state lands. The wells placed in the Muddy and Fall River/Lakota cases were placed where petrophysical properties were deemed best, scrutinized from porosity-thickness and permeability-thickness maps of the model distributions. This was done to give an initial assessment of the "best case" scenario for each, as each model contained relatively thin reservoir intervals with a high degree of heterogeneity. Maximum bottomhole pressure constraints were used in all of the cases, calculated from formation depth in well locations using a pressure gradient of 0.6 psi/ft., employed to mitigate the potential of fracturing the rock during injection. One case was conducted in exception, in which a bottomhole pressure constraint was calculated using a gradient of 0.7 psi/ft. This case was conducted to assess storage performance with slightly higher injection pressure constraints, a scenario which may occur if site-specific measurements of fracture pressure in overlying sealing formations indicate the fracture pressure gradient is greater than what would be assumed in default (0.6 psi/ft.). Perforations were set in sandstone components of each formation.

Base cases (P50 cases with four vertical injection wells) were simulated for each of the formations of interest (Table 4.6). In the Lower Sundance and Minnelusa simulations, P10 (conservative) and P90 (optimistic) cases with four vertical injection wells were run. After scrutinizing the results for the Muddy and Lakota/Fall River cases, which indicated rather poor storage performance, a decision was made to supplement the P50 results only with P90 cases with four vertical injection wells for these two models. Additionally, P50 cases with six vertical injection wells, brine extraction, and horizontal wells were run. Brine extraction cases were run with four injection wells and one production well. Of the horizontal well cases, a subset was run with one well, but with lateral length varied from 0.25 to 1 mi, and another subset of cases was run with four horizontal wells with 1-mile laterals.

Results

The base case (P50 models with four vertical injection wells) simulation results indicated the Muddy and Lakota/Fall River Formations would likely not be suitable for CO_2 storage at the scale required of the project. The relatively thin nature of each formation and the inherent geologic heterogeneity (discontinuous nature of sand bodies) resulted in rapid pressure buildup during the simulations, which limited injectivity. Therefore, P10 (conservative) cases were foregone, and

Table 4.6 Simulation Case Matrix

Formation	Scenario	Four Injection Wells, 0.6-psi/ft. BHP* Constraint	Four Injection Wells, 0.7-psi/ft. BHP Constraint	Six Injection Wells	Brine Extraction 5-Spot	One Horizontal Well, 0.25-mi/1-mi lateral	Four Horizontal Wells, 1-mi lateral
Muddy	P10						
Muddy	P50	X					
Muddy	P90	X					
Lakota/ Fall River	P10						
Lakota/ Fall River	P50	X					
Lakota/ Fall River	P90	X					
Lower Sundance	P10	X					
Lower Sundance	P50	X		X	X	X	X
Lower Sundance	P90	X					
Minnelusa	P10	X					
Minnelusa	P50	X	X	X	X	X	X
Minnelusa	P90	X					

* Bottomhole pressure.

only P90 (optimistic) cases were simulated for each of these formations. Yet even with petrophysical properties as good as what would be expected of a P90 scenario, the results indicate neither formation individually would be able to receive 50 million tonnes of CO_2 in a 25-year time frame based on the scenarios investigated. These formations, however, are not being excluded from future investigative activities, as there may be some potential for integration of these units in a stacked storage scenario.

The Minnelusa Formation base case result was nearly 31 million tonnes of stored CO_2 in a 25-year time frame. A similar case was conducted but with a BHP constraint calculated using a pressure gradient of 0.7 psi/ft. (the base case used a gradient of 0.6 psi/ft.), and the result was just over 48 million tonnes of CO_2 stored in a 25-year time frame. This result illustrated the importance of understanding fracture pressure gradient at future potential injection sites. Data may be generated in future characterization activities (i.e., microfracture testing in sealing units overlying injection targets) to support increasing of permitted injection pressure above gradients considered in default when fracture pressure data are absent. The impact of increasing injection pressure constraints may be significant, as indicated by these results.

An additional Minnelusa Formation case was simulated using six vertical wells, in which two additional wells were added on Wyoming state sections to the west of Dry Fork Station. Using the 0.6-psi/ft. BHP constraint, the case resulted in the storage of nearly 60 million tonnes of CO_2 over a 25-year time frame.

The P90 (optimistic) Minnelusa Formation simulation case using four wells and a 0.6-psi/ft. BHP gradient constraint resulted in the storage of 197 million tonnes of CO_2 in a 25-year time frame. This result, while considered a rather unlikely scenario, indicated that if Minnelusa petrophysical properties were even slightly better than those present in the P50 geologic model, 50 million tonnes of stored CO_2 is certainly achievable in the Minnelusa Formation. The Lower Sundance P90 (optimistic) case with four wells resulted in 81 million tonnes of stored CO_2.

Horizontal well cases were run using the Lower Sundance and Minnelusa models to investigate the potential benefit to future potential injection scenarios. Single vertical well cases were simulated for both the Lower Sundance and Minnelusa model to provide a basis for comparison, which resulted in the storage of 7 million tonnes and 12 million tonnes of CO_2, respectively. Two horizontal well cases were run for each model, cases using one horizontal well but varying lateral length from 0.25- to 1 mi. The results were 10.4 and 12 million tonnes of CO_2 in the Lower Sundance and 18.1 and 23.8 million tonnes of CO_2 in the Minnelusa model. Therefore, a horizontal well with lateral length of 0.25 mi enabled an increase of 48% more injected CO_2 mass in comparison to a vertical well in the Lower Sundance model, and the difference in injected CO_2 mass between horizontal wells with 0.25- and 1-mi laterals was 15%. In the Minnelusa model, the difference in injected CO_2 mass between a single vertical well and a horizontal well with a 0.25-mi lateral was 51%, and the difference in injected CO_2 mass between horizontal wells with 0.25- and 1-mi laterals was 31%. Because the 1-mi lateral cases appeared to show significant increases in the resulting injectivity over both vertical wells and horizontal wells with shorter laterals, an additional simulation case was run for both the Lower Sundance and Minnelusa model using four horizontal wells with 1-mi laterals.

Cases with four horizontal wells with 1-mi laterals ended up with 21.8 million tonnes in the Lower Sundance and 56 million tonnes in the Minnelusa Formation. Compared to the base case results (four vertical injection wells), the cases with four horizontal wells showed increases of 12% in the Lower Sundance model and 82% in the Minnelusa model. The difference observed in effectiveness of horizontal wells is thought to relate to average formation thickness in the study area. Even though horizontal wells provide much greater contact with the injection interval, suggesting overall injectivity should be higher, injectivity will still be limited by pressure buildup. The sands of the Lower Sundance Formation are relatively thin; therefore, pressure buildup from either horizontal or vertical wells are likely to reach pressure limits relatively quickly, resulting in similar stored CO_2 masses between the cases. The Minnelusa Formation, being relatively thick, appears to allow pressure dispersion from horizontal wells to occur more liberally throughout a greater reservoir volume, resulting in significantly more stored CO_2 in comparison to scenarios using vertical wells.

Brine extraction cases were also conducted using the Lower Sundance and Minnelusa models. The injection well pattern used in the base case simulations (four vertical wells)

was used in the brine extraction cases, with a production well placed near the center of the cluster to act as a large-scale 5-spot pattern. The Lower Sundance brine extraction case resulted in the storage of 26 million tonnes of CO_2, an increase of 33% over the base case result with only the four injection wells. The Minnelusa brine extraction case resulted in the storage of 43 million tonnes of CO_2, an increase of 39% over the base case result with only the four injection wells.

One Upper Minnelusa case was simulated to observe the long-term pressure response and disposition of injected CO_2. The six-well (vertical) case was simulated for 100 years postinjection (125 years in total). The results indicated that the pressure buildup associated with injection is expected to dissipate rather quickly, with pressure conditions after 100 years of postinjection monitoring resembling that of preinjection conditions. CO_2 migrated in the structural updip direction (east) under the effects of buoyancy at a very slow rate, on the order of tens of feet per year. If this migration rate were to continue, injected CO_2 would take tens of thousands of years to reach a Minnelusa outcrop to the east (approximately 70 miles). However, this rate is likely overestimated, as this simple calculation does not account for the effects of structural traps that exist in the Minnelusa (small eolian dunefield traps which would likely slow buoyant migration significantly), the effects of relative permeability and residual trapping, dissolution of CO_2 which would negate migration under the effects of buoyancy, or mineralization of dissolved CO_2 (i.e., formation of carbonate minerals), which would permanently trap injected CO_2. Therefore, the results give confidence that, with the integration of an adequate regional wellbore integrity assessment to mitigate potential vertical migration pathways, risks related to conformance and containment of injected CO_2 are negligible. More details of this assessment are included in Appendix A.

To summarize these results, injection scenarios in the Muddy, Lakota/Fall River, and Lower Sundance appear to show a small likelihood of success in storing 50 million tonnes of CO_2 individually with the simulations considered in this study (Table 4.7). Achieving the desired magnitude of stored CO_2 would likely require a greater area and relatively higher number of wells. Injection scenarios in the Minnelusa Formation with four-to-six wells appear to be sufficient to achieve storage of 50 million tonnes of CO_2. However, stacked storage scenarios using multiple formations will be given consideration in future investigations, which may enable a reduction in permitted AoR, thus a reduction in associated financial burdens (i.e., pore space payments to landowners, costs associated with implementing monitoring technologies). Overall, these results have shown the ability to achieve 50 million tonnes of CO_2 stored in the region around Dry Fork Station in several different ways. These results provide a sound foundation for additional and improved modeling and simulation work during the Phase II effort, updated with site-specific characterization data, more finely tuned well placements, and tailored operational parameters for increased accuracy in predictive results.

Section 4.5 AoR Determination

The U.S. Environmental Protection Agency (EPA) requires owners or operators of Class VI injection wells to delineate the AoR for the proposed Class VI well, which is the region surrounding the proposed well where underground sources of drinking water (USDW) may be endangered by the injection activity (EPA, 2013). The delineation of an AoR is calculated from the pressure front. The pressure front is defined as the area around an injection well where, during injection, the hydraulic head of the formation fluid in the injection zone is equal to or greater than the [hydraulic] head of USDWs (EPA, 2013). This can be calculated using the following equation:

Table 4.7 Dry Fork CarbonSAFE Simulation Case Results – Cumulative CO_2 Injection (MM tonnes)

Formation	Scenario	Four Injection Wells, 0.6-psi/ft. BHP Constraint	Four Injection Wells, 0.7-psi/ft. BHP Constraint	Six Injection Wells	Brine Extraction 5-Spot	One Horizontal Well, 0.25-mi/1-mi lateral	Four Horizontal Wells, 1-mi lateral
Muddy	**P10**	**N/A**					
Muddy	**P50**	**13**					
Muddy	**P90**	**31**					
Lakota/ Fall River	**P10**	**N/A**					
Lakota/ Fall River	**P50**	**6**					
Lakota/ Fall River	**P90**	**7**					
Lower Sundance	**P10**	**7**					
Lower Sundance	**P50**	**20**		**25**	**26**	**10/12**	**22**
Lower Sundance	**P90**	**81**					
Minnelusa	**P10**	**6**					
Minnelusa	**P50**	**31**	**48**	**60**	**43**	**18/24**	**56**
Minnelusa	**P90**	**197**					

$$Pi = Pu + \rho ig \cdot (zu - zi)$$

[Eq. 2]

Where Pu is the initial fluid pressure in the USDW, ρi is the injection-zone fluid density, g is the acceleration due to gravity, zu is the representative elevation of the USDW, and zi is the representative elevation of the injection zone.

Because the scale of simulated CO_2 injection in the Muddy Formation model and the Fall River and Lakota Formations' model were significantly below the 50-million-tonne injection target, no AoR calculations were conducted. However, AoR calculations were conducted using the simulation results for the Lower Sundance and Upper Minnelusa models.

The lowermost USDW in the study area is the Fox Hills Formation. Interburden thickness (distance from the bottom of the Fox Hills Formation to the Lower Sundance and Minnelusa formations) was calculated from formation top depths. Fluid density for the Upper Minnelusa and Lower Sundance Formations both have estimated fluid density of 1025 kg/m^3. Using pressure results from the simulations, AoR maps were created for select scenarios. A map showing the CO_2 plume footprints and pressure front-calculated AoRs from the P10, P50, and P90 Minnelusa model simulation results (cases with four vertical injection wells) is shown in Figure 4.7. Additional AoR maps for Lower Sundance and other Minnelusa simulation results are included in Appendix A. Statistics regarding the calculated AoRs for simulation cases, which resulted in a stored CO_2 mass approaching or exceeding 50 million tonnes, are reported in Table 4.8 below.

Table 4.8 Total Area in AoR for Select Simulation Scenarios

Formation	Scenario	Stored CO_2, Mt	Area, mi^2
Upper Minnelusa	P50 – 0.7-psi/ft. BHP Constraint	48	202
Upper Minnelusa	P50 – six vertical injection wells	60	218
Upper Minnelusa	P50 – four horizontal wells	56	204
Upper Minnelusa	P50 – brine extraction 5-Spot	43	149
Upper Minnelusa	P90	197	165
Lower Sundance	P90	81	290

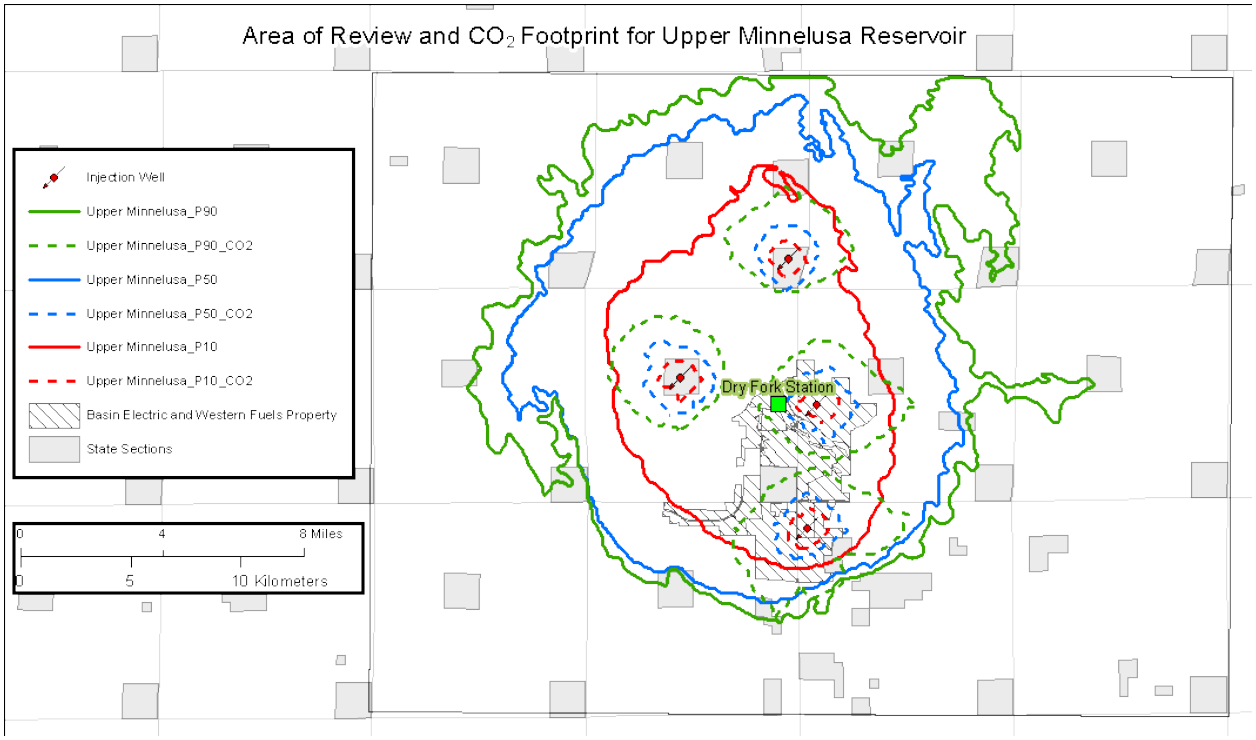

Figure 4.7 AoR map of the Upper Minnelusa Formation showing the P10, P50, and P90 pressure and CO_2 plume scenarios with four vertical injection wells. The P10, P50, and P90 cases resulted in CO_2 storage in the amounts of 5.6, 31, and 197 million tonnes, respectively.

Acknowledgment. The authors and project partners would like to thank BEPC for its participation in this study. Appreciation is also shown to GeoDigital Information, LLC, and TGS for providing important data sets for this study. The authors would also like to thank Schlumberger and CMG for providing access to the commercial modeling and simulation software required for this work.

Section 3.4 References

Computer Modelling Group (CMG), 2017, GEM user guide.

Deutsch, C.V., 2008, Fundamentals of geostatistics—principles and hands-on practice.

Minnelusa Sandstone of the Powder River Basin, 2000, GeoDigital Information, LLC, accessed from www.geodigitalinfo.com/index.html (subscription required).

Muddy Sandstone of the Northern Powder River Basin, 2000, GeoDigital Information, LLC, accessed from www.geodigitalinfo.com/index.html (subscription required).

Peck, W.A., Glazewski, K.A., Klenner, R.C.L., Gorecki, C.D., Steadman, E.N., and Harju, J.A., 2014, A workflow to determine CO_2 storage potential in deep saline formation: Energy Procedia, v. 63, p. 5231–5238.

Powder River Basin Geologic Framework, 2000, GeoDigital Information, LLC, accessed from_www.geodigitalinfo.com/index.html (subscription required).

Schlumberger, 2016, Petrel 2016: Petrel E&P Software Platform.

U.S. Department of Energy National Energy Technology Laboratory, 2010, Carbon sequestration atlas of the United States and Canada (3rd ed.).

U.S. Department of Energy National Energy Technology Laboratory, 2017–1845, Best practices— public outreach and education for geologic storage projects: 2017 revised edition (accessed July 13, 2018).

U.S. Environmental Protection Agency, 2013, Geologic sequestration of carbon dioxide Underground Injection Control (UIC) Program Class VI well area of review evaluation and corrective action guidance: EPA 816-R-13-005.

Wang A., Sun, B., and Yan, L., 2015, Improved density correlation for supercritical CO_2: Chemical Engineering and Technology, v. 38, no. 1, p. 75–84.

Chapter IV Appendix A – Modeling and Simulation

MODELLING AND SIMULATION

Model Construction

A.1 Introduction

Geologic models of the Muddy Formation, Fall River/Lakota Formations, Lower Sundance Formation, and Upper Minnelusa Formation were created to support numerical simulations of CO_2 injection and evaluation of dynamic CO_2 storage potential. Models were constructed based on a combination of measured subsurface characteristics and geologic interpretation. Modeling efforts were also used to assess the current availability and quality of data available within the Dry Fork Station study area and to identify key data acquisitions for future characterization activities. Modeling efforts resulted in visual and numerical representations of subsurface geologic/stratigraphic characteristics, including structure, heterogeneity, pressure, temperature, and petrophysical properties (porosity and permeability).

A.2 Data

Geocellular models for each formation were built with Schlumberger's Petrel E&P software platform (Schlumberger, 2016) using both public and private data. Each geocellular model encompasses a 766 mi^2 (18.2-mi × 42.2-mi) area around Dry Fork Station (Figure 4A-1). Publicly available data used in model development were mainly acquired from the Wyoming Oil and Gas Conservation Commission (WOGCC), including well locations, well datum values (i.e., kelly bushing [KB]), well logs, formation top depths, and core sample descriptions and analyses. Private data were acquired from two sources: GeoDigital Information, LLC (GDI) and TGS. Data acquired from GDI were in the form of three geologic studies related to the area ("Powder River Basin Geologic Framework," "Muddy Sandstone of the Northern Powder River Basin," and "Minnelusa Sandstone of the Powder River Basin"). Digital well logs from 80 wells were purchased from TGS for use in model development.

Existing well penetrations and their associated data sets comprise the primary source of information for the geologic models. A good number of wells penetrate the formations of interest surrounding the Dry Fork Station site, but a relatively lower concentration of data exists to the west. The closest well to Dry Fork Station that penetrates all the formations of interest is located approximately 1 mile to the northwest

(API 49005283880000). A large initial study area was delineated (766-mi^2; 18.2 mi × 42.2 miles), which included 3542 wells (Figure 4A-1). A smaller subset of this region served as the basis for simulation model extent (444-mi^2; 18.2 mi × 24.4 mi), centered on Dry Fork Station.

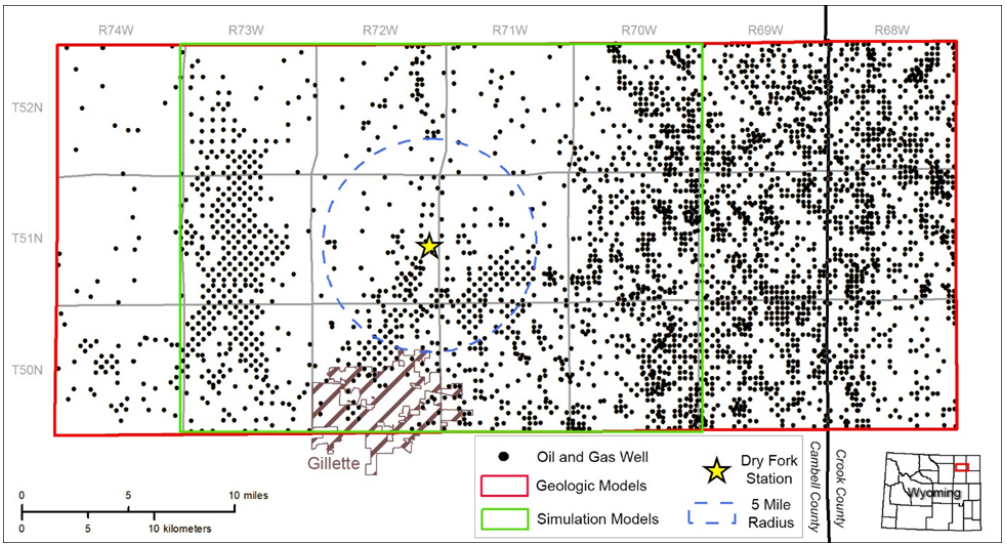

Figure 4A-1 Map showing the geologic model extent (red rectangle; 766 mi^2) and the smaller simulation model extent (green rectangle; 444 mi^2).

A.3 Structural Modeling

Modeling efforts focused on the Muddy Formation, Fall River/Lakota Formations, Lower Sundance Formation, and Upper Minnelusa Formation. Average depths and thicknesses across the study area along with expected depth and thickness at Dry Fork Station for each formation of interest are found in Table 4A-1.

Well top depths were compiled from multiple sources, including the WOGCC and GDI studies. Additional well tops for relevant formations were also picked in select wells based on well log characteristics. Formation top depths were then interpolated across the study area, creating structural surfaces for each the formations.

Table 4A-1 Petrophysical Property Statistics for Reservoir Lithofacies, All Models

Unit	Porosity, %		Permeability, mD	
	Range	Mean	Range	Geometric Mean
Muddy "Porous" Sandstone	6.4–26.8	16.9	1.0–1085	16.53
Muddy Silty-Sandstone	0.5–24.8	10.4	0.001–0.95	0.15
Fall River/Lakota Sandstone	2.6–16.1	9.79	0.02–60	0.82
Lower Sundance Sandstone	2.6–27.3	13.8	0.01–1745	2.73
Upper Minnelusa Sandstone	0.1–29.1	10.7	0.003–1700	5.35
Upper Minnelusa Dolostone	1.4–18.6	7.0	0.01–9.98	0.10

A.3.1 Muddy Formation

The Muddy Formation was further divided structurally by using members that are commonly used to divide the formation across the Powder River Basin (PRB). The members include the Rozet, Recluse, Cyclone, Ute, and Springen Ranch. The GDI study on the Muddy Formation in the northern PRB contained formation top depths for each of the members. Additional Muddy member tops were picked in select wells where they did not exist in the GDI study. Figure 4A-2 shows a typical well log display in the Muddy Formation near Dry Fork Station. Figure 4A-3 shows structure and isopach maps for the Muddy Formation within the geologic model (red rectangle in Figure 4A-1).

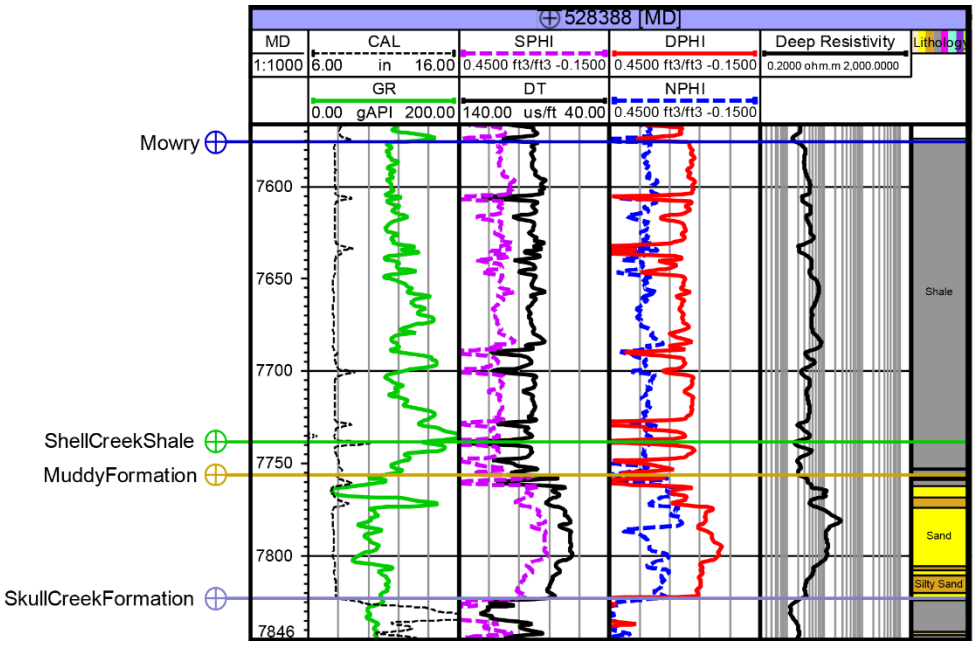

Figure 4A-2 Type log of the Muddy Formation near Dry Fork Station (API 49005283880000). Curves shown are (from left to right) caliper (CAL) and gamma ray (GR), sonic porosity (SPHI) and sonic travel time (DT), density porosity (DPHI) and neutron porosity (NPHI), deep resistivity, and lithology.

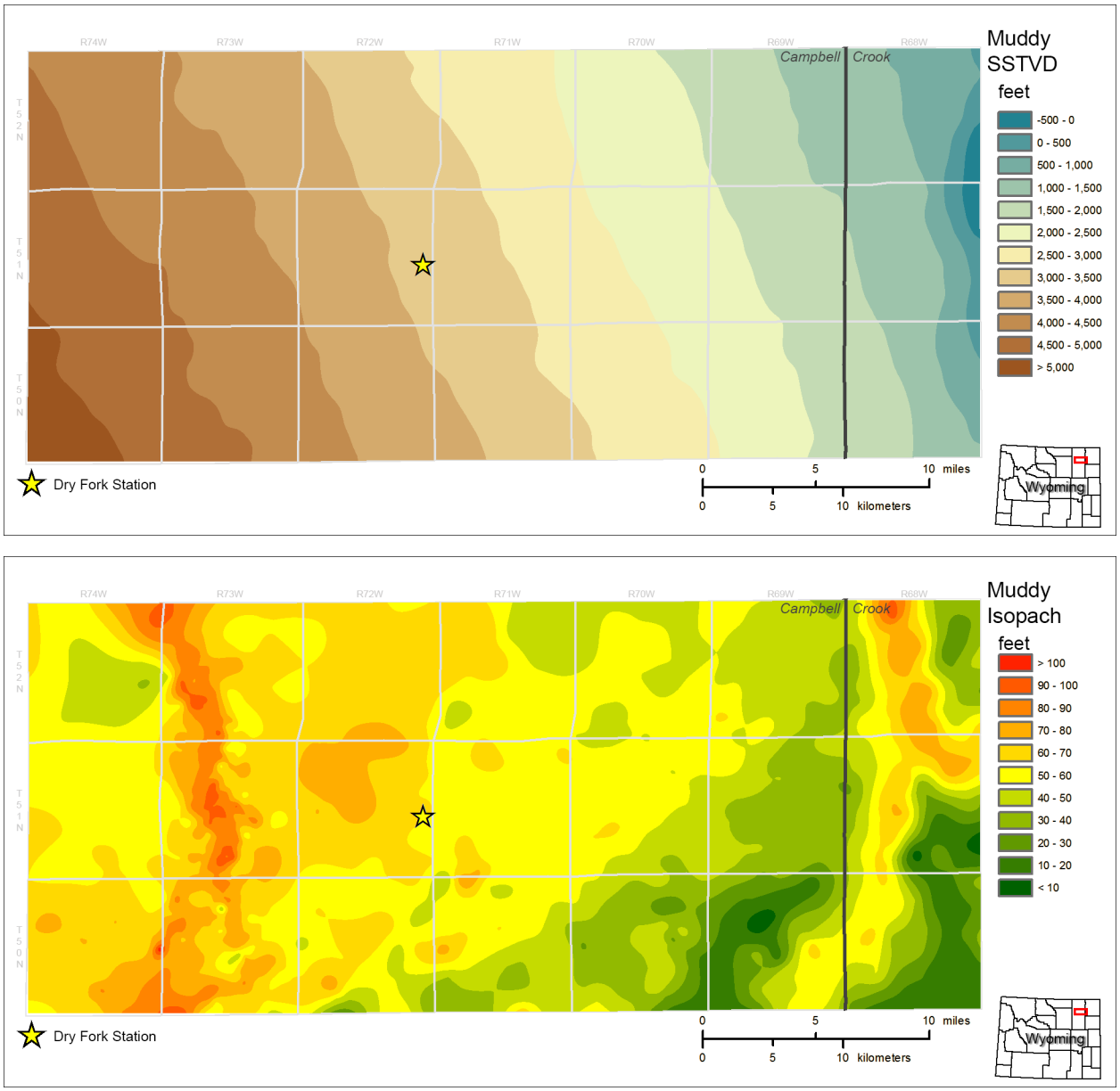

Figure 4A-3 Top: structure contour map of the top of the Muddy Formation (datum – mean sea level), bottom: isopach map of the Muddy Formation.

A.3.2 Fall River/Lakota Formations

The structural model of these formations was created with formation top depths from the Fall River, Fuson Shale, and Lakota Formations. The Fall River and Lakota

Formations make up the Inyan Kara Group within the PRB and are separated by the Fuson Shale. Figure 4A-4 shows a typical well log display in the Fall River and Lakota Formations near Dry Fork Station. Figures 4A-5 and 4A-6 show structure and isopach maps for the Fall River and Lakota Formations, respectively, within the geologic model (red rectangle in Figure 4A-1).

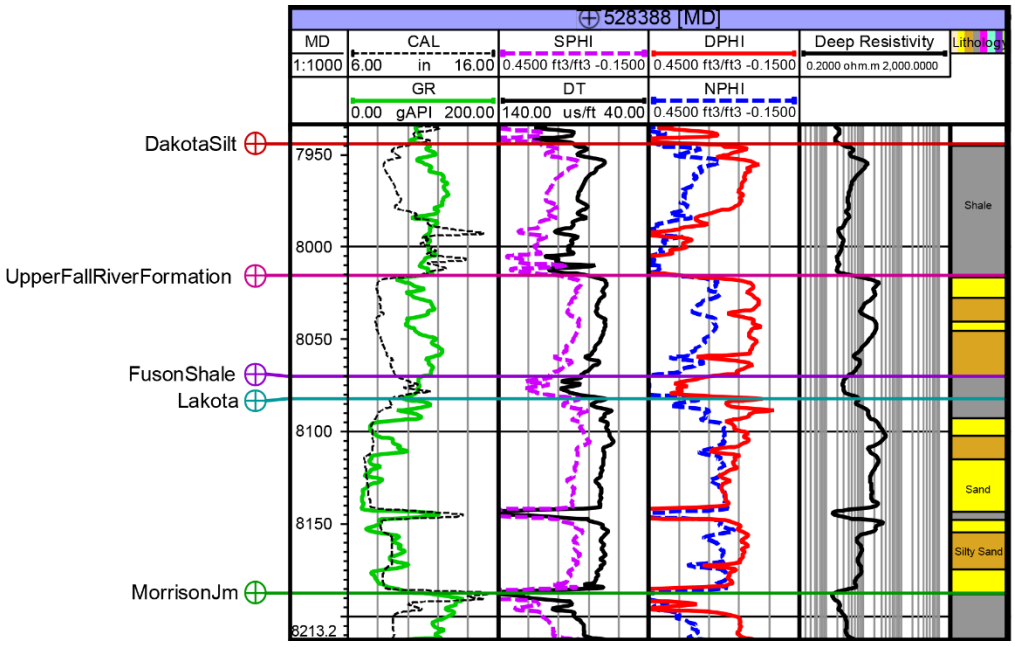

Figure 4A-4 Type log of the Fall River and Lakota Formations near Dry Fork Station (API 49005283880000). Curves shown are (from left to right) CAL and GR, SPHI and DT, DPHI and NPHI, deep resistivity, and lithology.

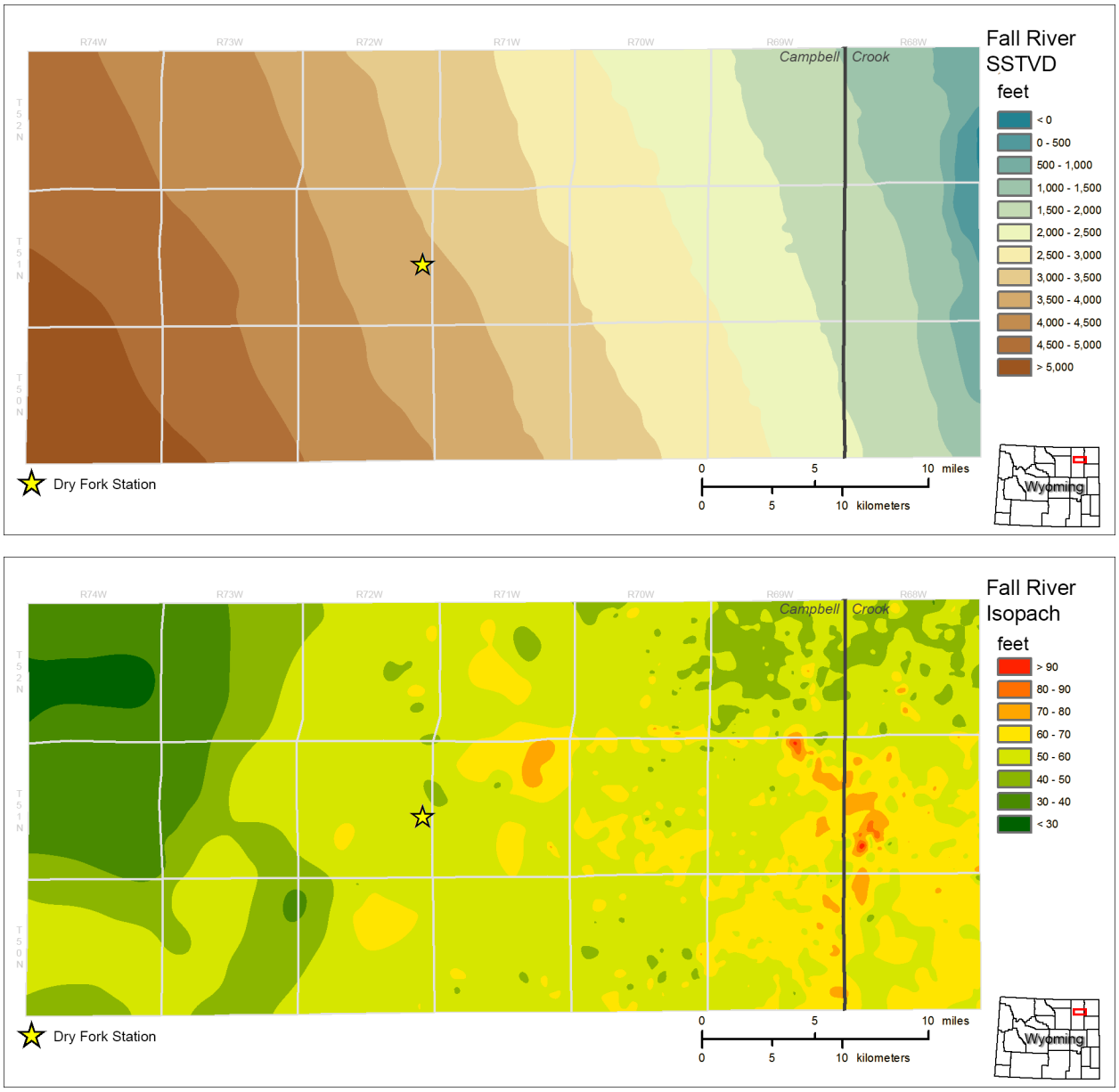

Figure 4A-5 Top: structure contour map of the top of the Fall River Formation (datum – mean sea level), bottom: isopach map of the Fall River Formation.

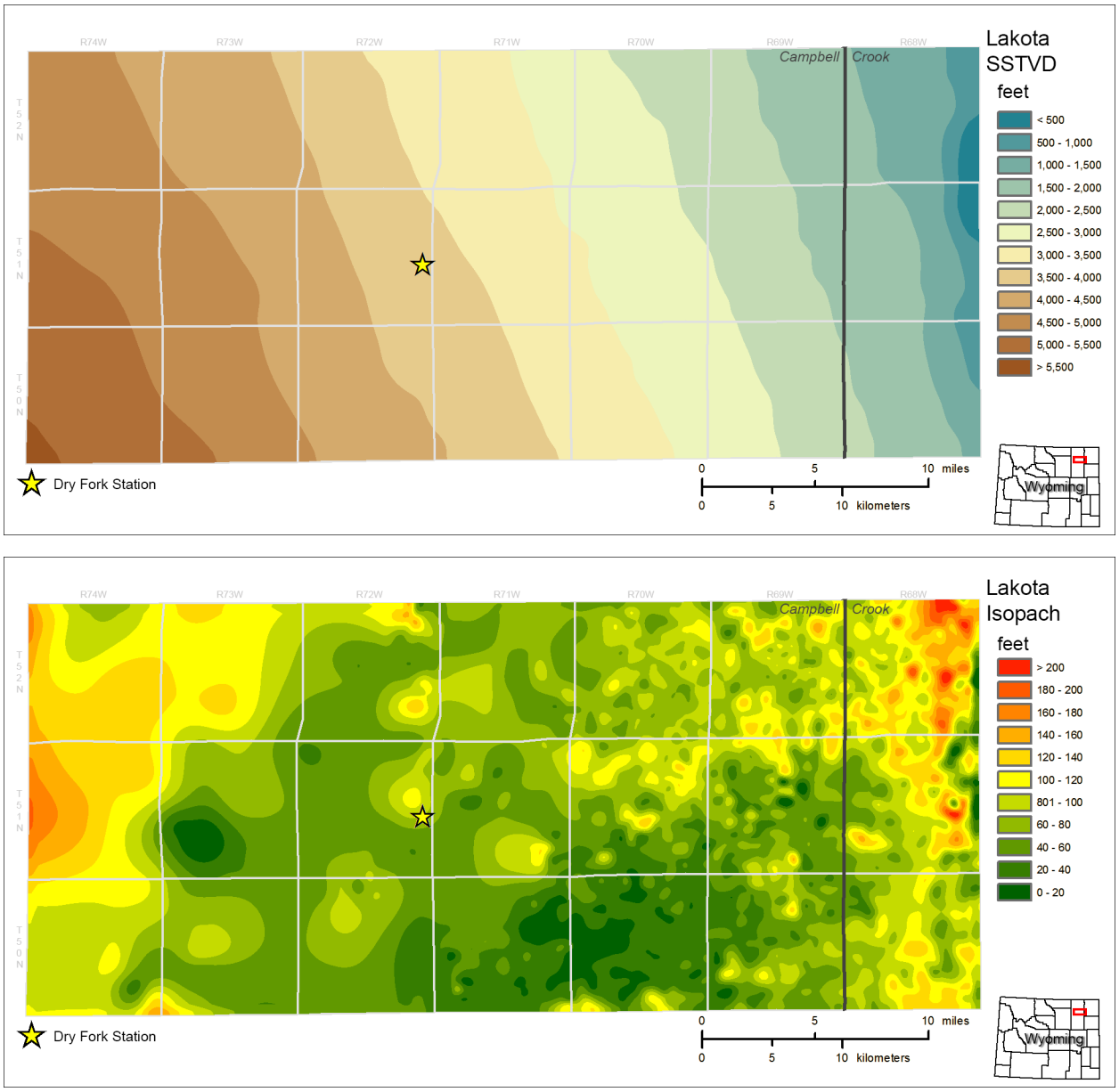

Figure 4A-6 Top: structure contour map of the top of the Lakota Formation (datum – mean sea level), bottom: isopach map of the Lakota Formation.

A.3.3 Lower Sundance Formation

The structural model of the Sundance Formation was divided into the informal upper and lower members. The Lower Sundance was then further divided into the Hulett and Canyon Springs members. Figure 4A-7 shows a typical well log display in the

Sundance Formation near Dry Fork Station. Figure 4A-8 shows structure and isopach maps for the Lower Sundance Formation within the geologic model (red rectangle in Figure 4A-1).

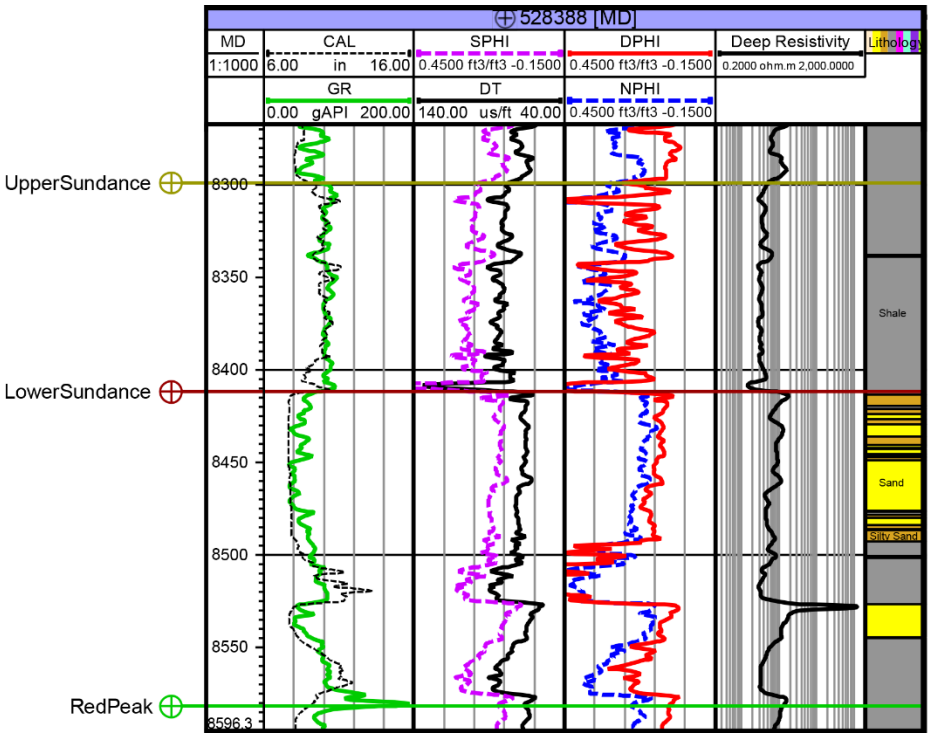

Figure 4A-7 Type log of the Sundance Formation near Dry Fork Station (API 49005283880000). Curves shown are (from left to right) CAL and GR, SPHI and DT, DPHI and NPHI, deep resistivity, and lithology.

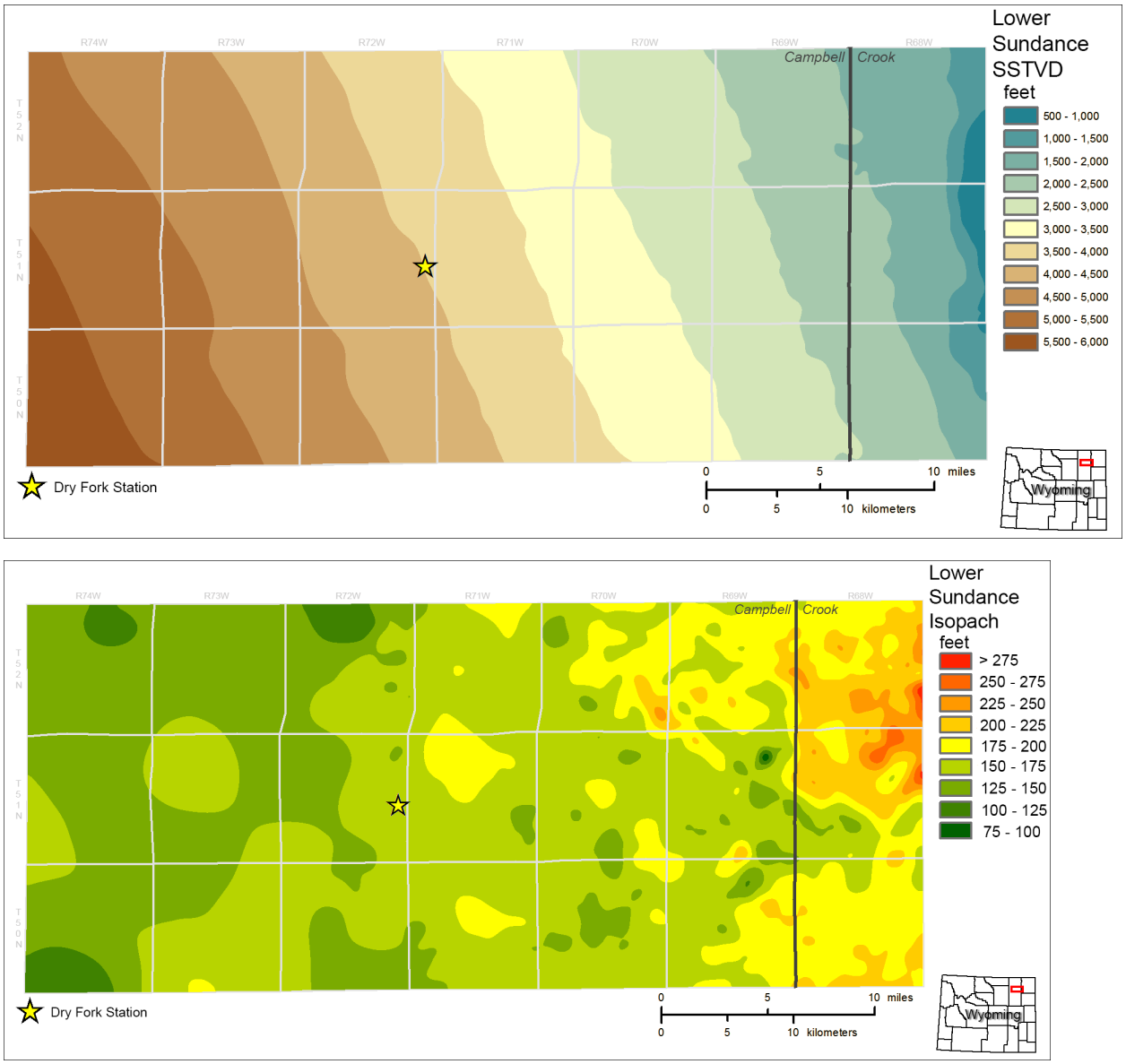

Figure 4A-8 Top: structure contour map of the top of the Lower Sundance Formation (datum – mean sea level), bottom: isopach map of the Lower Sundance Formation.

A.3.4 Upper Minnelusa Formation

The Minnelusa Formation is commonly divided into sandstone members within the PRB that are separated by carbonates. The GDI study on the Minnelusa Formation within the PRB divided the Upper Minnelusa into four sandstone intervals known as A–D. Sandstone intervals

A–D are separated by dolostone intervals. However, these members are not all laterally continuous, specifically the uppermost intervals (i.e., the A/B sands). Figure 4A-9 shows a typical well log display in the Minnelusa Formation near Dry Fork Station. Figure 4A-10 shows structure and isopach maps for the Upper Minnelusa Formation within the geologic model (red rectangle in Figure 4A-1).

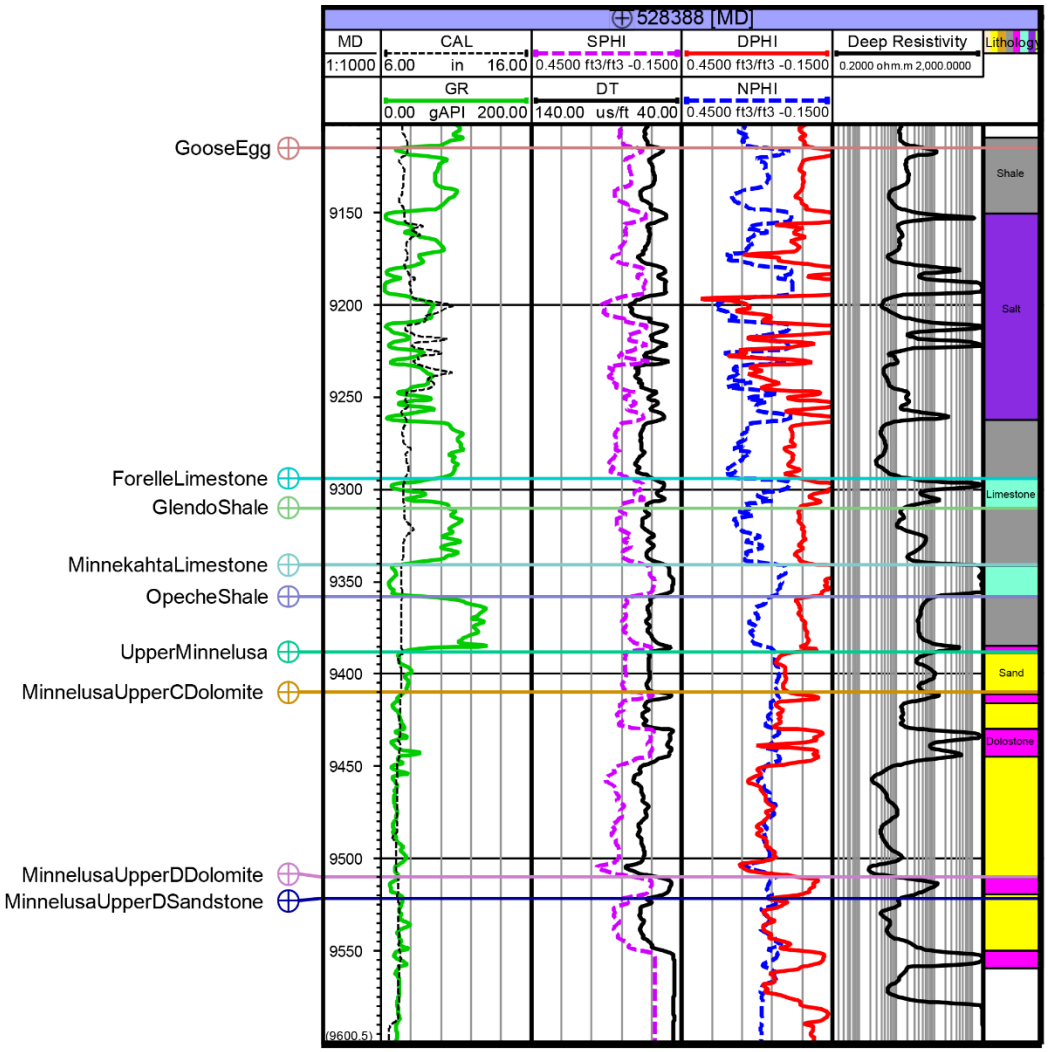

Figure 4A-9 Type log of the Upper Minnelusa near Dry Fork Station (API 49005283880000). Curves shown are (from left to right) CAL and GR, SPHI and DT, DPHI and NPHI, deep resistivity, and lithology.

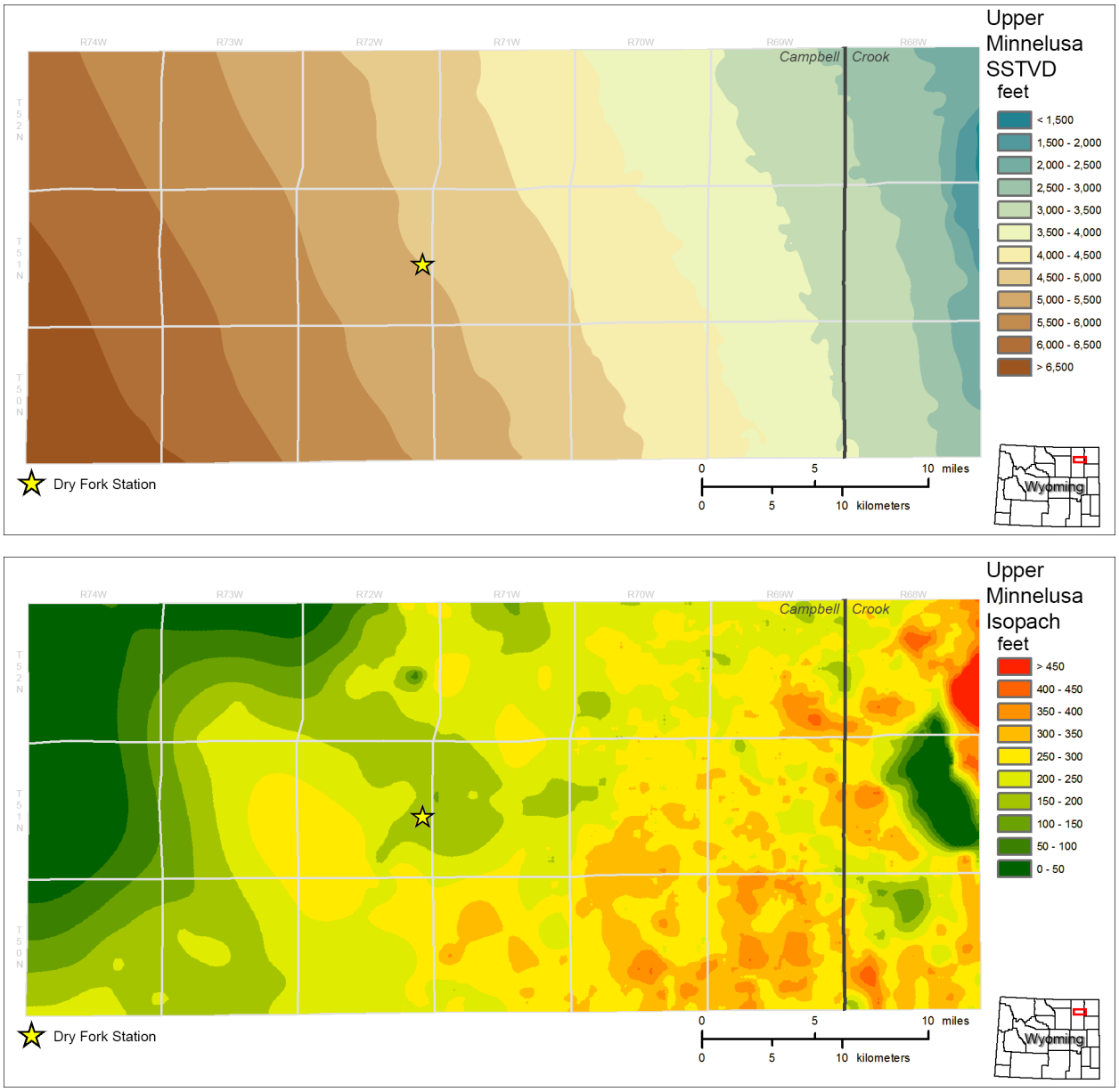

Figure 4A-10 Top: structure contour map of the top of the Upper Minnelusa Formation (datum – mean sea level), bottom: isopach map of the Upper Minnelusa Formation.

A.4 Facies Modeling

A.4.1 Muddy Formation

Muddy Formation lithologies were determined based on well log characteristics within the Muddy Formation along with core descriptions derived from the GDI study on the Northern Muddy. The Muddy was divided into three facies: sandstone, silty sandstone, and shale. “Porous” sandstone and gross sandstone isopach maps from the Muddy GDI study were digitized and used as probability trends for the sandstone distributions.

A.4.2 Fall River/Lakota Formations

The Fall River and Lakota Formations, along with the Fuson Shale, make up the Inyan Kara Group of the PRB. The facies model of the Fall River and Lakota Formations consisted of three lithologies: sandstone, silty sandstone, and shale. Lithofacies were assigned by using GRy log cutoffs and then distributed throughout the model to best represent the depositional environment of each formation.

A.4.3 Lower Sundance Formation

The lower Sundance Formation consists of two reservoir sandstone intervals: the lower Canyon Springs member and the Hulett Sandstone. The Canyon Springs member and Hulett Sandstone are separated by the shale/siltstone of the Stockade Beaver Shale. GR logs through the Lower Sundance interval were normalized and used to assign sandstone, silty sandstone, and shale lithofacies to the Lower Sundance Formation. Structural surfaces of the top and bottom of the Canyon Springs and Hulett Sandstone were used to constrain the sandstone facies distributions.

A.4.4 Upper Minnelusa Formation

Four sandstone/dolostone intervals (A–D) were modeled throughout the study area. These units represent four cycles during Upper Minnelusa deposition. The sandstone intervals represent times of relatively stable sea level when dunes developed in an eolian environment across the study area. During times of relative sea level rise, marine carbonates (later dolomitized) were deposited on top of the previously developed eolian dunes. Using well log interpretations, top and bottom structural surfaces were created for each sandstone interval and used to constrain sandstone facies distributions. All other cells within the Minnelusa Formation model were given properties of a dolostone lithofacies.

A.5 Petrophysical Property Modeling

Petrophysical properties (porosity and permeability) were distributed using variogram-based geostatistical methods with conditioning to the previously developed facies models. Variogram parameters used in these distributions were adapted from generalized variogram ranges based on depositional environment described by Deutsch (2008).

A.5.1 Muddy Formation

Petrophysical properties for the Muddy Formation (Table 4A-1) were derived from core data. These core data included petrophysical properties from core across the entire northern portion of the PRB. Additionally, core analysis were collected by the CEGR on five wells within the Dry Fork study area. Petrophysical properties were then divided into porous sandstone and silty sandstone based on a crossplot of the core analysis data. Porosities associated with permeability values above 1 mD were assigned to the porous sandstone lithofacies, and those below the cutoff were assigned to the silty-sandstone lithofacies (Figure 4A-11).

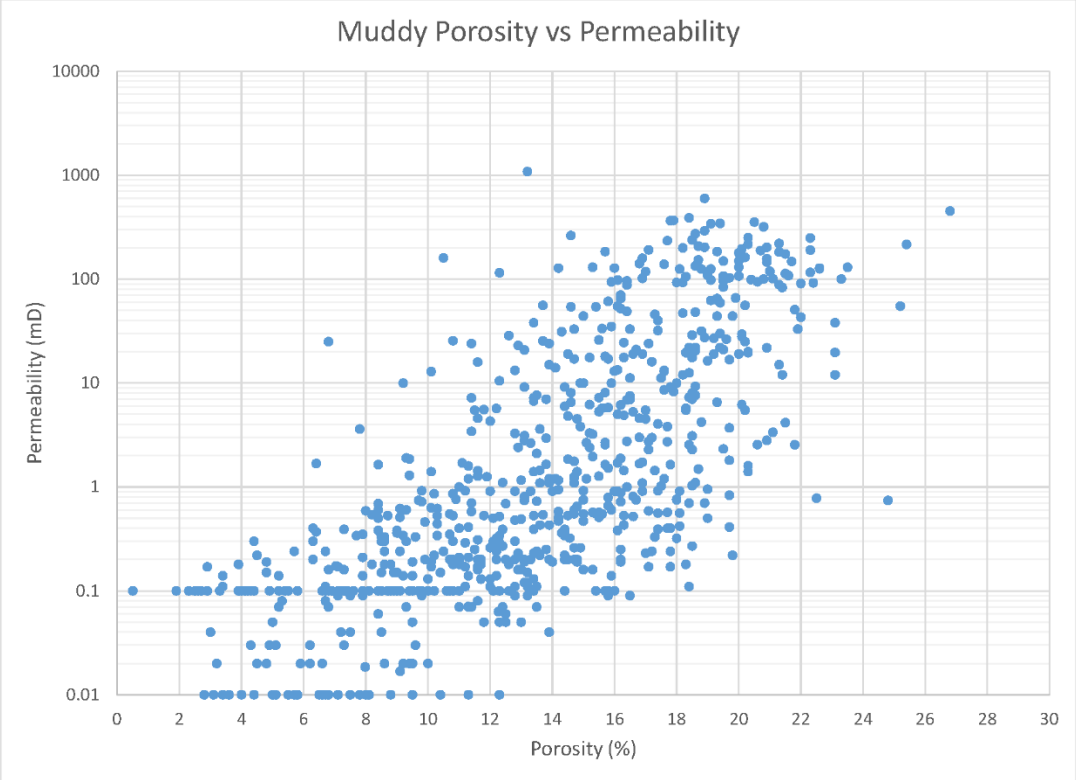

Figure 4A-11 Muddy Formation porosity-permeability crossplot.

A.5.2 Fall River/Lakota Formations

Limited petrophysical properties derived from core analysis were available in the Dry Fork study area for the Fall River/Lakota Formations. Petrophysical properties were instead sourced from Fall River/Lakota cored wells throughout the PRB (Figure 4A-12). Table 4A-1 contains some basic petrophysical statistics for the Fall River and Lakota Formations used in modeling efforts.

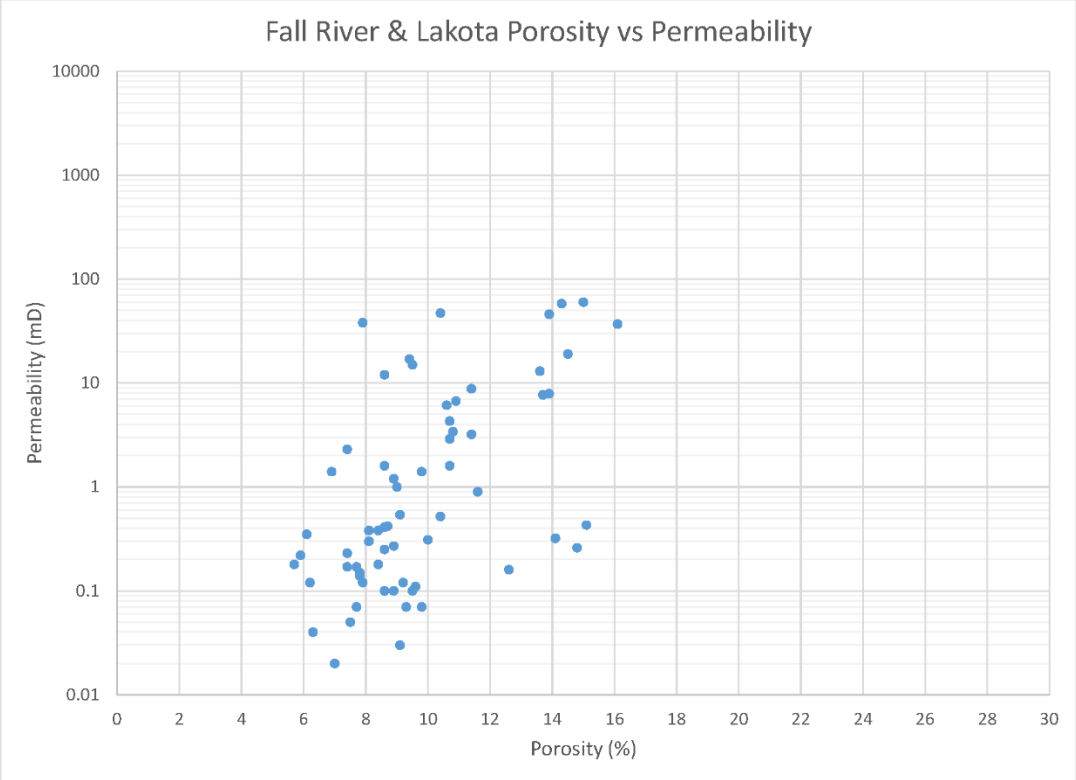

Figure 4A-12 Fall River/Lakota porosity-permeability crossplot.

A.5.3 Lower Sundance Formation

Petrophysical properties derived from core analysis were not available in the Dry Fork study area for the Lower Sundance Formation. Petrophysical properties were instead sourced from Lower Sundance cored wells throughout the PRB (Figure 4A-13). Table 4A-1 contains some basic petrophysical statistics for Lower Sundance Formation used in modeling efforts.

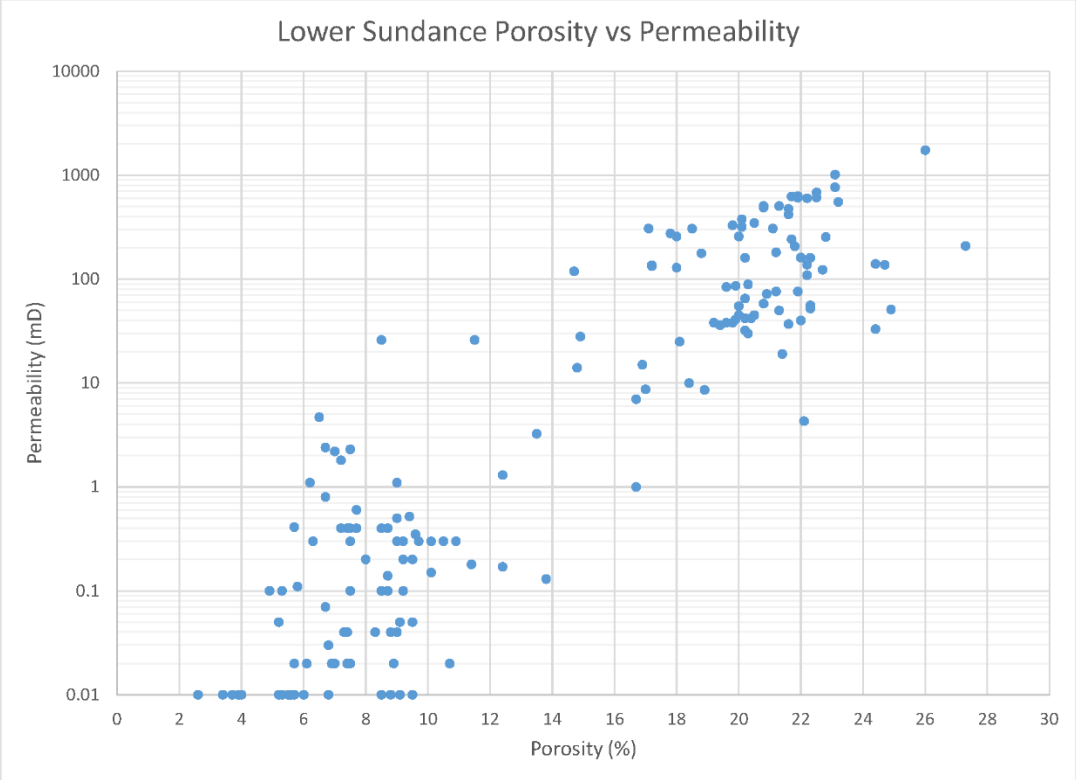

Figure 4A-13 Lower Sundance porosity-permeability crossplot.

A.5.4 Upper Minnelusa Formation

Site-specific petrophysical properties within the Dry Fork study area are very limited for the Upper Minnelusa Formation. Upper Minnelusa core analysis values were collected from the entire PRB for use in petrophysical modeling. CEGR also evaluated core samples from four wells within the Dry Fork study area for use in petrophysical modeling. The combined core sample analyses are shown in Figure 4A-14. Petrophysical properties for the formation were separated based on the two dominate reservoir and nonreservoir lithologies (sandstone and dolostone, respectively) in order to better represent each lithology within the formation (Table 4A-1).

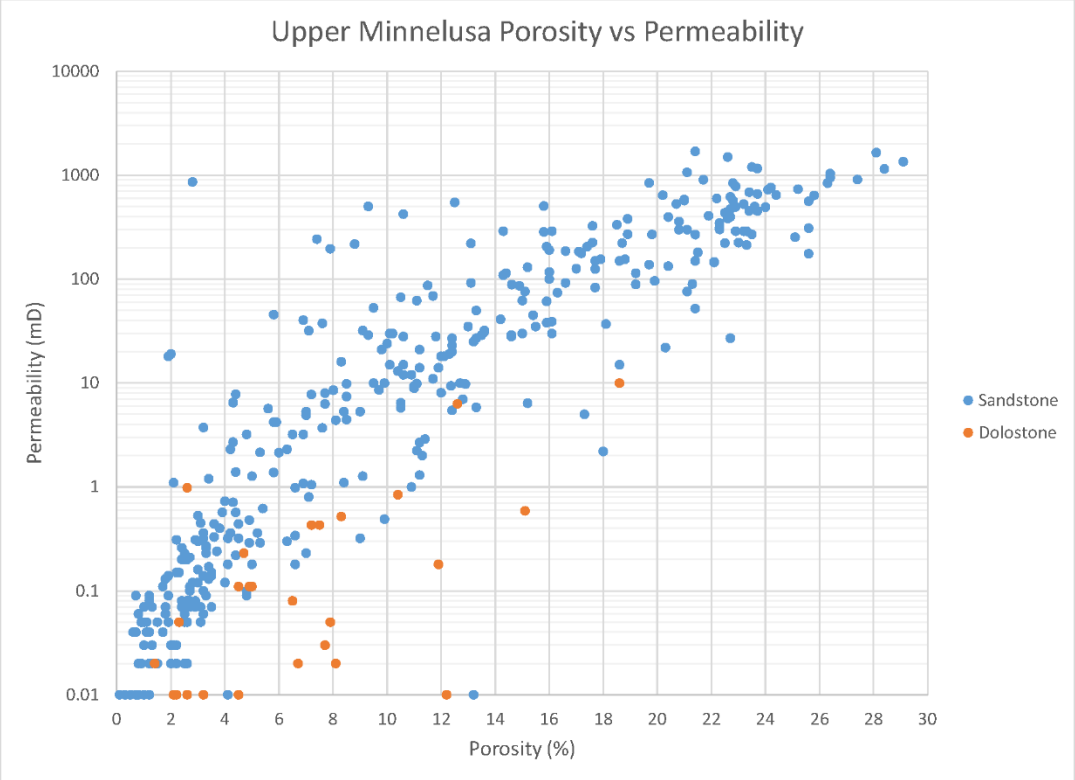

Figure 4A-14 Upper Minnelusa porosity-permeability crossplot.

A.6 Petrophysical Property Uncertainty

Multiple property distributions were developed for each model to address petrophysical property uncertainty. Petrophysical properties were distributed, which represented P10, P50, and P90 cases within each previously developed facies model. The P10 distribution represented a generally conservative case, with a 10% chance that the actual values were lower. The P50 distribution represented a median value, and the P90 distribution represented a more optimistic case, with a 10% chance that the values were higher.

A.6.1 Porosity

Porosity values from core sample analyses of each formation were used to determine the P10, P50, and P90 values and the standard deviation used in petrophysical modeling (Table 4A-2).

A.6.2 Permeability

Permeability values used in modeling efforts for each formation were based on core-measured values. Permeability was bivariately distributed using the previously modeled porosity property and a relationship derived from the core-measured porosity-permeability crossplots from each formation.

Table 4A-2 Petrophysical Uncertainty Model Cases

Model*	Case	Mean Porosity, %	GeoMean Permeability, mD
Muddy	P10	N/A	N/A
	P50	8.89	0.0098
	P90	12.14	0.03
Fall River/Lakota	P10	N/A	N/A
	P50	5.60	0.00052
	P90	7.0	0.00091
Lower Sundance	P10	6.21	0.0019
	P50	7.39	0.0033
	P90	9.89	0.011
Upper Minnelusa	P10	6.47	0.57
	P50	10.11	2.24
	P90	17.39	21.71

*Includes all lithologies

A.7 Other Reservoir Properties

Drillstem test results and temperature measurements within the study area were used for estimating pressure and temperature of each formation of interest to aid in numerical simulation efforts. Pressure and temperature gradients used for each formation are shown in Table 4A-3. Interestingly, three of the four target formations showed evidence of underpressured conditions in comparison to hydrostatic pore pressure gradient (0.433 psi/ft. for fresh water). No further action was taken to investigate the cause.

Table 4A-3 Pressure and Temperature Gradients for Each Formation of Interest

Formation	Pressure Gradient, psi/ft.	Temperature Gradient, °F/ft.
Muddy	0.31	0.013
Fall River/Lakota	0.44	0.014
Lower Sundance	0.39	0.014
Minnelusa	0.39	0.014

A.8 Volumetric Storage Resource Estimates

A.8.1 Methods

The models developed in this work, discussed in the previous sections, were used to estimate the static, volumetric CO_2 storage resource potential. The U.S. Department of Energy (DOE) National Energy Technology Laboratory (NETL) has developed multiple methods of such estimations (DOE NETL, 2010). One such method was specifically developed to estimate the CO_2 storage resource potential of a saline formation using the following equation:

$$G_{CO2} = A_t h_g \varphi_{tot} \rho E_{saline} \quad \text{[Eq. 1]}$$

Where A_t is the total area in consideration, h_g is the gross formation thickness, φ_{tot} is the total porosity (effective and ineffective porosity together), ρ is the expected CO_2 density

at the end of injection (after reaching maximum reservoir pressure constraints), and E_{saline} is the efficiency factor describing the fraction of the pore volume that will be occupied by the injected CO_2.

Storage resource potential estimates were determined using the workflow created by Peck and others (2014), which expanded upon the DOE methodology reported in the Carbon Sequestration Atlas III (DOE NETL, 2010). The footprints of existing oil and gas operations within the study area were excluded from the final storage potential estimates to avoid potential negative interaction between CO_2 storage and other subsurface activities. The study area used in the equation for each formation was 766 mi^2. Isopach maps were built to describe formation thickness. Porosity was derived from formation-specific core analysis data collected from wells within the PRB. CO_2 density was calculated using the method of Wang and others (2015) using pressure calculated from a gradient of 0.6 psi/ft., a constraint placed on simulated injection wells in avoidance of fracturing the rock. Saline storage efficiency (E_{saline}) values from Peck and others (2014) were used in these calculations. As described in Peck and others (2014), different E_{saline} values were used for each selected formation, because different amounts of data were available. For example, the greatest amount of information was known about the Muddy Formation; therefore, the highest efficiency values were used; in comparison, much less data were available for the lower Sundance Formation, thus the use of lower efficiency values. For each formation, storage resource potential was calculated using P10 (conservative), P50 (median), and P90 (optimistic) E_{saline} values and the other values used in Table 4A-4.

Table 4A-4 Parameters Used To Calculate CO_2 Storage Resource Potential

Unit	Mean Porosity (%)	Mean Thickness (ft.)	Mean CO_2 Density ($lb/ft.^3$)	P_{10} E_{saline} (%)	P_{50} E_{saline} (%)	P_{90} E_{saline} (%)
Muddy	13.2	25	50.74	7.4	14.0	24.0
Fall River/Lakota	7.1	128	50.75	1.62	4.41	9.53
Lower Sundance	13.8	162	50.76	1.62	4.41	9.53
Upper Minnelusa	10.7	165	50.78	7.4	14.0	24.0

Table 4A-4 Parameters Used to Calculate CO_2 Storage Resource Potential

	Porosity, %	Average Thickness, ft.	Average CO_2 Density, lb/ft^3	P10 E_{saline}, %	P50 E_{saline}, %	P90 E_{saline}, %
Muddy	13.2	25	50.74	7.40	14.00	24.00
Fall River/Lakota	7.1	128	50.75	1.62	4.41	9.53
Lower Sundance	13.8	162	50.76	1.62	4.41	9.53
Upper Minnelusa	10.7	165	50.78	7.40	14.00	24.00

The Muddy, Lakota/Fall River, and Minnelusa Formations all produce oil in the study area. A future potential CO_2 storage operation would be planned in such a way to avoid any potential detrimental impact on hydrocarbon resources, thus areas where oil fields exist were eliminated from the storage potential estimates of these formations. The Lower Sundance does not produce hydrocarbons in the study area, and therefore needed no such adjustment. Table 4A-5 presents the CO_2 storage resource estimates with the oil fields removed. Isopach maps, maps showing the P_{50} CO_2 storage potential estimates (with and without oil fields regions considered), and a combined CO_2 storage resource potential map (all formations), can be found in Figures 4A-15 through 4A-27.

Table A-5 CO_2 storage potential estimates for selected formations with oilfields removed.

Unit	P10		P50		P90	
	Sum, Mt	Mt/mi^2	Sum, Mt	Mt/mi^2	Sum, Mt	Mt/mi^2
Muddy	98	0.13	180	0.24	320	0.41
Fall River/Lakota	70	0.10	190	0.25	410	0.54
Lower Sundance	180	0.23	480	0.63	1000	1.40
Upper Minnelusa	500	0.66	950	1.20	1600	2.10
Combined	848	1.12	1800	2.32	3330	4.45

A.8.2 Muddy Formation

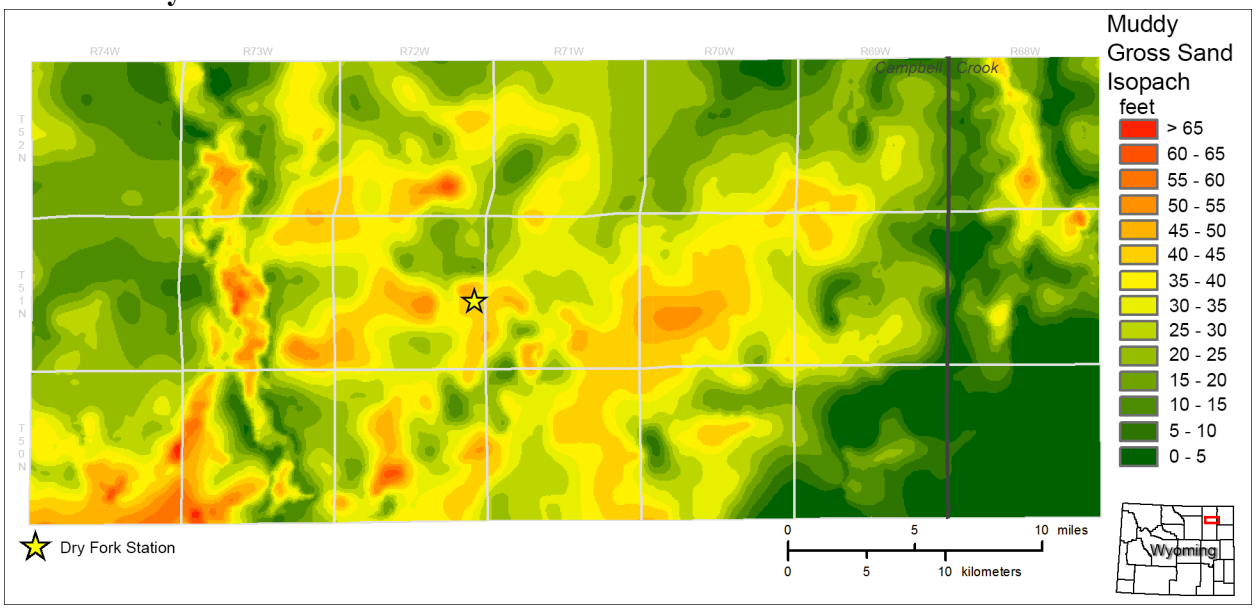

Figure 4A-15 Sandstone isopach map of the Muddy Formation.

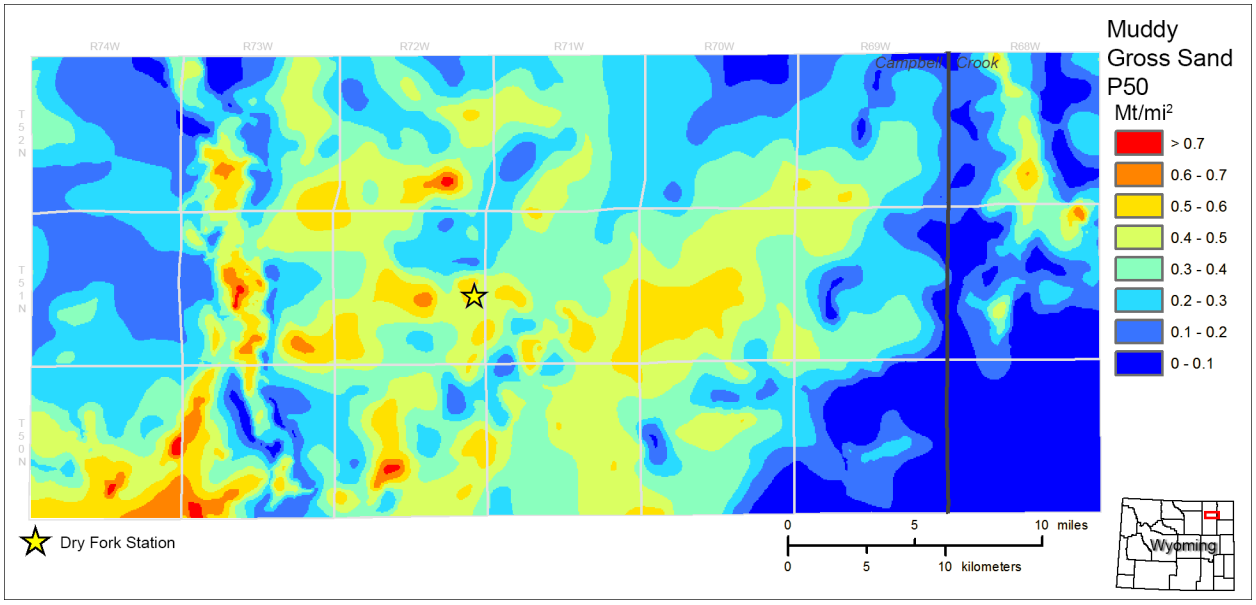

Figure 4A-16 Map of the Muddy Formation estimated P50 CO_2 storage resource potential (million tonnes/mi^2).

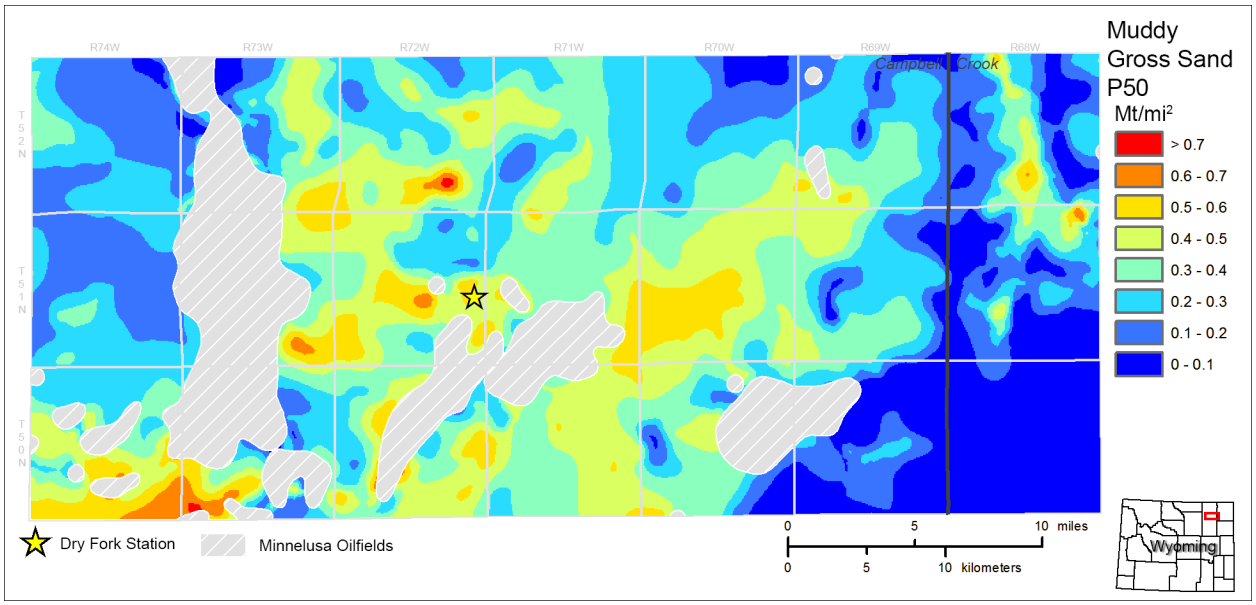

Figure 4A-17 Map of the Muddy Formation estimated P50 CO_2 storage resource potential (million tonnes/mi^2) with oil fields removed.

A.8.3 Fall River/Lakota Formations

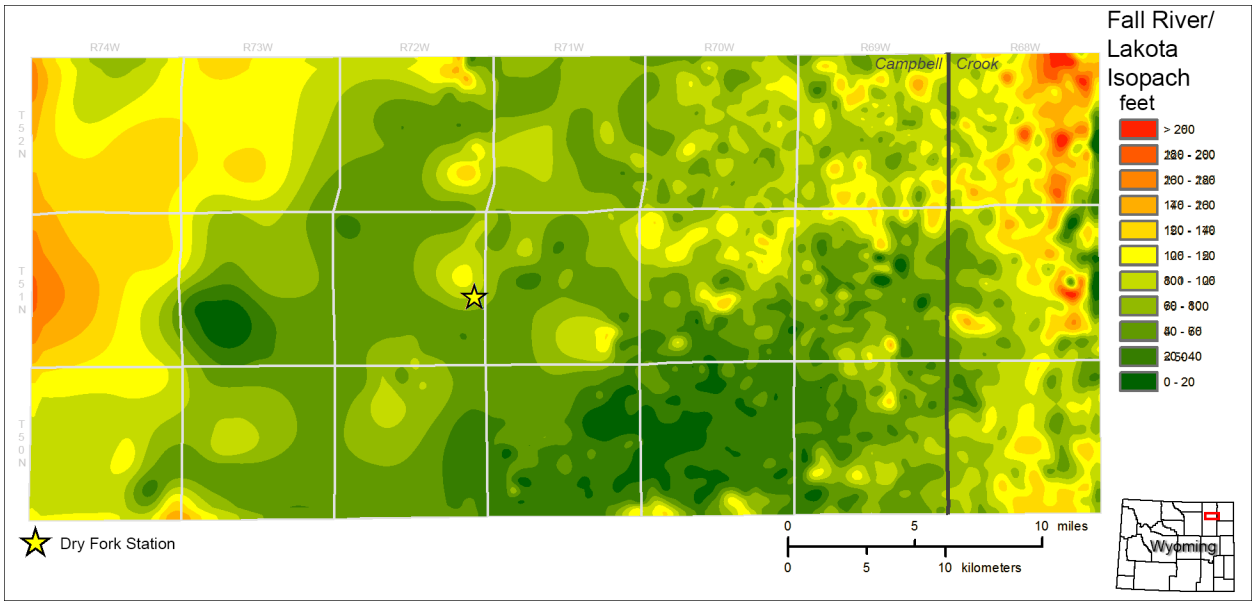

Figure 4A-18 Isopach map of the Fall River and Lakota Formations.

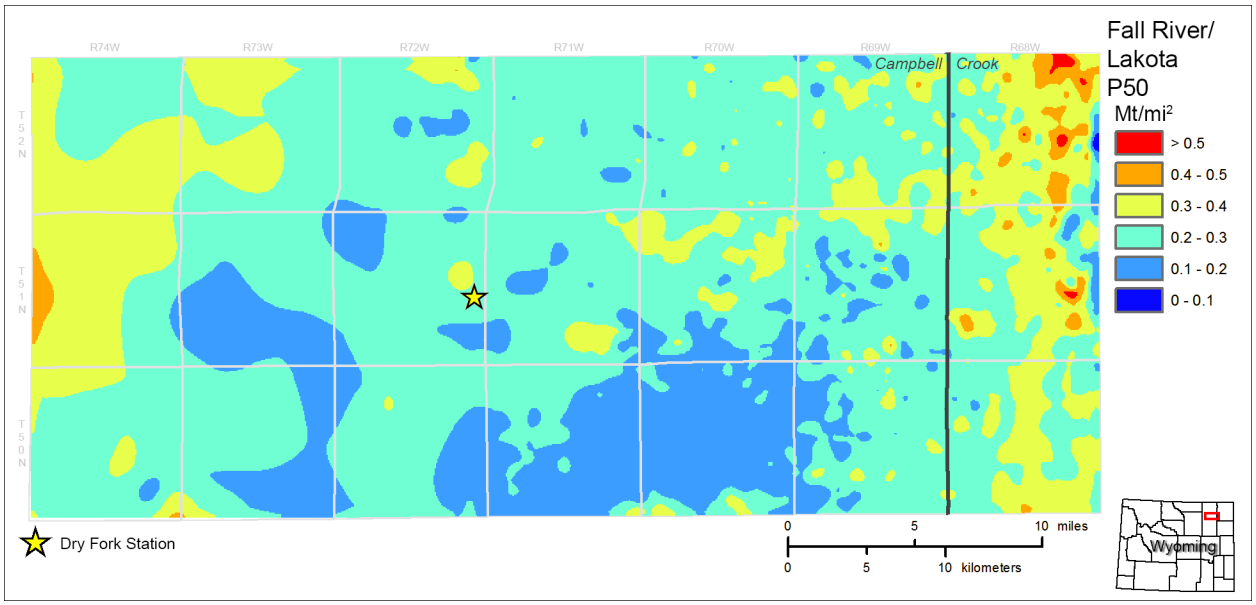

Figure 4A-19 Map of the Fall River and Lakota Formations' estimated P50 CO_2 storage resource potential (million tonnes/mi^2).

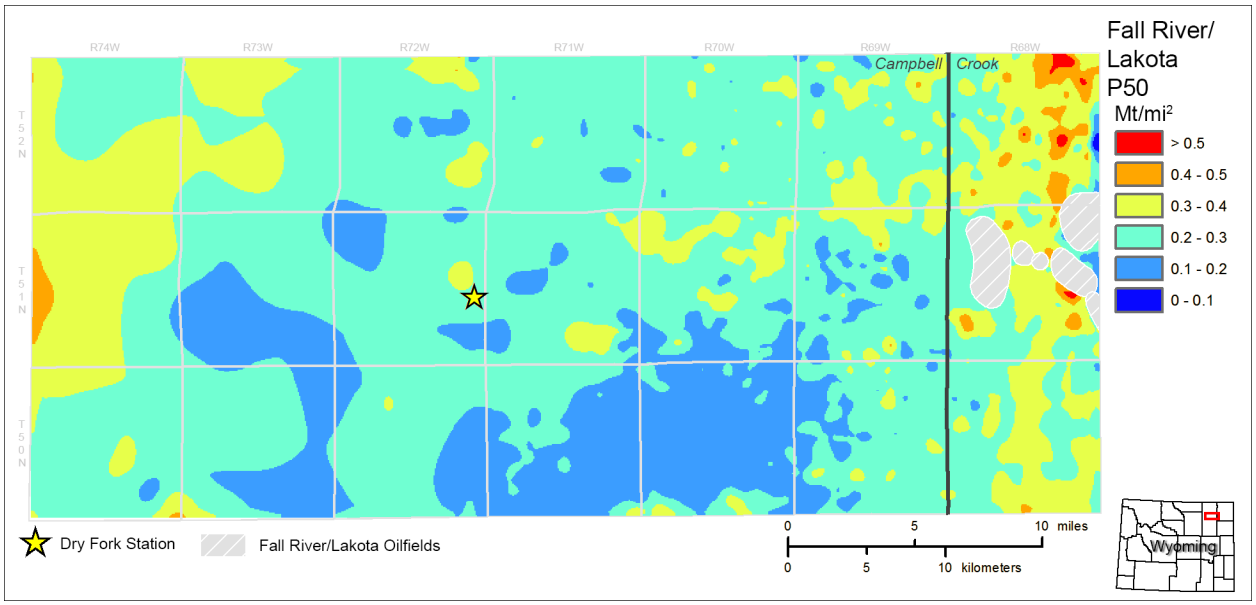

Figure 4A-20 Map of the Fall River and Lakota Formations' estimated P50 CO_2 storage resource potential (million tonnes/mi^2) with oil fields removed.

A.8.4 Lower Sundance Formation

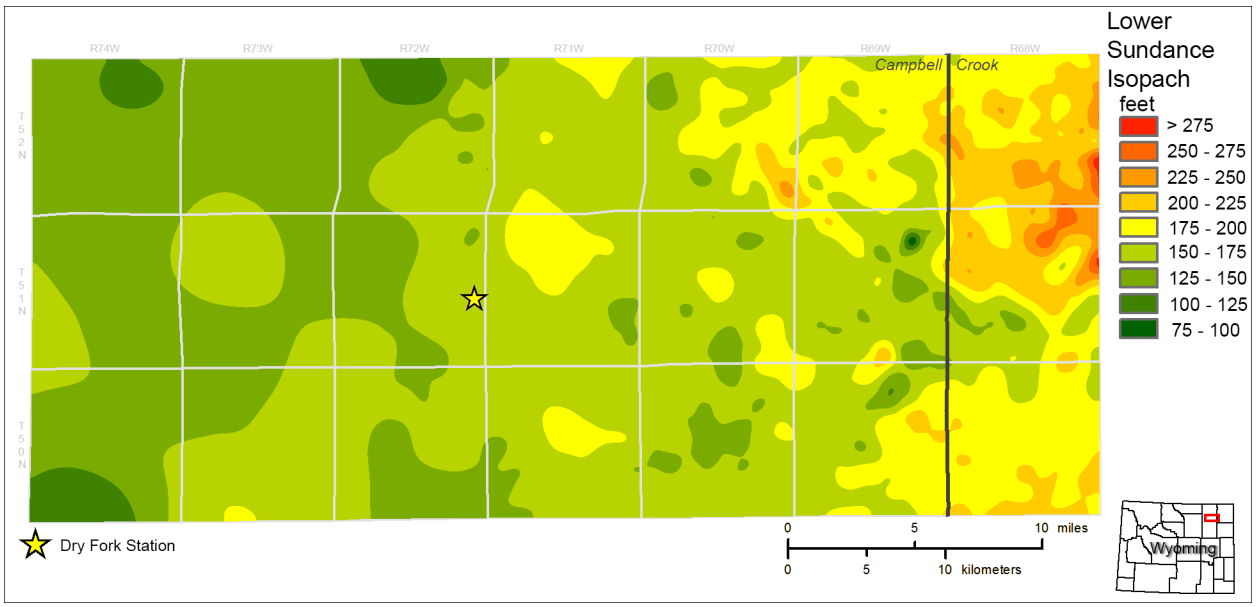

Figure 4A-21 Isopach map of the Lower Sundance Formation.

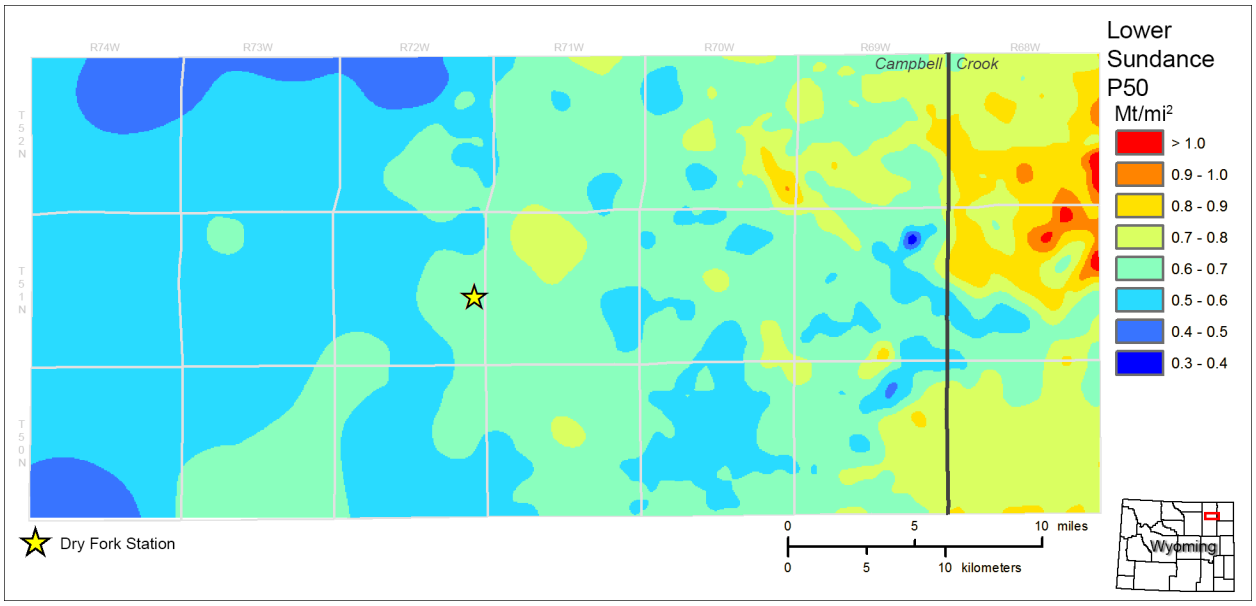

Figure 4A-22 Map of the Lower Sundance Formation estimated P50 CO_2 storage resource potential (million tonnes/mi^2).

A.8.5 Upper Minnelusa Formation

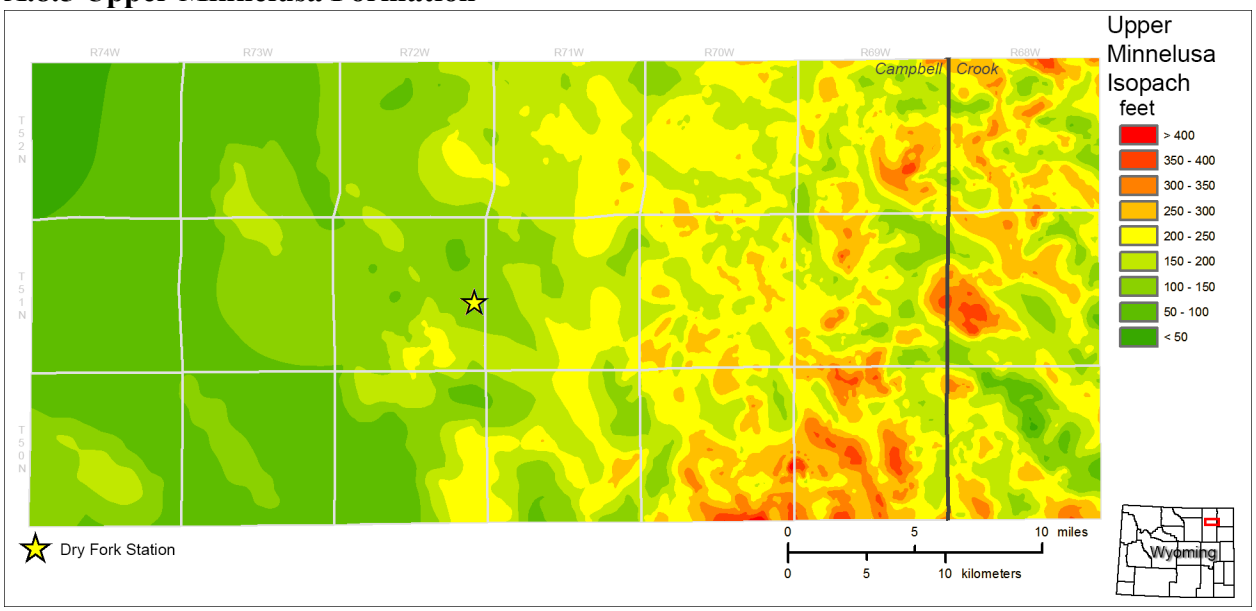

Figure 4A-23 Sandstone isopach map of the Upper Minnelusa Formation.

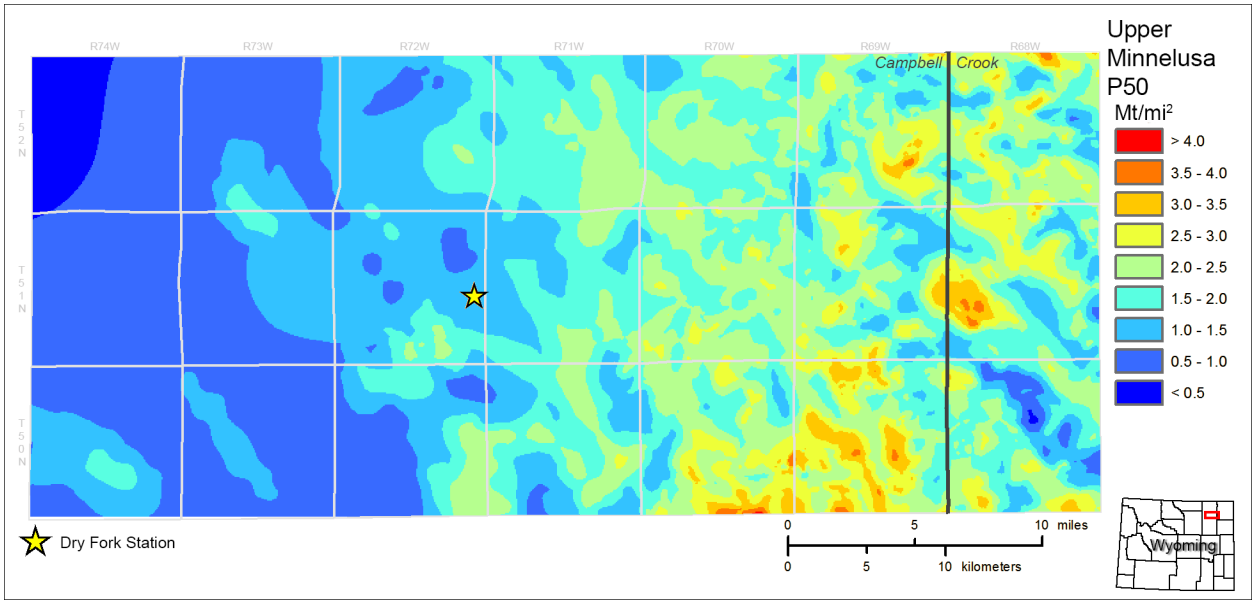

Figure 4A-24 Map of the Upper Minnelusa Formation estimated P50 CO_2 storage resource potential (million tonnes/mi^2).

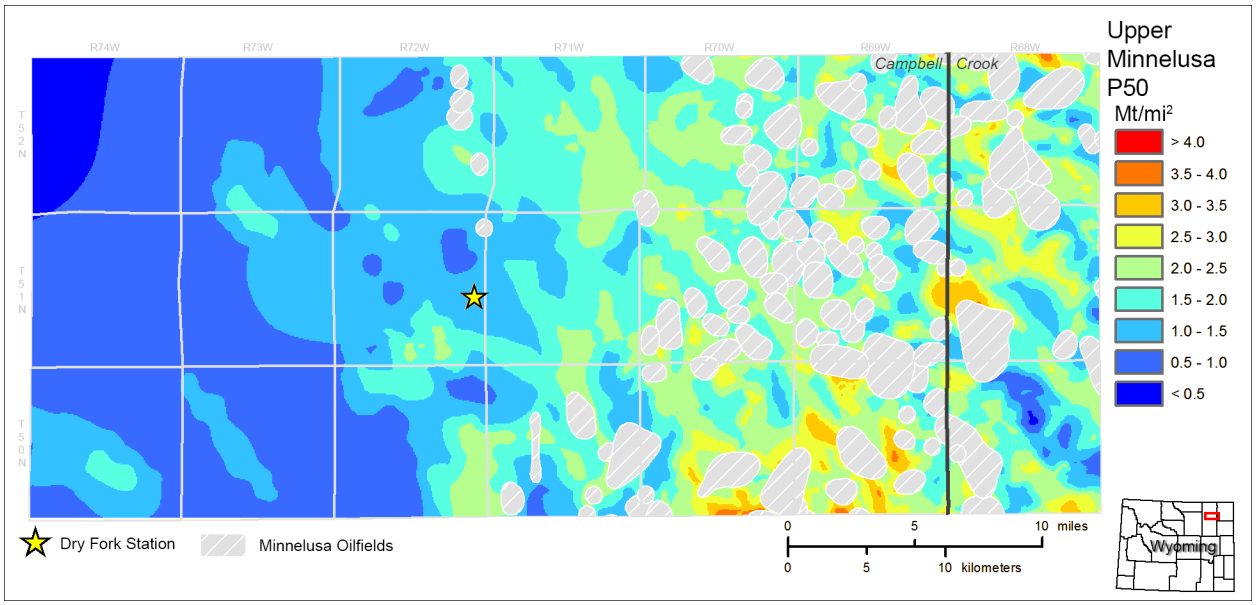

Figure 4A-25 Map of the Upper Minnelusa Formation estimated P50 CO_2 storage resource potential (million tonnes/mi^2) with oil fields removed.

A.8.6 Combined Formations

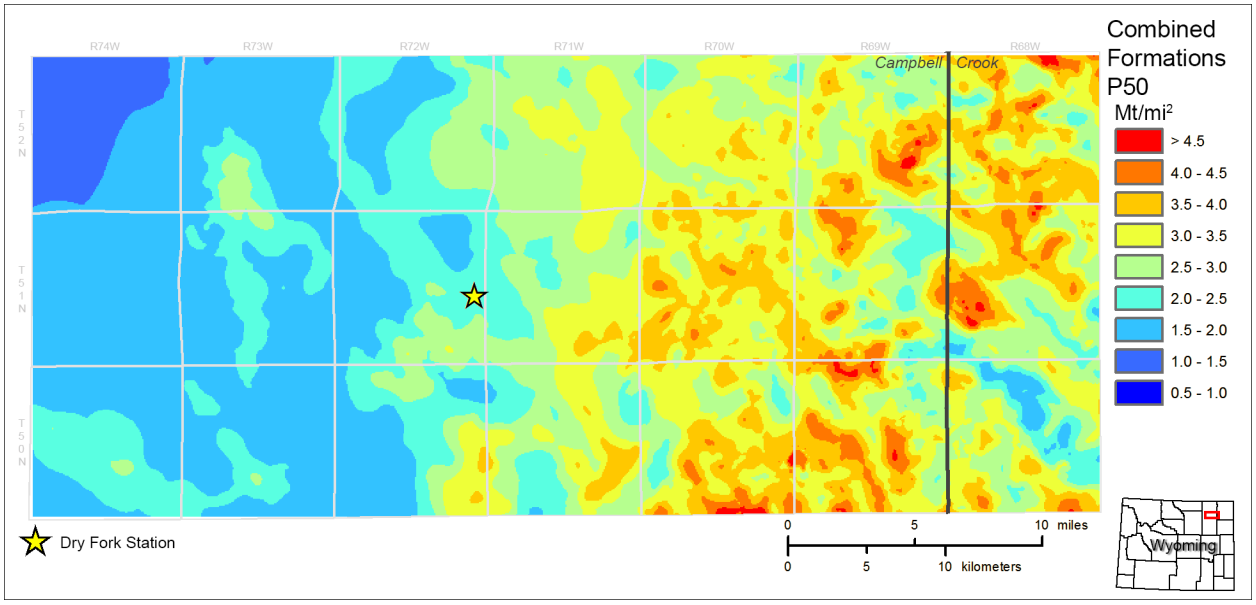

Figure 4A-26 Map of the combined formations' estimated P50 CO_2 storage resource potential (million tonnes/mi^2).

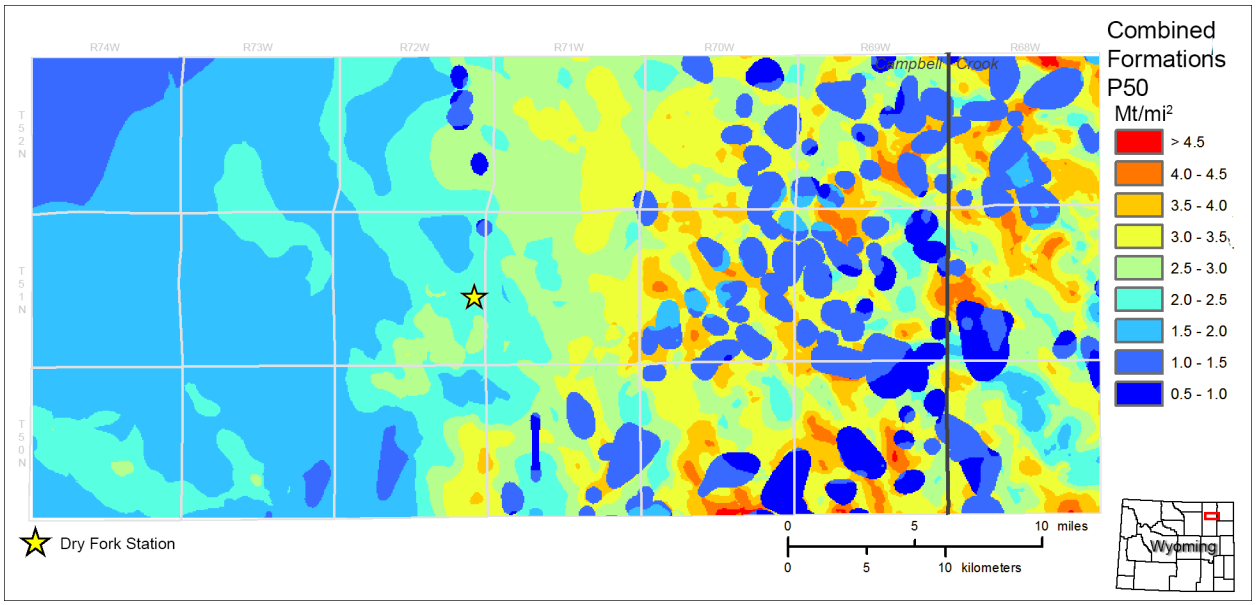

Figure 4A-27 Map of the combined formations' estimated P50 CO_2 storage resource potential (million tonnes/mi^2) with oil fields removed.

A.9 Numerical Simulation

Numerical simulation of CO_2 injection was conducted using the models described in the previous sections. These simulations were run to test formation responses to injection and the probability of successful storage. Simulations were performed using Computer Modelling Group Ltd.'s (CMG's) GEM software (CMG, 2017). The intent of each simulation was to assess the potential of storing fifty million tonnes of CO_2 over a twenty-five year timeframe.

A.9.1 Scenario Design

With the exception of Muddy and Fall River/Lakota cases, simulated wells were placed to maximize pore space use on BEPC, Western Fuels, and Wyoming state lands. The wells placed in the Muddy and Fall River/Lakota cases were placed where petrophysical properties were deemed best, scrutinized from porosity-thickness and permeability-thickness maps of the models' distributions. This was done to give an initial assessment

of the 'best case' scenario for each, as each model contained relatively thin reservoir intervals with a high degree of heterogeneity. Maximum bottomhole pressure constraints were used in all of the cases, calculated from formation depth in well locations using a pressure gradient of 0.6 psi/ft., employed to mitigate the potential of fracturing the rock during injection. One case was conducted in exception, in which a bottomhole pressure constraint was calculated using a gradient of 0.7 psi/ft. This case was conducted to assess storage performance with slightly higher injection pressure constraints, a scenario which may occur if site specific measurements of fracture pressure in overlying sealing formations indicate the fracture pressure gradient is greater than what would be assumed in default (0.6 psi/ft.). Perforations were set in sandstone components of each formation.

Base cases (P_{50} cases with four vertical injection wells) were simulated for each of the formations of interest. In the Lower Sundance and Minnelusa simulations, P10 (conservative) and P_{90} (optimistic) cases with four vertical injection wells were run. After scrutinizing the results for the Muddy and Lakota/Fall River cases, which indicated rather poor storage performance, a decision was made to supplement the P_{50} results only with P90 cases with four vertical injection wells for these two models. Additionally, P_{50} cases with six vertical injection wells, brine extraction, and horizontal wells were run. Brine extraction cases were run with four injection wells and one production well. Of the horizontal well cases, a subset were run with one well but with lateral length varied from 0.25 mile to one mile, and another subset of cases were run with four horizontal wells with one mile laterals.

A.9.2 Results

Results of all simulations are included in Table 4A-6 below.

Figure 4A-27 shows the base case results for all models. The base case (P_{50} models with four vertical injection wells) simulation results indicated the Muddy and Lakota/Fall River Formations would likely not be suitable for CO_2 storage at the scale required of the project. The relatively thin nature of each formation and the inherent geologic heterogeneity (discontinuous nature of sand bodies) resulted in rapid pressure build-up during the simulations, which limited injectivity. Therefore, P_{10} (conservative) cases were foregone and only P_{90} (optimistic) cases were simulated for each of these formations. Yet even with petrophysical properties as good as what would be expected of a P_{90} scenario, the results indicate neither formation individually would be able to receive 50 million tonnes of CO_2 in a 25-year time frame based on the scenarios investigated. These formations, however, are not being excluded from future investigative activities, as there may be some potential for integration of these units in a stacked storage scenario.

The Minnelusa Formation base case result was nearly 31 million tonnes of stored CO_2 in a 25-year timeframe. A similar case was conducted but with a BHP constraint calculated using a pressure gradient of 0.7 psi/ft. (the base case used a gradient of 0.6 psi/ft.), and the result was just over 48 million tonnes of CO_2 stored in a 25-year timeframe. This result illustrated the importance of understanding fracture pressure gradient at future potential injection sites. Data may be generated in future characterization activities (i.e., micro-fracture testing in sealing units overlying injection targets) to support increasing of permitted injection pressure above gradients considered in default when fracture pressure data is absent. The impact of increasing injection pressure constraints may be significant, as indicated by these results.

An additional Minnelusa Formation case was simulated using six vertical wells, in which two additional wells were added on Wyoming state sections to the west of DFS. Using the 0.6 psi/ft. BHP constraint, the case resulted in the storage of nearly 60 million tonnes of CO_2 over a 25-year timeframe.

The P_{90} (optimistic) Minnelusa Formation simulation case using four wells and a 0.6 psi/ft. BHP gradient constraint resulted in the storage of 197 million tonnes of CO_2 in a 25-year timeframe. This result, while considered a rather unlikely scenario, indicated that if Minnelusa petrophysical properties were even slightly better than those present in the P_{50} geologic model, 50 million tonnes of stored CO_2 is certainly achievable in the Minnelusa Formation. The Lower Sundance P_{90} (optimistic) case with four wells resulted in 81 million tonnes of stored CO_2.

Horizontal well cases were run using the Lower Sundance and Minnelusa models to investigate the potential benefit to future potential injection scenarios. Single vertical well cases were simulated for both the Lower Sundance and Minnelusa model to provide a basis for comparison, which resulted in the storage of seven million tonnes and twelve million tonnes of CO_2 respectively. Two horizontal well cases were run for each model, cases using one horizontal well but varying lateral length from 0.25 mi to 1 mi. The results were 10.4 and 12 million tonnes of CO_2 in the Lower Sundance and 18.1 and 23.8 million tonnes of CO_2 in the Minnelusa model. Therefore, a horizontal well with lateral length of 0.25 mi enabled an increase of 48% more injected CO_2 mass in comparison to a vertical well in the Lower Sundance model, and the difference in injected CO_2 mass between horizontal wells with 0.25 and 1 mi laterals was 15%. In the Minnelusa model, the difference in injected CO_2 mass between a single vertical well and a horizontal well with a 0.25 mi lateral was 51%, and the difference in injected CO_2 mass between horizontal wells with 0.25 and 1 mi laterals was 31%. Because the one-mile lateral cases appeared to show significant increases in the resulting injectivity over both vertical wells and horizontal wells with shorter laterals, an additional simulation case was run for both

the Lower Sundance and Minnelusa model using four horizontal wells with 1-mile laterals.

Cases with four horizontal wells with 1 mi laterals ended up with 21.8 million tonnes in the Lower Sundance and 56 million tonnes in the Minnelusa Formation. Compared to the base case results (four vertical injection wells), the cases with four horizontal wells showed increases of 12% in the Lower Sundance model and 82% in the Minnelusa model. The difference observed in effectiveness of horizontal wells is thought to relate to average formation thickness in the study area. Even though horizontal wells provide much greater contact with the injection interval, suggesting overall injectivity should be higher, injectivity will still be limited by pressure build-up. The sands of the Lower Sundance Formation are relatively thin, therefore pressure build-up from either horizontal or vertical wells are likely to reach pressure limits relatively quickly, resulting in similar stored CO_2 masses between the cases. The Minnelusa Formation, being relatively thick, appears to allow pressure dispersion from horizontal wells to occur more liberally throughout a greater reservoir volume, resulting in significantly more stored CO_2 in comparison to scenarios using vertical wells.

Brine extraction cases were also conducted using the Lower Sundance and Minnelusa models. The injection well pattern used in the base case simulations (four vertical wells) was used in the brine extraction cases, with a production well placed near the center of the cluster to act as a large-scale 5-spot pattern. The Lower Sundance brine extraction case resulted in the storage of 26 million tonnes of CO_2, an increase of 33% over the base case result with only the four injection wells. The Minnelusa brine extraction case resulted in the storage of 43 million tonnes of CO_2, an increase of 39% over the base case result with only the four injection wells.

One Upper Minnelusa case was simulated to observe the long-term pressure response and disposition of injected CO_2. The six-well (vertical) case was simulated for 100 years post-injection (125 years in total). The results indicated that the pressure build-up associated with injection is expected to dissipate rather quickly, with pressure conditions after 100 years of post-injection monitoring resembling that of pre-injection conditions. CO_2 migrated in the structural updip direction (east) under the effects of buoyancy at a very slow rate, on the order of tens of feet per year. If this migration rate were to continue, injected CO_2 would take tens of thousands of years to reach a Minnelusa outcrop to the east (approximately 70 miles). However, this rate is likely overestimated, as this simple calculation does not account for the effects of structural traps that exist in the Minnelusa (small eolian dunefield traps, which would likely slow buoyant migration significantly), the effects of relative permeability and residual trapping, dissolution of CO_2, which would negate migration under the effects of buoyancy, or mineralization of dissolved CO_2 (i.e., formation of carbonate minerals), which would permanently trap injected CO_2. Therefore, the results give confidence that, with the integration of an adequate regional wellbore integrity assessment to mitigate potential vertical migration pathways, risks related to conformance and containment of injected CO_2 are negligible.

Graphs showing cumulative stored CO_2 (tonne), maps showing CO_2 plume footprint (gas per unit area – total; ft.), and maps showing the pressure distribution at the conclusion of simulated CO_2 injection are shown in Figures 4A-29 through 4A-44 below. Maps showing long-term CO_2 migration potential (gas per unit area – total; ft.) and 100-year post-injection pressure distribution from the six-well Upper Minnelusa case are shown in Figures 4A-45 through 4A-48.

To summarize these results, injection scenarios in the Muddy, Lakota/Fall River, and Lower Sundance appear to show a small likelihood of success in storing 50 million tonnes of CO_2 individually with the simulations considered in this study. Achieving the desired magnitude of stored CO_2 would likely require a greater area and relatively higher number of wells. Injection scenarios in the Minnelusa Formation with four-to-six wells appear to be sufficient to achieve storage of 50 million tonnes of CO_2. However, stacked storage scenarios using multiple formations will be given consideration in future investigations, which may enable a reduction in permitted AoR, thus a reduction in associated financial burdens (i.e., pore space payments to landowners, costs associated with implementing monitoring technologies). Overall, these results have shown the ability to achieve 50 million tonnes of CO_2 stored in the region around Dry Fork Station in several different ways. These results provide a sound foundation for additional and improved modeling and simulation work during the Phase II effort, updated with site specific characterization data, more finely-tuned well placements, and tailored operational parameters for increased accuracy in predictive results.

Table 4A-6 Dry Fork CarbonSAFE Simulation Case Results – Cumulative CO_2 Injection (MMtonnes)

Formation	Scenario	4 Injection Wells 0.6 psi/ft. BHP Constraint	4 Injection Wells 0.7 psi/ft. BHP Constraint	6 Injection Wells	Brine Extraction 5-Spot	1 Horizontal Well 0.25 mi/ 1 mi lateral	4 Horizontal Wells 1 mi lateral
Muddy	P_{10}	N/A					
Muddy	P_{50}	13					
Muddy	P_{90}	31					
Lakota/ Fall River	P_{10}	N/A					
Lakota/ Fall River	P_{50}	6					
Lakota/ Fall River	P_{90}	7					
Lower Sundance	P_{10}	7					
Lower Sundance	P_{50}	20		25	26	10/12	22
Lower Sundance	P_{90}	81					
Minnelusa	P_{10}	6					
Minnelusa	P_{50}	31	48	60	43	18/24	56
Minnelusa	P_{90}	197					

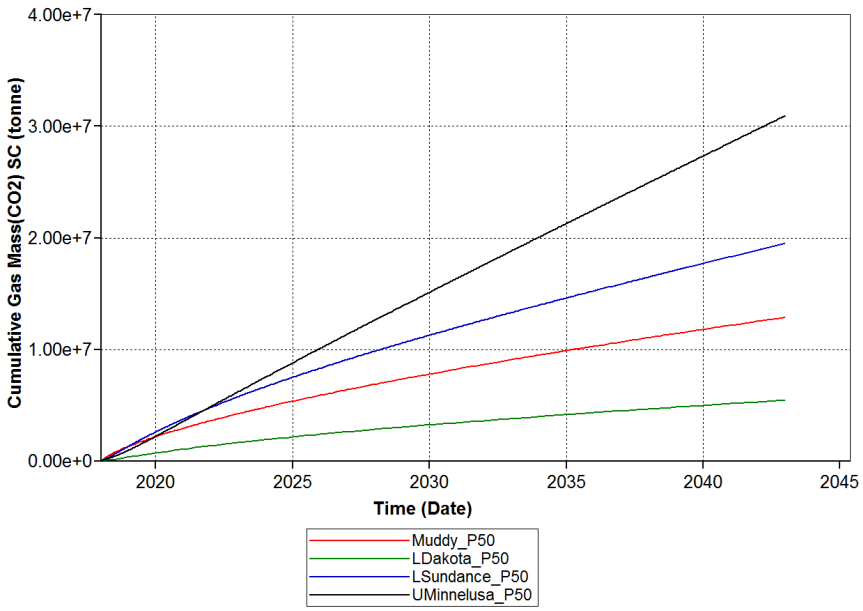

Figure 4A-28 Cumulative injected CO_2 mass (tonne) for all models' P50 simulation (base case simulations; 4 vertical injection wells).

Muddy Formation

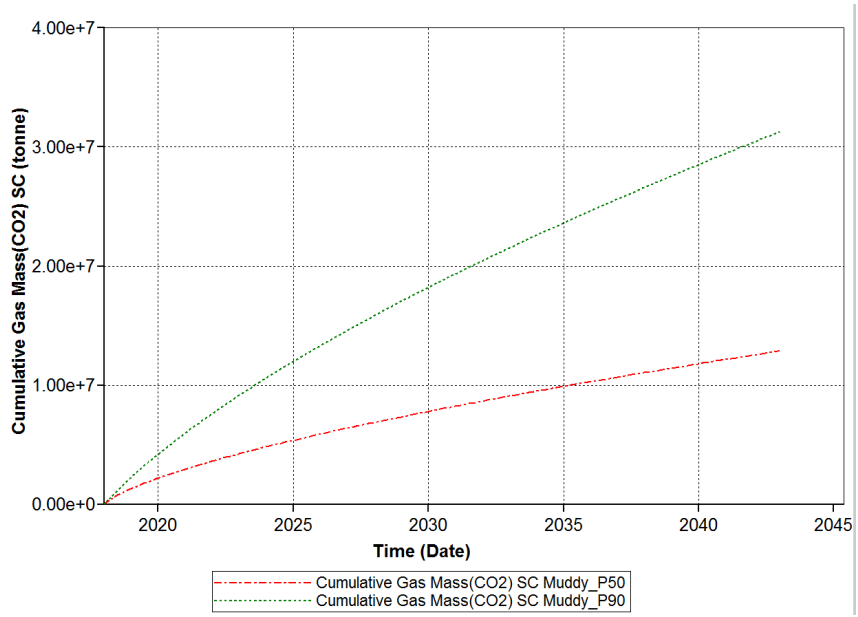

Figure 4A-29 Cumulative injected CO_2 mass (tonne) for the Muddy model's base case (P50 petrophysical properties with four vertical injection wells) and P90 simulation case.

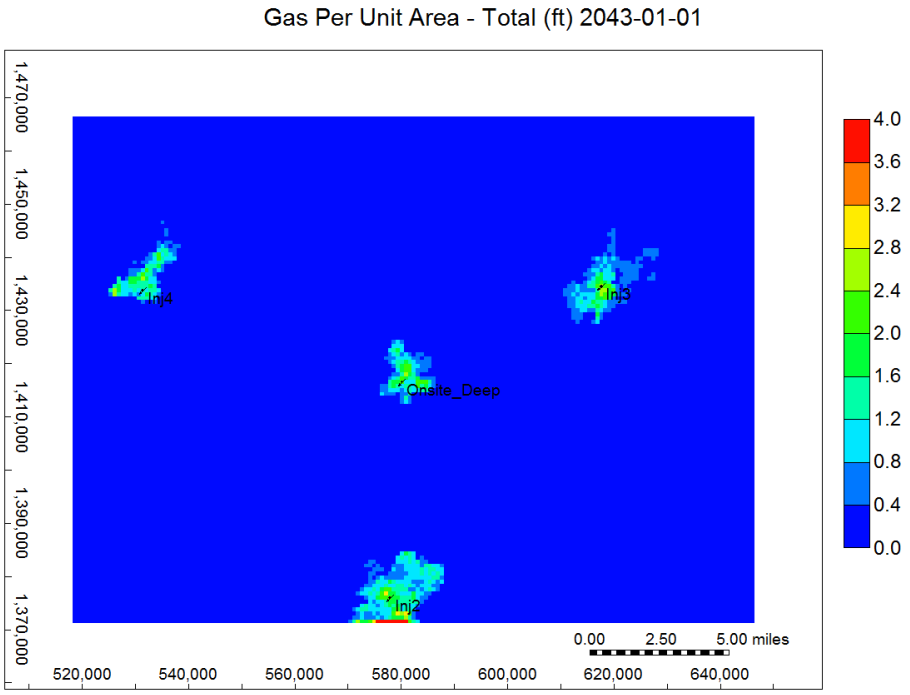

Figure 4A-30 Muddy Formation base case (P50 petrophysical properties with four vertical injection wells) showing gas per unit area – total (ft.) after 25 years of CO_2 injection. This simulation case resulted in the injection of 13 million tonnes of CO_2.

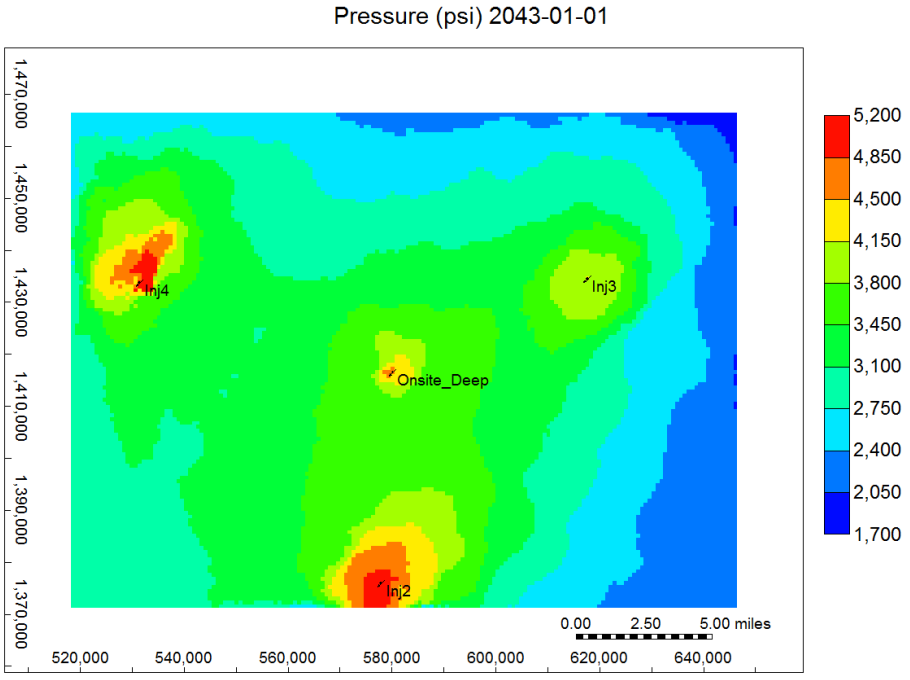

Figure 4A-31 Muddy Formation base case (P50 petrophysical properties with four vertical injection wells) showing pressure distribution after 25 years of CO_2 injection. This simulation case resulted in the injection of 13 million tonnes of CO_2.

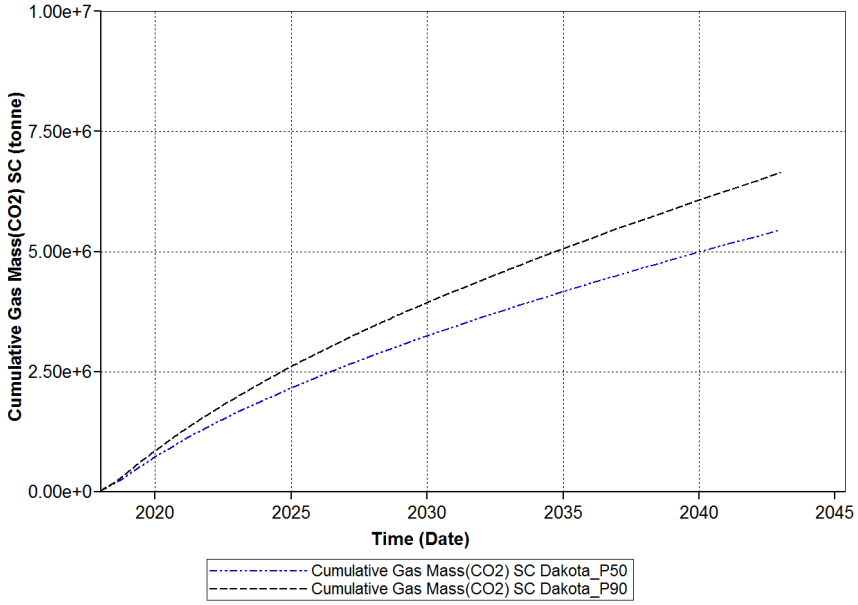

Figure 4A-32 Cumulative injected CO_2 mass (tonne) for the Fall River/Lakota model's base case (P50 petrophysical properties with four vertical injection wells) and P90 simulation case.

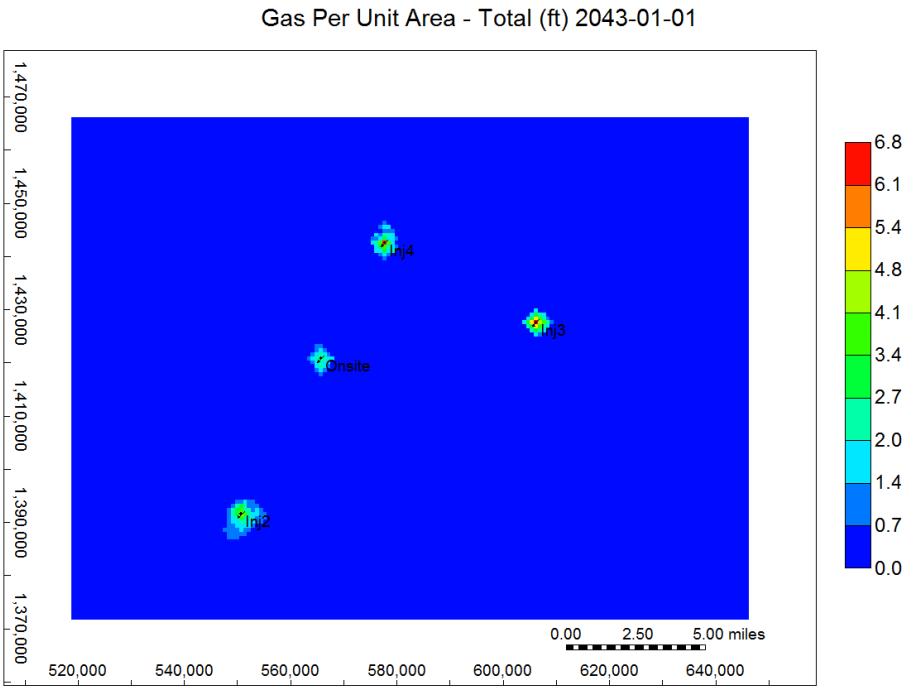

Figure 4A-33 Fall River/Lakota Formation base case (P50 petrophysical properties with four vertical injection wells) showing gas per unit area – total (ft.) after 25 years of CO_2 injection. This simulation case resulted in the injection of 6 million tonnes of CO_2.

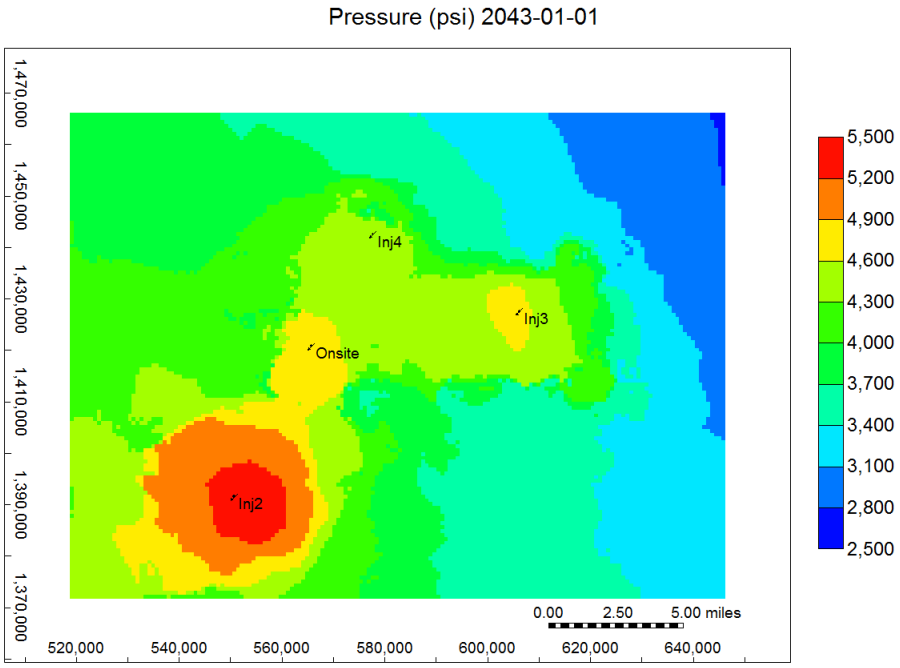

Figure 4A-34 Fall River/Lakota Formation base case (P50 petrophysical properties with four vertical injection wells) showing pressure distribution after 25 years of CO_2 injection. This simulation case resulted in the injection of 6 million tonnes of CO_2.

Lower Sundance Formation

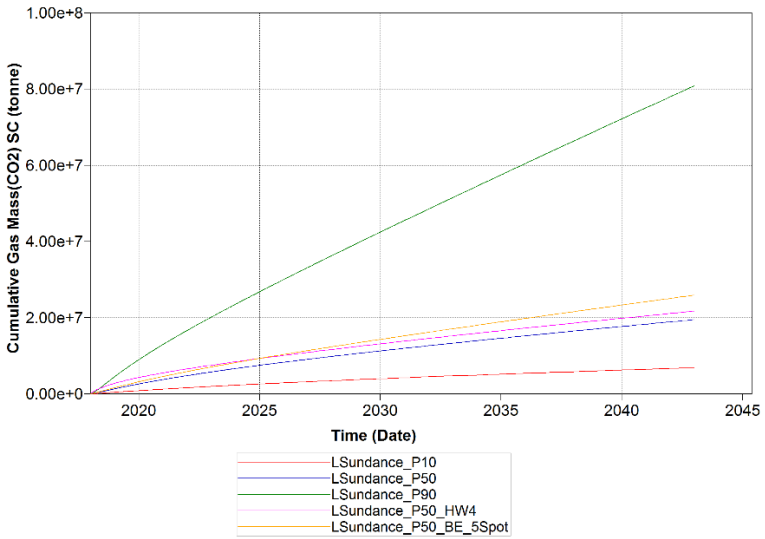

Figure 4A-35 Cumulative injected CO_2 mass (tonne) for the Lower Sundance model's base case (P50 petrophysical properties with four vertical injection wells), P10, P90, 4-horizontal well, and 5-spot brine extraction (four vertical injection wells and one brine extraction well) simulation cases.

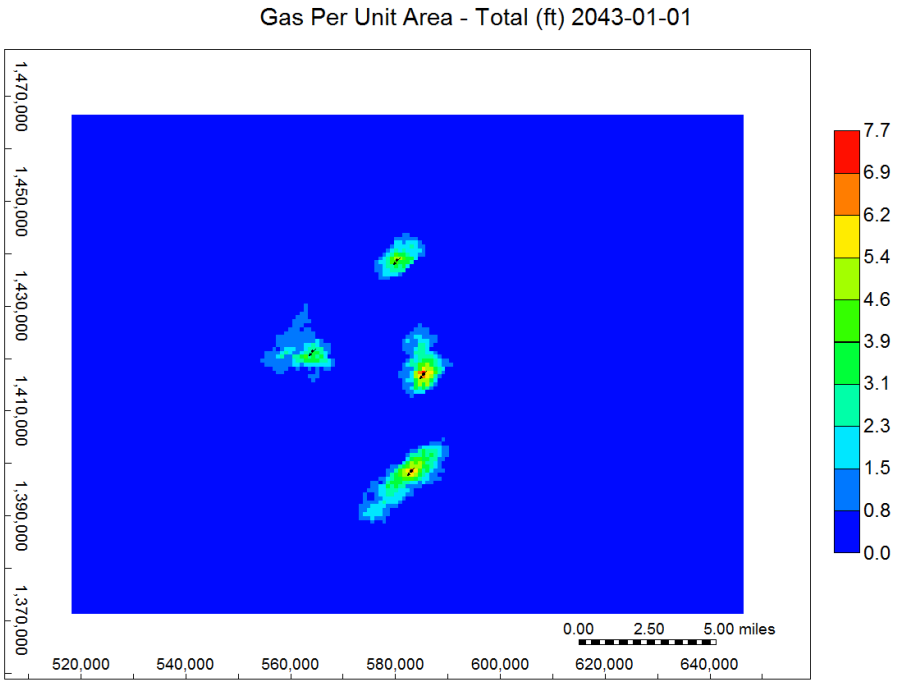

Figure 4A-36 Lower Sundance Formation base case (P50 petrophysical properties with four vertical injection wells) gas per unit area – total map (ft.) after 25 years of CO_2 injection. This simulation case resulted in the injection of 20 million tonnes of CO_2.

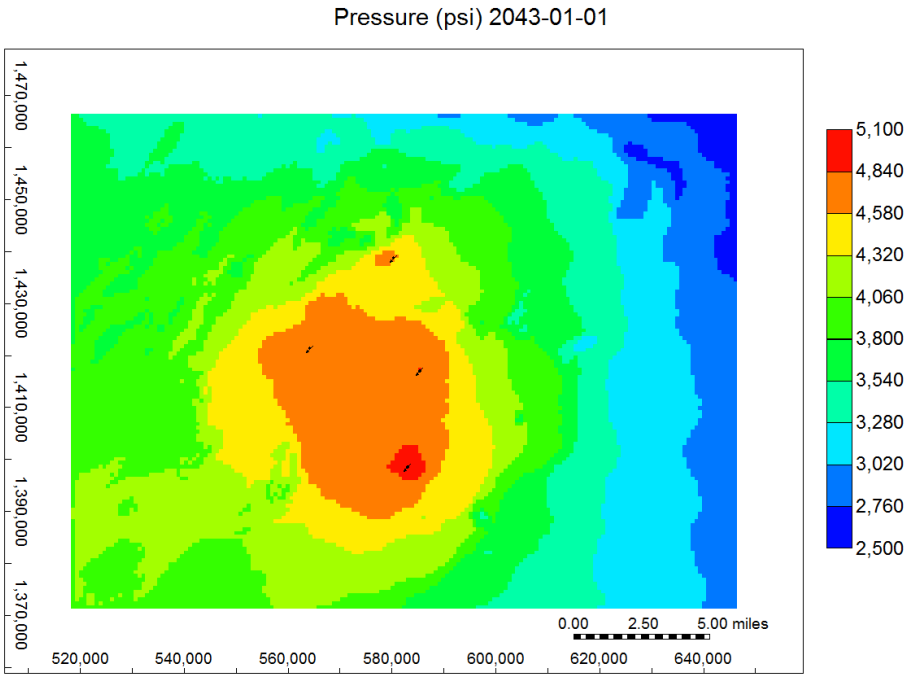

Figure 4A-37 Lower Sundance Formation base case (P50 petrophysical properties with four vertical injection wells) showing pressure distribution after 25 years of CO_2 injection. This simulation case resulted in the injection of 20 million tonnes of CO_2.

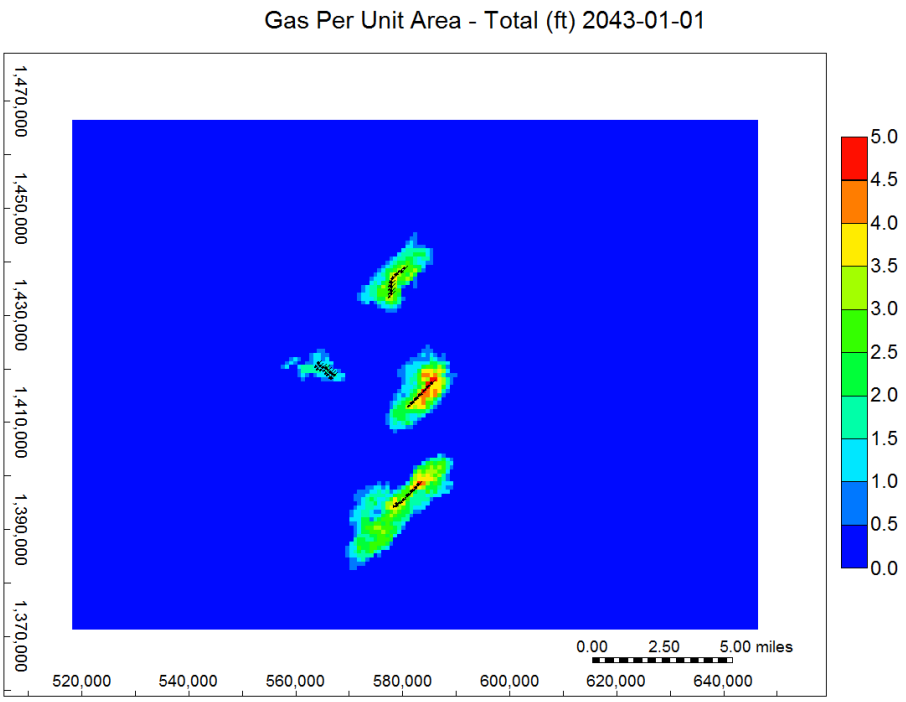

Figure 4A-38 Lower Sundance Formation P50 case with four horizontal injection wells showing gas per unit area – total (ft.) after 25 years of CO_2 injection. This simulation case resulted in the injection of 22 million tonnes of CO_2.

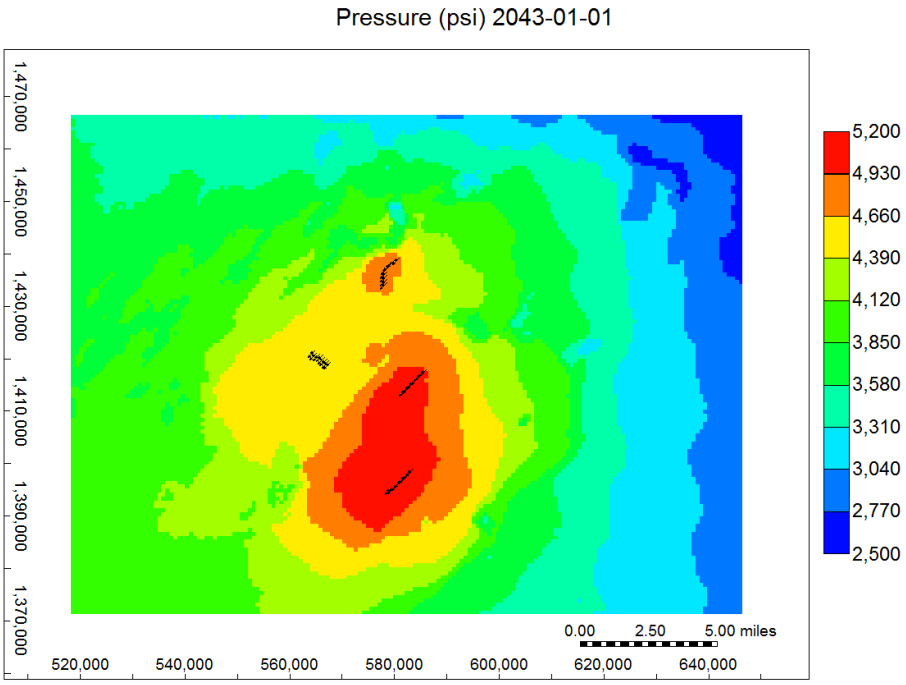

Figure 4A-39 Lower Sundance Formation P50 case with four horizontal injection wells showing pressure distribution after 25 years of CO_2 injection. This simulation case resulted in the injection of 22 million tonnes of CO_2.

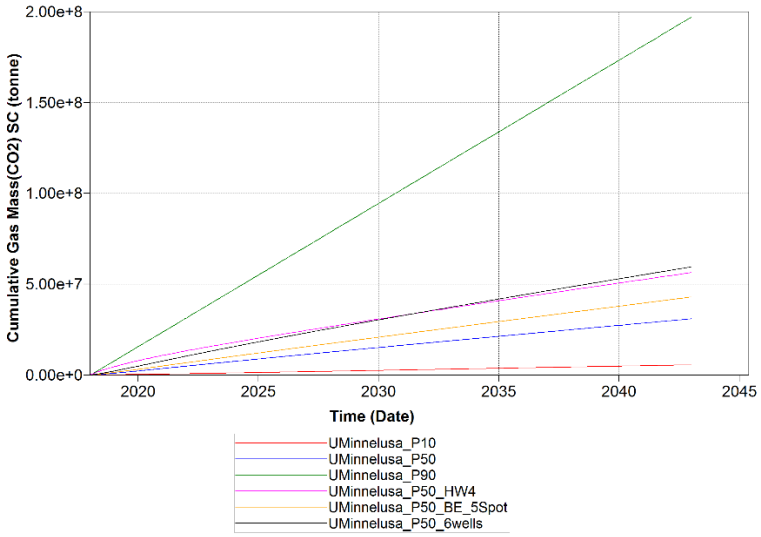

Figure 4A-40 Cumulative injected CO_2 mass (tonne) for the Upper Minnelusa model's base case (P50 petrophysical properties with four vertical injection wells), P10, P90, 4-horizontal well, 5-spot brine extraction (four vertical injection wells and one brine extraction well), and 6-vertical well simulation cases.

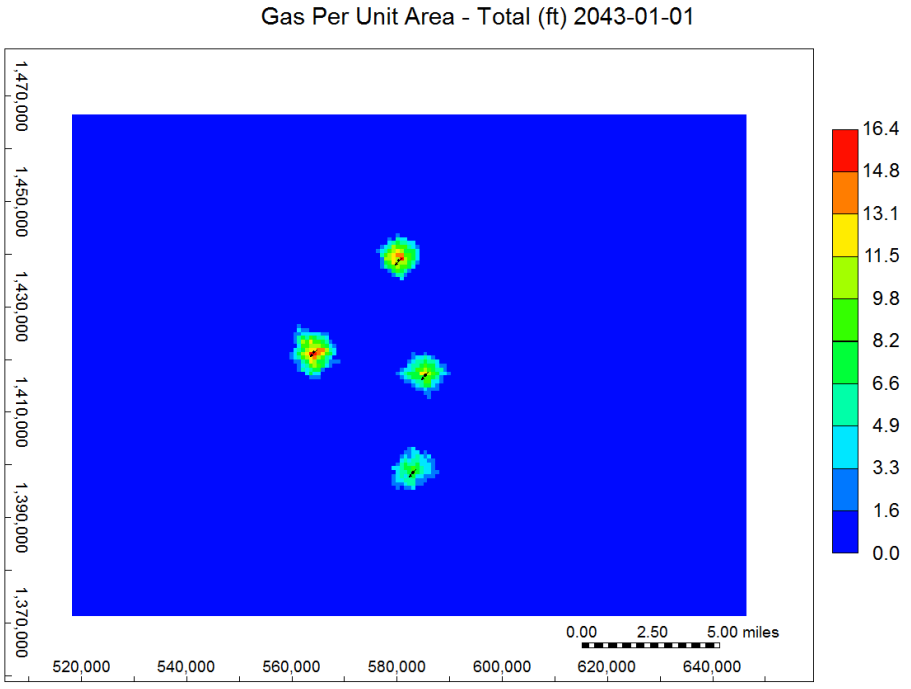

Figure 4A-41 Upper Minnelusa Formation base case (P50 petrophysical properties with four vertical injection wells) gas per unit area – total map (ft.) after 25 years of CO_2 injection. This simulation case resulted in the injection of 31 million tonnes of CO_2.

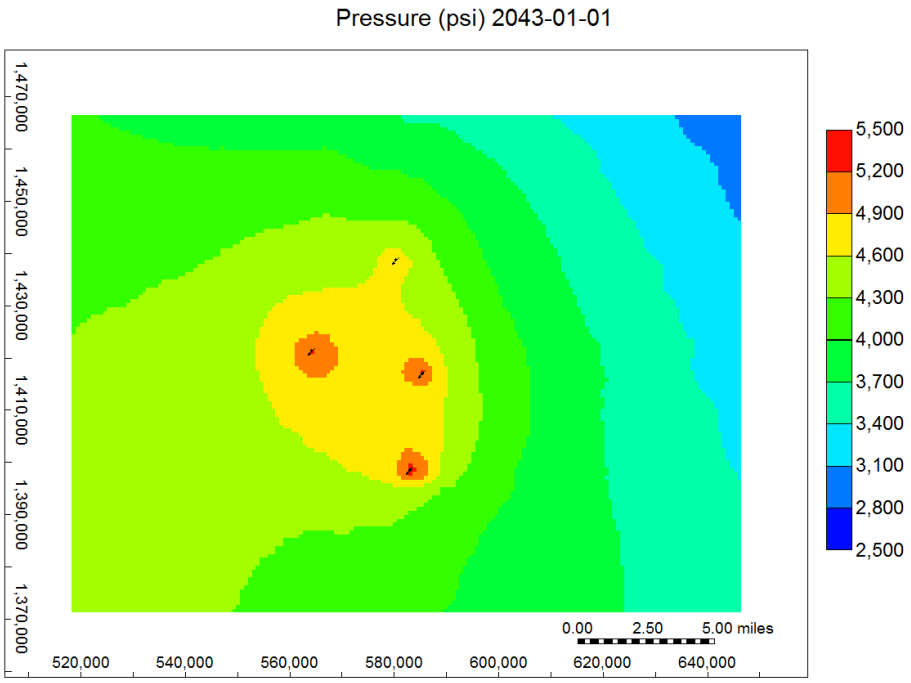

Figure 4A-42 Upper Minnelusa Formation base case (P50 petrophysical properties with four vertical injection wells) showing pressure distribution after 25 years of CO_2 injection. This simulation case resulted in the injection of 31 million tonnes of CO_2.

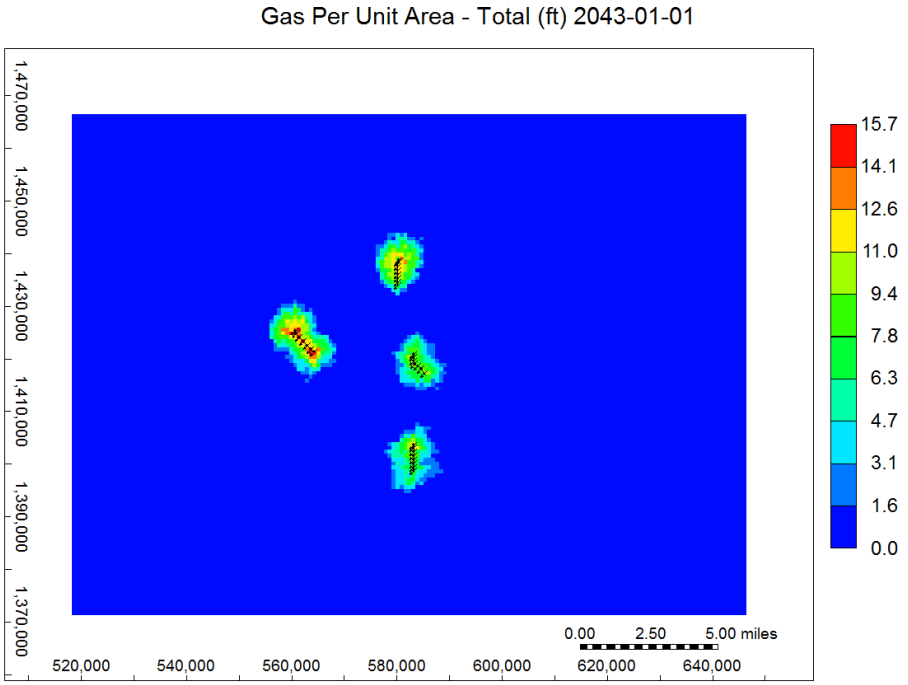

Figure 4A-43 Upper Minnelusa Formation P50 case with four horizontal injection wells showing gas per unit area – total (ft.) after 25 years of CO_2 injection. This simulation case resulted in the injection of 56 million tonnes of CO_2.

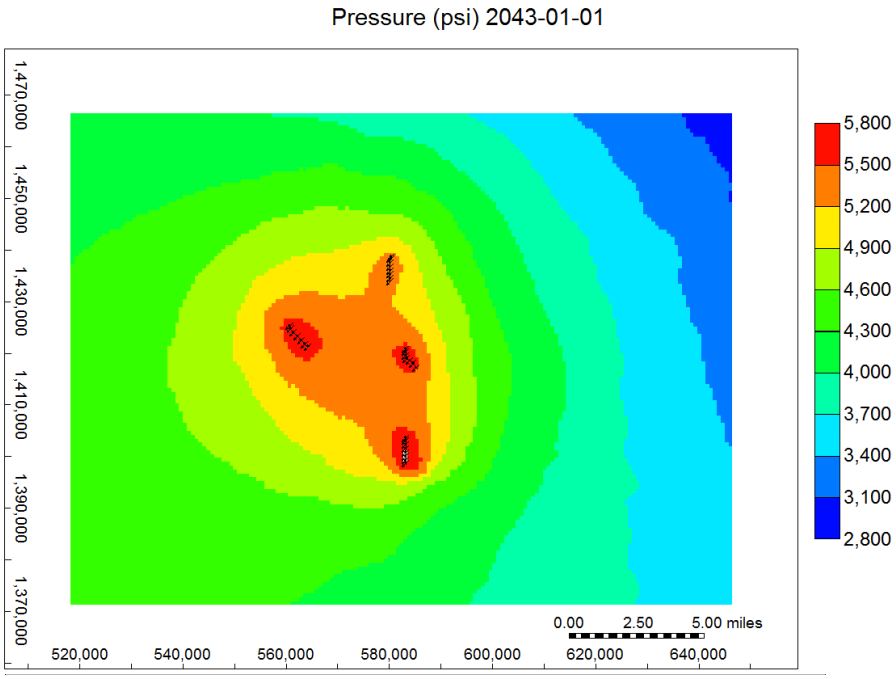

Figure 4A-44 Upper Minnelusa Formation P50 case with four horizontal injection wells showing pressure distribution after 25 years of CO_2 injection. This simulation case resulted in the injection of 56 million tonnes of CO_2.

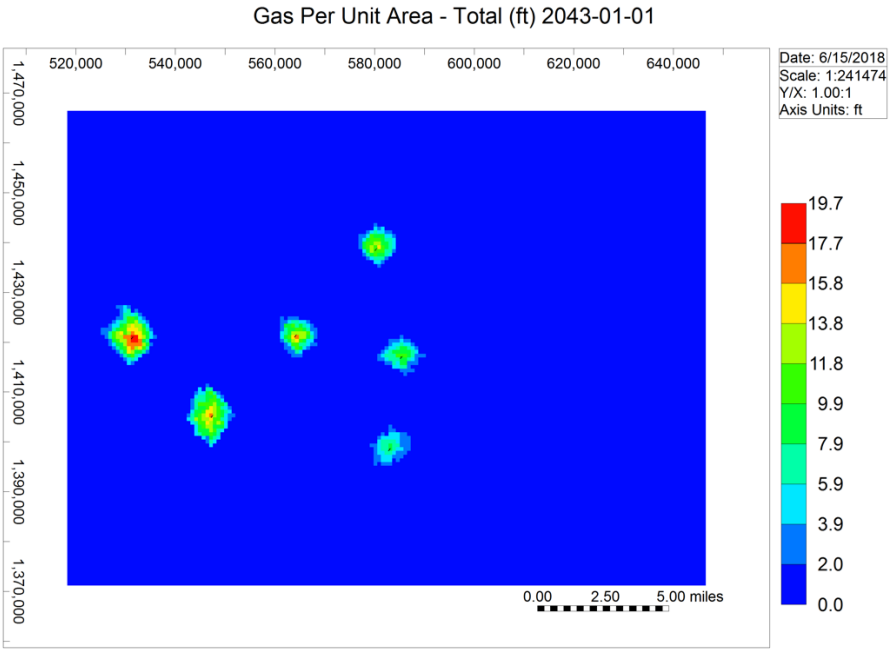

Figure 4A-45 Upper Minnelusa Formation P50 case with six vertical injection wells showing a gas per unit area – total map (ft.) after 25 years of CO_2 injection. This simulation case resulted in the injection of 60 million tonnes of CO_2.

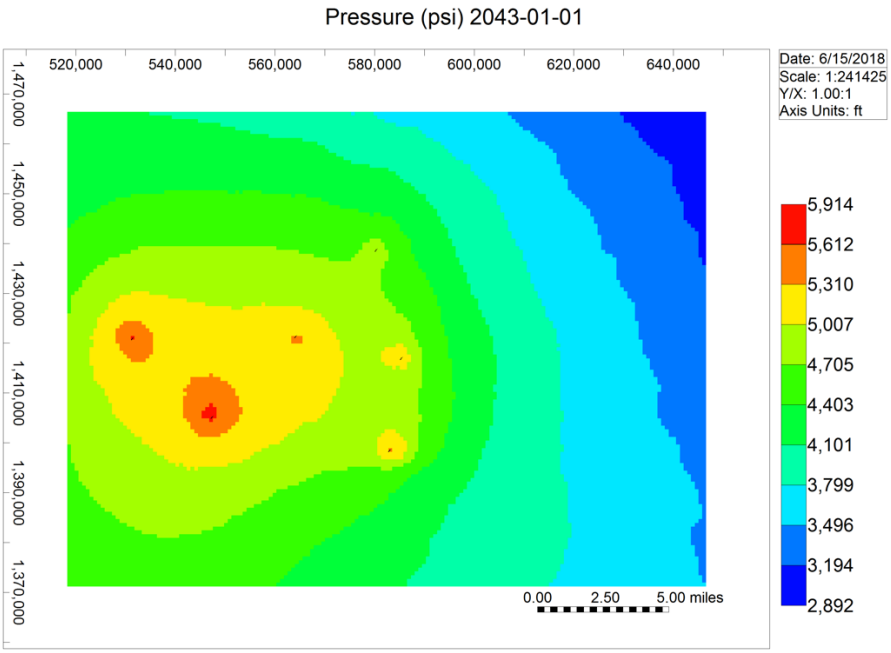

Figure 4A-46 Upper Minnelusa Formation P50 case with six vertical injection wells showing pressure distribution after 25 years of CO_2 injection. This simulation case resulted in the injection of 60 million tonnes of CO_2.

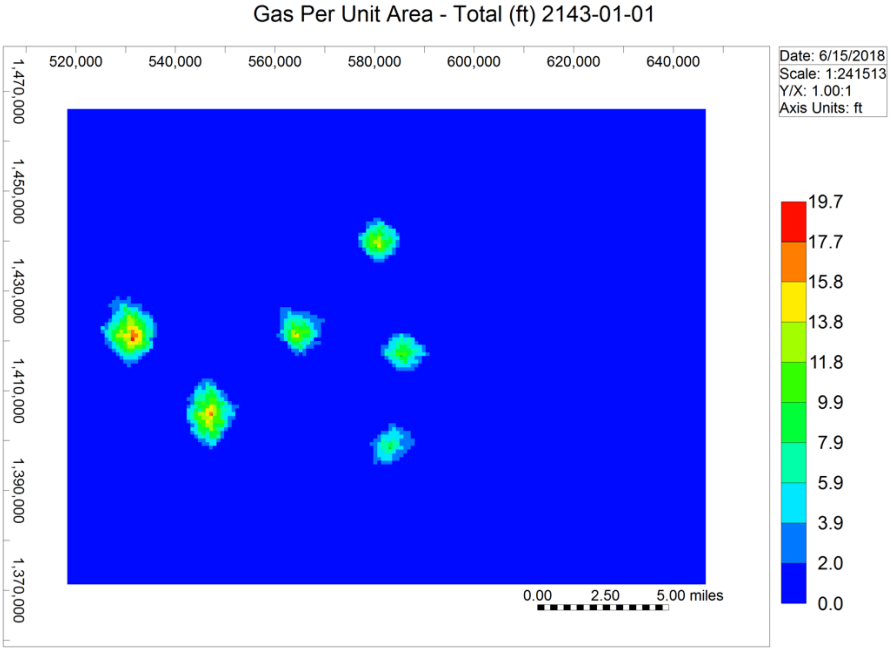

Figure 4A-47 Upper Minnelusa Formation P50 case with six vertical injection wells showing a gas per unit area – total map (ft.) after 100 years after the cessation of CO_2 injection. This simulation case resulted in the injection of 60 million tonnes of CO_2. After 100 years of monitoring, the injected CO_2 migrated very slowly in the structural up-dip direction (east).

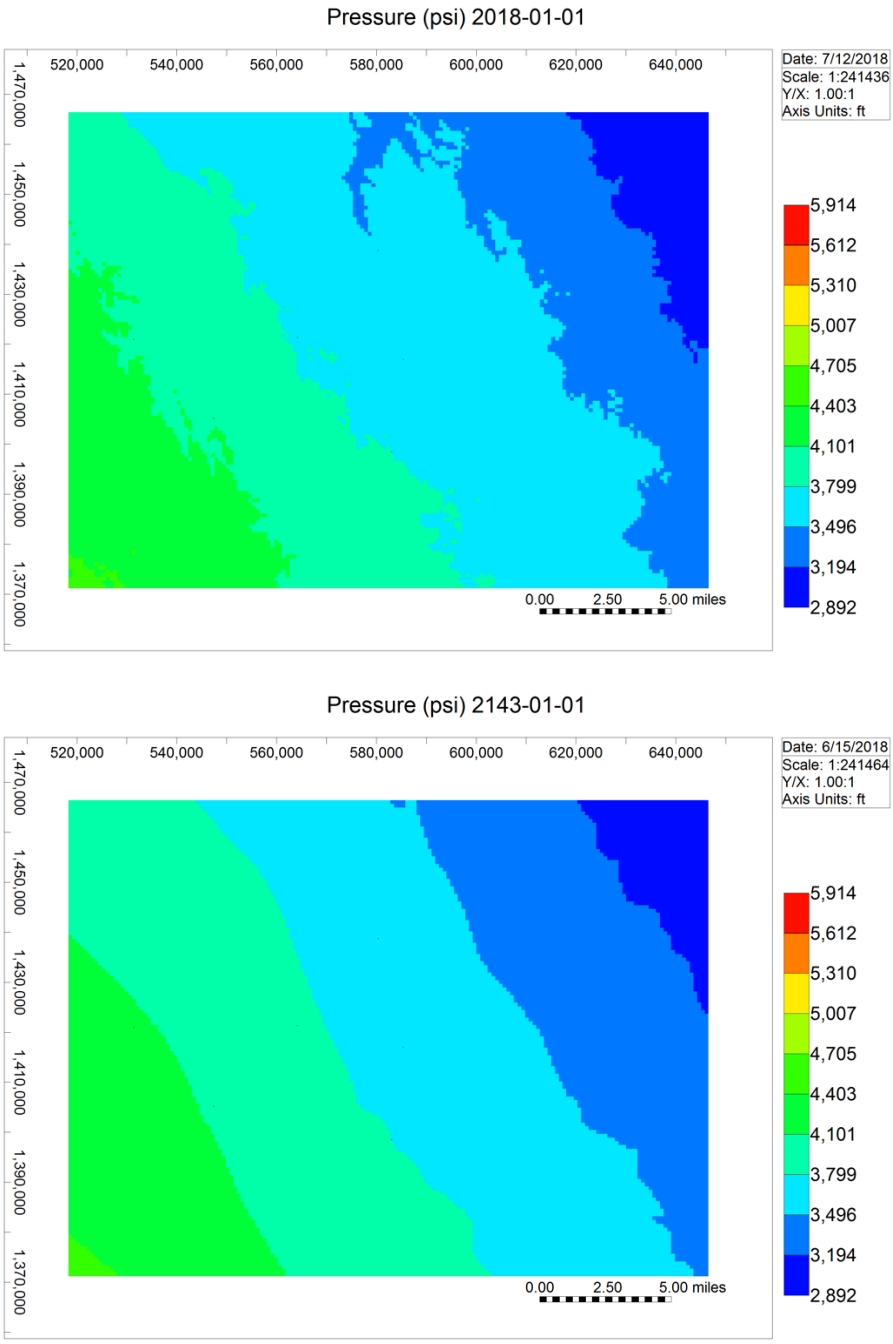

Figure 4A-48 Minnelusa model initial (prior to simulated injection) pressure distribution (top) and the pressure distribution 100 years after the end of simulated injection (bottom). Within 100 years of CO_2 injection cessation the pressure distribution is nearly the same as conditions prior to simulated injection.

A.10 Area of Review Determination

The Environmental Protection Agency requires owners or operators of Class VI injection wells to delineate the AoR for the proposed Class VI well, which is the region surrounding the proposed well where underground sources of drinking water (USDW) may be endangered by the injection activity (EPA, 2013). The delineation of an AoR is calculated from the pressure front. The pressure front is defined as, "the area around an injection well where, during injection, the hydraulic head of the formation fluid in the injection zone is equal to or greater than the [hydraulic] head of USDWs." (EPA, 2013). This can be calculated using the following equation:

$$Pi,=Pu+\rho ig\cdot(zu-zi)$$

[Eq-1]

Where Pu is the initial fluid pressure in the USDW, ρi is the injection-zone fluid density, g is the acceleration due to gravity, zu is the representative elevation of the USDW, and zi is the representative elevation of the injection zone.

Because the scale of simulated CO_2 injection in the Muddy Formation model and the Fall River and Lakota Formations' model were significantly below the 50 million tonne injection target, no AoR calculations were conducted. However, AoR calculations were conducted using the simulation results for the Lower Sundance and Upper Minnelusa models.

The lowermost USDW in the study area is the Fox Hills Formation. Interburden thickness (distance from the bottom of the Fox Hills Formation to the Lower Sundance and Minnelusa formations) was calculated from formation top depths. Fluid density for the Upper Minnelusa and Lower Sundance Formations both have estimated fluid density of 1025 kg/m^3. Using pressure results from the simulations, AoR maps were created for select scenarios (Figures 4A-45 through 4A-51). Statistics regarding the calculated AoRs for simulation cases, which resulted in a stored CO_2 mass approaching or exceeding 50 million tonnes, are reported in Table 4A-7 below.

Table 4A-7 Total Area in AoR for Select Simulation Scenarios.

Formation	**Scenario**	**Stored CO_2 (Mt)**	**Area (mi^2)**
Upper Minnelusa	P_{50} - 0.7 BHP Constraint	48	202
Upper Minnelusa	P_{50} - 6 Vertical Injection Wells	60	218
Upper Minnelusa	P_{50} - 4 Horizontal Wells	56	204
Upper Minnelusa	P_{50} - Brine Extraction 5-Spot	43	149

Upper Minnelusa	P_{90}	197	165
Lower Sundance	P_{90}	81	290

A.10.1 Lower Sundance Formation

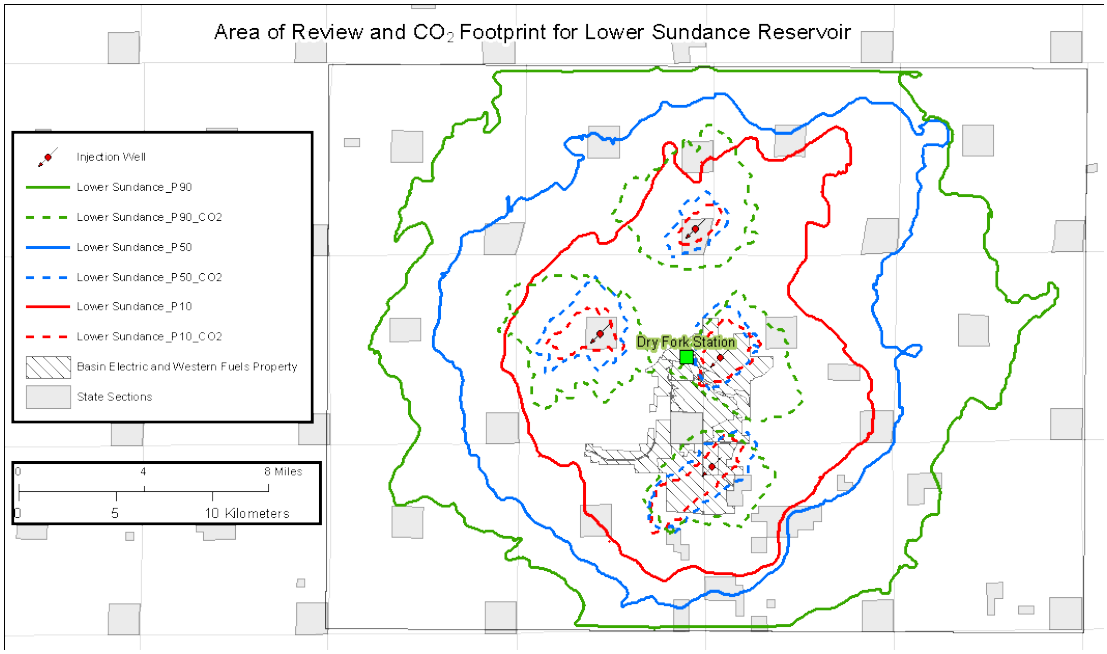

Figure 4A-49 P10 and P50 and P90. Area of review map of the Lower Sundance showing the P10, P50, and P90 pressure and CO_2 plume scenario with four vertical injection wells. The P10, P50, and P90 cases resulted in CO_2 storage in the amounts of 7, 20, and 81 million tonnes, respectively.

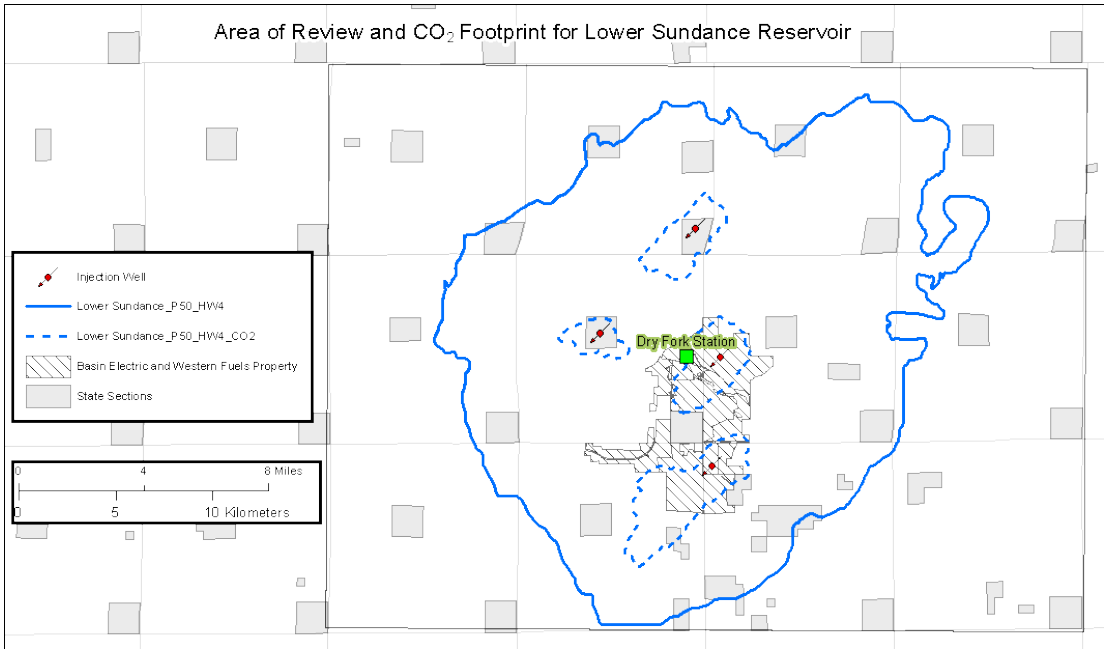

Figure 4A-50 AoR map of the Lower Sundance case with four horizontal wells showing the pressure front and CO_2 plume. This case resulted in 22 million tonnes of stored CO_2.

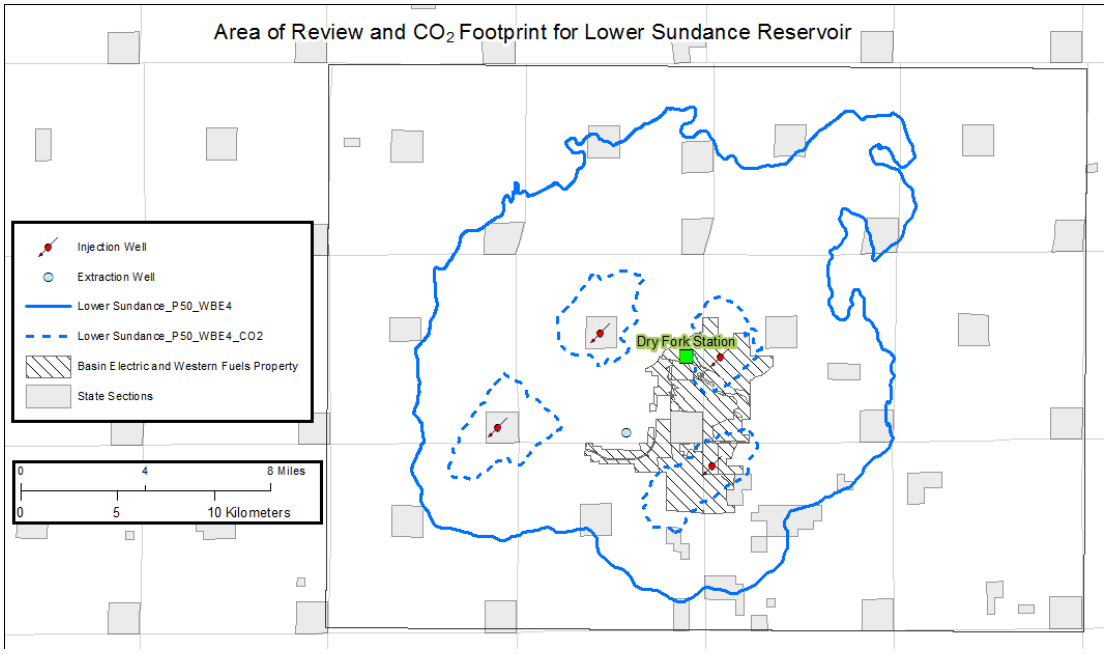

Figure 4A-51 AoR map of the Lower Sundance case with four vertical injection wells and one brine extraction well (5-spot) showing the pressure front and CO_2 plume. This case resulted in 26 million tonnes of stored CO_2.

A.10.2 Minnelusa Formation

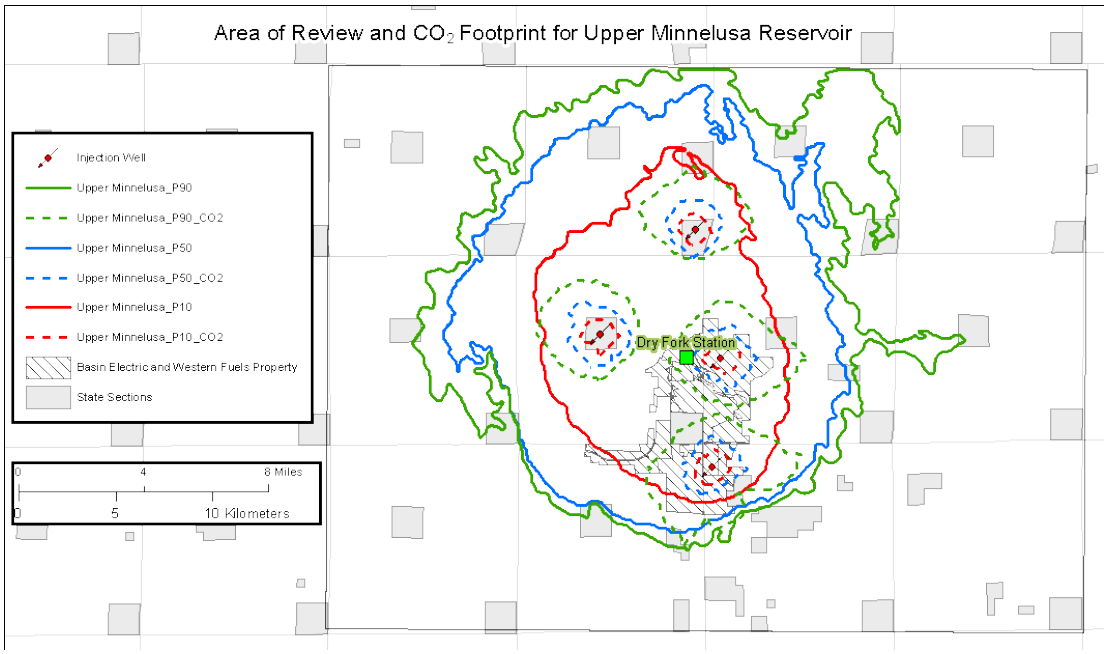

Figure 4A-52 Minnelusa P10/P50/P90 area of review map showing the pressure and CO_2 plume bounds with four vertical injection wells. The P10, P50, and P90 cases resulted in CO_2 storage in the amounts of 6, 31, and 197 million tonnes, respectively.

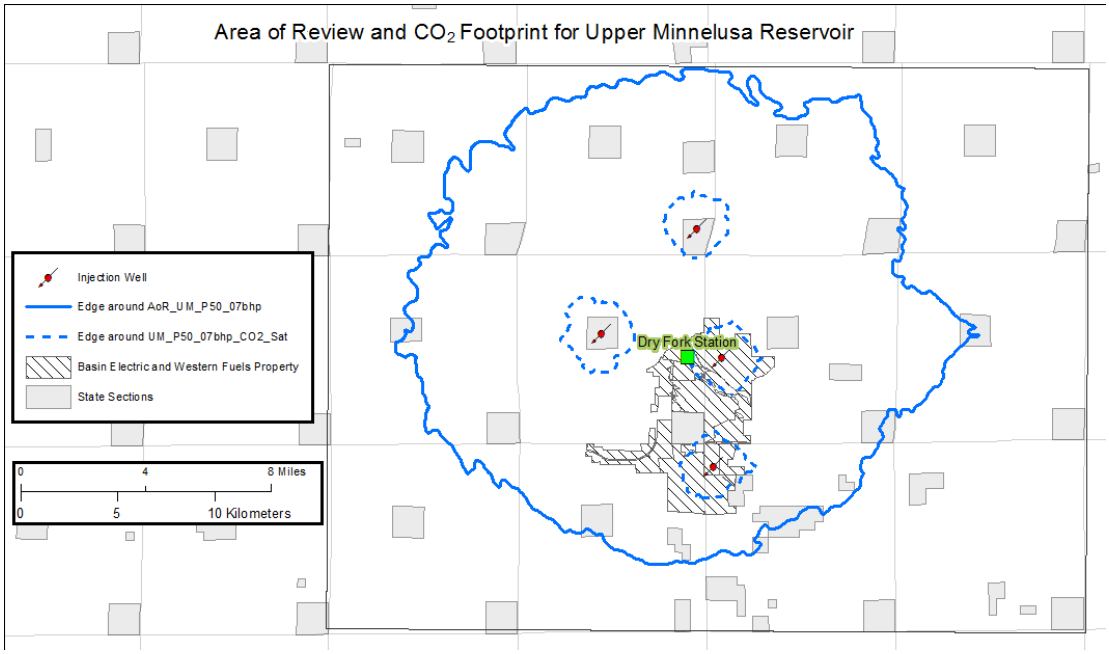

Figure 4A-53 AoR map of the Upper Minnelusa case with four vertical injection wells with maximum BHP pressure constraints calculated using a fracture gradient of 0.7 psi/ft. showing the pressure front and CO_2 plume. This case resulted in 48 million tonnes of stored CO_2.

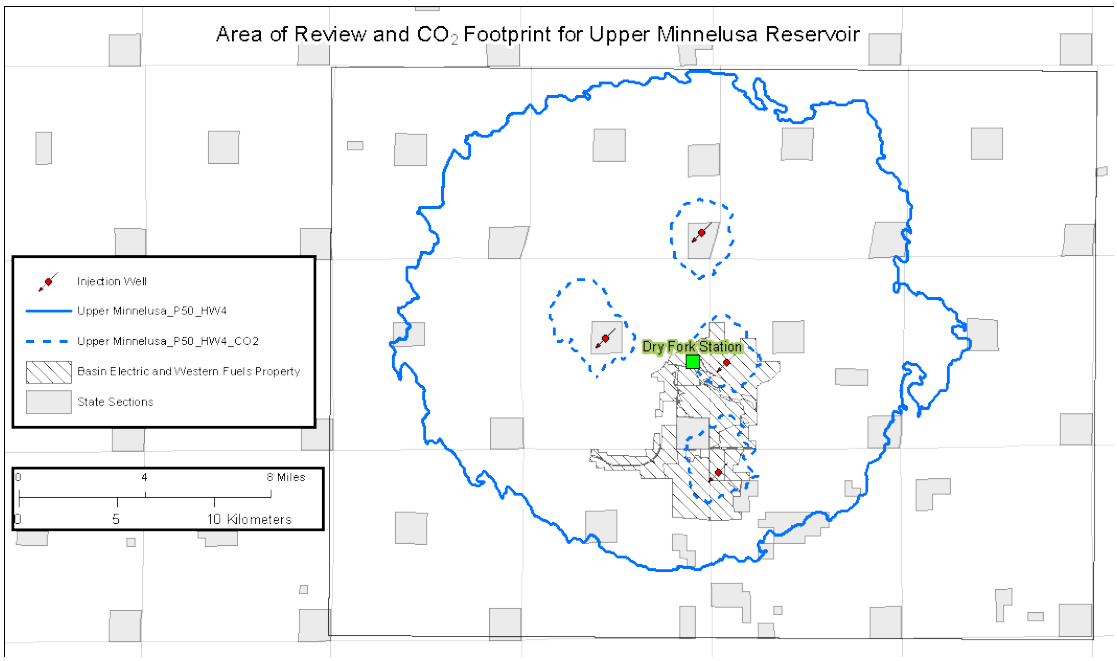

Figure 4A-54 AoR map of the Upper Minnelusa case with four horizontal injection wells showing the pressure front and CO_2 plume. This case resulted in 56 million tonnes of stored CO_2.

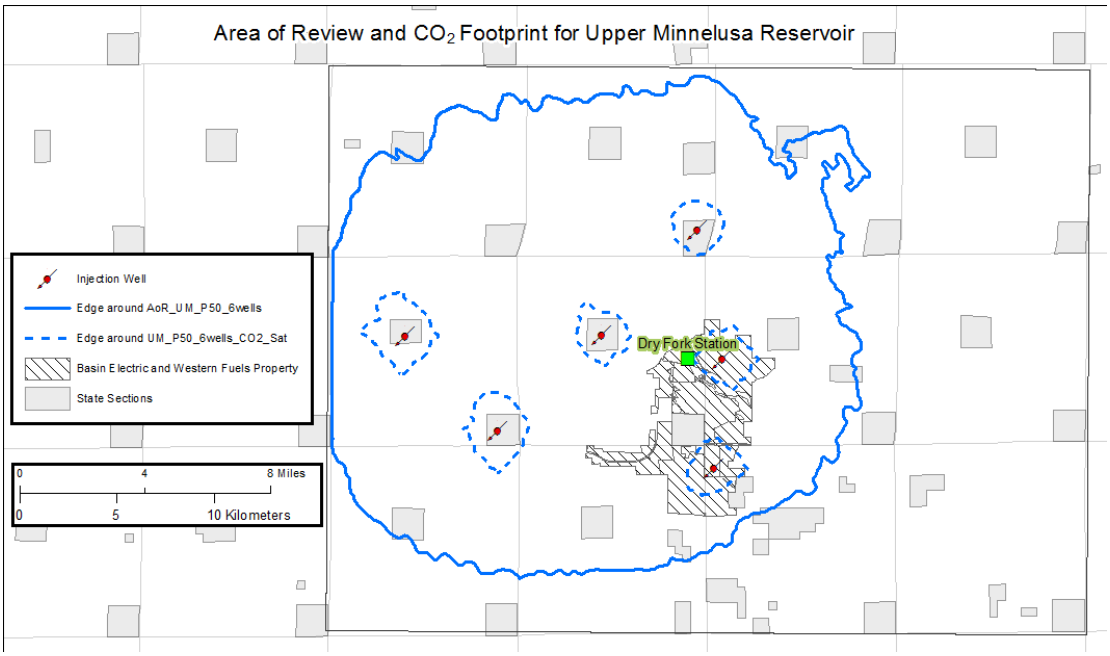

Figure 4A-55 AoR map of the Upper Minnelusa case with six vertical injection wells showing the pressure front and CO_2 plume. This case resulted in 60 million tonnes of stored CO_2.

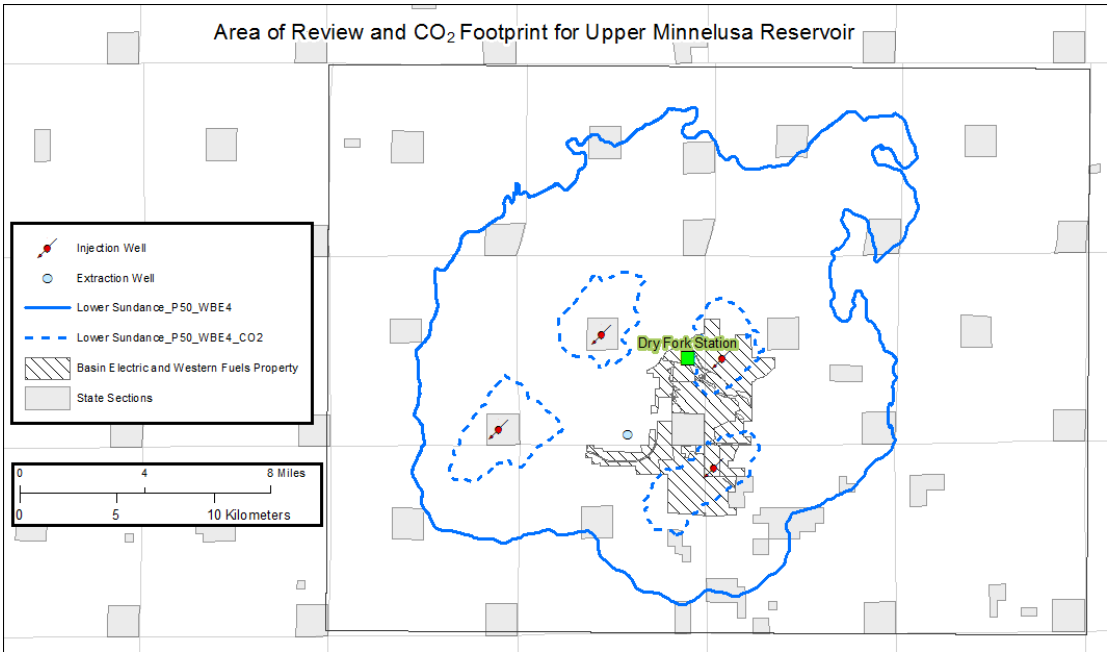

Figure 4A-56 AoR map of the Upper Minnelusa case with four vertical injection wells and one brine extraction well (5-spot) showing the pressure front and CO_2 plume. This case resulted in 43 million tonnes of stored CO_2.

Chapter IV Appendix B – Characterization Well Designs and Cost Estimates

B.1.1 Stratigraphic Test Well Drilling and Completion

B.1.1.1 Estimated Drilling Plan for a Stratigraphic Test Well

Operator:	TBD	Start Date	1-Jul-18
Well Name:	STRAT WELL 01	End Drilling Date	31-Jul-18
Rig:	TBD	End Drilling Date (IPM + %NPT):	31-Jul-18
Field: (if applicable)			

Operation Description	Estimated Time				ROP	Date	
	[hrs]	[Days]	[Days]	[ft]	[ft/hr]	Start	Finish
17-1/2" Hole Section							
Pre-spud Safety Meeting	8.00	0.33	0.33	0		1-Jul-18 06:00	1-Jul-18 14:00
Drill rat and mouse holes, make up bit	8.00	0.67	0.67	0		1-Jul-18 14:00	1-Jul-18 22:00
Drill 17-1/2" hole @ 3754 ft MD	**15.02**	1.29	1.29	**3,754**	**250.0**	1-Jul-18 22:00	2-Jul-18 13:00
Circulate	0.50	1.31	1.31	3,754		2-Jul-18 13:00	2-Jul-18 13:30
POOH	2.00	1.40	1.40	3,754		2-Jul-18 13:30	2-Jul-18 15:30
Wireline Logs	8.00	1.73	1.73	3,754		2-Jul-18 15:30	2-Jul-18 23:30
Run Surface Casing - Cement	6.00	1.98	1.98	3,754		2-Jul-18 23:30	3-Jul-18 05:30
Wait on Cement	12.00	2.48	2.48	3,754		3-Jul-18 05:30	3-Jul-18 17:30
17-1/2" Hole Section Sub Total	59.52	2.48	2.48	3,754		3-Jul-18 05:30	3-Jul-18 17:30
12-1/4" Hole Section			0.00	0			
Nipple up BOPs	12.00	2.98	2.98	3,754		3-Jul-18 17:30	4-Jul-18 05:30
Make up 12-1/4" BHA	6.00	3.23	3.23	3,754		4-Jul-18 05:30	4-Jul-18 11:30
Drill Float/Shoe and LOT/FIT	6.00	3.48	3.48	3,754		4-Jul-18 11:30	4-Jul-18 17:30
Drill 12-1/4" hole @ 6124 ft MD	**27.88**	4.64	4.64	**6,124**	**85.0**	4-Jul-18 17:30	5-Jul-18 21:23
Circulate	0.50	4.66	4.66	6,124		5-Jul-18 21:23	5-Jul-18 21:53
POOH	2.00	4.75	4.75	6,124		5-Jul-18 21:53	5-Jul-18 23:53
Wireline Logs	8.00	5.08	5.08	6,124		5-Jul-18 23:53	6-Jul-18 07:53
Run Intermediate Casing - Cement	6.00	5.33	5.33	6,124		6-Jul-18 07:53	6-Jul-18 13:53
Wait on Cement	12.00	5.83	5.83	6,124		6-Jul-18 13:53	7-Jul-18 01:53
12-1/4" Hole Section Sub Total	80.38	5.83	5.83	6,124		7-Jul-18 01:53	7-Jul-18 01:53
8-3/4" Hole Section			0.00	0			
Make up 8-3/4" BHA	6.00	6.08	6.08	6,124		7-Jul-18 01:53	7-Jul-18 07:53
Drill Float/Shoe and LOT/FIT	6.00	6.33	6.33	6,124		7-Jul-18 07:53	7-Jul-18 13:53
Drill 8-3/4" hole @ 7600 ft MD	**29.52**	7.56	7.56	**7,600**	**50.0**	7-Jul-18 13:53	8-Jul-18 19:25
Trip for Muddy Core, Make up Core Barrel	12.00	8.06	8.06	7,600		8-Jul-18 19:25	9-Jul-18 07:25
Core Muddy 65' @ 7665 ft MD	**4.64**	8.25	8.25	**7,665**	**14.0**	9-Jul-18 07:25	9-Jul-18 12:03
Trip for Core, MU Reaming Assembly, Trip in to Ream	16.00	8.92	8.92	7,665		9-Jul-18 12:03	10-Jul-18 04:03
Ream 65'	8.13	9.26	9.26	7,665		10-Jul-18 04:03	10-Jul-18 12:11
Trip, MU BHA, Trip in to Drill to next core pt.	12.00	9.76	9.76	7,665		10-Jul-18 12:11	11-Jul-18 00:11
Drill 8-3/4" hole @ 7864 ft MD	**3.98**	9.92	9.92	**7,864**	**50.0**	11-Jul-18 00:11	11-Jul-18 04:09
Trip for Core, Make up Core Barrel, Trip in to Core	16.00	10.59	10.59	7,864		11-Jul-18 04:09	11-Jul-18 20:09
Core Inyan Kara 115' @ 7979 ft MD	**8.85**	10.96	10.96	**7,979**	**13.0**	11-Jul-18 20:09	12-Jul-18 05:00
Trip for Core, MU Reaming Assembly, Trip in to Ream	16.00	11.63	11.63	7,979		12-Jul-18 05:00	12-Jul-18 21:00
Ream 115'	14.38	12.22	12.22	7,979		12-Jul-18 21:00	13-Jul-18 11:23
Trip, MU BHA, Trip in to Drill to next core pt.	12.00	12.72	12.72	7,979		13-Jul-18 11:23	13-Jul-18 23:23
Drill 8-3/4" hole @ 8218 ft MD	**4.78**	12.92	12.92	**8,218**	**50.0**	13-Jul-18 23:23	14-Jul-18 04:10
Trip for Core, Make up Core Barrel, Trip in to Core	16.00	13.59	13.59	8,218		14-Jul-18 04:10	14-Jul-18 20:10
Core L Sundance 120' @ 8338 ft MD	**29.92**	14.84	14.84	**8,338**	**12.0**	14-Jul-18 20:10	16-Jul-18 02:05
Trip for Core, MU Reaming Assembly, Trip in to Ream	16.00	15.50	15.50	8,338		16-Jul-18 02:05	16-Jul-18 18:05
Ream 120'	15.00	16.13	16.13	8,338		16-Jul-18 18:05	17-Jul-18 09:05
Trip, MU BHA, Trip in to Drill to next core pt.	12.00	16.63	16.63	8,338		17-Jul-18 09:05	17-Jul-18 21:05
Drill 8-3/4" hole @ 9241 ft MD	**20.07**	17.46	17.46	**9,241**	**45.0**	17-Jul-18 21:05	18-Jul-18 17:09
Trip for Core, Make up Core Barrel	16.00	18.13	18.13	9,241		18-Jul-18 17:09	19-Jul-18 09:09
Core U & M Minnelusa 250' @ 9491 ft MD	**115.30**	22.94	22.94	**9,491**	**10.0**	19-Jul-18 09:09	24-Jul-18 04:27
Trip for Core, MU Reaming Assembly, Trip in to Ream	16.00	23.60	23.60	9,491		24-Jul-18 04:27	24-Jul-18 20:27
Ream 250'	31.25	24.90	24.90	9,491		24-Jul-18 20:27	26-Jul-18 03:42
Trip, MU BHA, Trip in to Drill to total depth.	12.00	25.40	25.40	9,491		26-Jul-18 03:42	26-Jul-18 15:42
Drill 8-3/4" hole @ 10200 ft MD	**17.73**	26.14	26.14	**10,200**	**40.0**	26-Jul-18 15:42	27-Jul-18 09:25
Circulate	6.00	26.39	26.39	10,200		27-Jul-18 09:25	27-Jul-18 15:25
POOH and rig down MWD	16.00	27.06	27.06	10,200		27-Jul-18 15:25	28-Jul-18 07:25
Wireline Logs	60.00	29.56	29.56	10,200		28-Jul-18 07:25	30-Jul-18 19:25
Plug and Abandon	12.00	30.06	30.06	10,200		30-Jul-18 19:25	31-Jul-18 07:25
Rig down	16.00	30.73	30.73	10,200		31-Jul-18 07:25	31-Jul-18 23:25
8-3/4" Hole Section Sub Total	597.53	30.73	30.73				
TOTALS	**737.43**	**30.73**	**30.73**				

NPT + Contingency %:	0.00%
Time per Connection [Minutes]:	15.00
Time per Connection Technical Limit [Minutes]:	14.00
Contract Time vs Planned Time Calculation	
Planned Time:	30.73
Planned Time + 0%	30.73

Figure 4B-1 Drilling procedure for a stratigraphic test well.

B.1.1.2 Stratigraphic Test Well Drilling Time Line

The estimated time line includes 31 days required for drilling, coring, logging, and plugging of a stratigraphic test well, which is shown in Figure 4B-2.

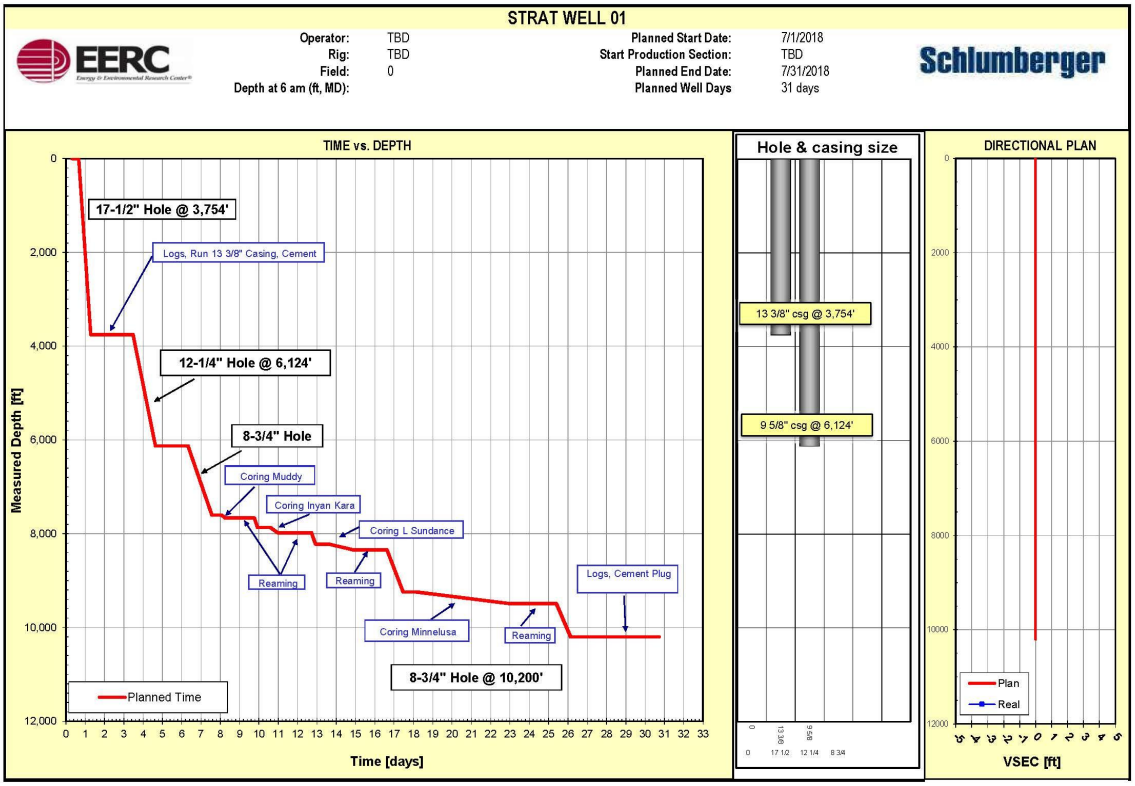

Figure 4B-2 Proposed time line for a stratigraphic test well, including drilling, coring, logging, and plugging.

B.1.1.3 Stratigraphic Test Well Cost Estimate

Dry Fork CarbonSAFE I Strat. Test Well - Wyoming
AUTHORIZATION FOR EXPENDITURES - Est Cost

In US $

Operator:	EERC	Project Type :	CO_2 Storage
Contract Area:	Wyoming	Well Name :	Stratigraphic Test Well
Contract Area #:		Well Type :	
Prepared by	WR, GV, JK, NM	Platform/Tripod :	AFE #: 1 of 3
		Field/Structure :	Date: 29-Jan-18
		Basin :	PRB

Location _____ Surface Coordinate _____
Surface Elev. _____ Elevation _____

	PROGRAM	ACTUAL
Spud Date		
Compl Date		
In Service		
Drilling Days		

	PROGRAM	ACTUAL
Rig Days	31	
Total Depth	10,200	
Well Cost $/Ft.	$0.00	
Well Cost $/Day	$0.00	

Close Out Date: _____ Completion Type: Cased Hole Well Status: Pre Permit

	Description	Dry Hole Budget	Completed Budget	Total Budget	Actual Expenditure	Actual Over/Under	% Over/Under
1	**TANGIBLE COSTS**						
2	Casing	361,112	0	361,112	$0	361,112	100%
3	Casing Accessories; Float Equip & Liners	7,845	0	7,845	$0	7,845	100%
4	Tubing		0	0	$0	0	
5	Well Equipment - Surface	15,000	0	15,000	$0	15,000	100%
6	Well Equipment - Subsurface	0	0	0	$0	0	
7	Other Tangible Costs	0	0	0	$0	0	
8	Contingency	0	0	0	$0	0	
9	**Total Tangible Costs**	**$383,957**	**$0**	**$383,957**	**$0**	383,957	100%
10	**INTANGIBLE COSTS**						
11	**PREPARATION & TERMINATION**						
12	Surveys	7,000	0	7,000	$0	7,000	100%
13	Location Staking & Positioning	4,500	0	4,500	$0	4,500	100%
14	Wellsite & Access Road Preparation	80,000	0	80,000	$0	80,000	100%
15	Service Lines & Communications	27,200	0	27,200	$0	27,200	100%
16	Water Systems	0	0	0	$0	0	
17	Rigging Up/Rigging Down/ Mob/Demob	200,000	0	200,000	$0	200,000	100%
19	**Total Preparations/MOB**	**$318,700**	**$0**	**$318,700**	**$0**	318,700	100%
20	**DRILLING - W/O OPERATIONS**						
21	Contract Rig	732,480	0	732,480	$0	732,480	100%
22	Drlg Rig Crew/Contract Rig Crew/Catering	0	0	0	$0	0	
23	Mud, Chem & Engineering Servs	119,880	0	119,880	$0	119,880	100%
24	Water	15,000	0	15,000	$0	15,000	100%
25	Bits, Reamers & Coreheads	41,890	0	41,890	$0	41,890	100%
26	Equipment Rentals	74,545	0	74,545	$0	74,545	100%
27	Directional Drlg & Surveys	282,548	0	282,548	$0	282,548	100%
28	Closed Loop and Disposal	98,600	0	98,600	$0	98,600	100%
29	Casing & Wellhead Installation & Inspection	30,000	0	30,000	$0	30,000	100%
30	Cement, Cementing & Pump Fees	140,000	0	140,000	$0	140,000	100%
31	Misc. H2S Services	0	0	0	$0	0	
32	**Total Drilling Operations**	**$1,534,943**	**$0**	**$1,534,943**	**$0**	1,534,943	100%
33	**FORMATION EVALUATION**						
34	Coring	220,000	0	220,000	$0	220,000	100%
35	Mud Logging Services	0	0	0	$0	0	
36	Drillstem Tests	0	0	0	$0	0	
37	Open Hole Elec Logging Services	270,000	0	270,000	$0	270,000	100%
39	**Total Formation Evaluation**	**$490,000**	**$0**	**$490,000**	**$0**	490,000	100%
40	**COMPLETION**						
41	Casing, Liner, Wellhead & Tubing Installation	0	0	0	$0	0	
42	Remedial Cementing and Fees	0	0	0	$0	0	
43	Cased Hole Elec Logging Services	25,000	0	25,000	$0	25,000	100%
44	Perforating & Wireline Services	0	0	0	$0	0	
45	Stimulation Treatment	0	0	0	$0	0	
46	Production Tests	0	0	0	$0	0	
48	**Total Completion Costs**	**$25,000**	**$0**	**$25,000**	**$0**	25,000	100%
49	**GENERAL**						
50	Supervision	179,800	0	179,800	$0	179,800	100%
51	Insurance	0	0	0	$0	0	
52	Permits & Fees	45,000	0	45,000	$0	45,000	100%
53	Marine Rental & Charters	0	0	0	$0	0	
54	Helicopter & Aviation Charges	0	0	0	$0	0	
55	Land Transportation	23,000	0	23,000	$0	23,000	100%
56	Other Transportation	0	0	0	$0	0	
57	Fuel & Lubricants Non Rig	60,000	0	60,000	$0	60,000	100%
58	Camp Facilities	20,500	0	20,500	$0	20,500	100%
59	Allocated Overhead - Well Construction Contractor	227,545	0	227,545	$0	227,545	100%
60	Allocated Overhead - Main Office	0	0	0	$0	0	
61	Allocated Overhead - Overseas	0	0	0	$0	0	
62	Contingency Intangibles	0	0	0	$0	0	
64	**Total General Costs**	**$555,845**	**$0**	**$555,845**	**$0**	555,845	100%
65	**TOTAL INTANGIBLE COSTS**	**$2,924,488**	**$0**	**$2,924,488**	**$0**	2,924,488	100%
	TOTAL TANGIBLE COSTS	**$383,957**	**$0**	**$383,957**	**$0**	383,957	100%
66	**TOTAL WELL COST**	**$3,308,446**	**$0**	**$3,308,446**	**$0**	**$3,308,446**	**100%**
67							
68							
69							
70							

Operator	Approved By:			**Remarks**
	Position			This AFE assumes the well will be drilled to TD, cored and logged, then abandoned. It assumes an intermediate casing string will be required. The P&A will be such that it will be easily re-entered at some later date for completion as either a monitor well or injection well. The entire well configuration can be downsized if necessary to save cost. It also assumes the well construction supervising company will apply a markup to every item.
	Date			
Operator Approval	Approved By:			
	Position			
	Date			

Figure 4B-3 Stratigraphic test well cost estimate.

B.1.2 Monitoring Well Drilling and Completion

B.1.2.1 Estimated Drilling Plan for a Monitoring Well

Operator:	TBD	Start Date	1-Jul-18
Well Name:	MONITOR WELL 01	End Drilling Date	3-Aug-18
Rig:	TBD	End Drilling Date (IPM + %NPT):	3-Aug-18
Field: (if applicable)		End Completion Date	17-Aug-2018

Operation Description	Estimated Time				ROP	Date	
	[hrs]	[Days]	[Days]	[ft]	[ft/hr]	Start	Finish
17-1/2" Hole Section							
Pre-spud Safety Meeting	8.00	0.33	0.33	0		1-Jul-18 06:00	1-Jul-18 14:00
Drill rat and mouse holes, make up bit	8.00	0.67	0.67	0		1-Jul-18 14:00	1-Jul-18 22:00
Drill 17-1/2" hole @ 3754 ft MD	**15.02**	1.29	1.29	**3,754**	**250.0**	1-Jul-18 22:00	2-Jul-18 13:00
Circulate	0.50	1.31	1.31	3,754		2-Jul-18 13:00	2-Jul-18 13:30
POOH	2.00	1.40	1.40	3,754		2-Jul-18 13:30	2-Jul-18 15:30
Wireline Logs	8.00	1.73	1.73	3,754		2-Jul-18 15:30	2-Jul-18 23:30
Run Surface Casing - Cement	6.00	1.98	1.98	3,754		2-Jul-18 23:30	3-Jul-18 05:30
Wait on Cement	12.00	2.48	2.48	3,754		3-Jul-18 05:30	3-Jul-18 17:30
17-1/2" Hole Section Sub Total	**59.52**	**2.48**	**2.48**	**3,754**		3-Jul-18 05:30	3-Jul-18 17:30
12-1/4" Hole Section			0.00	0			
Nipple up BOPs	12.00	2.98	2.98	3,754		3-Jul-18 17:30	4-Jul-18 05:30
Make up 12-1/4" BHA	6.00	3.23	3.23	3,754		4-Jul-18 05:30	4-Jul-18 11:30
Drill Float/Shoe and LOT/FIT	6.00	3.48	3.48	3,754		4-Jul-18 11:30	4-Jul-18 17:30
Drill 12-1/4" hole @ 6124 ft MD	**27.88**	4.64	4.64	**6,124**	**85.0**	4-Jul-18 17:30	5-Jul-18 21:23
Circulate	0.50	4.66	4.66	6,124		5-Jul-18 21:23	5-Jul-18 21:53
POOH	2.00	4.75	4.75	6,124		5-Jul-18 21:53	5-Jul-18 23:53
Wireline Logs	8.00	5.08	5.08	6,124		5-Jul-18 23:53	6-Jul-18 07:53
Run Intermediate Casing - Cement	6.00	5.33	5.33	6,124		6-Jul-18 07:53	6-Jul-18 13:53
Wait on Cement	12.00	5.83	5.83	6,124		6-Jul-18 13:53	7-Jul-18 01:53
12-1/4" Hole Section Sub Total	**80.38**	**5.83**	**5.83**	**6,124**		7-Jul-18 01:53	7-Jul-18 01:53
8-3/4" Hole Section			0.00	0			
Make up 8-3/4" BHA	6.00	6.08	6.08	6,124		7-Jul-18 01:53	7-Jul-18 07:53
Drill Float/Shoe and LOT/FIT	6.00	6.33	6.33	6,124		7-Jul-18 07:53	7-Jul-18 13:53
Drill 8-3/4" hole @ 7600 ft MD	**29.52**	7.56	7.56	**7,600**	**50.0**	7-Jul-18 13:53	8-Jul-18 19:25
Trip for Muddy Core, Make up Core Barrel	12.00	8.06	8.06	7,600		8-Jul-18 19:25	9-Jul-18 07:25
Core Muddy 65' @ 7665 ft MD	**4.64**	8.25	8.25	**7,665**	**14.0**	9-Jul-18 07:25	9-Jul-18 12:03
Trip for Core, MU Reaming Assembly, Trip in to Ream	16.00	8.92	8.92	7,665		9-Jul-18 12:03	10-Jul-18 04:03
Ream 65'	8.13	9.26	9.26	7,665		10-Jul-18 04:03	10-Jul-18 12:11
Trip, MU BHA, Trip in to Drill to next core pt.	12.00	9.76	9.76	7,665		10-Jul-18 12:11	11-Jul-18 00:11
Drill 8-3/4" hole @ 7864 ft MD	**3.98**	9.92	9.92	**7,864**	**50.0**	11-Jul-18 00:11	11-Jul-18 04:09
Trip for Core, Make up Core Barrel, Trip in to Core	16.00	10.59	10.59	7,864		11-Jul-18 04:09	11-Jul-18 20:09
Core Inyan Kara 115' @ 7979 ft MD	**8.85**	10.96	10.96	**7,979**	**13.0**	11-Jul-18 20:09	12-Jul-18 05:00
Trip for Core, MU Reaming Assembly, Trip in to Ream	16.00	11.63	11.63	7,979		12-Jul-18 05:00	12-Jul-18 21:00
Ream 115'	14.38	12.22	12.22	7,979		12-Jul-18 21:00	13-Jul-18 11:23
Trip, MU BHA, Trip in to Drill to next core pt.	12.00	12.72	12.72	7,979		13-Jul-18 11:23	13-Jul-18 23:23
Drill 8-3/4" hole @ 8218 ft MD	**4.78**	12.92	12.92	**8,218**	**50.0**	13-Jul-18 23:23	14-Jul-18 04:10
Trip for Core, Make up Core Barrel, Trip in to Core	16.00	13.59	13.59	8,218		14-Jul-18 04:10	14-Jul-18 20:10
Core L Sundance 120' @ 8338 ft MD	**29.92**	14.84	14.84	**8,338**	**12.0**	14-Jul-18 20:10	16-Jul-18 02:05
Trip for Core, MU Reaming Assembly, Trip in to Ream	16.00	15.50	15.50	8,338		16-Jul-18 02:05	16-Jul-18 18:05
Ream 120'	15.00	16.13	16.13	8,338		16-Jul-18 18:05	17-Jul-18 09:05
Trip, MU BHA, Trip in to Drill to next core pt.	12.00	16.63	16.63	8,338		17-Jul-18 09:05	17-Jul-18 21:05
Drill 8-3/4" hole @ 9241 ft MD	**20.07**	17.46	17.46	**9,241**	**45.0**	17-Jul-18 21:05	18-Jul-18 17:09
Trip for Core, Make up Core Barrel	16.00	18.13	18.13	9,241		18-Jul-18 17:09	19-Jul-18 09:09
Core U & M Minnelusa 250' @ 9491 ft MD	**115.30**	22.94	22.94	**9,491**	**10.0**	19-Jul-18 09:09	24-Jul-18 04:27
Trip for Core, MU Reaming Assembly, Trip in to Ream	16.00	23.60	23.60	9,491		24-Jul-18 04:27	24-Jul-18 20:27
Ream 250'	31.25	24.90	24.90	9,491		24-Jul-18 20:27	26-Jul-18 03:42
Trip, MU BHA, Trip in to Drill to total depth.	12.00	25.40	25.40	9,491		26-Jul-18 03:42	26-Jul-18 15:42
Drill 8-3/4" hole @ 10200 ft MD	**17.73**	26.14	26.14	**10,200**	**40.0**	26-Jul-18 15:42	27-Jul-18 09:25
Circulate	6.00	26.39	26.39	10,200		27-Jul-18 09:25	27-Jul-18 15:25
POOH and rig down MWD	16.00	27.06	27.06	10,200		27-Jul-18 15:25	28-Jul-18 07:25
Wireline Logs	60.00	29.56	29.56	10,200		28-Jul-18 07:25	30-Jul-18 19:25
Run casing and cement	36.00	31.06	31.06	10,200		30-Jul-18 19:25	1-Aug-18 07:25
Rig down	16.00	31.73	31.73	10,200		1-Aug-18 07:25	1-Aug-18 23:25
De-mobilize Drilling Rig	32.00	33.06	33.06	10,200		1-Aug-18 23:25	3-Aug-18 07:25
8-3/4" Hole Section Sub Total	**653.53**	**33.06**	**33.06**				
Completion	(Days)						
Move-in and Rig up Workover rig (assuming daylight hrs)	1.00	34.06	34.06	10200.00		3-Aug-18 06:00	4-Aug-18 06:00
Install tubing head adapter and nipple up BOP, pressure test	1.00	35.06	35.06	10200.00		4-Aug-18 06:00	5-Aug-18 06:00
Bit and scrapper run, reverse circ in clean KCl water, trip out and la	1.00	36.06	36.06	10200.00		5-Aug-18 06:00	6-Aug-18 06:00
Run Cased Hole logs and perforate injection zone	1.00	37.06	37.06	10200.00		6-Aug-18 06:00	7-Aug-18 06:00
RIH With RBP and Packer, isolate zone, Swab and obtain fluid sam	2.00	39.06	39.06	10200.00		7-Aug-18 06:00	9-Aug-18 06:00
Perforate deepest permeable zone above seal	1.00	40.06	40.06	10200.00		9-Aug-18 06:00	10-Aug-18 06:00
RIH With RBP and Packer, isolate zone, Swab and obtain fluid sam	3.00	43.06	43.06	10200.00		10-Aug-18 06:00	13-Aug-18 06:00
RIH With Intelligent packer system and control lines	4.00	47.06	47.06	10200.00		13-Aug-18 06:00	17-Aug-18 06:00
Rig down Workover rig and move off	0.50	47.56	47.56	10200.00		17-Aug-18 06:00	17-Aug-18 18:00
Completion Sub Total	**14.50**	**47.56**	**47.56**				
TOTALS	**1141.43**	**47.56**	**47.56**				

NPT + Contingency %:	0.00%
Time per Connection [Minutes]:	15.00
Time per Connection Technical Limit [Minutes]:	14.00
Contract Time vs Planned Time Calculation	
Planned Time:	47.56
Planned Time + 0%	47.56

Figure 4B-4 Drilling procedure for a monitoring well.

B.1.2.2 Monitoring Well Drilling Time Line

SLB estimates 42 days required for drilling, coring, logging, and completion of a monitoring well, which is shown in Figure 4B-5.

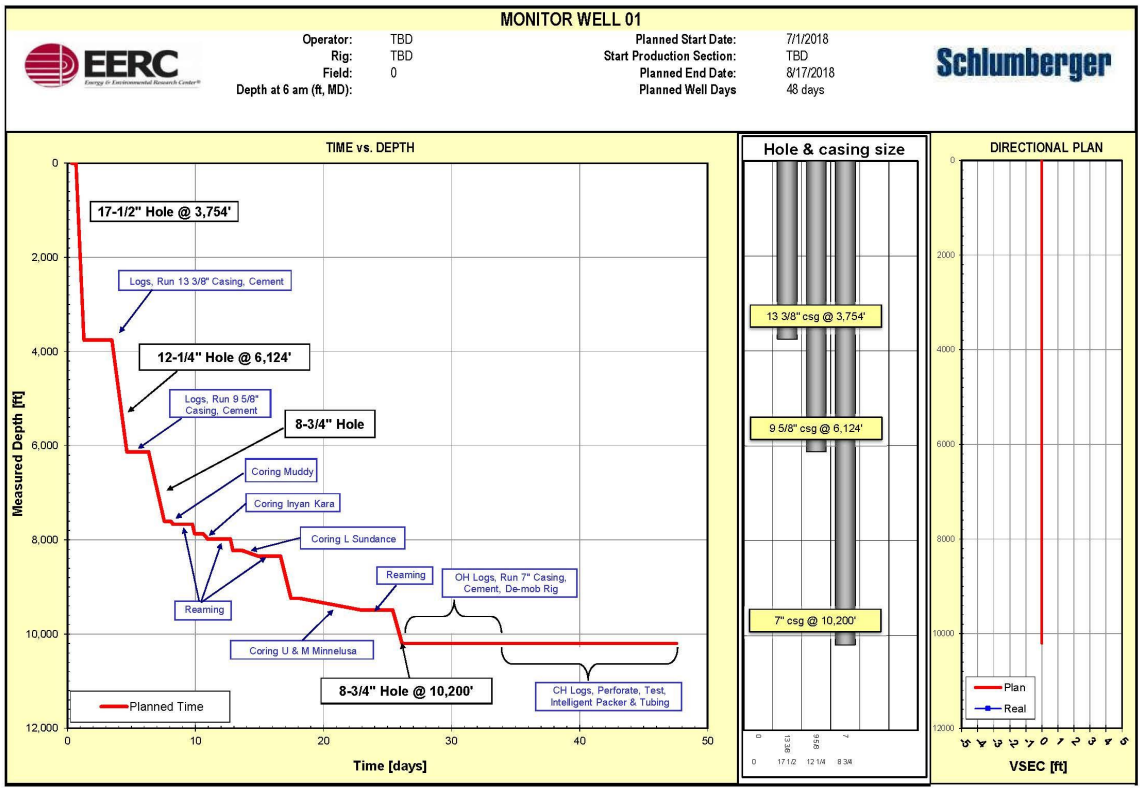

Figure 4B-5 Proposed time line for a monitoring well, including drilling, coring, logging, and completion.

B.1.2.3 Monitoring Well Cost Estimate

EERC

Dry Fork CarbonSAFE Monitor Well - Wyoming

AUTHORIZATION FOR EXPENDITURES - Est Cost

Schlumberger

In US $

Operator:	EERC	Project Type :	CO_2 Storage		
Contract Area:	Wyoming	Well Name :	Monitor Well		
Contract Area #:		Well Type :	MMV		
Prepared by	WR, GV, JK, NM	Platform/Tripod :		AFE #:	2 of 3
		Field/Structure :		Date:	29-Jan-18
		Basin :	PRB		

Location _____ Surface Coordinate _____

Surface Elev. _____ Elevation _____

	PROGRAM	ACTUAL
Spud Date		
Compl Date		
In Service		
Drilling Days		

	PROGRAM	ACTUAL
Rig Days	33	
Total Depth	10,200	
Well Cost $/Ft.	$0.00	
Well Cost $/Day	$0.00	

Close Out Date: _____ Completion Type: Cased Hole Well Status: Pre Permit

	Description	Dry Hole Budget	Completed Budget	Total Budget	Actual Expenditure	Actual Over/Under	% Over/Under
1	**TANGIBLE COSTS**						
2	Casing	361,112	218,600	579,712	$0	579,712	100%
3	Casing Accessories; Float Equip & Liners	7,845	18,698	26,544	$0	26,544	100%
4	Tubing		225,120	225,120	$0	225,120	100%
5	Well Equipment - Surface	15,000	134,000	149,000	$0	149,000	100%
6	Well Equipment - Subsurface	0	835,000	835,000	$0	835,000	100%
7	Other Tangible Costs	0	0	0	$0	0	
8	Contingency	0	0	0	$0	0	
9	**Total Tangible Costs**	**$383,957**	**$1,431,418**	**$1,815,376**	**$0**	1,815,376	100%
10	**INTANGIBLE COSTS**						
11	**PREPARATION & TERMINATION**						
12	Surveys	7,000	0	7,000	$0	7,000	100%
13	Location Staking & Positioning	4,500	0	4,500	$0	4,500	100%
14	Wellsite & Access Road Preparation	80,000	0	80,000	$0	80,000	100%
15	Service Lines & Communications	28,900	0	28,900	$0	28,900	100%
16	Water Systems	0	0	0	$0	0	
17	Rigging Up/Rigging Down/ Mob/Demob	200,000	0	200,000	$0	200,000	100%
19	**Total Preparations/MOB**	**$320,400**	**$0**	**$320,400**	**$0**	320,400	100%
20	**DRILLING - W/O OPERATIONS**						
21	Contract Rig	772,760	180,000	952,760	$0	952,760	100%
22	Drlg Rig Crew/Contract Rig Crew/Catering	0	0	0	$0	0	
23	Mud, Chem & Engineering Servs	120,720	30,000	150,720	$0	150,720	100%
24	Water	15,000	24,000	39,000	$0	39,000	100%
25	Bits, Reamers & Coreheads	41,890	0	41,890	$0	41,890	100%
26	Equipment Rentals	73,270	6,769	80,039	$0	80,039	100%
27	Directional Drlg & Surveys	240,548	0	240,548	$0	240,548	100%
28	Closed Loop and Disposal	98,600	0	98,600	$0	98,600	100%
29	Casing & Wellhead Installation & Inspection	32,500	33,000	65,500	$0	65,500	100%
30	Cement, Cementing & Pump Fees	80,000	80,000	160,000	$0	160,000	100%
31	Misc. H2S Services	0	0	0	$0	0	
32	**Total Drilling Operations**	**$1,475,288**	**$353,769**	**$1,829,057**	**$0**	1,829,057	100%
33	**FORMATION EVALUATION**						
34	Coring	220,000	0	220,000	$0	220,000	100%
35	Mud Logging Services	0	0	0	$0	0	
36	Drillstem Tests	0	0	0	$0	0	
37	Open Hole Elec Logging Services	270,000	0	270,000	$0	270,000	100%
39	**Total Formation Evaluation**	**$490,000**	**$0**	**$490,000**	**$0**	490,000	100%
40	**COMPLETION**						
41	Casing, Liner, Wellhead & Tubing Installation	0	0	0	$0	0	
42	Remedial Cementing and Fees	0	0	0	$0	0	
43	Cased Hole Elec Logging Services	25,000	50,000	75,000	$0	75,000	100%
44	Perforating & Wireline Services	0	35,000	35,000	$0	35,000	100%
45	Stimulation Treatment	0	50,000	50,000	$0	50,000	100%
46	Production Tests	0	0	0	$0	0	
48	**Total Completion Costs**	**$25,000**	**$135,000**	**$160,000**	**$0**	160,000	100%
49	**GENERAL**						
50	Supervision	221,950	24,750	246,700	$0	246,700	100%
51	Insurance	0	0	0	$0	0	
52	Permits & Fees	45,000	0	45,000	$0	45,000	100%
53	Marine Rental & Charters	0	0	0	$0	0	
54	Helicopter & Aviation Charges	0	0	0	$0	0	
55	Land Transportation	23,000	0	23,000	$0	23,000	100%
56	Other Transportation	0	0	0	$0	0	
57	Fuel & Lubricants Non Rig	52,500	0	52,500	$0	52,500	100%
58	Camp Facilities	22,000	0	22,000	$0	22,000	100%
59	Allocated Overhead - Well Construction Contractor	232,755	100,397	333,152	$0	333,152	100%
60	Allocated Overhead - Main Office	0	0	0	$0	0	
61	Allocated Overhead - Overseas	0	0	0	$0	0	
62	Contingency Intangibles	0	0	0	$0	0	
64	**Total General Costs**	**$597,205**	**$125,147**	**$722,352**	**$0**	722,352	100%
65	**TOTAL INTANGIBLE COSTS**	**$2,907,893**	**$613,915**	**$3,521,809**	**$0**	3,521,809	100%
	TOTAL TANGIBLE COSTS	**$383,957**	**$1,431,418**	**$1,815,376**	**$0**	1,815,376	100%
66	**TOTAL WELL COST**	**$3,291,851**	**$2,045,334**	**$5,337,184**	**$0**	**$5,337,184**	**100%**
67							
68							
69							
70							

Operator	Approved By:			**Remarks**
	Position			Instal intelligent packer system with data recording system (Line 6) to isolate injection interval and deepest USDW above sealing formation. If well is specifically drilled to be a monitor well it can be downsized to 7 7/8" borehole, 5 1/2" casing and 2 7/8" tubing to reduce cost.
	Date			
Operator Approval	Approved By:			
	Position			
	Date			

Figure 4B-6 Monitoring well cost estimate.

B.1.3 Injection Well Drilling and Completion

B.2.3.1 Estimated Drilling Plan for an Injection Well

Operator:	TBD	Start Date	1-Jul-18
Well Name:	INJECTION WELL	End Drilling Date	3-Aug-18
Rig:	TBD	End Drilling Date (IPM + %NPT):	3-Aug-18
Field: (if applicable)		End Completion Date	10-Aug-2018

Operation Description	Estimated Time				ROP	Date	
	[hrs]	[Days]	[Days]	[ft]	[ft/hr]	Start	Finish
17-1/2" Hole Section							
Pre-spud Safety Meeting	8.00	0.33	0.33	0		1-Jul-18 06:00	1-Jul-18 14:00
Drill rat and mouse holes, make up bit	8.00	0.67	0.67	0		1-Jul-18 14:00	1-Jul-18 22:00
Drill 17-1/2" hole @ 3754 ft MD	**15.02**	1.29	1.29	**3,754**	**250.0**	1-Jul-18 22:00	2-Jul-18 13:00
Circulate	0.50	1.31	1.31	3,754		2-Jul-18 13:00	2-Jul-18 13:30
POOH	2.00	1.40	1.40	3,754		2-Jul-18 13:30	2-Jul-18 15:30
Wireline Logs	8.00	1.73	1.73	3,754		2-Jul-18 15:30	2-Jul-18 23:30
Run Surface Casing - Cement	6.00	1.98	1.98	3,754		2-Jul-18 23:30	3-Jul-18 05:30
Wait on Cement	12.00	2.48	2.48	3,754		3-Jul-18 05:30	3-Jul-18 17:30
17-1/2" Hole Section Sub Total	**59.52**	**2.48**	**2.48**	**3,754**		3-Jul-18 05:30	3-Jul-18 17:30
12-1/4" Hole Section			0.00	0			
Nipple up BOPs	12.00	2.98	2.98	3,754		3-Jul-18 17:30	4-Jul-18 05:30
Make up 12-1/4" BHA	6.00	3.23	3.23	3,754		4-Jul-18 05:30	4-Jul-18 11:30
Drill Float/Shoe and LOT/FIT	6.00	3.48	3.48	3,754		4-Jul-18 11:30	4-Jul-18 17:30
Drill 12-1/4" hole @ 6124 ft MD	**27.88**	4.64	4.64	**6,124**	**85.0**	4-Jul-18 17:30	5-Jul-18 21:23
Circulate	0.50	4.66	4.66	6,124		5-Jul-18 21:23	5-Jul-18 21:53
POOH	2.00	4.75	4.75	6,124		5-Jul-18 21:53	5-Jul-18 23:53
Wireline Logs	8.00	5.08	5.08	6,124		5-Jul-18 23:53	6-Jul-18 07:53
Run Intermediate Casing - Cement	6.00	5.33	5.33	6,124		6-Jul-18 07:53	6-Jul-18 13:53
Wait on Cement	12.00	5.83	5.83	6,124		6-Jul-18 13:53	7-Jul-18 01:53
12-1/4" Hole Section Sub Total	**80.38**	**5.83**	**5.83**	**6,124**		7-Jul-18 01:53	7-Jul-18 01:53
8-3/4" Hole Section			0.00	0			
Make up 8-3/4" BHA	6.00	6.08	6.08	6,124		7-Jul-18 01:53	7-Jul-18 07:53
Drill Float/Shoe and LOT/FIT	6.00	6.33	6.33	6,124		7-Jul-18 07:53	7-Jul-18 13:53
Drill 8-3/4" hole @ 7600 ft MD	**29.52**	7.56	7.56	**7,600**	**50.0**	7-Jul-18 13:53	8-Jul-18 19:25
Trip for Muddy Core, Make up Core Barrel	12.00	8.06	8.06	7,600		8-Jul-18 19:25	9-Jul-18 07:25
Core Muddy 65' @ 7665 ft MD	**4.64**	8.25	8.25	**7,665**	**14.0**	9-Jul-18 07:25	9-Jul-18 12:03
Trip for Core, MU Reaming Assembly, Trip in to Ream	16.00	8.92	8.92	7,665		9-Jul-18 12:03	10-Jul-18 04:03
Ream 65'	8.13	9.26	9.26	7,665		10-Jul-18 04:03	10-Jul-18 12:11
Trip, MU BHA, Trip in to Drill to next core pt.	12.00	9.76	9.76	7,665		10-Jul-18 12:11	11-Jul-18 00:11
Drill 8-3/4" hole @ 7864 ft MD	**3.98**	9.92	9.92	**7,864**	**50.0**	11-Jul-18 00:11	11-Jul-18 04:09
Trip for Core, Make up Core Barrel, Trip in to Core	16.00	10.59	10.59	7,864		11-Jul-18 04:09	11-Jul-18 20:09
Core Inyan Kara 115' @ 7979 ft MD	**8.85**	10.96	10.96	**7,979**	**13.0**	11-Jul-18 20:09	12-Jul-18 05:00
Trip for Core, MU Reaming Assembly, Trip in to Ream	16.00	11.63	11.63	7,979		12-Jul-18 05:00	12-Jul-18 21:00
Ream 115'	14.38	12.22	12.22	7,979		12-Jul-18 21:00	13-Jul-18 11:23
Trip, MU BHA, Trip in to Drill to next core pt.	12.00	12.72	12.72	7,979		13-Jul-18 11:23	13-Jul-18 23:23
Drill 8-3/4" hole @ 8218 ft MD	**4.78**	12.92	12.92	**8,218**	**50.0**	13-Jul-18 23:23	14-Jul-18 04:10
Trip for Core, Make up Core Barrel, Trip in to Core	16.00	13.59	13.59	8,218		14-Jul-18 04:10	14-Jul-18 20:10
Core L Sundance 120' @ 8338 ft MD	**29.92**	14.84	14.84	**8,338**	**12.0**	14-Jul-18 20:10	16-Jul-18 02:05
Trip for Core, MU Reaming Assembly, Trip in to Ream	16.00	15.50	15.50	8,338		16-Jul-18 02:05	16-Jul-18 18:05
Ream 120'	15.00	16.13	16.13	8,338		16-Jul-18 18:05	17-Jul-18 09:05
Trip, MU BHA, Trip in to Drill to next core pt.	12.00	16.63	16.63	8,338		17-Jul-18 09:05	17-Jul-18 21:05
Drill 8-3/4" hole @ 9241 ft MD	**20.07**	17.46	17.46	**9,241**	**45.0**	17-Jul-18 21:05	18-Jul-18 17:09
Trip for Core, Make up Core Barrel	16.00	18.13	18.13	9,241		18-Jul-18 17:09	19-Jul-18 09:09
Core U & M Minnelusa 250' @ 9491 ft MD	**115.30**	22.94	22.94	**9,491**	**10.0**	19-Jul-18 09:09	24-Jul-18 04:27
Trip for Core, MU Reaming Assembly, Trip in to Ream	16.00	23.60	23.60	9,491		24-Jul-18 04:27	24-Jul-18 20:27
Ream 250'	31.25	24.90	24.90	9,491		24-Jul-18 20:27	26-Jul-18 03:42
Trip, MU BHA, Trip in to Drill to total depth.	12.00	25.40	25.40	9,491		26-Jul-18 03:42	26-Jul-18 15:42
Drill 8-3/4" hole @ 10200 ft MD	**17.73**	26.14	26.14	**10,200**	**40.0**	26-Jul-18 15:42	27-Jul-18 09:25
Circulate	6.00	26.39	26.39	10,200		27-Jul-18 09:25	27-Jul-18 15:25
POOH and rig down MWD	16.00	27.06	27.06	10,200		27-Jul-18 15:25	28-Jul-18 07:25
Wireline Logs	60.00	29.56	29.56	10,200		28-Jul-18 07:25	30-Jul-18 19:25
Run casing and cement	36.00	31.06	31.06	10,200		30-Jul-18 19:25	1-Aug-18 07:25
Rig down	16.00	31.73	31.73	10,200		1-Aug-18 07:25	1-Aug-18 23:25
De-mobilize Drilling Rig	32.00	33.06	33.06	10,200		1-Aug-18 23:25	3-Aug-18 07:25
8-3/4" Hole Section Sub Total	**653.53**	**33.06**	**33.06**				
Completion	(Days)						
Move-in and Rig up Workover rig (assuming daylight hrs)	1.00	34.06	34.06	10200.00		2-Aug-18 06:00	3-Aug-18 06:00
Install tubing head adapter and nipple up BOP, pressure test	1.00	35.06	35.06	10200.00		3-Aug-18 06:00	4-Aug-18 06:00
Bit and scrapper run, reverse circ in clean KCl water, trip out and lay	1.00	36.06	36.06	10200.00		4-Aug-18 06:00	5-Aug-18 06:00
Run Cased Hole logs and perforate injection zone	1.00	37.06	37.06	10200.00		5-Aug-18 06:00	6-Aug-18 06:00
RIH With RBP and Packer, isolate zone, Swab and obtain fluid samp	2.00	39.06	39.06	10200.00		6-Aug-18 06:00	8-Aug-18 06:00
RIH packer, P/T gauges and chrome tubing	2.00	41.06	41.06	10200.00		8-Aug-18 06:00	10-Aug-18 06:00
Rig down Workover rig and move off	0.50	41.56	41.56	10200.00		10-Aug-18 06:00	10-Aug-18 18:00
Completion Sub Total	**8.50**	**41.56**	**41.56**				
TOTALS	**997.43**	**41.56**	**41.56**				

NPT + Contingency %:	0.00%
Time per Connection [Minutes]:	15.00
Time per Connection Technical Limit [Minutes]:	14.00
Contract Time vs Planned Time Calculation	
Planned Time:	41.56
Planned Time + 0%	41.56

Figure 4B-7 Drilling procedure for a monitoring well.

B.1.3.2 Injection Well Drilling Time Line

SLB estimates 48 days required for drilling, coring, logging, and completion of an injection well, which is shown in Figure 4B-8.

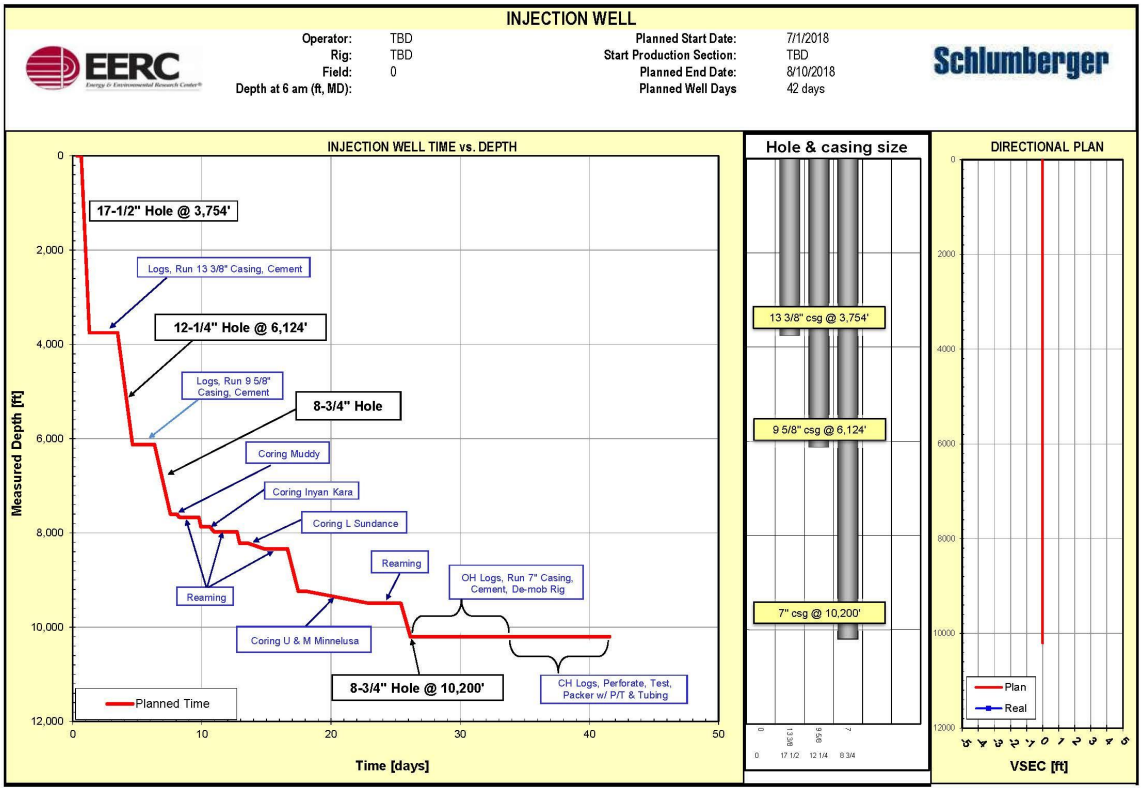

Figure 4B-8 Proposed time line for an injection well, including drilling, coring, logging, and completion.

B.2.3.3 Injection Well Cost Estimate

EERC

Dry Fork CarbonSAFE Injection Well - Wyoming

AUTHORIZATION FOR EXPENDITURES - Est Cost

Schlumberger

In US $

Operator:	EERC	Project Type :	CO_2 Storage		
Contract Area:	Wyoming	Well Name :	Injection Well		
Contract Area #:		Well Type :	Class VI		
Prepared by	WR, GV, JK, NM	Platform/Tripod :		AFE #:	3 of 3
		Field/Structure :		Date:	29-Jan-18
		Basin :	PRB		

Location _____ Surface Coordinate _____

Surface Elev. _____ Elevation _____

	PROGRAM	ACTUAL
Spud Date		
Compl Date		
In Service		
Drilling Days		

	PROGRAM	ACTUAL
Rig Days	33	
Total Depth	10,200	
Well Cost $/Ft.	$0.00	
Well Cost $/Day	$0.00	

Close Out Date: _____ Completion Type: Cased Hole Well Status: Pre Permit

	Description	Dry Hole Budget	Completed Budget	Total Budget	Actual Expenditure	Actual Over/Under	% Over/Under
1	**TANGIBLE COSTS**						
2	Casing	361,112	218,600	579,712	$0	579,712	100%
3	Casing Accessories; Float Equip & Liners	7,845	18,698	26,544	$0	26,544	100%
4	Tubing		225,120	225,120	$0	225,120	100%
5	Well Equipment - Surface	15,000	105,763	120,763	$0	120,763	100%
6	Well Equipment - Subsurface	0	110,000	110,000	$0	110,000	100%
7	Other Tangible Costs	0	0	0	$0	0	
8	Contingency	0	0	0	$0	0	
9	**Total Tangible Costs**	**$383,957**	**$678,181**	**$1,062,139**	**$0**	1,062,139	100%
10	**INTANGIBLE COSTS**						
11	**PREPARATION & TERMINATION**						
12	Surveys	7,000	0	7,000	$0	7,000	100%
13	Location Staking & Positioning	4,500	0	4,500	$0	4,500	100%
14	Wellsite & Access Road Preparation	80,000	0	80,000	$0	80,000	100%
15	Service Lines & Communications	27,200	0	27,200	$0	27,200	100%
16	Water Systems	0	0	0	$0	0	
17	Rigging Up/Rigging Down/ Mob/Demob	200,000	0	200,000	$0	200,000	100%
19	**Total Preparations/MOB**	**$318,700**	**$0**	**$318,700**	**$0**	318,700	100%
20	**DRILLING - W/O OPERATIONS**						
21	Contract Rig	732,480	108,000	840,480	$0	840,480	100%
22	Drlg Rig Crew/Contract Rig Crew/Catering	0	0	0	$0	0	
23	Mud, Chem & Engineering Servs	118,170	30,000	148,170	$0	148,170	100%
24	Water	15,000	0	15,000	$0	15,000	100%
25	Bits, Reamers & Coreheads	41,890	0	41,890	$0	41,890	100%
26	Equipment Rentals	73,270	6,769	80,039	$0	80,039	100%
27	Directional Drlg & Surveys	240,548	0	240,548	$0	240,548	100%
28	Closed Loop and Disposal	98,600	0	98,600	$0	98,600	100%
29	Casing & Wellhead Installation & Inspection	32,500	33,000	65,500	$0	65,500	100%
30	Cement, Cementing & Pump Fees	160,000	80,000	240,000	$0	240,000	100%
31	Misc. H2S Services	0	0	0	$0	0	
32	**Total Drilling Operations**	**$1,512,458**	**$257,769**	**$1,770,227**	**$0**	1,770,227	100%
33	**FORMATION EVALUATION**						
34	Coring	220,000	0	220,000	$0	220,000	100%
35	Mud Logging Services	0	0	0	$0	0	
36	Drillstem Tests	0	0	0	$0	0	
37	Open Hole Elec Logging Services	270,000	0	270,000	$0	270,000	100%
39	**Total Formation Evaluation**	**$490,000**	**$0**	**$490,000**	**$0**	490,000	100%
40	**COMPLETION**						
41	Casing, Liner, Wellhead & Tubing Installation	0	0	0	$0	0	
42	Remedial Cementing and Fees	0	0	0	$0	0	
43	Cased Hole Elec Logging Services	25,000	50,000	75,000	$0	75,000	100%
44	Perforating & Wireline Services	0	35,000	35,000	$0	35,000	100%
45	Stimulation Treatment	0	0	0	$0	0	
46	Production Tests	0	0	0	$0	0	
48	**Total Completion Costs**	**$25,000**	**$85,000**	**$110,000**	**$0**	110,000	100%
49	**GENERAL**						
50	Supervision	197,200	0	197,200	$0	197,200	100%
51	Insurance	0	0	0	$0	0	
52	Permits & Fees	45,000	200,000	245,000	$0	245,000	100%
53	Marine Rental & Charters	0	0	0	$0	0	
54	Helicopter & Aviation Charges	0	0	0	$0	0	
55	Land Transportation	23,000	0	23,000	$0	23,000	100%
56	Other Transportation	0	0	0	$0	0	
57	Fuel & Lubricants Non Rig	52,500	0	52,500	$0	52,500	100%
58	Camp Facilities	22,000	0	22,000	$0	22,000	100%
59	Allocated Overhead - Well Construction Contractor	233,291	55,959	289,250	$0	289,250	100%
60	Allocated Overhead - Main Office	0	0	0	$0	0	
61	Allocated Overhead - Overseas	0	0	0	$0	0	
62	Contingency Intangibles	0	0	0	$0	0	
64	**Total General Costs**	**$572,991**	**$255,959**	**$828,950**	**$0**	828,950	100%
65	**TOTAL INTANGIBLE COSTS**	**$2,919,149**	**$598,728**	**$3,517,877**	**$0**	3,517,877	100%
	TOTAL TANGIBLE COSTS	**$383,957**	**$678,181**	**$1,062,139**	**$0**	1,062,139	100%
66	**TOTAL WELL COST**	**$3,303,107**	**$1,276,909**	**$4,580,016**	**$0**	**$4,580,016**	**100%**
67							
68							
69							
70							

Operator	Approved By:			**Remarks**
	Position			Exact completed well configuration will ultimately be determined by the EPA administrator. This AFE includes downhole P/T gauges and annular P monitor. It does assume chrome casing below packer and chrome tubing. It also includes CO2 resistant cement with each string cemented to surface. There is a rough estimate of the additional cost to support the application of a class VI license. This AFE also assumes it is the Strat test completed as a Class VI injection well.
	Date			
Operator Approval	Approved By:			
	Position			
	Date			

Figure 4B-9 Injection well cost estimate.

B.2 Seismic Survey Designs and Cost Estimates Report

Schlumberger produced multiple designs and cost estimates for 3-D surface seismic surveys, varying with source/receiver layout and resolution. The goal was to identify acquisition parameters and associated cost estimates to enable proper planning for future acquisition. The seismic data will be used for site characterization purposes. The data may also serve as a baseline for future time-lapse surveys (4-D seismic investigations) to identify changes in fluid saturations and pressure during and following CO_2 injection. The anticipated survey area footprint is 3.5 mi × 3.5 mi, centered on the characterization well location. A map showing the anticipated seismic footprint and characterization well location is shown in Figure 4B.10.

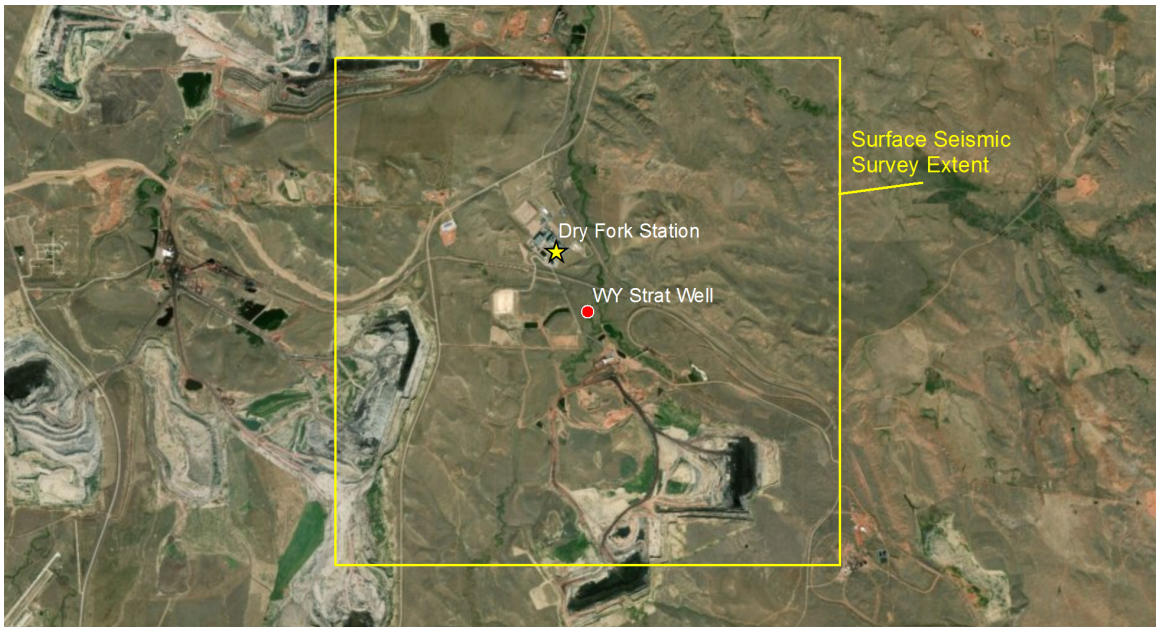

Figure 4B-10 Map showing the extent of the anticipated 3-D seismic survey (yellow square 3.5 miles on a side), the location of the planned characterization well, and the location of Dry Fork Station.

Three survey design options were explored, and the cost estimate was calculated for each option. Option 1 is the least dense and has the least cost. Option 2 has greater resolution and cost than Option 1 but less than Option 3. Option 3 is a high-resolution acquisition geometry, and the smaller source and receiver intervals help in modeling linear noise and subtracting (attenuating) it safely without compromising data quality. Survey designs were performed taking into account a 10,000-ft offset requirement. Fold plots were generated for 7650-, 7900-, 8250-, and 9300-ft offsets which, approximately, corresponds to the same value in depth for each. These depths of interest coincide approximately with the stratigraphic intervals of interest, including the Muddy, Fall River/Lakota, Lower Sundance, and Minnelusa Formations.

Seismic Survey Option 1

Table 4B-1 Seismic Survey Option 1 Acquisition Parameters

Option 1	
Acquisition Parameters	
Acquisition Geometry	Orthogonal
Recording Patch	16 Lines × 96 Stations
Channels Live	1536 Channels
Source Lines Heading	360°
Receiver Lines Heading	90°
Bin Size	110 ft. × 110 ft.
Sources	
Source Line Interval	1320 ft.
Source Point Interval	220 ft.
Number of Lines	15
Energy Source Type	Vibroseis × 2 (2 crews), AHV-IV Buggies
Vibroseis Sweep Parameters	Nonlinear 2 – 100 Hz 12-sec Sweep Two sweeps per Source Point Five second Listen Time
Receivers	
Recording System	Inova Hawk
Receiver Line Interval	1320 ft.
Receiver Point Interval	220 ft.
Number of Lines	15
Source-to-Detector Offset Distances	
Minimum	155.563 ft.
Maximum	14,788.531 ft.
Maximum (inline)	10,450.005 ft.
Maximum (crossline)	10,450.004 ft.

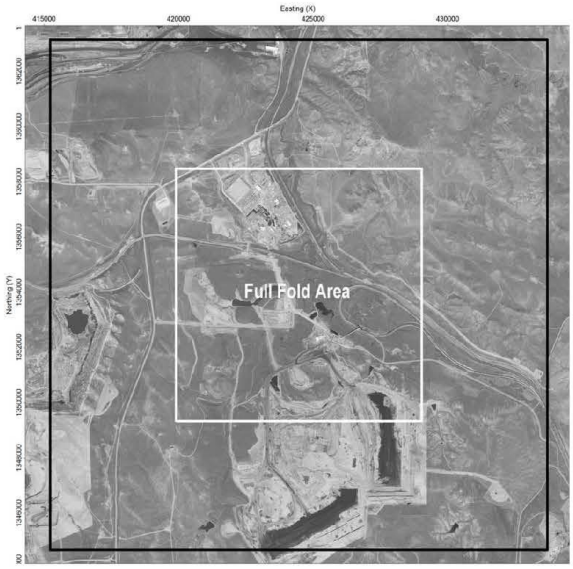

Total and Full Fold Areas

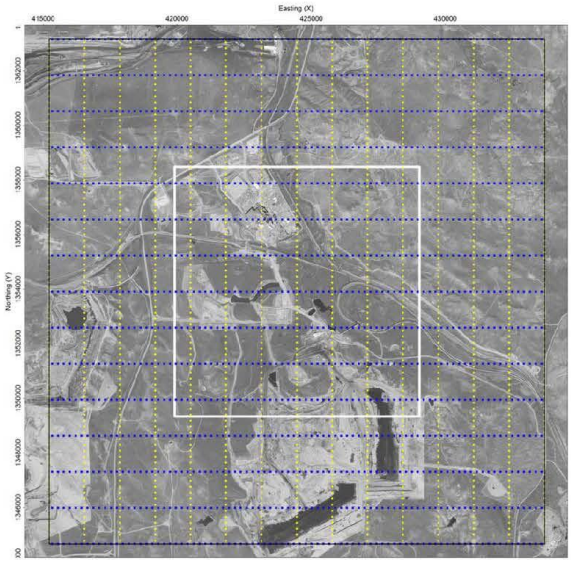

Sources and Detectors locations

Figure 4B-11 Map views of seismic survey Option 1 showing total and full fold areas (top) and source/receiver layout (bottom).

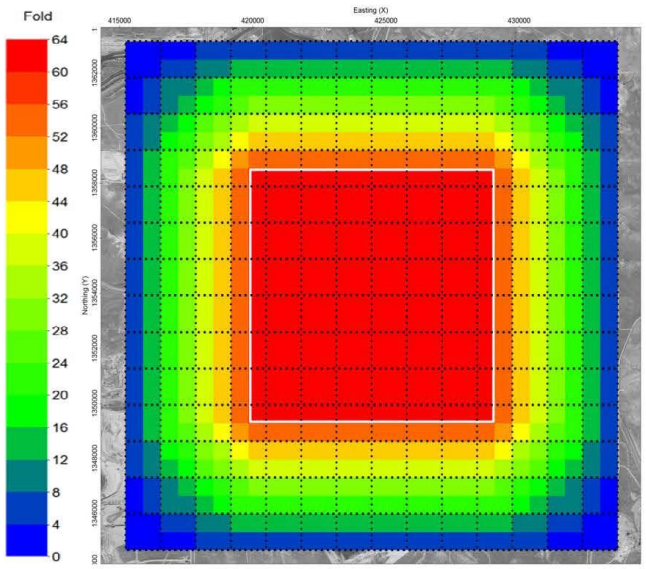

Fold: All Offsets

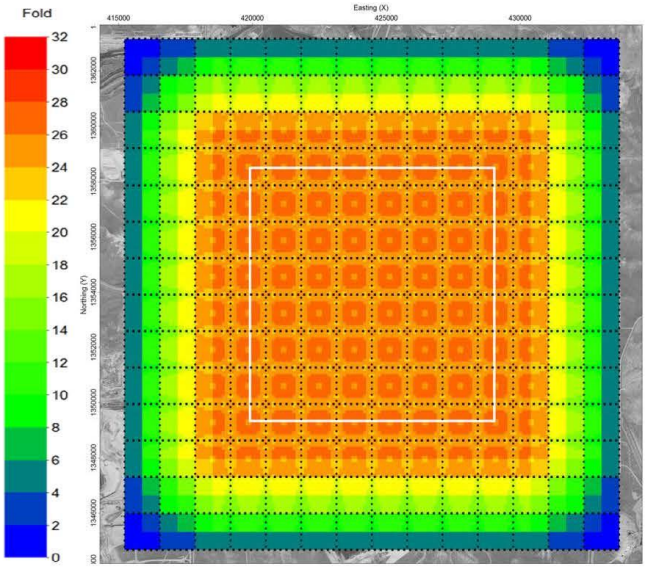

Fold: Offsets 0 – 7650 feet (~ Muddy)

Figure 4B-12 Map views of seismic survey Option 1 showing fold from all offsets (top) and fold coverage for offsets of 0–7650 ft. (approximately at Muddy Formation depth, bottom).

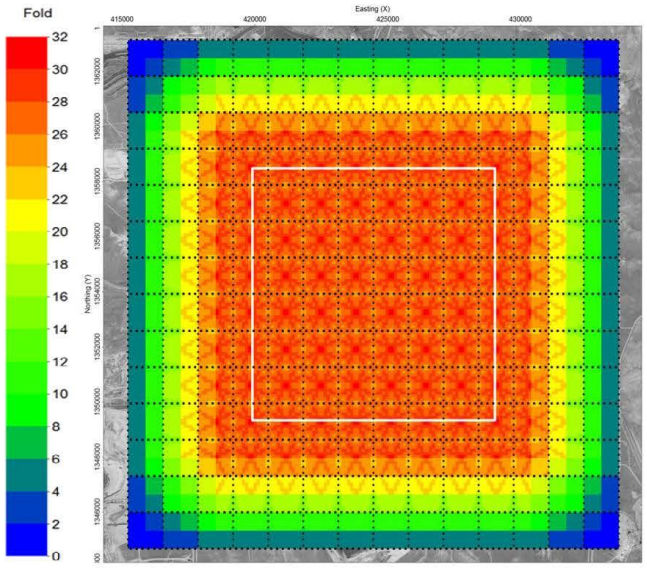

Fold: Offsets 0 – 7900 feet (~ Fall River (Dakota))

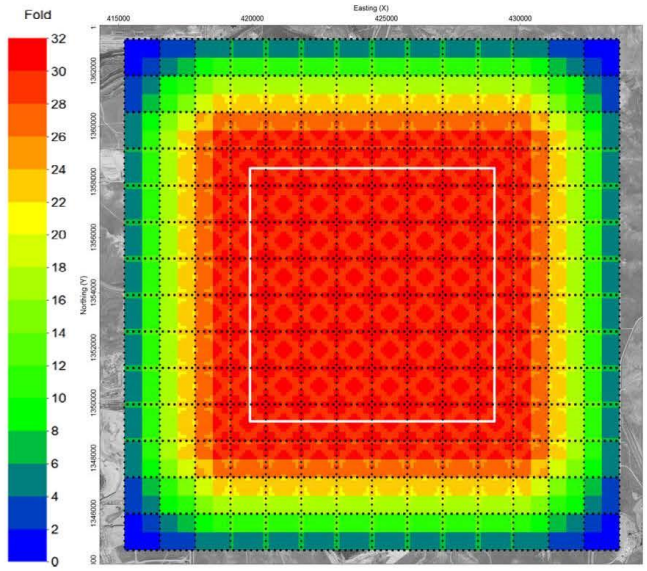

Fold: Offsets 0 – 8250 feet (~ Lakota)

Figure 4B-13 Map views of seismic survey Option 1 showing fold from offsets of 0–7900 ft. (approximately at Fall River Formation depth, top) and fold coverage for offsets of 0–8250 ft. (approximately at Lakota Formation depth, bottom).

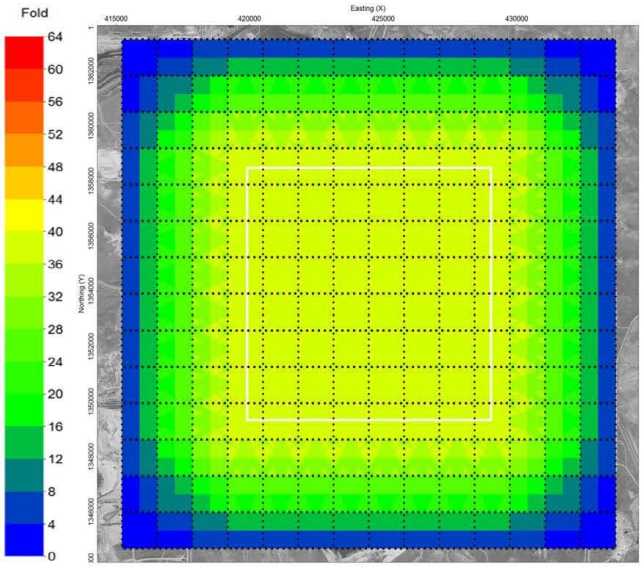

Fold: Offsets 0 – 9300 feet (~ Lower Sundance)

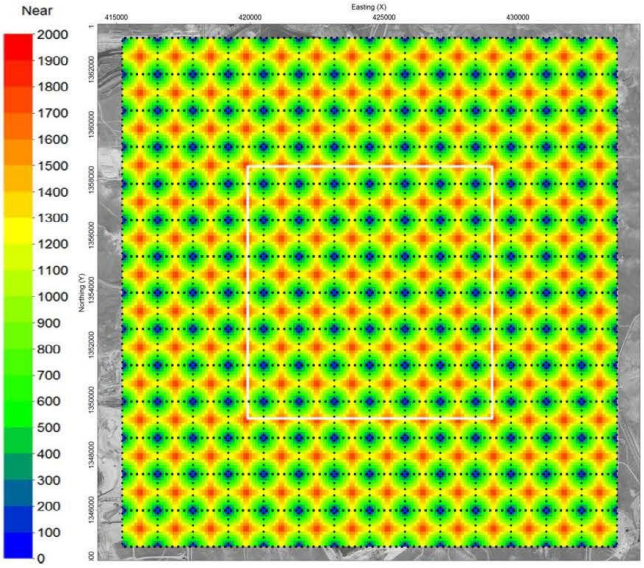

Minimum Offset

Figure 4B-14 Map views of seismic survey Option 1 showing fold from offsets of 0–9300 ft. (approximately at Lower Sundance Formation depth, top) and minimum offset (bottom).

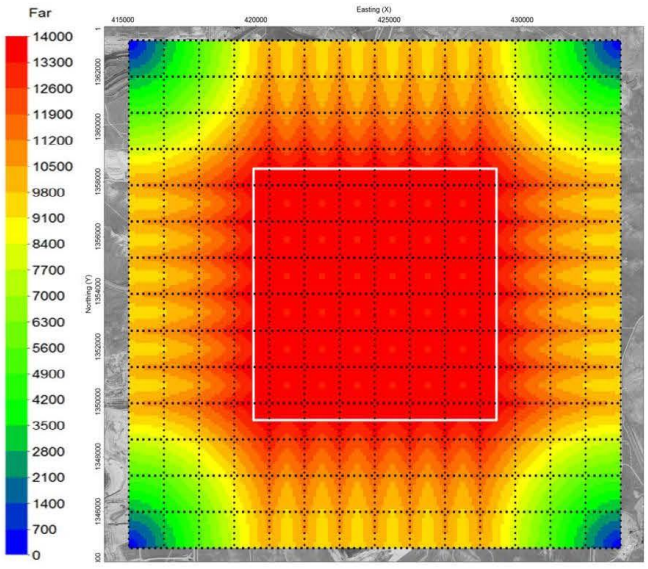

Maximum Offset

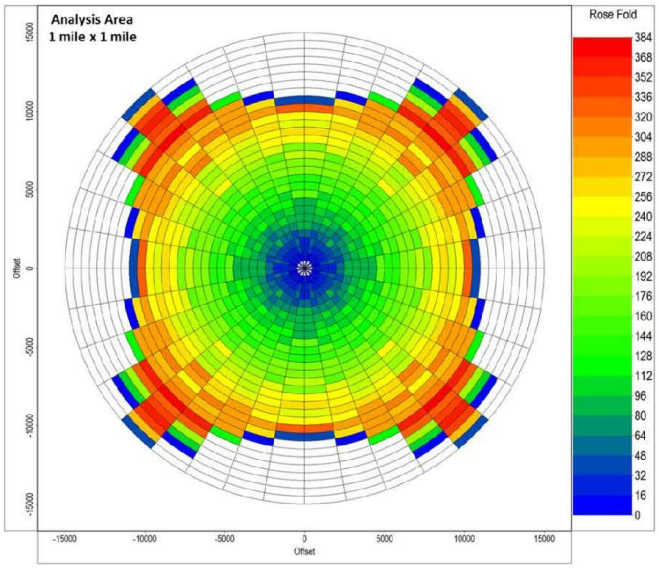

Offset/Azimuth Distribution

Figure 4B-15 Map views of seismic survey Option 1 showing maximum offset (top) and offset/azimuth distribution (bottom).

Cost estimates for Option 1 are included in Table 4B-2. These estimates include costs associated with permitting, surveying, and acquisition. Final numbers will rely on finalized project parameters and execution of mutually agreeable contract with the vendor.

Table 4B-2 Cost Estimates for Seismic Survey Option 1

Option 1 Cost Estimate		
Description	**Estimated Cost, $**	**Comments**
Recording	197,225	Acquisition crew
Vibroseis Trucking	21,200	Assuming × 4 vibrators from Denver and Return
Environmental Services	–	At cost if required
Cutting or Dozing	–	At cost if required
Survey	30,240	Two GPS crews, one field supervisor, two hazard surveyors, and 1 survey manager
Drilling or Explosives	–	At cost if required
Helicopter	–	At cost if required
Permit Agents	30,000	Assuming surface agent for 30 man-days and mineral agent for 10 man-days
Permit Fees	156,800	Assuming 100% private lands at $2000 per acre access fees
Project Management and Admin. Fees	65,320	Management of all project phases plus contractor admin. Fees
Water Well Test and PPV Monitoring	–	At cost if required
Total Estimated Project Cost	500,785	

Seismic Survey Option 2

Table 4B-3 Seismic Survey Option 2 Acquisition Parameters

Option 2	
Acquisition Parameters	
Acquisition Geometry	Orthogonal
Recording Patch	24 lines × 192 stations
Channels Live	4608 channels
Source Lines Heading	360°
Receiver Lines Heading	90°
Bin Size	110 ft. × 110 ft.
Sources	
Source Line Interval	880 ft.
Source Point Interval	110 ft.
Number of Lines	22
Energy Source Type	Vibroseis × 2 (two crews), AHV-IV buggies
Vibroseis Sweep Parameters	Nonlinear 2 – 100 Hz 12-second sweep Two sweeps per source point Five-second listen time
Receivers	
Recording System	Inova Hawk
Receiver Line Interval	880 ft.
Receiver Point Interval	110 ft.
Number of Lines	22
Source-to-Detector Offset Distances	
Minimum	77.782 ft.
Maximum	14,856.31 ft.
Maximum (inline)	10,505.01 ft.
Maximum (crossline)	10,505.004 ft.

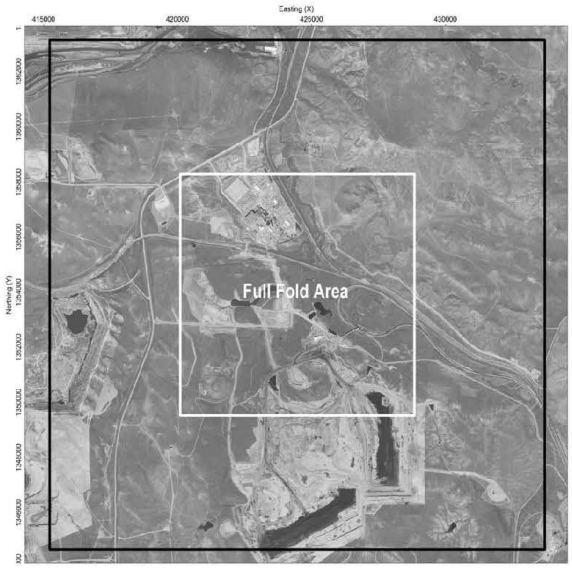

Total and Full Fold Areas

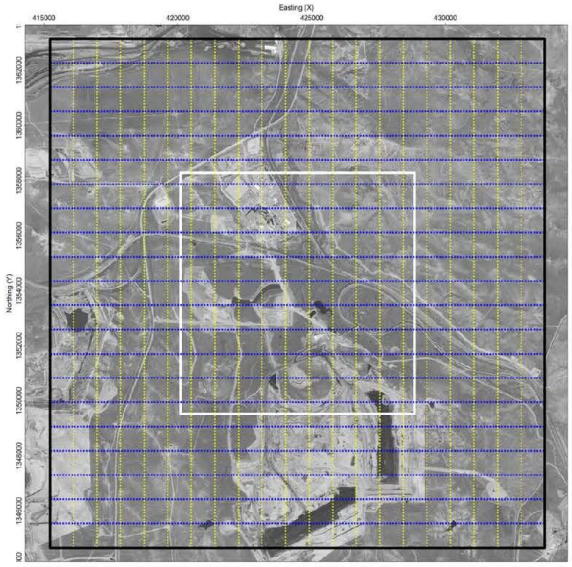

Sources and Detectors locations

Figure 4B-16 Map views of seismic survey Option 2 showing total and full fold areas (top) and source/receiver layout (bottom).

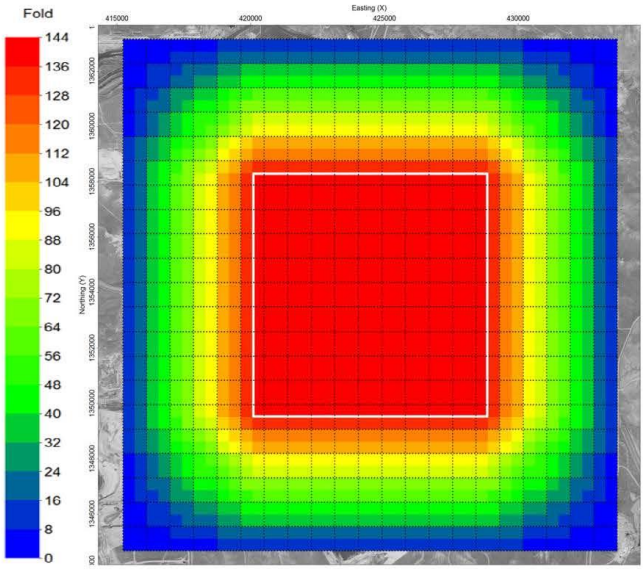

Fold: All Offsets

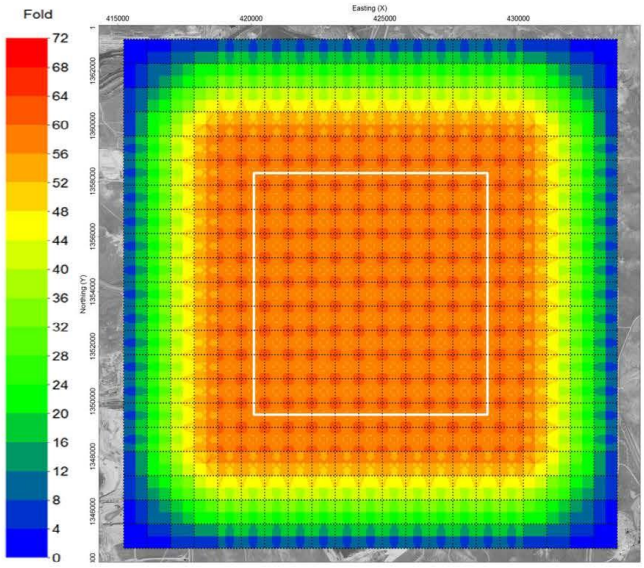

Fold: Offsets 0 – 7650 feet (~ Muddy)

Figure 4B-17 Map views of seismic survey Option 2 showing fold from all offsets (top) and fold coverage for offsets of 0–7650 ft. (approximately at Muddy Formation depth, bottom).

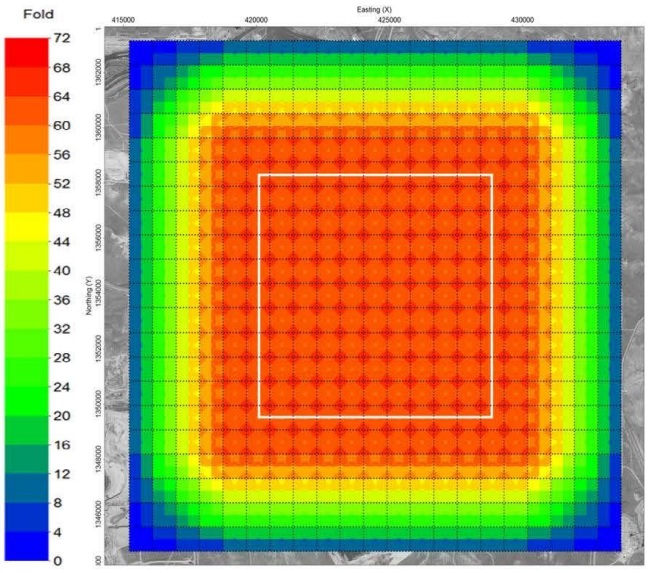

Fold: Offsets 0 – 7900 feet (~ Fall River (Dakota))

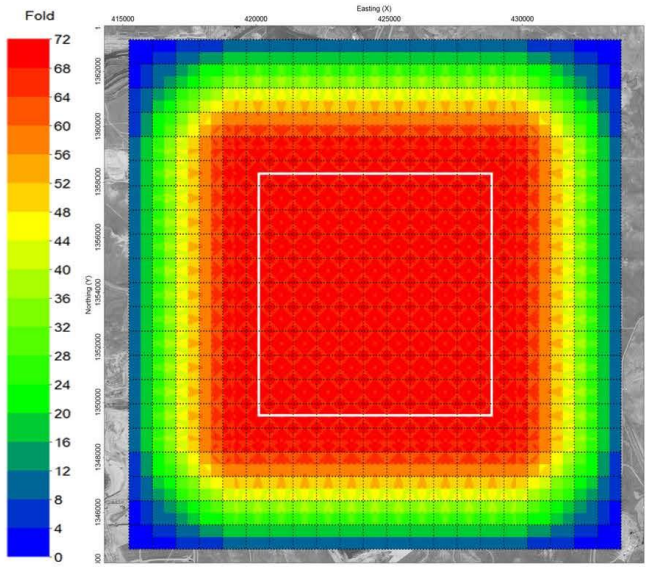

Fold: Offsets 0 – 8250 feet (~ Lakota)

Figure 4B-18 Map views of seismic survey Option 2 showing fold from offsets of 0–7900 ft. (approximately at Fall River Formation depth, top) and fold coverage for offsets of 0–8250 ft. (approximately at Lakota Formation depth, bottom).

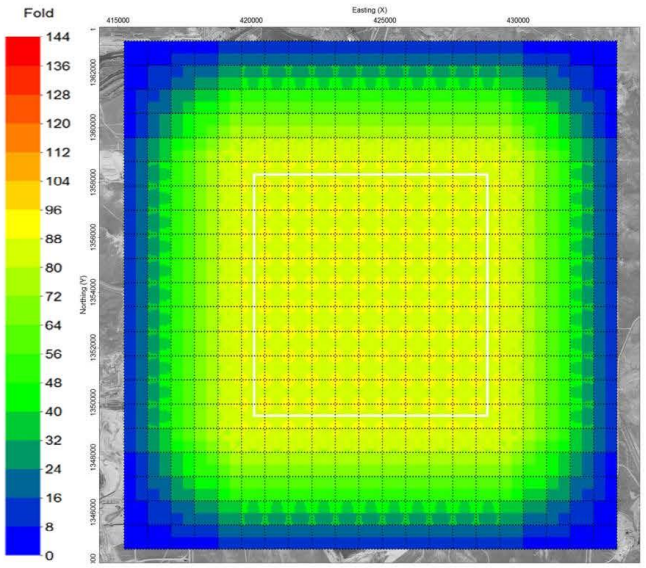

Fold: Offsets 0 – 9300 feet (~ Lower Sundance)

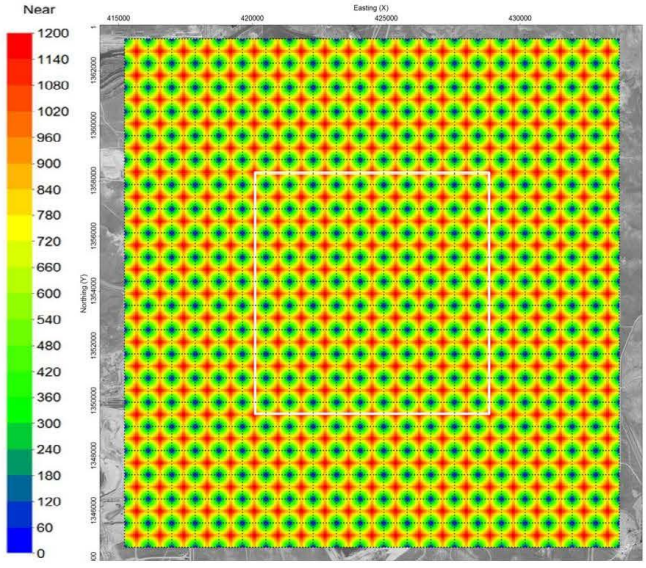

Minimum Offset

Figure 4B-19 Map views of seismic survey Option 1 showing fold from offsets of 0–9300 ft. (approximately at Lower Sundance Formation depth, top) and minimum offset (bottom).

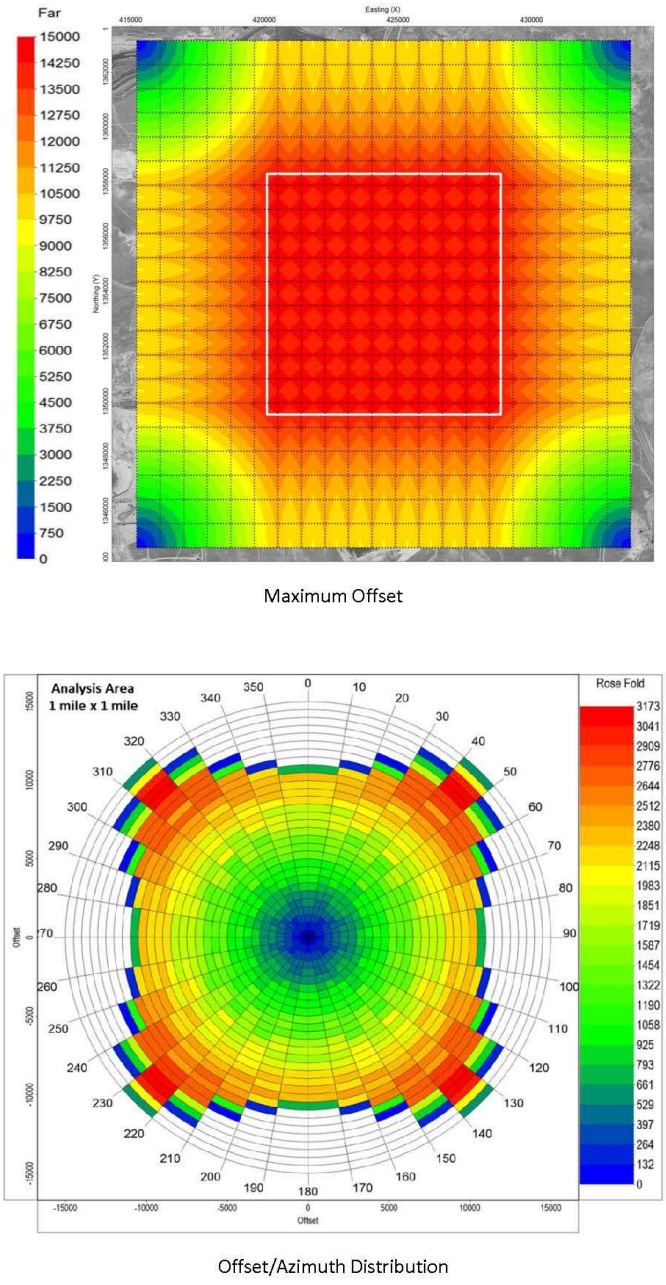

Figure 4B-20 Map views of seismic survey Option 1 showing maximum offset (top) and offset/azimuth distribution (bottom).

Cost estimates for Option 2 are included in Table 4B-4. These estimates include costs associated with permitting, surveying, and acquisition. Final numbers will rely on finalized project parameters and execution of mutually agreeable contract with the vendor.

Table 4B-4 Cost Estimates for Seismic Survey Option 2

Option 2 Cost Estimate		
Description	**Estimated Cost, $**	**Comments**
Recording	324,258	Acquisition crew
Vibroseis Trucking	21,200	Assuming × 4 vibrators from Denver and return
Environmental Services	–	At cost if required
Cutting or Dozing	–	At cost if required
Survey	73,920	Two GPS crews, one field supervisor, two hazard surveyors, and one survey manager
Drilling or Explosives	–	At cost if required
Helicopter	–	At cost if required
Permit Agents	30,000	Assuming surface agent for 30 man-days and mineral agent for 10 man-days
Permit Fees	156,800	Assuming 100% private lands at $2000 per acre access fees
Project Management and Admin. Fees	90,927	Management of all project phases plus contractor admin. Fees
Water Well Test and PPV Monitoring	–	At cost if required
Total Estimated Project Cost	697,105	

Seismic Survey Option 3

Table 4B-5 Seismic Survey Option 3 Acquisition Parameters

Option 3	
Acquisition Parameters	
Acquisition Geometry	Orthogonal
Recording Patch	32 lines × 504 stations
Channels Live	16,128 Channels
Source Lines Heading	360°
Receiver Lines Heading	90°
Bin Size	20 ft. × 40 ft.
Sources	
Source Line Interval	720 ft.
Source Point Interval	80 ft.
Number of Lines	26
Energy Source Type	Vibroseis × 2 (two crews), AHV-IV buggies
Vibroseis Sweep Parameters	Nonlinear 2 – 100 Hz 12-second sweep Two sweeps per source point Five-second listen time
Receivers	
Recording System	Inova Hawk
Receiver Line Interval	640 ft.
Receiver Point Interval	40 ft.
Number of Lines	29
Source-to-Detector Offset Distances	
Minimum	44.721 ft.
Maximum	14,326.325 ft.
Maximum (inline)	10,060.006 ft.
Maximum (crossline)	10,200.005 ft.

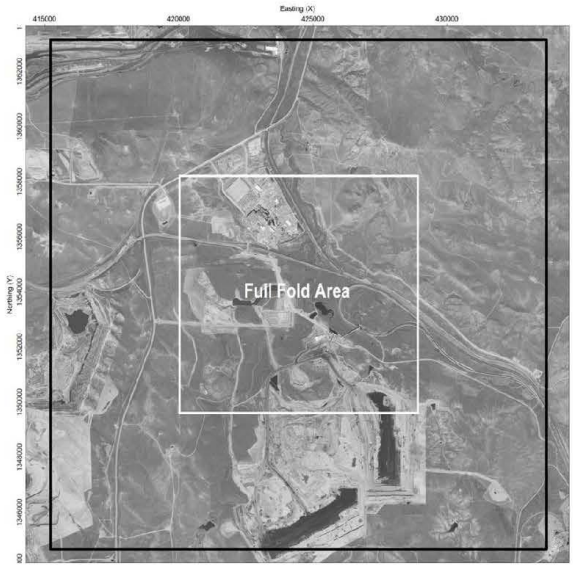

Total and Full Fold Areas

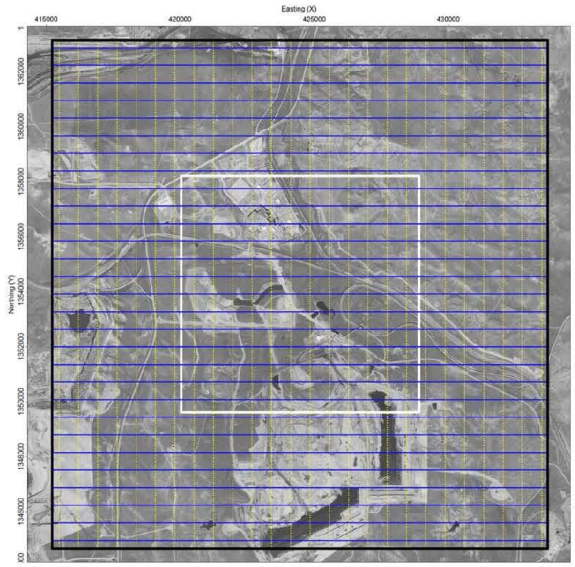

Sources and Detectors locations

Figure 4B-21 Map views of seismic survey Option 3 showing total and full fold areas (top) and source/receiver layout (bottom).

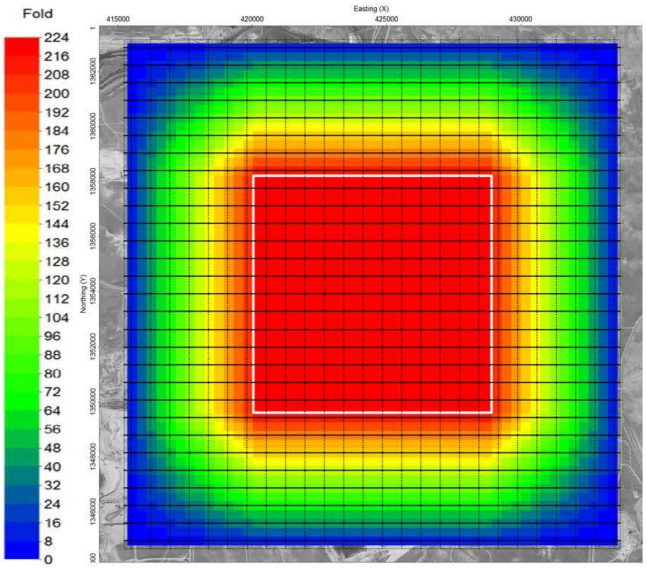

Fold: All Offsets

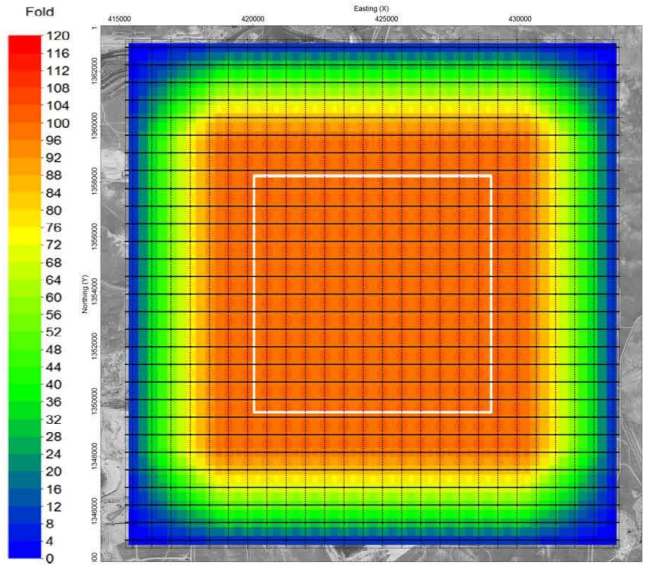

Fold: Offsets 0 – 7650 feet (~ Muddy)

Figure 4B-22 Map views of seismic survey Option 3 showing fold from all offsets (top) and fold coverage for offsets of 0–7650 ft. (approximately at Muddy Formation depth, bottom).

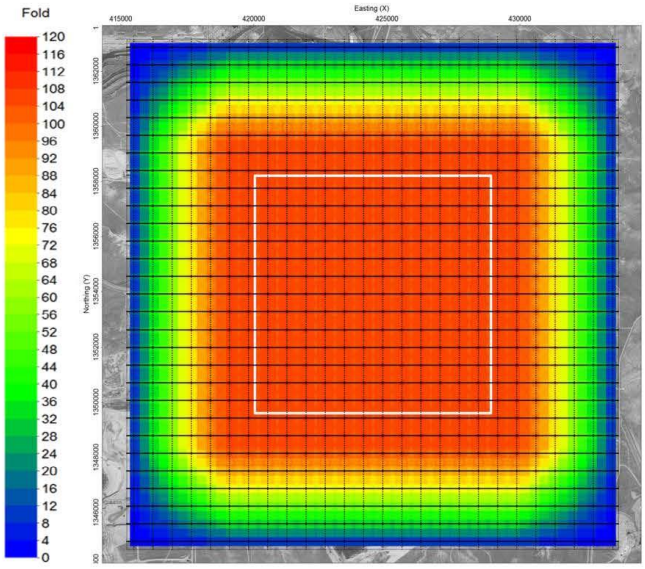

Fold: Offsets 0 – 7900 feet (~ Fall River (Dakota))

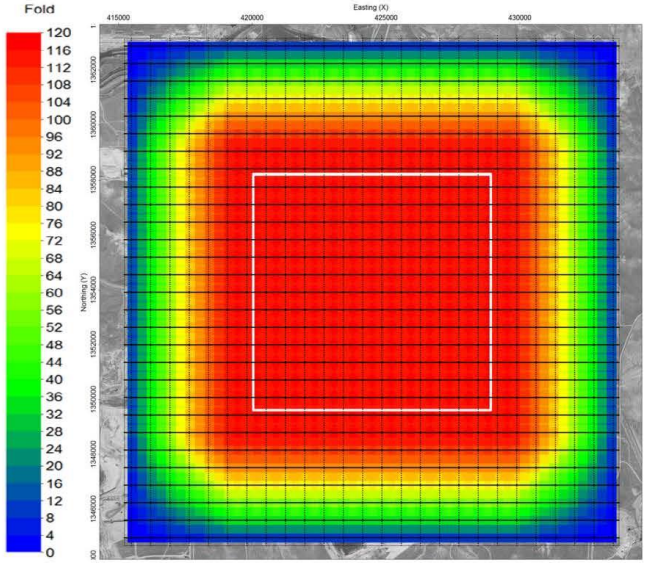

Fold: Offsets 0 – 8250 feet (~ Lakota)

Figure 4B-23 Map views of seismic survey Option 3 showing fold from offsets of 0–7900 ft. (approximately at Fall River Formation depth, top) and fold coverage for offsets of 0–8250 ft. (approximately at Lakota Formation depth, bottom).

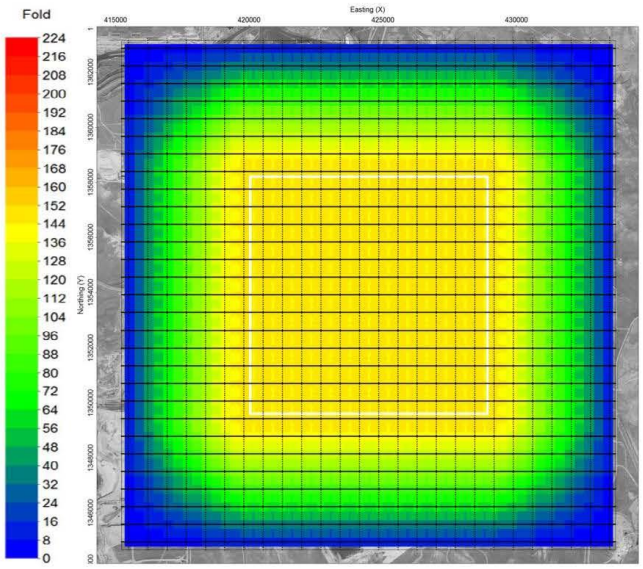

Fold: Offsets 0 – 9300 feet (~ Lower Sundance)

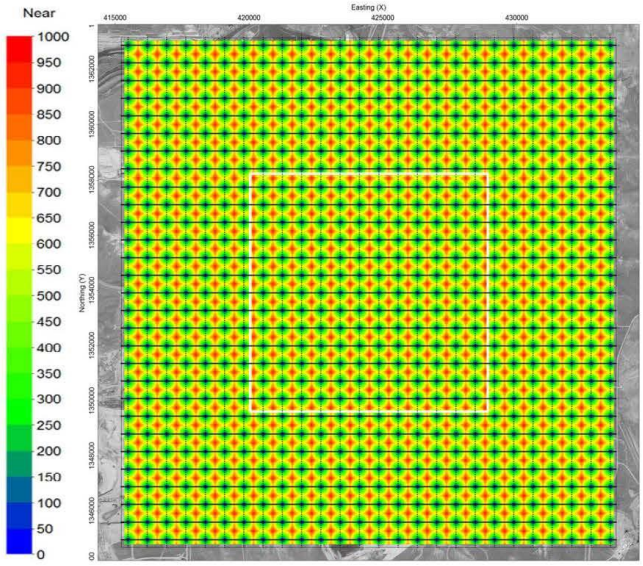

Minimum Offset

Figure 4B-24 Map views of seismic survey Option 1 showing fold from offsets of 0–9300 ft. (approximately at Lower Sundance Formation depth, top) and minimum offset (bottom).

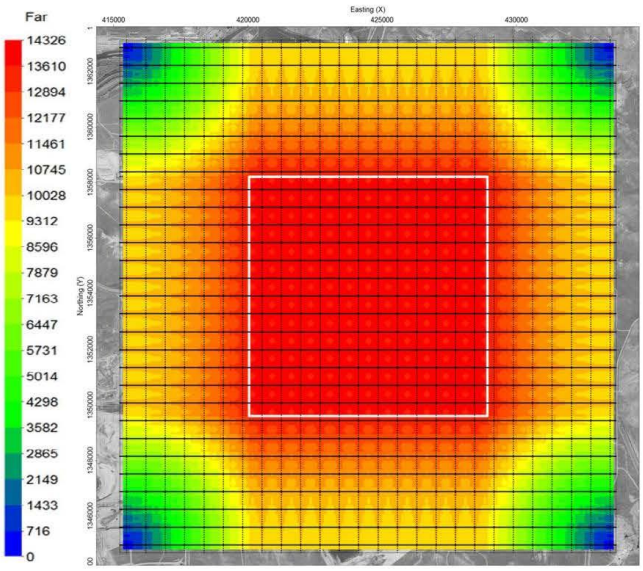

Maximum Offset

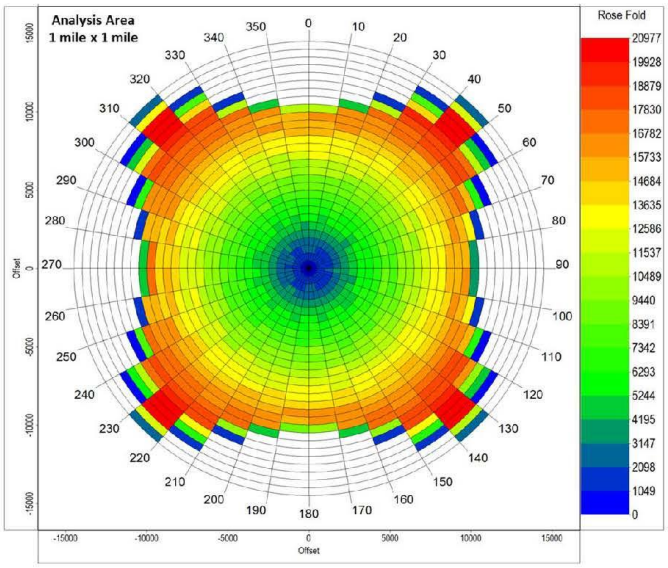

Offset/Azimuth Distribution

Figure 4B-25 Map views of seismic survey Option 1 showing maximum offset (top) and offset/azimuth distribution (bottom).

Cost estimates for Option 1 are included in Table 4B-6. These estimates include costs associated with permitting, surveying, and acquisition. Final numbers will rely on finalized project parameters and execution of a mutually agreeable contract with the vendor.

Table 4B-6 Cost Estimates for Seismic Survey Option 3

Option 3 Cost Estimate		
Description	**Estimated Cost, $**	**Comments**
Recording	720,545	Acquisition crew
Vibroseis Trucking	26,500	Assuming × 4 vibrators from Denver and return
Environmental Services	–	At cost if required
Cutting or Dozing	–	At cost if required
Survey	155,680	Two GPS crews, one field supervisor, two hazard surveyors, and one survey manager
Drilling or Explosives	–	At cost if required
Helicopter	–	At cost if required
Permit Agents	30,000	Assuming surface agent for 30 man-days and mineral agent for 10 man-days
Permit Fees	156,800	Assuming 100% private lands at $2000 per acre access fees
Project Management and Admin. Fees	163,429	Management of all project phases plus contractor admin. Fees
Water Well Test and PPV Monitoring	–	At Cost if Required
Total Estimated Project Cost	1,252,954	

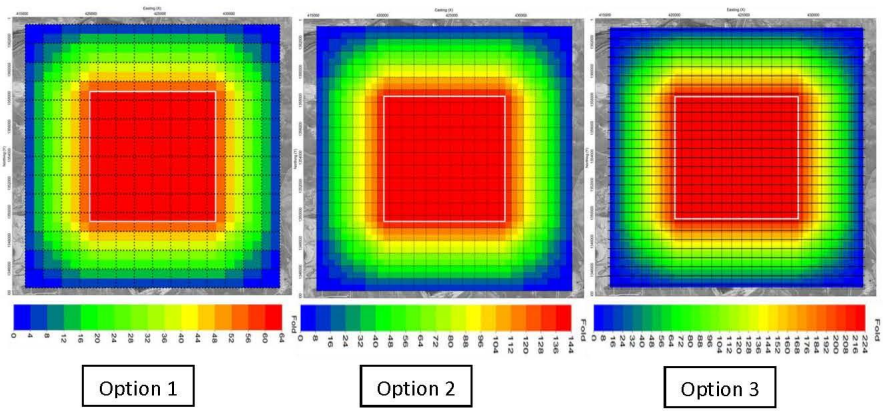

Figure 4B-26 Comparison of data resolution and fold density for each of the three seismic survey options.

Chapter IV Appendix B Summary

- Option 1 has the lowest fold of coverage in general and at target reservoirs; Option 3 has the highest fold of coverage.

- Data collected using Option 3 geometry can, potentially, have lower noise levels because of the higher fold. Additionally, the small source point and receiver interval in Option 3 allows the recording of unaliased noise that can be modeled and subtracted safely during processing without compromising data quality.

- Field-testing of sweep frequency band and length and number of sweeps and listen time is recommended.

- Some source and receiver locations might change because of obstacles or infrastructure not accounted for during the survey design. If that is the case, infield geometry quality control is recommended to verify that adequate fold of coverage is maintained.

Chapter V: NRAP Modeling and Validation

George J. Koperna and Anne Oudinot

Advanced Resources International, Inc.
4501 Fairfax Drive, Suite 910
Arlington, VA 22203

Section 5.1 Executive Summary

The United States Department of Energy, National Energy Technology Laboratory (USDOE-NETL) is sponsoring research as part of the Carbon Storage Assurance Facility Enterprise (CarbonSAFE) initiative. This program seeks to mitigate carbon emissions from the burning of fossil fuels and addresses key research gaps in the deployment of large-scale (50+ million metric tons) carbon capture and storage (CCS).

USDOE-NETL requested that awarded projects evaluate a suite of sponsored reduced order modeling tools designed to help stakeholders evaluate and then mitigate potential risks associated with subsurface injection of carbon dioxide (CO_2). Developed by the National Risk Assessment Partnership (NRAP), these tools assess environmental risks associated with leakage and induced seismicity for reservoirs, confining units, wells, and aquifers. This report outlines their use in relation to the CarbonSAFE Phase I project at the University of Wyoming, Center for Economic Geology Research's, Dry Fork Station (DFS) Test Site.

To support this request, this report describes in detail the ten available NRAP reduced-order models, their use, required inputs, and the available outputs. Out of the ten tools, one of the ROMs was further studied in application to the Dry Fork Station CarbonSAFE project.

With numerical models being generated to assess CO_2 storage capacity in the Minnelusa formation as part of the Dry Fork Station CarbonSAFE Project, the Reservoir Evaluation and Visualization (REV) tool was analyzed with available GEM datasets. The initial phase of the evaluation, which consisted in getting the tool to run, was made difficult by compatibility issues and the existence of various versions of the tool. Once that issue was resolved, the tool functioned properly. However, the results obtained didn't fully compare with simulator results. While the visual display represents roughly the extent of the plumes, there is a distortion issue, which requires some support from the NETL NRAP personnel. In addition, computation of the plume areas is erroneous.

Section 5.1 Introduction

Review of NRAP Tools

The United States Department of Energy, National Energy Technology Laboratory (USDOE-NETL) is sponsoring research as part of the Carbon Storage Assurance Facility Enterprise (CarbonSAFE) initiative. This program seeks to mitigate carbon emissions from the burning of fossil fuels and addresses key research gaps in the deployment of large-scale (50+ million metric tons) carbon capture and storage (CCS).

Initial awards were made in two phases of the initiative: I) integrated CCS pre-feasibility and II) storage complex feasibility. Phase I awards focused on assembling a team capable of building a techno-economic CCS development plan, based on a high-level characterization of the basin with

available geologic information. Phase II built on Phase I by collecting new subsurface geologic data in the field to improve the subsurface evaluations, risk assessments, and flow modeling. The additional data have been used to demonstrate that the storage complex was adequate to meet programmatic needs (50+ million metric tonnes). This information also informs Phase II baseline monitoring and outreach plan development.

Within each Phase, USDOE-NETL requested that awarded projects evaluate a suite of sponsored reduced order modeling tools designed to help stakeholders evaluate and then mitigate potential risks associated with subsurface injection of carbon dioxide (CO_2). Developed by the National Risk Assessment Partnership (NRAP), these tools assess environmental risks associated with leakage and induced seismicity for reservoirs, confining units, wells, and aquifers. This report outlines their use in relation to the CarbonSAFE Phase I project at the University of Wyoming, Center for Economic Geology Research's, Dry Fork Station (DFS) Test Site.

Site Background

The DFS Test Site is located within the Powder River Basin, just north of Gillette, Wyoming (**Figure 5.2.1**). The site is strategically located near a large diameter CO_2 transmission pipeline as well as Basin Electric Power Cooperative's coal-fired Dry Fork Power Station, which emits 3.3 million tons of CO_2 per annum.

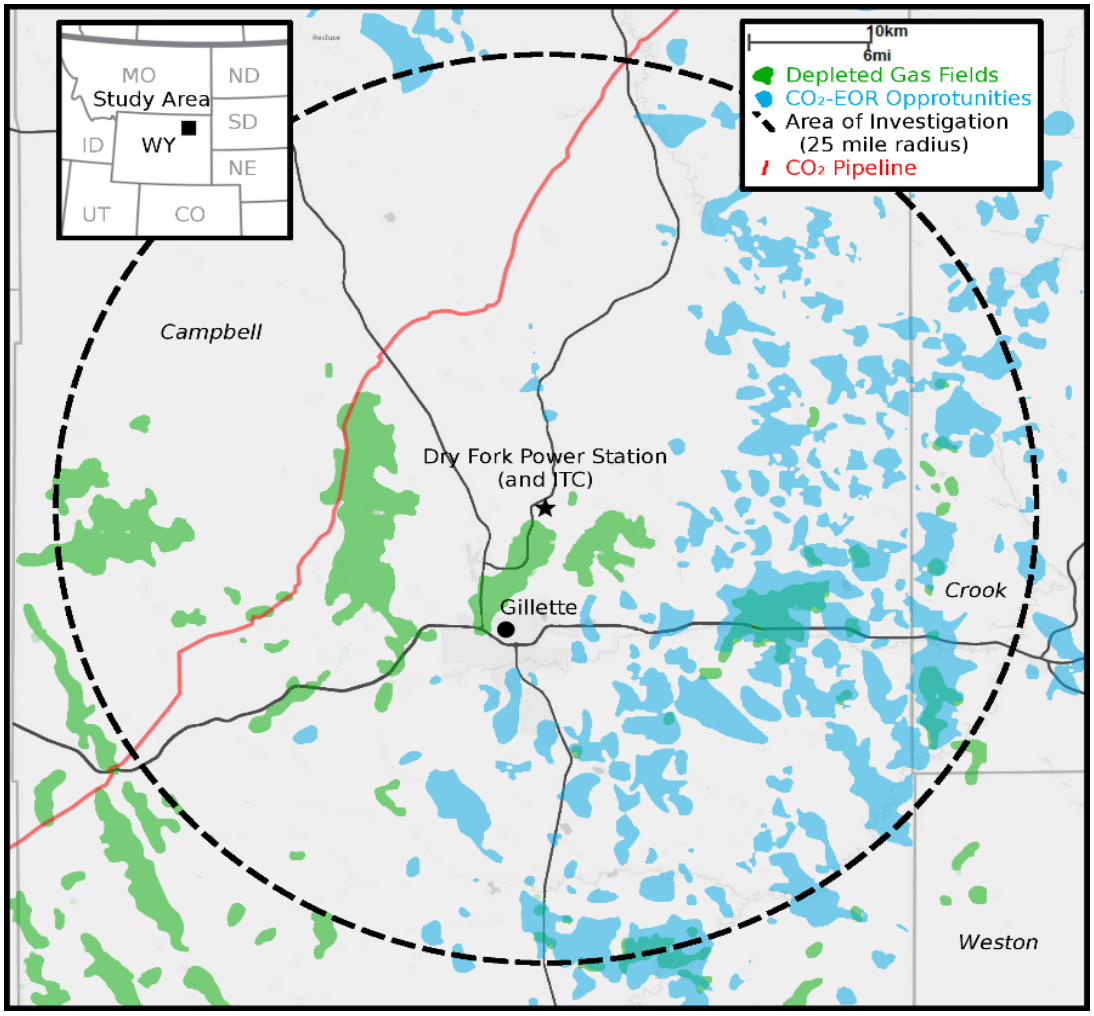

Figure 5.2.1 Dry Fork Station Study Area

The major goal of this current study is to identify and characterize high quality potential reservoirs suitable for storage of 50 + million metric tons of anthropogenic carbon dioxide (CO_2) and the sealing formations that would trap it in place. Four major saline formations have been identified as potential storage complexes in Phase I of this project, and these are the Pennsylvanian Minnnelusa formation, the Jurassic Sundance formation, the Cretaceous Lakota and Fall River formations, and the Muddy formation. Should any of these formations be suitable for storage, the Dry Fork Station plant, along with the plant's proximal CO_2 transmission infrastructure, could make this a storage hub for the Rocky Mountain Region.

Section 5.1 NRAP Tools

There are ten NRAP tools (listed below) available for use and evaluation of this project. The following sections discuss the tools, their input parameters, and their expected output. One of the tools was selected to test datasets collected from the ongoing work of the CarbonSAFE Phase I project at the DFS test site: the Reservoir Evaluation and Visualization Tool (REV).

NRAP Tools:

- Aquifer Influence Model (AIM)
- Designs for Risk Evaluation and Management (DREAM) Tool
- Ground Motion Prediction Applications to Potential Induced Seismicity (GMPIS)
- Multiple Source Leakage Reduced-Order Model (MSLR)
- NRAP Integrated Assessment Model–Carbon Storage (NRAP-IAM-CS)
- NRAP Seal Barrier Reduced Order Model (NSEALR)
- Reservoir Evaluation and Visualization Tool (REV)*
- Reservoir Reduced-Order Model Generator RROM- Gen
- Short-Term Seismic Forecasting (STSF)
- Well Leakage Analysis Tool (WLAT)

** Tools that were selected to be tested using datasets from the DFS test site.*

The following discussions highlight use of the NRAP tool employed in this study. Similar descriptions of the remaining nine tools can be found in Appendix 1.

Reservoir Evaluation and Visualization Tool (REV)

Introduction. The REV tool is a numerical modeling post-processing visualization tool that uses time-lapse CO_2 saturation and pressure outputs from various specific reservoir simulators to generate CO_2 saturation maps and pressure differential (as compared to initial reservoir pressure) maps based on a user- specified threshold. A threshold is being defined as a minimum value for the parameter evaluated. If a grid cell in the model has a value at or above the user-specified threshold, this cell is considered to be inside the plume.

Input. REV accepts inputs, from eight different simulators listed below. While each simulator is different, REV requires from each two types of information: a grid file (contains description of the model grid) and a dynamic file (contains time-lapse CO_2 saturation and pressure information). Sample files are provided for some of the simulators and their format is also described in the manual.

- Two-Phase Three Dimensional (TP3D),
- Finite Element Heat and Mass (FEHM),
- Computer Modeling Group-Generalized Equation of State Model (CMG-GEM),
- NRAP-Integrated Assessment Model-Carbon Storage (NRAP-IAM-CS),
- Transport of Unsaturated Groundwater and Heat 2 (TOUGH2),
- Subsurface Transport Over Multiple Phases (STOMP),
- Exploration Consultants Limited Implicit Program for Simulation Engineers (ECLIPSE) and
- PETREL (ECLIPSE's pre and post-processor).

Figure 5.3.1 shows the REV input/output tab with a drop-down menu to select the simulator (CMG-GEM chosen here as an example). Zipped files can also be loaded into the model and REV will unzip them automatically.

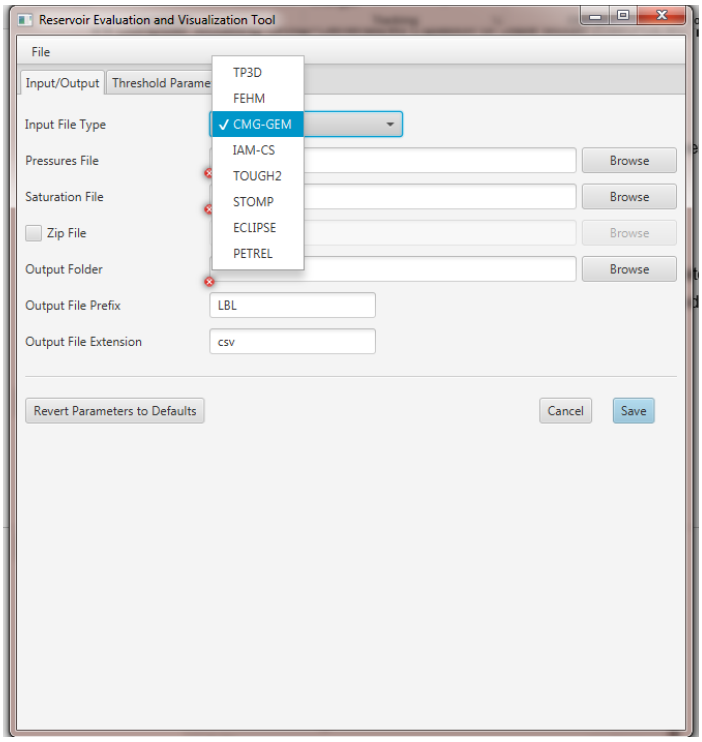

Figure 5.3.1 REV Input/ Output Tab

There are three types of threshold that can be defined by the user.

- critical CO_2 saturation to detect areas of free phase CO_2 in the formation,
- differential pressure to detect areas of elevated pressure, and
- saturation-pressure product.

Multiple thresholds can be specified at the same time, **Figure 5.3.2.**

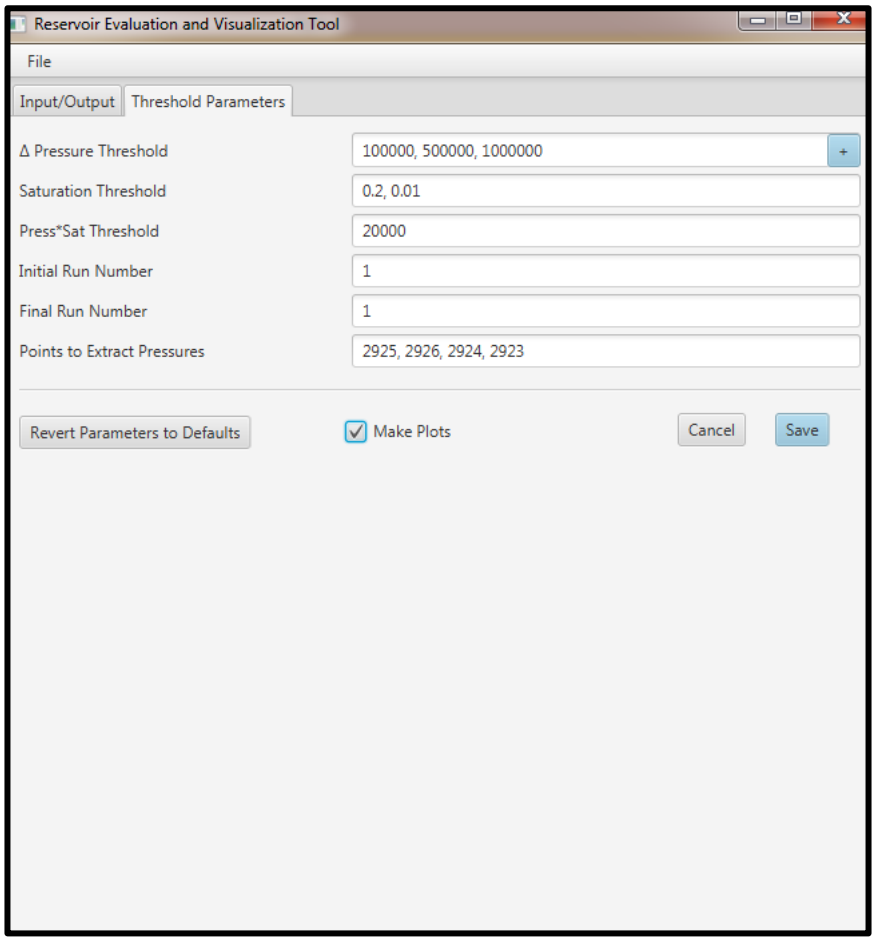

Figure 5.3.2 REV Threshold Parameters Tab

Output

REV outputs come in two different formats:

- Graphical display of differential pressure and saturation maps versus time. These files will have a png (portable network graphics) extension, **Figure 5.3.3**. **Figure 5.3.3** shows the evolution of the differential pressure plume (or area of increased pressure of 0.5MPa or more than initial pressure) at various times over the life of the injection project. Any grid block in the plume will be colored in red whereas any grid block outside the plume will be colored in blue.
- Quantitatively, for each threshold input (differential pressure, saturation, and pressure saturation product), a csv (comma separated value) file will be generated with the computed maximum plume area at each time step.

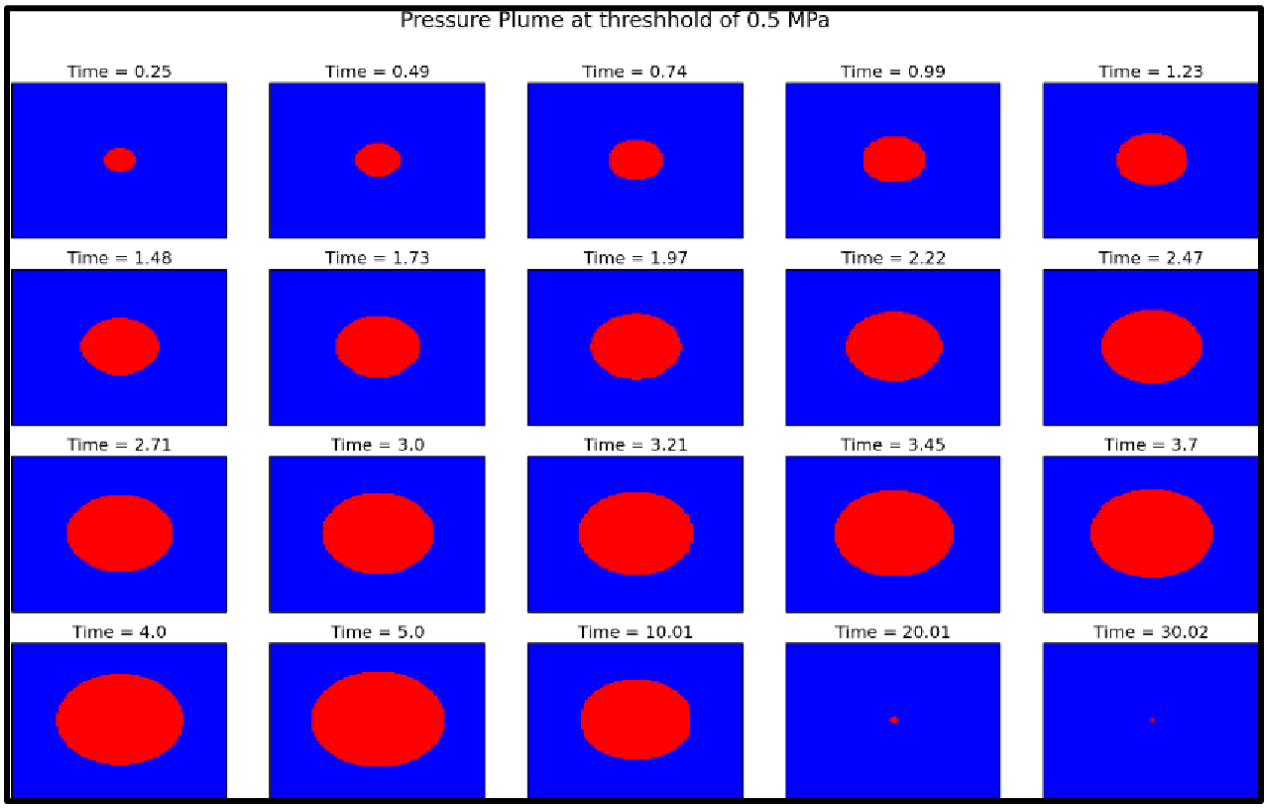

Figure 5.3.3 Example of Visualization from Sample File– Pressure Plumes

NRAP Tools Computer Requirements

Table 5.3.1 summarizes the list of the reviewed reduced order models with their corresponding computer requirements for use. This also highlights the drawbacks that might be encountered when a model requires other supporting software to be downloaded (GoldSim is required for NRAP-IAM-CS and NSealR for example) or an operating system not always available to the user (STSF is only available on Linux or Mac only for example).

Table 5.3.1 ROMs Computer Requirements

	OS	Requirements
AIM	Windows 64-bit	Java Version 8 or newer
	Linux and OSX	Oracle JRE version 8u41 and the R scripting language
DREAM	Windows 64-bit	Java Version 8 or newer
	Mac	
GMPIS	Windows 64-bit	Java Version 8 update 46 or newer
MSLR	Windows 64-bit	Java Version 8 update 50 or newer
NRAP-IAM-CS	Windows 2003/ XP/ Vista / 7	GoldSim 11.1.02 is required
NSealR	Windows 2003/ XP/ Vista / 7	GoldSim 11.1.02 is required
REV	Windows 64-bit	Java Version 8 update 40 or newer
RROM-Gen	Windows 64-bit	Java Version 8 update 40 or newer
STSF	Mac or Linux	Java Version 8 update 40 or newer
WLAT	Windows	Java Version 8 or newer

Section 5.2 ROM Evaluation

REV Evaluation

At the time the NRAP tools were to be evaluated with project data, numerical models were being generated to assess CO_2 storage capacity. With pressure and saturation maps over time being an output of this assessment, evaluation of the REV (Reservoir Evaluation and Visualization, section 2.1 of this report) tool was a logical extension for the project team.

For this storage capacity assessment, Computer Modeling Group's compositional reservoir simulator GEM was used to model the CO_2 injection process into the Pennsylvanian Minnelusa sandstone formation. The case chosen for this evaluation looked at injecting CO_2 over a period of 25 years into the Minnelusa formation through four injectors without brine extraction. Average petrophysical characteristics (50^{th} percentile) from the available data (permeability, porosity, thickness) were used to build this model, which resulted in 31 million metric tonnes of stored CO_2 over the 25-year injection period. A 3D view of the model is shown on **Figure 5.4.1**.

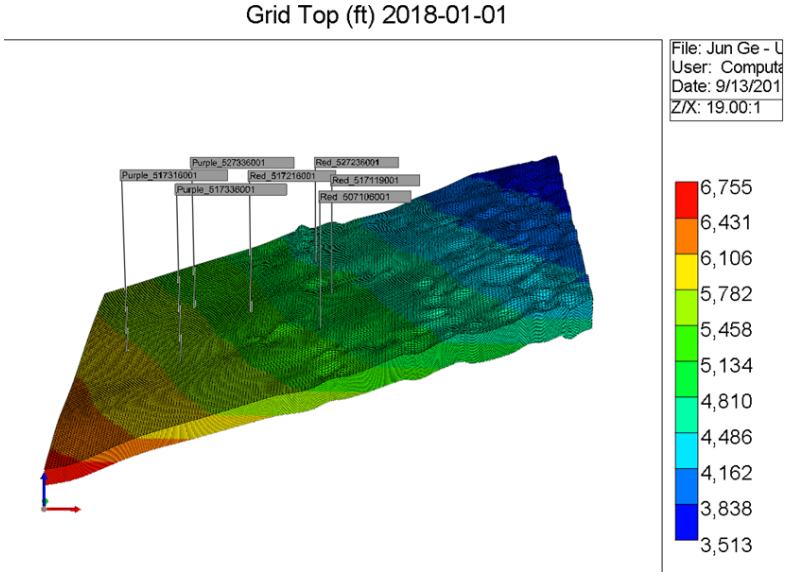

Figure 5.4.1 GEM Minnelusa Model 3D View

The version of the REV tool to be tested is supposed to be the publicly available version 2016-11-1-2, which can be downloaded from the NETL EDX website. The tool was tested first with the GEM sample files provided and worked properly. **Figure 5.4.2** from the example files shows what a differential pressure plume over time looks like.

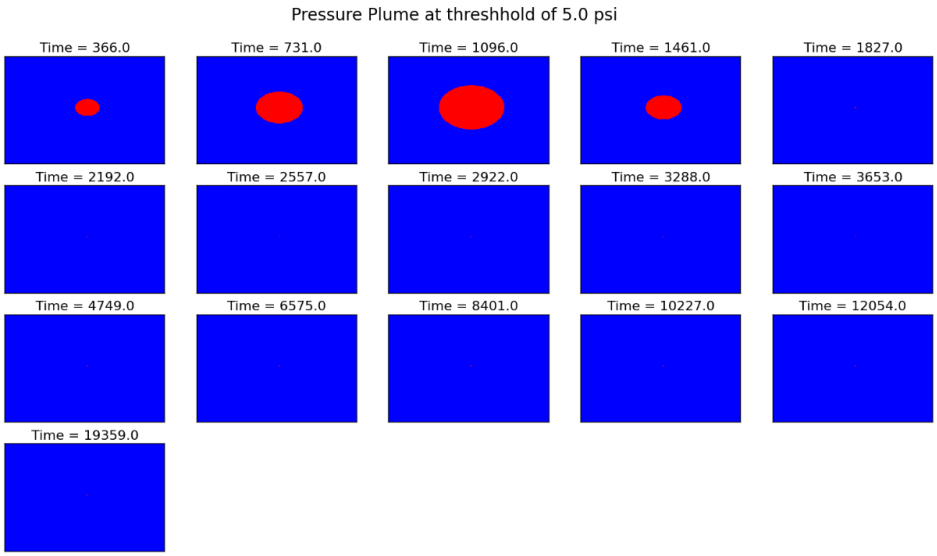

Figure 5.4.2 Example of Visualization from Sample File– Differential Pressure Plumes

As described in section 2.1 of this report, and as the example in the REV manual shows, REV uses as inputs time-lapse reservoir pressure and saturation data from the simulation work and provides as outputs differential pressure and CO_2 saturation plumes based on a threshold (minimum value) defined by the user. If a grid cell has a value above the defined threshold, this cell will be considered part of the plume.

The first step of the process consists in generating the required input files to be loaded into REV. For GEM, two types of files, simply pressure and saturation over time, are required and easily generated from Results 3D, GEM's post processor. The pressure file contains the coordinates of each grid block in the model and its corresponding pressure while the saturation file contains the coordinates of each grid block and its corresponding CO_2 saturation. Following the first step of testing the example files, after the project's GEM output files were loaded, an error message stating a file format issue made the model impossible to run (**Figure 5.4.3**).

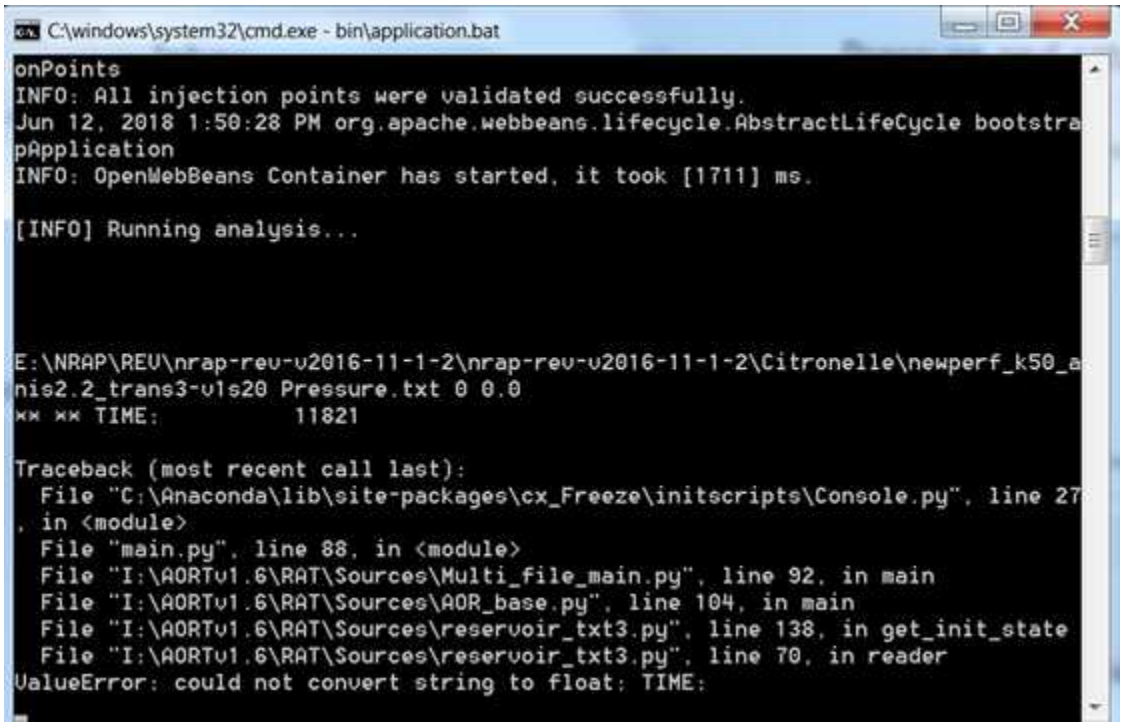

Figure 5.4.3 REV Error Message

CMG was contacted, and it was confirmed that the pressure and saturation files generated had the proper format. However, it is worth noting that the CMG pressure and saturation outputs need to be generated by any Results (post-processor) version prior to 2017 for proper format as confirmed by the technical support of CMG. The publicly available version of the tool has not been updated to take into account the new file format generated by the 2017 GEM release. After a considerable amount of time spent researching the issue, the existence of a newer 2017 REV version (version 2017-03-1-2-1) provided by EERC, but not publicly available on the EDX website, solved the problem. In the meantime, NETL had been working on a patch and sent another working version. Consequently, all the testing described below uses version 2017-03-1-2-1 of the tool.

The second step in the process consists in defining the differential pressure and CO_2 saturation thresholds (lower limit). For this exercise, an initial differential pressure minimum value of 100 psi (over initial pressure) and a CO_2 saturation minimum of 0.02 (or 2% gas saturation) were chosen, **Figure 5.4.4**. As stipulated in the manual, the tool doesn't deal with units. Because the simulation units are in pound per square-inch (psi) and feet, thresholds have to be defined in the same units. As mentioned above, any grid cell with an increase in pressure of 100 psi or more over initial pressure will be considered as being inside the pressure influenced area, and any grid cell with a gas saturation higher than 0.02 will be considered inside the CO_2 plume.

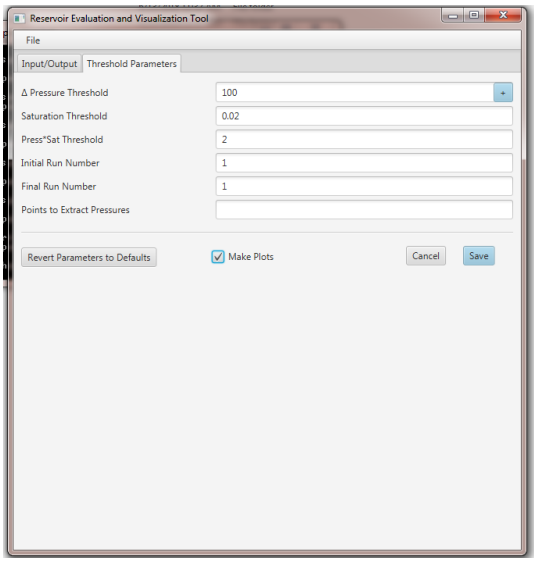

Figure 5.4.4 REV Threshold Tab

Once the analysis is running, the DOS windows on **Figure 5.4.5** appears and remains the same. This DOS window does not show the status of the process and remains idle until the conclusion of the visualization effort. The GEM pressure and saturation maps were output on a yearly basis over the 25-year injection period, and the tool was able to render results within a 10-hour timeframe.

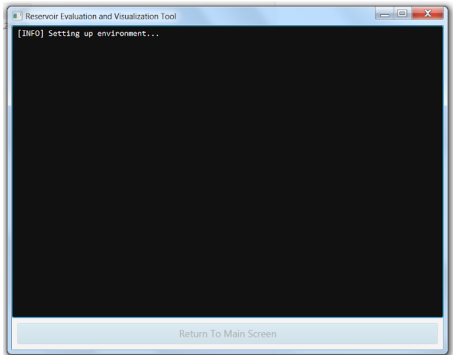

Figure 5.4.5 REV DOS Windows

Figure 5.4.6 shows the gas saturation map after 25 years of injection from GEM where the location of the four injection wells is easily detected while **Figure 5.4.7** shows the corresponding gas saturation maps from REV at various time steps on a yearly basis with a defined minimum CO_2 saturation value of 0.02. The saturation map at the end of the 25-year injection period will be the last image of the REV series of maps (highlighted in red on **Figure 5.4.7**). The saturation plumes displayed by the REV tool show three main areas of increased CO_2 saturation (in red), which are representative of the location of the four injection wells if we consider that the two central plumes got lumped together, but the shapes of the plumes are not representative of the GEM results. While the GEM plumes are quite round, the REV plumes are very elongated or distorted. The NRAP support at NETL was contacted regarding this graphical display issue, but this issue had not been resolved prior to the preparation of this report.

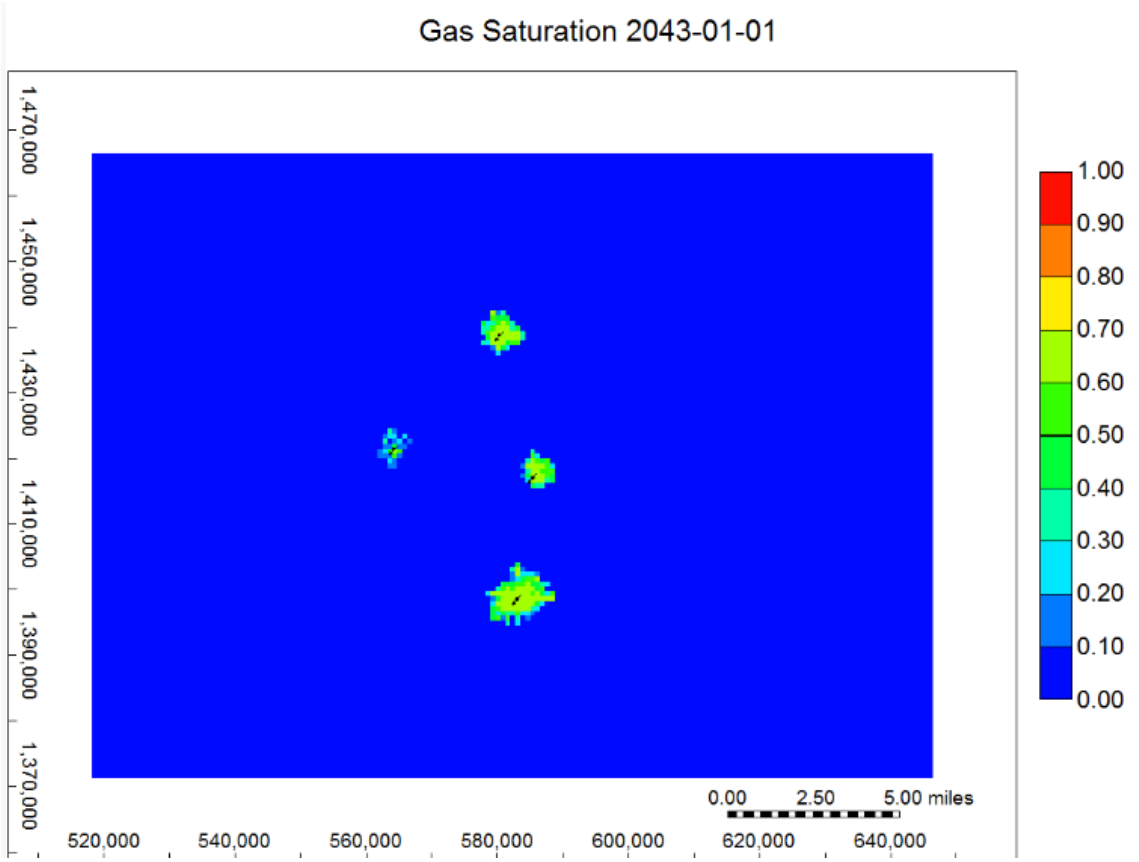

Figure 5.4.6 GEM Gas Saturation Map at End of 25-year Injection Period –

Minnelusa Formation

Figure 5.4.7 REV Gas Saturation Maps – Upper Minnelusa Formation

Next, a comparison of the differential pressure maps from REV with the GEM pressure maps was made. **Figure 5.4.8a** shows the initial pressure in the model (varying from about 3000 psi to 4500 psi), and **Figure 5.4.8b** shows the pressure at the end of the 25-year injection period. Areas of increased pressure (reaching about 5000 psi or on the order of 1000 psi over initial pressure) can easily be spotted around the four injectors, and an overall increase in pressure is noticeable over most of the model area.

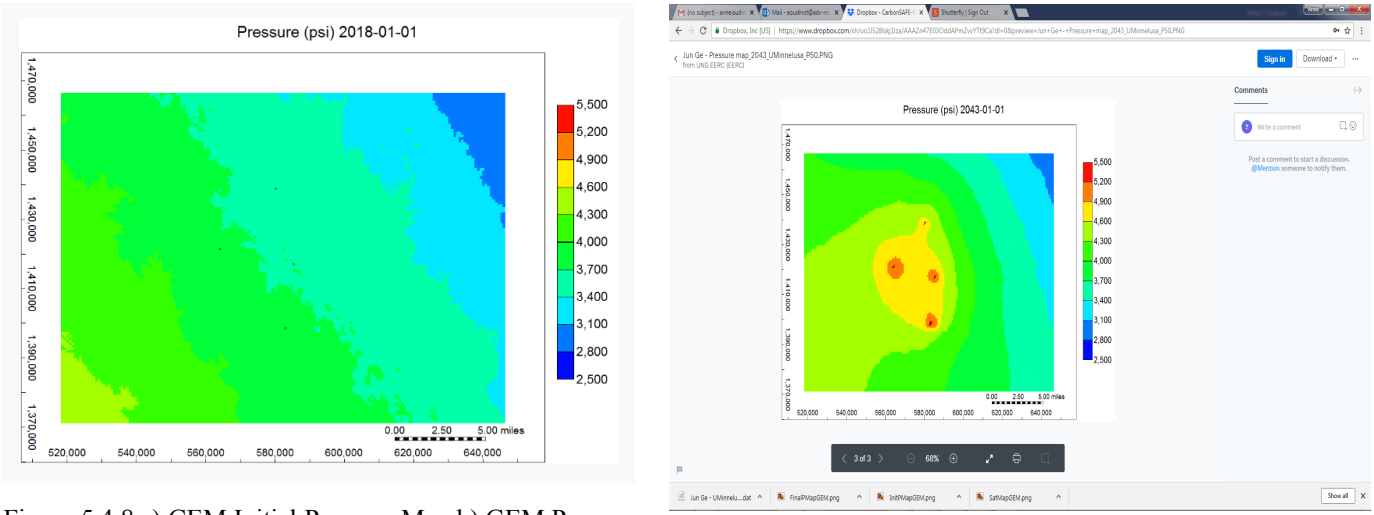

Figure 5.4.8 a) GEM Initial Pressure Map b) GEM Pressure Map at End of 30-year Injection Period

For comparison**, Figure 5.4.9** shows time-lapse pressure maps on a yearly basis from REV with a differential pressure threshold of 100 psi (any grid block with a pressure value more than a 100 psi over initial pressure will be considered in the plume). The evolution (increase in size) of the differential pressure plume can be seen over time. Analyzing the results, they seem quite consistent with the GEM output (**Figure 5.4.8b**), indicating the pressure differential over most of the model area is greater than 100 psi. However, as noticed with the CO_2 saturation maps, the shape of the area of elevated pressure is rather distorted. In addition, there is no definition of the pressure interface indicating areas of elevated pressure.

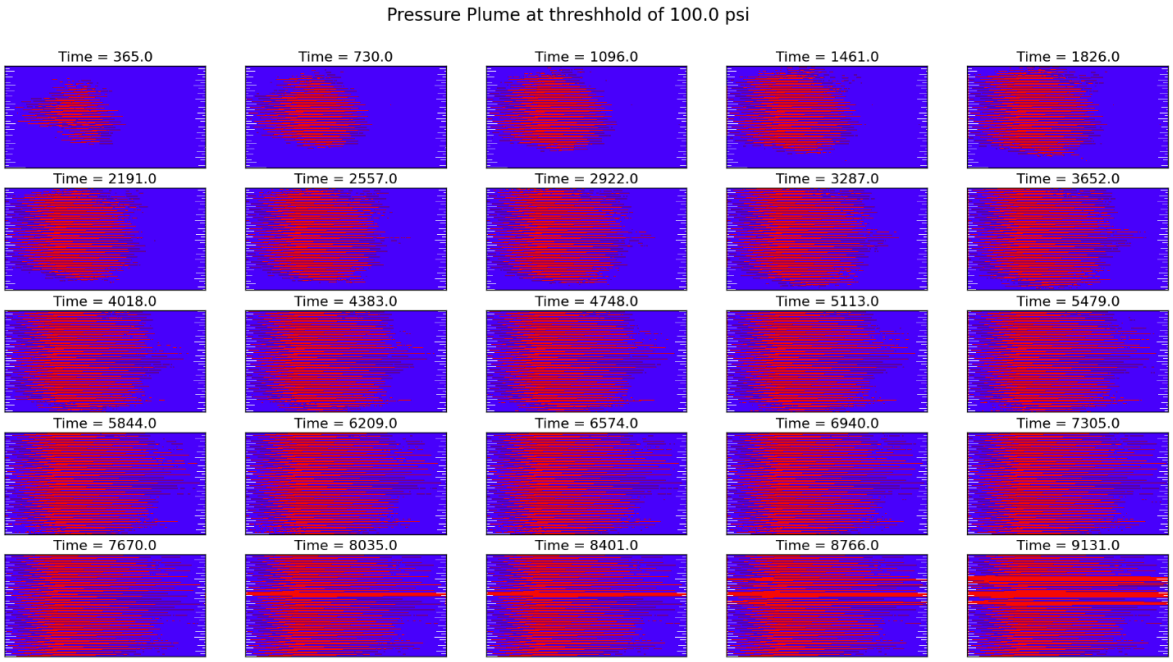

Figure 5.4.9 REV Pressure Plumes at 100 psi Threshold

Because the differential pressure plume is only based on a minimum value and not a range of values, it is difficult to highlight the various areas of elevated pressure, especially the higher pressure around the injectors. In an effort to try to improve the results, analyses were run with additional differential pressure thresholds of 250 psi, 500 psi, 750 psi, and 1000 psi (knowing that the maximum pressure increase around the injectors is on the order of a 1000 psi) to get a better plume definition. **Figures 5.4.10 to 5.4.13** show the differential pressure results for thresholds of 250 psi, 500 psi, 750 psi and 1000 psi, respectively.

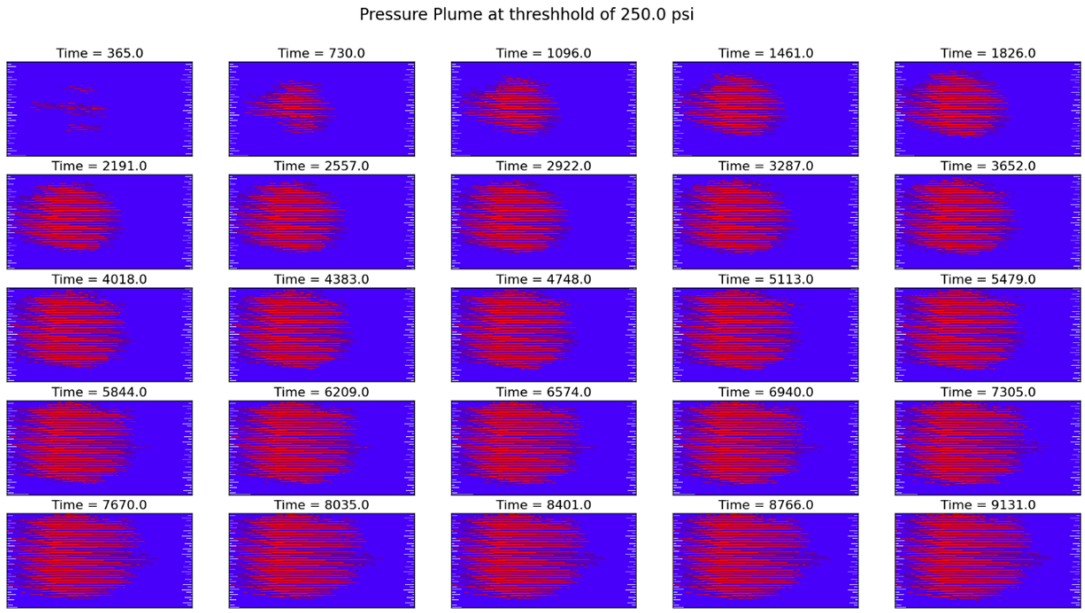

Figure 5.4.10 REV Differential Pressure Plumes at 250 psi Threshold

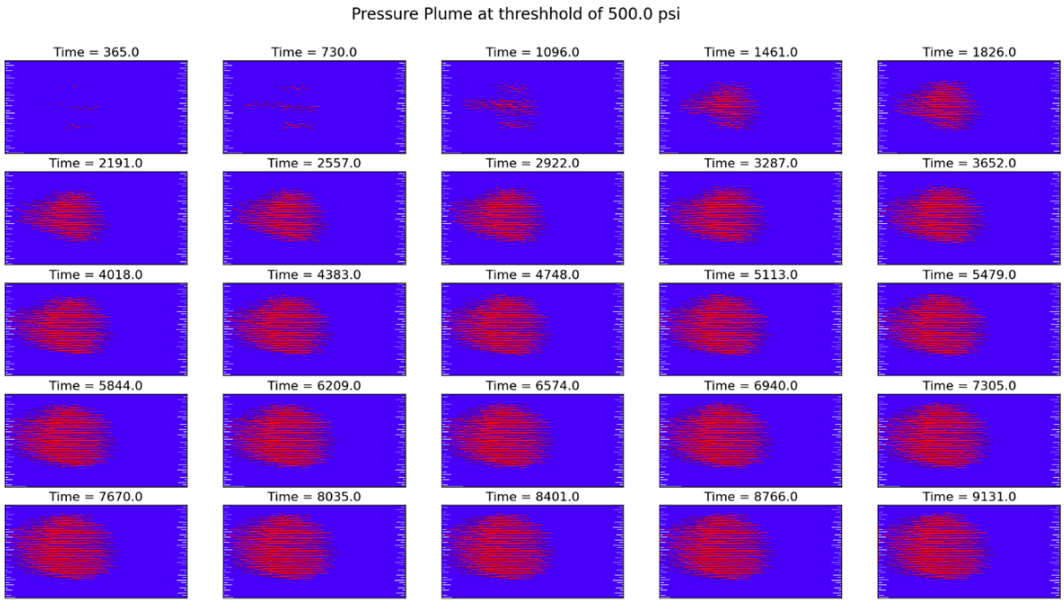

Figure 5.4.11 REV Differential Pressure Plumes at 500 psi Threshold

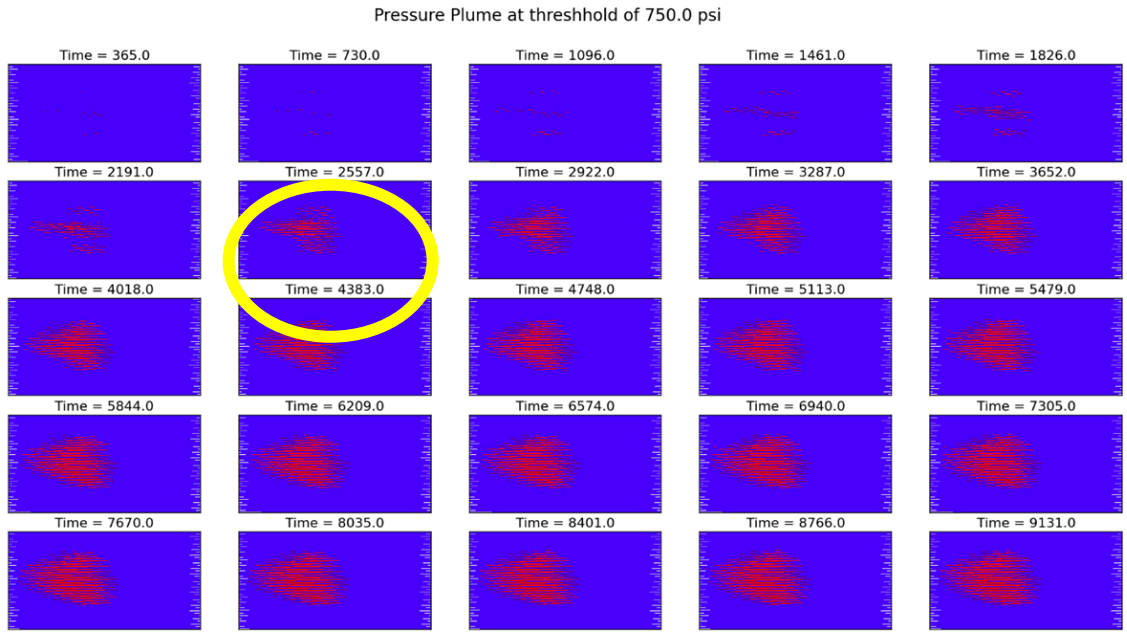

Figure 5.4.12 REV Differential Pressure Plumes at 750 psi Threshold

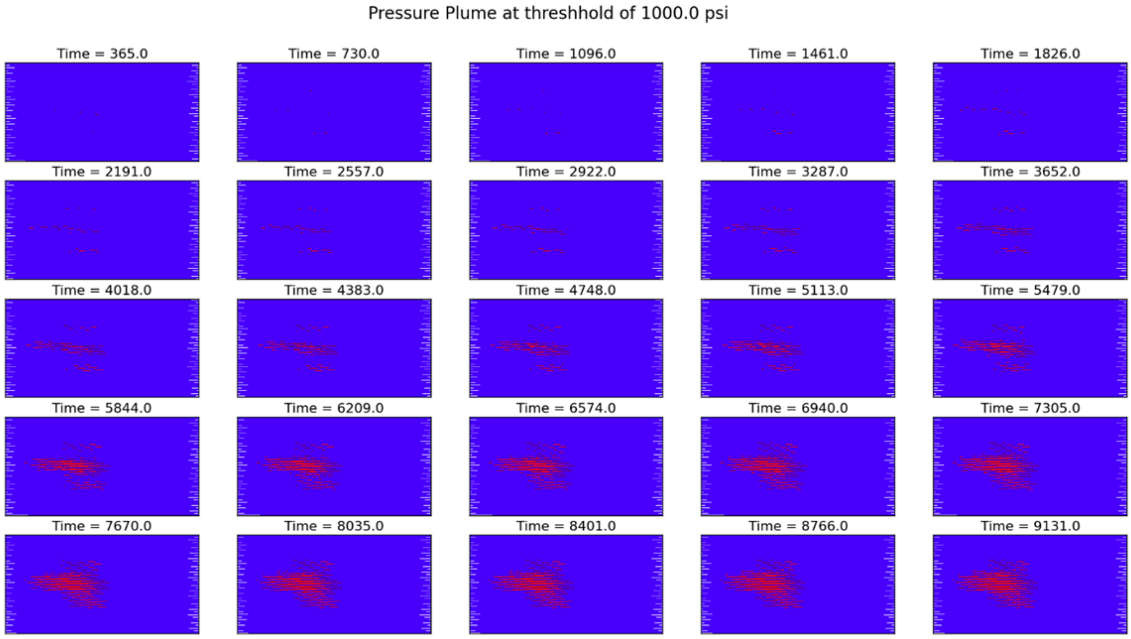

Figure 5.4.13 REV Differential Pressure Plumes at 1000 psi Threshold

These new maps (even though distorted) now allow us to more easily locate the areas of elevated pressure around the injectors and also refine the gain in pressure. Despite the distortion, they are representative of the GEM results.

In addition to the differential pressure and saturation maps, the maximum size of the plumes at each threshold is also given as a REV output as shown on **Figure 5.4.14.** For each of the thresholds evaluated, the maximum plume size will be at the end of the 25-year injection period. The model area is about 12 billion square feet, so the maximum pressure plume size at a threshold of 100 psi of more than 15 billion square feet is erroneous. This particular case (last image of **Figure 5.4.9**) shows huge distortion, which might be at the origin of the erroneous plume size calculation. While it is not possible to compare exactly the areas of the plumes between REV and GEM, based on the size of the numerical model, the REV pressure plume sizes all seem overestimated.

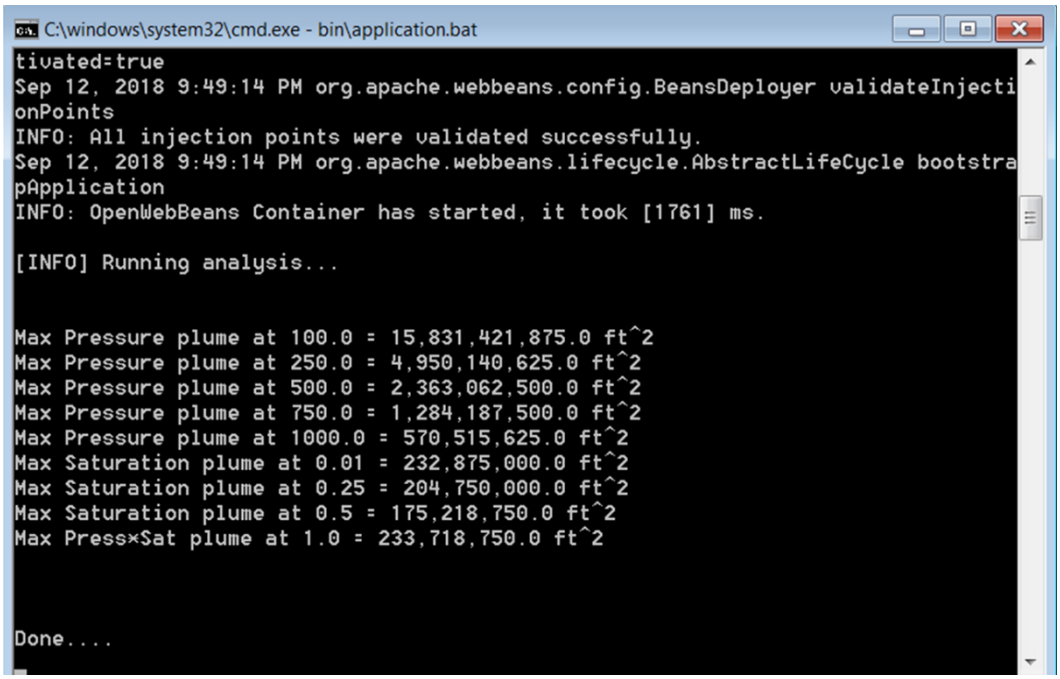

Figure 5.4.14 REV Analysis Plume Sizes – Minnelusa Formation

Recommendations:

The following is a list of comments and recommendations based on findings from the study:

- Only one version of the REV tool is available to users. However, updated ROMs are provided to users experiencing difficulty. Known issues should be identified to the users and patches provided via the EDX portal.
- It would be very useful if the manual stipulated which version of each simulator is supported by the tool. With regular updates to reservoir simulators in the industry, file formats change, and hence, can render the tool unusable.
- It would be very helpful to be able to see the progress of the analysis with something similar to a progress bar.
- There is a display issue for the differential pressure and saturation maps, which needs to be further investigated.
- Computation of plume sizes seems erroneous and needs to be further investigated.

Section 5.3 Recommendations

This report describes in detail the ten available NRAP reduced-order models, their use, required inputs, and the available outputs. Out of the ten tools, only one of the ROMs was further studied in application to the Dry Fork Station CarbonSAFE project.

With numerical models being generated to assess CO_2 storage capacity in the Minnelusa formation as part of the Dry Fork Station CarbonSAFE Project, the Reservoir Evaluation and Visualization (REV) tool was analyzed with available GEM datasets. The initial phase of the evaluation, which consisted in getting the tool to run, was made difficult by compatibility issues and the existence of various versions of the tool. Once that issue was resolved, the tool functioned properly. However,

the results obtained didn't fully compare with simulator results. While the visual display represents roughly the extent of the plumes, there is a distortion issue, which requires some support from the NETL NRAP personnel. In addition, computation of the plume areas is erroneous.

Chapter V References

1. Douglass, J.; Edwards, B.; Convertito, V.; Sharma, N.; Tramelli, A.; Kraaijpoel, D.; Cabrera, B.; Maercklin, N.; Troise, C. Predicting ground motion from induced earthquakes in geothermal areas. *Bull. Seis. Soc. Am.* **2013,** *103*, 1875–1897.
2. Abrahamson, N.; Silva, W. Summary of the Abrahamson & Silva NGA Ground-Motion Relations. *Earthquake Spectra* **2008,** *24*, 67–97.
3. Boore, D.; Atkinson, G. Ground-Motion Prediction Equations for the Average Horizontal Component of PGA, PGV, and 5%-Damped PSA at Spectral Periods between 0.01 s and 10.0 s. *Earthquake Spectra* **2008,** *24*, 99–138.
4. Britter, R. E.; McQuaid, J. D. *Workbook on the dispersion of dense gases*; Contract Research Report 17 Health and Safety Executive, Sheffield, UK, 1988.
5. Ogata, Y. Statistical-models for earthquake occurrences and residual analysis for point-processes. *J. Am. Stat. Assoc.* **1988,** *83*, 9–27.
6. Bachmann, C. E.; Wiemer, S.; Woessner, J.; Hainzl, S. Statistical analysis of the induced basel 2006 earthquake sequence: Introducing a probability-based monitoring approach for enhanced geothermal systems. *Geophys. J. Int.* **2011,** *186*, 793–807. DOI:10.1111/j.1365-246X.2011.05068.x.
7. Zyvoloski, G. A. *FEHM: A control volume finite element code for simulating subsurface multi-phase multi-fluid heat and mass transfer*; Report LAUR-07-3359; Los Alamos National Laboratory: Los Alamos, NM, 2007.
8. Nordbotten, J. M.; Celia, M. A.; Bachu, S.; Dahle, H. K. Semianalytical Solution for CO_2 Leakage through an Abandoned Well. *Environmental Science & Technology* **2005,** *39*, 602–611.
9. Pan, L.; Webb, S. W.; Oldenburg, C. M. Analytical Solution for Two-Phase Flow in a Wellbore Using the Drift-Flux Model. *Advances in Water Resources* **2011a,** *34,* 1656–1665.

Chapter V Appendix A

1.1 Aquifer Influence Model (AIM)

Introduction. The AIM tool predicts the size of a CO_2 leak into an overlying aquifer. Two reduced order models (ROMs), one an unconfined carbonate model and the second a confined alluvium model, can be employed to perform the numerical calculations. Monte Carlo techniques are used to review the results in a probabilistic context.

The software application accepts input data for a specific ROM. The major input panels are leak rate models, aquifer characteristics, and control parameters. The tool has been developed as an early stage screening tool where "site specific knowledge is expected to be low and only moderate levels of accuracy should be expected."

Input/Output Data. At a high level, the input variables may be grouped into three categories. They are 1) the leakage locations and their number, 2) the rate of flow of brine and CO_2 at those positions, and 3) the characteristics of the aquifer into which the leakage occurs. AIM results are given in terms of the plume size for each of nine water quality facets (pH, total dissolved solids, four trace metals, and three organic compounds, **Figure 5A-21**) as well as the flux of CO_2.

Figure 5A-19 show the tab for inputs of the leakage rate model. At the bottom of the tab, a drawing of the leak scenario explains what each parameter corresponds to and what an acceptable range for each parameter is. As highlighted in red, several scenarios (input by the user) will be run using Monte-Carlo probabilistic techniques.

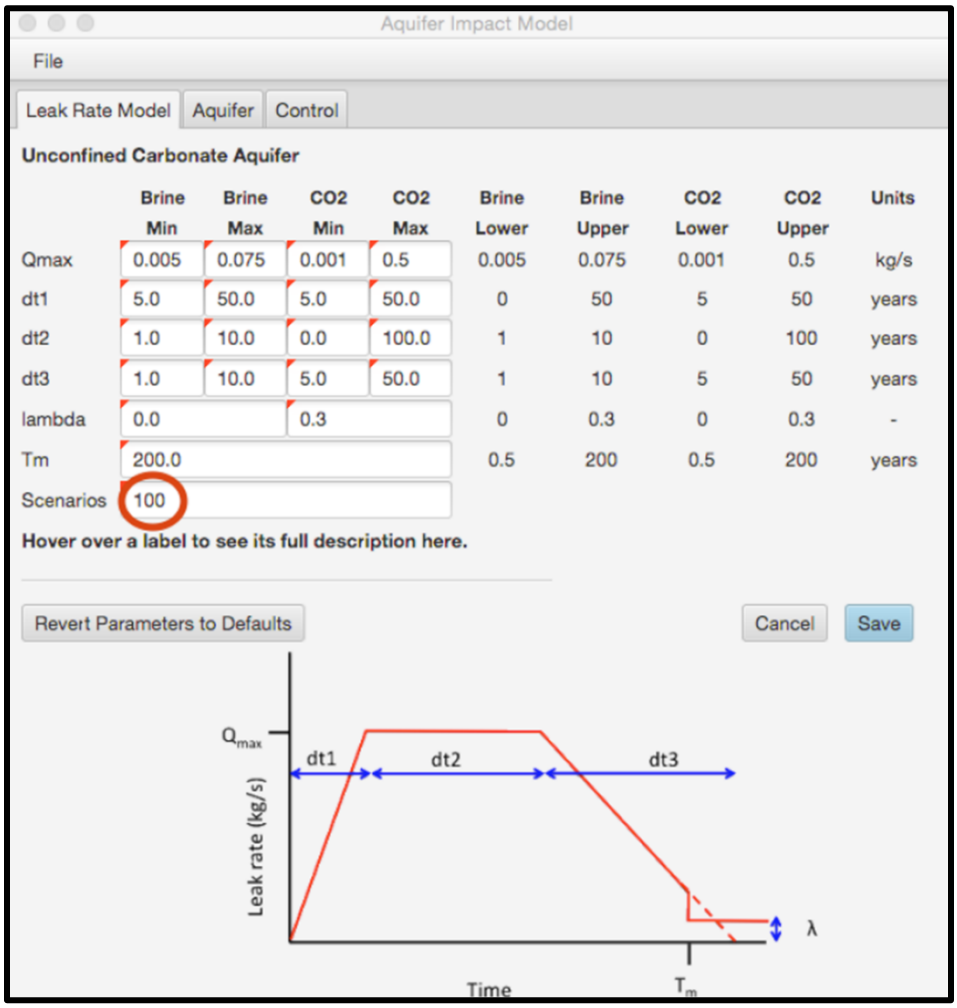

Figure 5A-19 Leak Rate Model Tab and Inputs

Figure 5A-20 shows the numerous inputs necessary to describe the aquifer for each option (unconfined carbonate or confined alluvium).

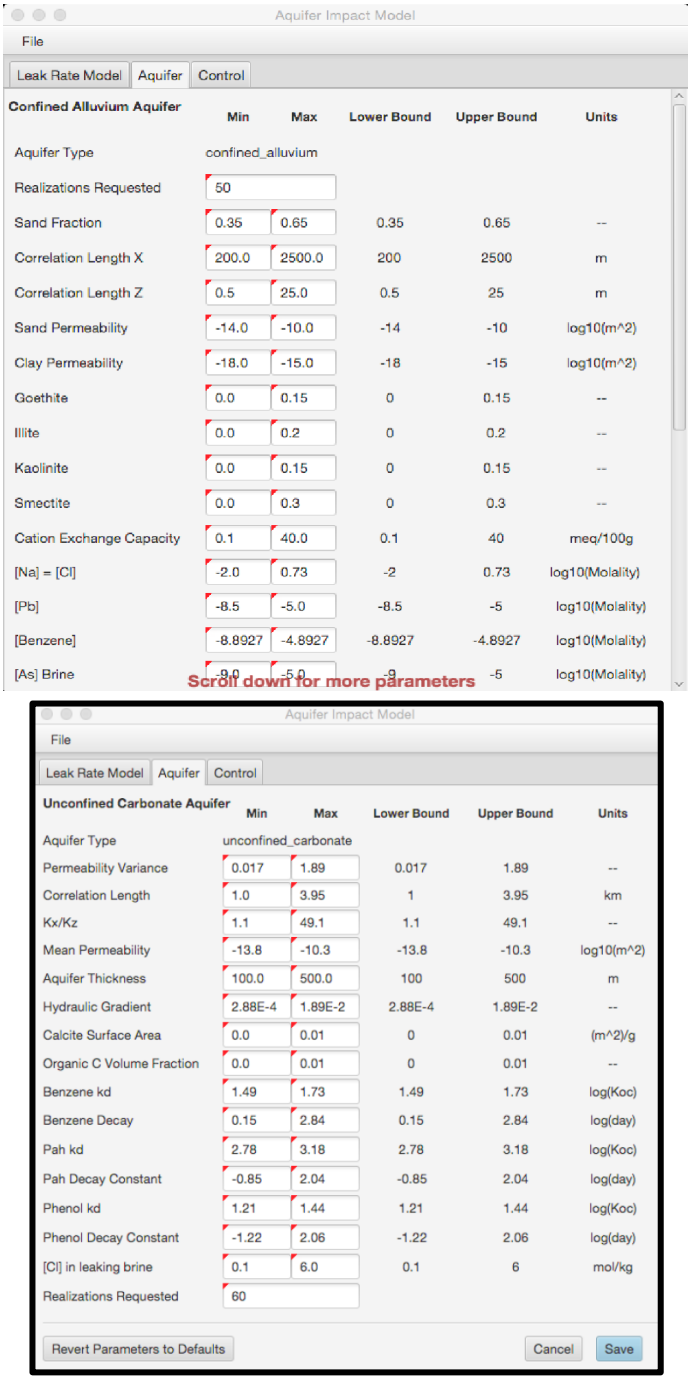

Figure 5A-20 a) Unconfined Carbonate Aquifer and b) Confined Alluvium Aquifer Tab and Inputs

Note: to convert from m^2 to Darcy multiply by 1.013249966e+12

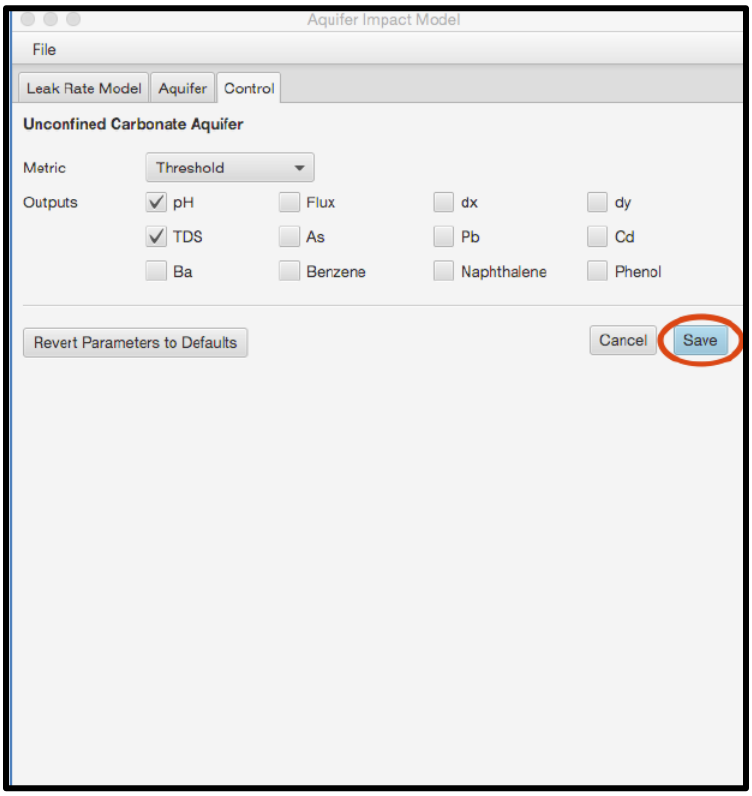

Figure 5A-21 Control Tab and Inputs

1.2 Designs for Risk Evaluation and Management (DREAM) Tool

Introduction. The DREAM software application was constructed to be a monitoring program design tool to minimize the time to first detection of a subsurface CO_2 leak. When executing the program, there are three components that comprise the software: 1) a Java input and execution wizard, 2) a results visualization protocol, and 3) a results plotting tool.
Input/Output Data. DREAM leverages user-provided CO_2 leakage modeling results to optimize the outlay of monitoring tools and wells available. These inputs may include any modeling results developed from physics-based, porous media flow models, including pressure, temperature, gas saturation, etc. The various windows/panes for the software are described below.

DREAM Welcome. The software opens to the welcome window, which contains links to the software development manual, references, and acknowledgments.

Input Directory. This pane requests the directory containing the CO_2 leakage simulation output files in HDF5 format. If the output files are not currently in HDF5 format, the Launch Converter button can be used to convert the ASCII data into the desired structure.

Porosity. The porosity of the system is required to calculate aquifer volumes. Additional zones can be provided along with porosity data from an external file. This data can be saved for future use elsewhere.

Scenario Weighting. Modeled leakage scenarios, which have been created in subfolders for input, are listed and are each assigned a default weighting of 1.0. This represents the likelihood of the potential leakage scenario. The larger the number is the greater the potential for leakage.

Leakage Criteria for Monitoring Parameters. Based on the flow modeling output of the imported simulations, DREAM will generate a table of monitoring parameters. The application requires the monitoring technology to be deployed for each selected parameter, the total cost, the detection criteria, and the ranges for the detection criteria. In addition, the triggering nodes (elements that meet the detection criteria) can be found and the solution spaces (set of nodes where leakage is present) selected. The leakage nodes and the optimum monitoring locations can be viewed through the Launch Visualization button.

Minimum Triggered Monitoring Devices. Input the minimum number of sensors required.

Configuration Settings. The application designs the monitoring program based on user input specifications regarding the total sensor budget and number of wells. If well spacing limitations are known, this can be input, as well.

Exclude Locations. Should monitoring nodes be excluded from the configuration, they may be deselected on this pane. If the user has incorporated a Google map of the storage site, this can also be used to confirm locations.

Run DREAM. Prior to running the software, output directories and best achievable monitoring protocols (no budget) are available to manage the output and set the expectation prior to running the requested number of configurations to determine the budgeted monitoring optimization.

Formatted software output accepted for DREAM input includes NUFT (Non-isothermal, Unsaturated Flow and Transport Model), STOMP (Subsurface Transport Over Multiple Phases), and TECPLOT (which is a post-processing simulation tool).

While executing, two windows pop up to show progress. The first is the DREAM visualization window, which shows the monitoring configuration being tested. The second is a window with four performance plots showing the time to detection results for new configurations, the best configurations, each realization, and the percentage leak detected. The program generates several useful output files in .CSV format for user review. **Figure 5A-22** shows an example from the Visualization Tool.

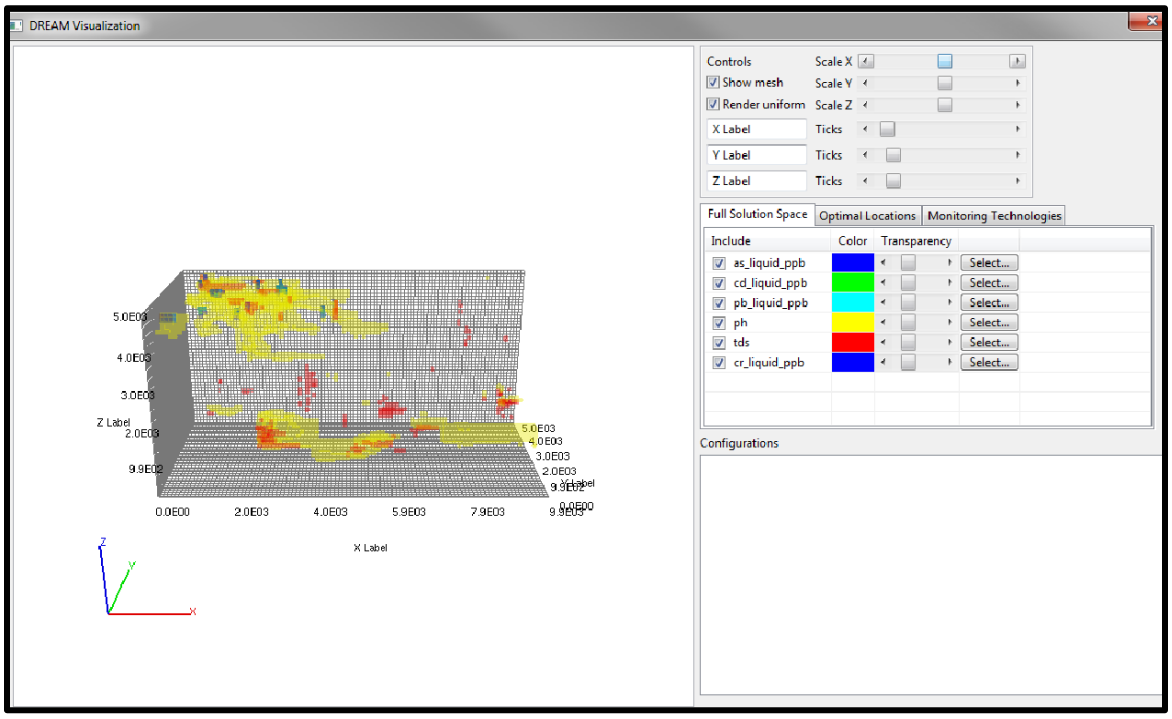

Figure 5A-22 DREAM Visualization Tool – Full Solution Space

1.3 Ground Motion Prediction Applications to Potential Induced Seismicity (GMPIS)

Introduction. The GMPIS tool predicts the distribution of potential ground movement due to induced seismicity (IS) caused by CO_2 injection and accompanied by accelerated/triggered tectonic-related seismicity. Because of the limited seismicity data due to CO_2 injection, ground motion prediction equations were adapted and developed from data derived from active geothermal sites (Douglas et al, 2013)[1] to obtain peak ground acceleration and peak ground velocity. The database includes nearly 4,000 records from Switzerland, Germany, France, the Netherlands, California, and Iceland. One limitation to the tool is that induced seismicity is regionally dependent. Because of the lack of data on injection IS, global IS data with uncertainties have to be applied via a simplified site amplification model. The site amplification models of Abrahamson and Silva (2008)[5] and Boore and Atkinson (2008)[3] were incorporated to adjust the ground motion prediction equations (GMPEs). These models estimate the shallow shear-wave velocity, typically in the upper 30 meters (Vs30), with direct measurements based on geology, slope or terrain, and other local velocity observations.

The major input panels for the ROM include a Master, description of induced seismicity characteristics, and description of tectonic seismicity characteristics.

Input/Output Data. At a high level, the input variables may be grouped into three categories. They are 1) the location of the site 2) for induced seismicity, the properties of the induced earthquake, and 3) for the tectonic seismicity, fault characteristics and properties of the earthquake.

1.3.1 Site Location

The Master tab allows the user to define the bounding coordinates of the studied area as well as the number of evenly spaced sites in that area. The user can also upload personal topographic maps in the model. This tab allows for specific outputs to be generated, such as a ShakeMap (maps of ground motion from the USGS Earthquake Hazard Program) or a detailed output. **Figure 5A-23** shows the 'Master' tab in the GMPIS model.

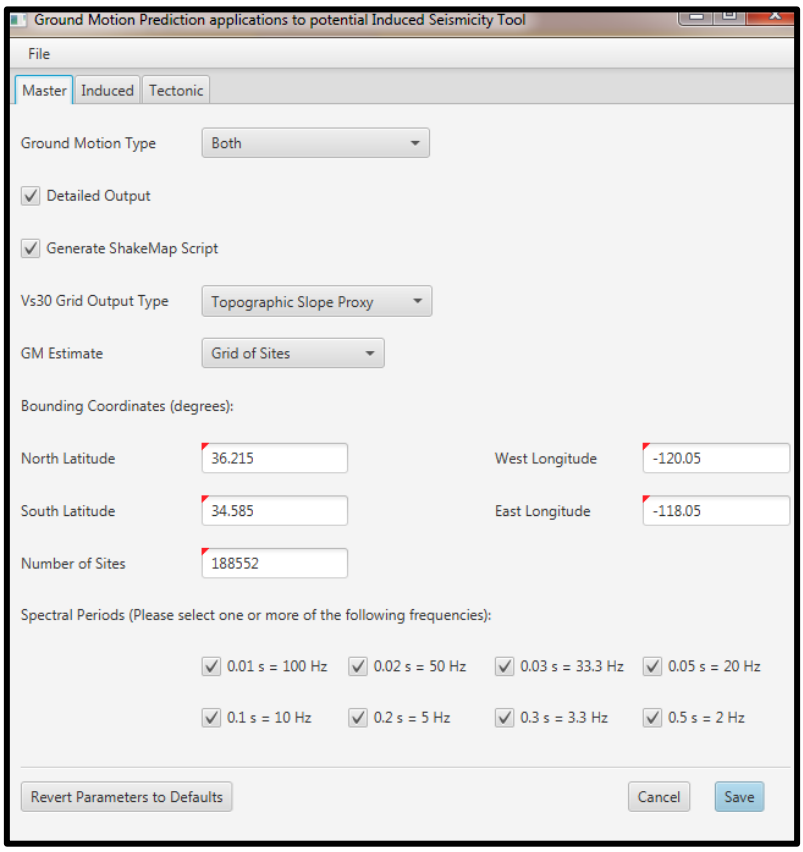

Figure 5A-23 GMPIS "Master" Input Page

1.3.2 Induced Seismicity Characteristics

Under the induced tab, characteristics pertinent to the earthquake induced by the CO_2 injection are input. These are the earthquake coordinates as well as its magnitude and its depth. The user specifies which site amplification method to be used for site specific corrections (Abrahamson and Silva or Boore and Atkinson). **Figure 5A-24** shows the 'Induced' tab.

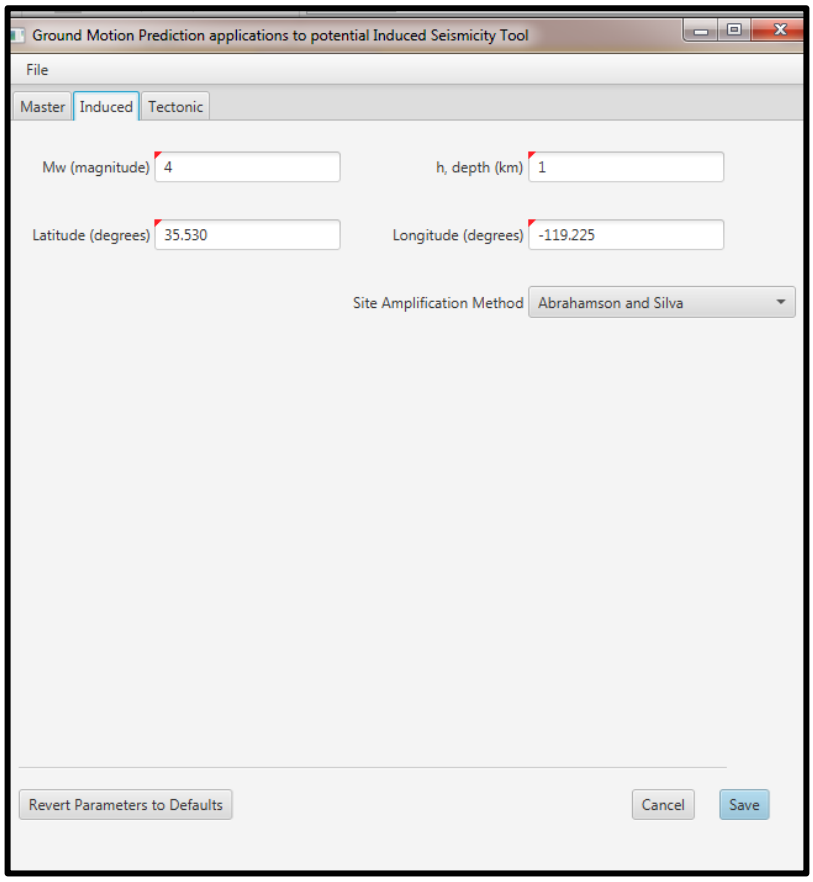

Figure 5A-24 GMPIS "Induced" Input Page

1.3.3 Tectonic Seismicity Characteristics

Under the 'Tectonic' tab, the characteristics of the rupture surface (fault), which was triggered during CO_2 injection, are input. These include the type of fault, the fault dip, exact coordinates along the fault, and the top depth of the fault as well as the magnitude of the triggered earthquake. **Figure 5A-25** shows the 'Tectonic' tab.

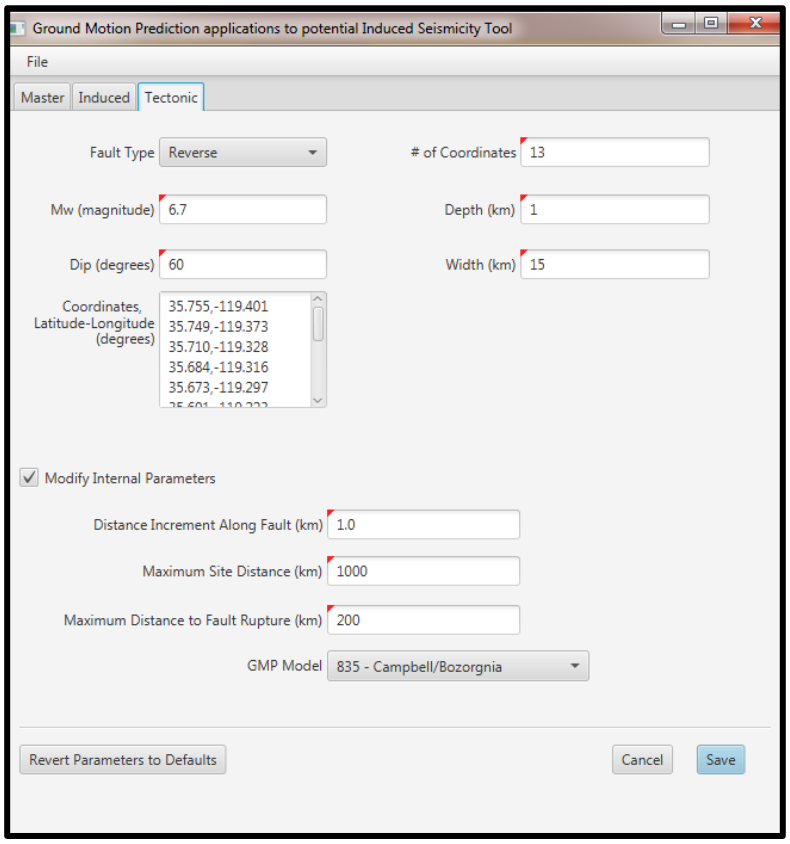

Figure 5A-25 GMPIS "Tectonic" Input Page

1.3.4 GMPIS Outputs

GMPIS simulation results are a flat file containing peak ground velocity and acceleration at each defined location over the area of interest as well as input files for graphic packages.

1.4 Multiple Source Leakage Reduced-Order Model (MSLR)

Introduction. The MSLR tool predicts if receptors are within a critical radius of eventual multiple CO_2 leakage sources. The MSLR is developed as both a built-in tool in the NRAP-IAM-CS (Integrated Assessment Model for Carbon Storage) and as a standalone module. The Britter and McQuaid (1988)[4] correlations for predicting plume extent and concentration of dense gases during potential gas releases were used, but are only applicable to single source releases. A superposition approach was developed to handle multiple leakage sources. This tool is mainly intended for scoping studies.

Input/Output Data. The main inputs to the MSLR are CO_2 leakage rates, wind speed, leakage sources' location, receptors' locations (limited to 100), and the critical CO_2 concentration (the threshold concentration limit above which CO_2 is considered to become hazardous).

1.4.1 MSLR Main Inputs

The model main inputs include atmospheric conditions (temperature and pressure to compute air density and wind speed) as well as the source of the CO_2 leakage temperature (to compute CO_2 density) and time. The main inputs are shown on **Figure 5A-26**.

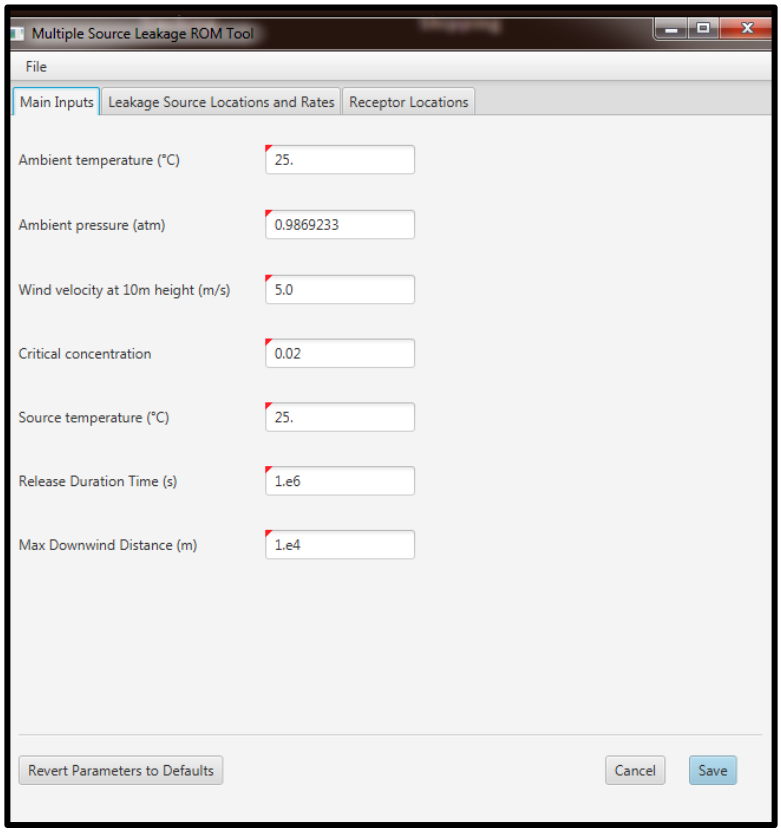

Figure 5A-26 MSLR Main Input Tab

1.4.2 MSLR Leakage Source Locations and Rates

Up to 1,000 sources of CO_2 leakage can be input in the model. For each source, location (coordinates) and leakage rate are required. If the ROM is used as part of the NRAP-IAM-CS model, leakage locations and rates can be passed from other modules. If the ROM is used as a standalone, the information needs to be entered into the 'Leakage Source Locations and Rates' tab as illustrated in **Figure 5A-27**.

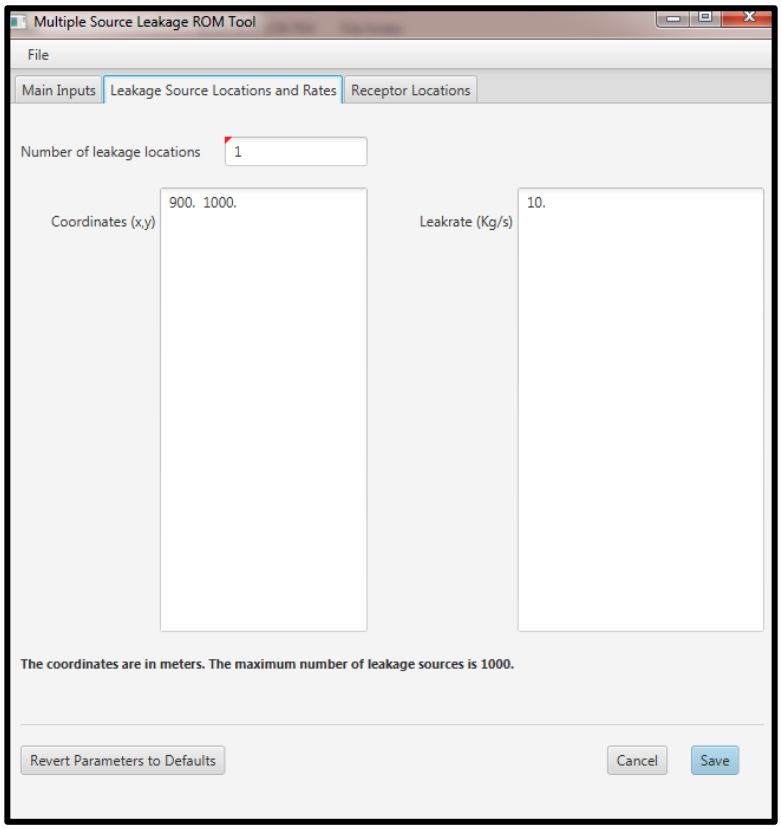

Figure 5A-27 MSLR Leakage Source Locations and Rates Tab

1.4.3 MSLR Receptor Locations

Up to 100 receptors (locations at which the user wants to know if the dense gas concentration exceeds the critical value defined) can be defined. If the ROM is used as part of the NRAP-IAM-CS model, receptor locations are provided through a specific text file. If the ROM is used as a standalone, the information needs to be entered into the 'Receptor Locations' tab as illustrated in **Figure 5A-28**.

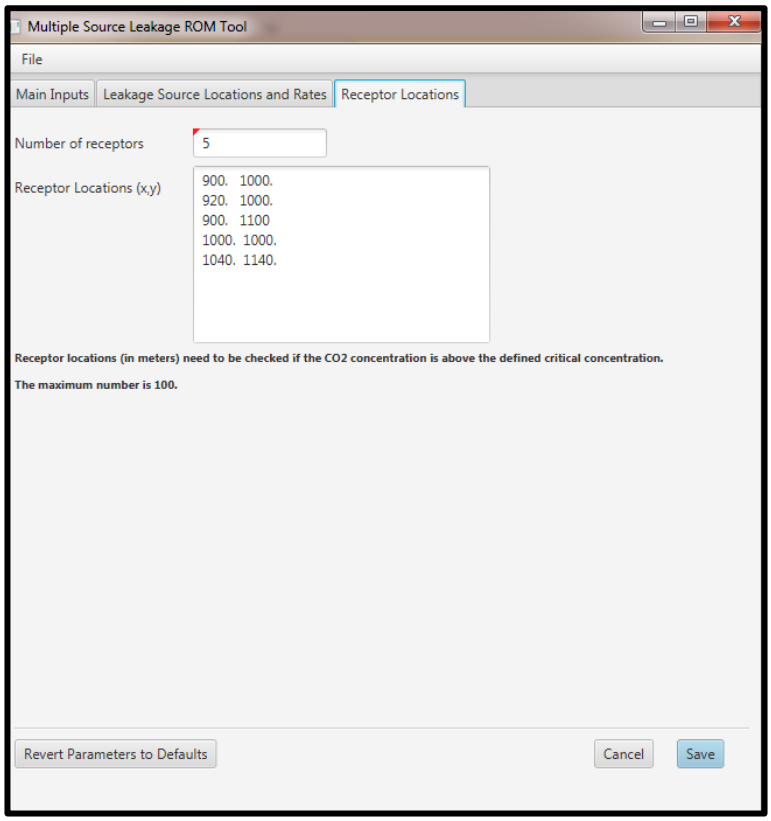

Figure 5A-28 MSLR Receptor Locations Tab

1.4.4 MSLR Outputs

If used as a standalone evaluation tool, MSLR results are in the format of a text file (graphical outputs are currently not available) and include the list of the receptors where the critical CO_2 concentration has been reached as well as the critical radius of each leakage zone to define the critical zone. When used within the NRAP-IAM-CS, graphic visualization is available.

To prove the validity of the superposition method and Britter and McQuaid monograph built into MSLR, the model has been tested against Fluidyn-PANACHE (family of software modules for modeling atmospheric flows) for single and multiple source releases. Results are in very good accordance and can be viewed in the tool's user manual.

1.5 NRAP Integrated Assessment Model–Carbon Storage (NRAP-IAM-CS)

Introduction. The NRAP-IAM-CS software is constructed to provide probabilistic simulations modeling the long-term fate of CO_2. Several ROMs make up the program, allowing subsurface modeling to be conducted within the storage reservoir, through leakage pathways and in shallower reservoirs. This does include leaky wellbores. Modeling results are provided in terms of volumes in place, plume extent, and impact on other resources, such as shallow groundwater wells or the atmosphere.

GoldSim is required to be installed in order to run the model, which must be purchased or provided as an academic or 30-day evaluative license (available at: https://www.goldsim.com/Forms/Evaluation.aspx).

Input/ Output. NRAP-IAM-CS can operate in two modes. The first type is a scoping level input array that employs simplified model geometry and constant geologic properties. Later, when more data is available, the model can be run in a detailed mode to describe the spatial variability of subsurface properties, well locations, and leakage pathways.

Model input data can be categorized as follows:

1. Scenario Type and Inputs
    a. Direct leakage to atmosphere through wells (requires reservoir, legacy wells, and land surface information)
    b. Leakage to groundwater through wells (requires reservoir, legacy wells, shallow aquifer, and intermediate reservoir and land surface information)
    c. Area of review (requires reservoir, seal, legacy wells, and land surface information)

Once the type of scenario has been chosen, the site needs to be described.

2. Site Characteristics
    a. Simple (built-in model)

One main assumption for the simple site is that there is one single injection well. The CO_2 injection rate can be specified by the user but will be limited by the maximum frac pressure, if reached. Main reservoir inputs include depth, thickness, permeability, porosity, water, and CO_2 residual saturations (constant or distributed).

    b. Complex

A lookup table option is available for the complex option and allows the user to import spatially variable inputs, such as land surface elevation, reservoir elevation, thickness, permeability, temperature, CO_2 saturation, dissolved CO_2 concentration, and pressure. All inputs must be generated on a 100 by 100 grid.

3. Wellbore Characteristics

NRAP-IAM-CS uses the wellbore leakage WLAT reduced-order model (described in Appendix 1, section 1.9) to calculate CO_2 and brine leakage rates.

    a. Locations options

This is a very flexible option which allows the user to input coordinates for existing well(s) or let the software generate random location(s) for a specified number of wells over a specific area using a normal distribution.

    b. Permeability options

Three permeability options are available, which include: constant cement permeability for all the wells, variable permeability using available distribution options, or an open wellbore model (refer to Appendix 1, section 1.9 of the WLAT Reduced Order Model for more details).

4. Shallow Aquifer and Intermediate Reservoir

The simulations for the shallow aquifer plumes are from multiphase reactive chemistry models using the FEHM (Finite Element Heat and Mass) and STOMP (Subsurface Transport Over Multiple Phases) models. The shallow aquifer and intermediate reservoir section requires the input of physical and hydrologic and geochemical parameters.

a. Physical parameters
b. This section allows the user to fill in physical properties, such as elevation, thickness, pressure, temperature, permeability, and porosity for each of the shallow aquifer and the intermediate reservoir Hydrologic and geochemical parameters

This section allows the user to fill in a complex table of inputs for 16 different aquifer hydrologic (permeability, permeability anisotropy, aquifer thickness, etc.) and geochemical (benzene, pH, and phenol decay constants, for example) parameters. Each of these parameters can be defined as constant, or a distribution can be selected, which will be applied during Monte Carlo analysis.

5. Surface Environment Characteristics (land surface information)

In this section, the leakage from the wells or/and faults that make it to the atmosphere is input into the atmospheric dispersion model, which computes the changes in CO_2 concentration above the sequestration site based upon external factors (such as wind speed, ambient temperature, and ambient pressure). More details are provided in Appendix 1, section 1.4 on the MSLR (Multiple Source Leakage Reduced Order Model) tool.

Using GoldSim output and the results viewer, animations of contour plots or three-dimensional realizations can be seen.

1.6 NRAP Seal Barrier Reduced Order Model (NSEALR)

Introduction. NSEALR models the flow or leakage of CO_2 through low permeability formations overlying storage horizons. These strata, often called cap rocks or confining units, are a primary characterization criterion that must be input in order to quantify leakage/seepage potential from storage pools. The model currently assumes a 1D (vertically), two-phase flow of CO_2 through a brine saturated rock under CO_2 supercritical conditions.

GoldSim is required to be installed in order to run the model, which must be purchased or provided as an academic or 30-day evaluative license (available at: https://www.goldsim.com/Forms/Evaluation.aspx).

Input/ Output. As can be seen on **Figure 5A-29**, there are 7 different sections for inputs, the top 5 for seal-related properties, and the 2 additional sections for general reservoir parameters.

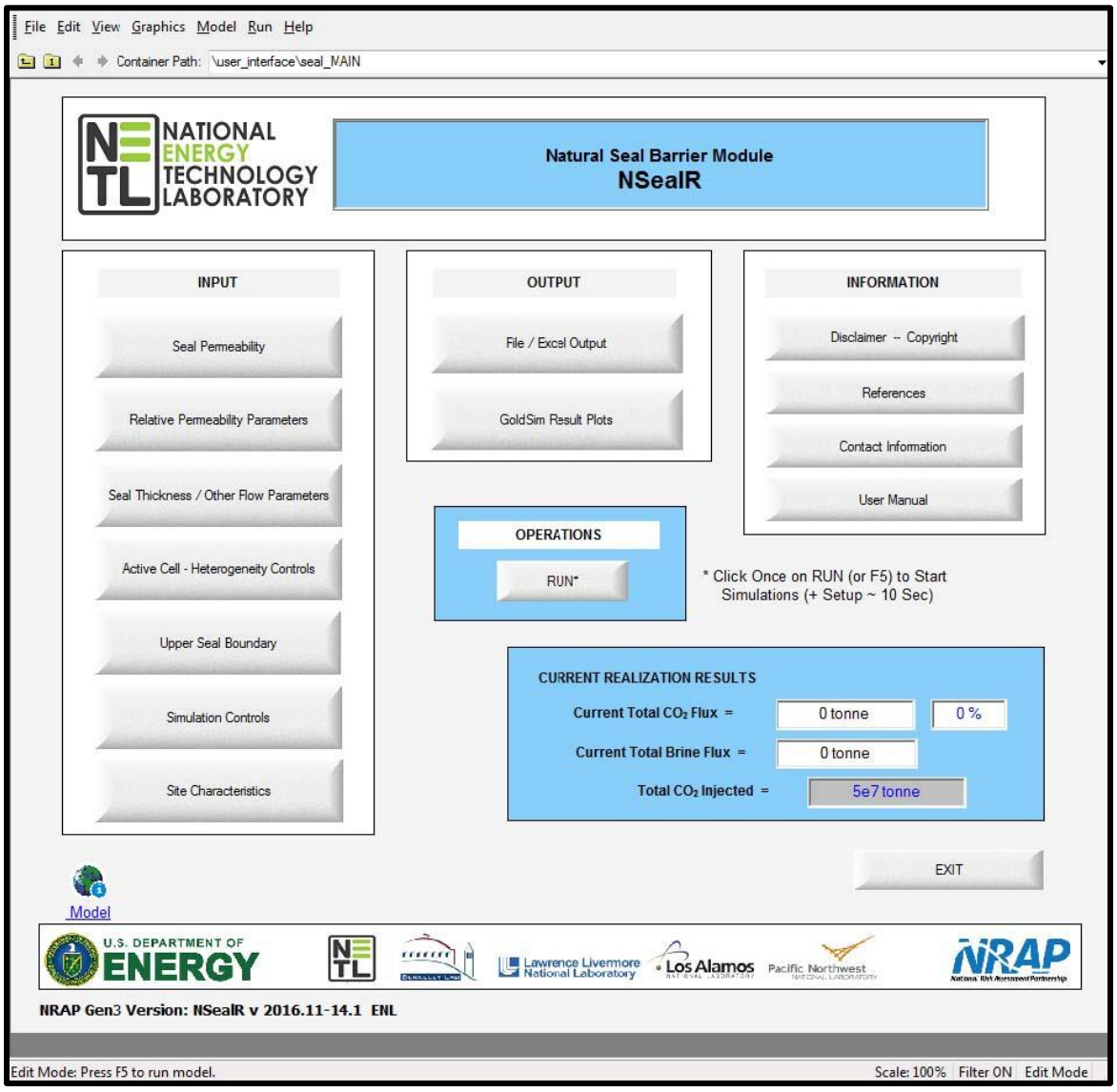

Figure 5A-29 NsealR Main Dashboard

1.6.1 Seal Permeability

There are 5 different options available for a seal permeability model: (1) constant flux; (2) user defined constant permeability and porosity for each cell; (3) definition of permeability and porosity across the area of interest using stochastic distributions; (4) user defined equivalent permeability and porosity for each cell using the fractured rock model; and (5) a user defined permeability map input using a text file. Additional information regarding the different permeability models can be found in Appendix A of NSealR's user manual. All the required inputs are shown on **Figure 5A-30**.

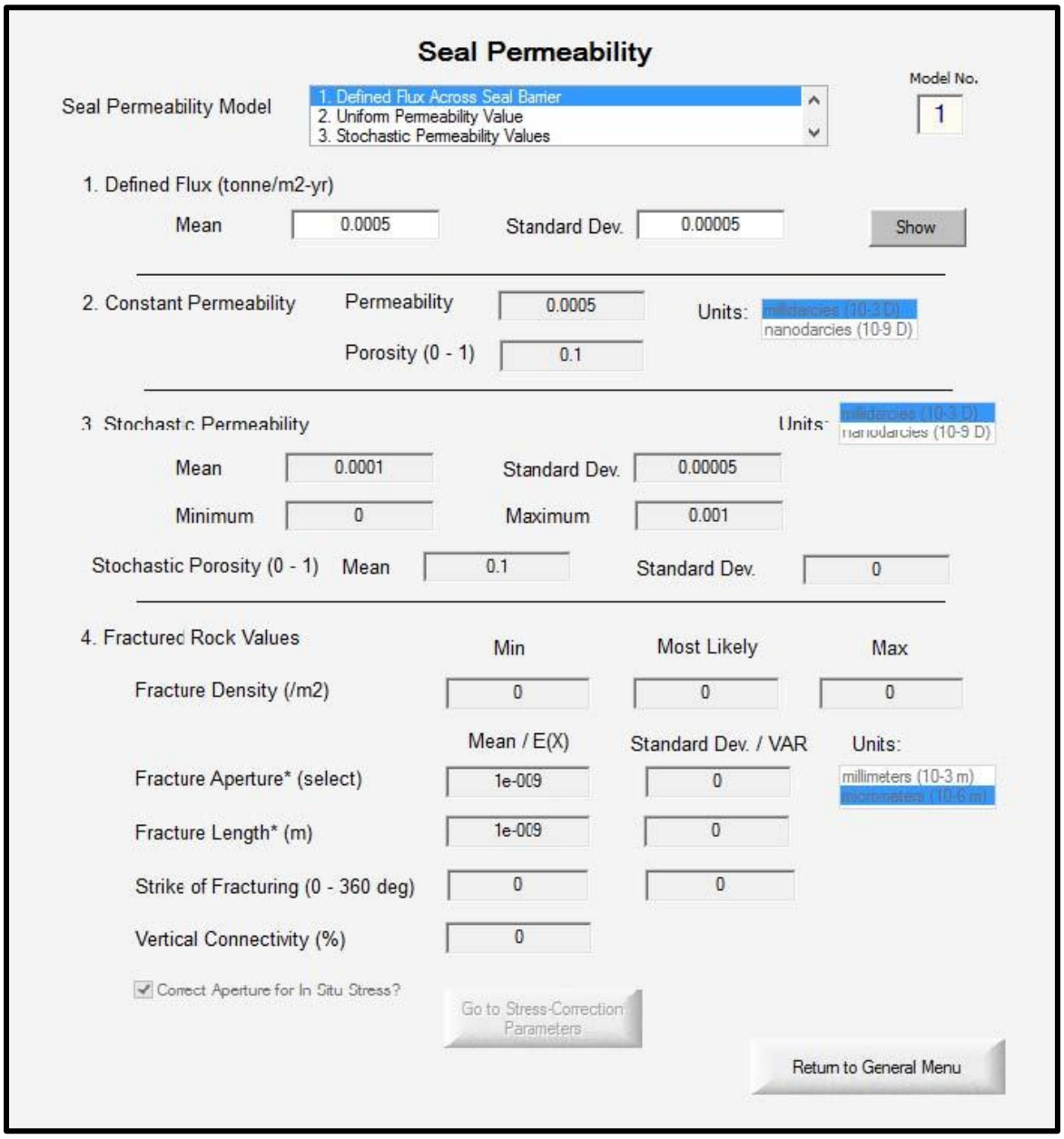

Figure 5A-30 Seal Permeability Dashboard

1.6.2 Two-Phase Flow and Relative Permeability

Two-phase model parameters can be entered as a single value or as a variable value (using a uniform distribution). The model currently supports four different two-phase models: Purcell Model, Brooks-Corey model, van Genuchten-Mualem model, and LET general model. These relative permeability models are all described in great detail in Appendix C of NSealR's user manual. **Figure 5A-31** highlights all the inputs required.

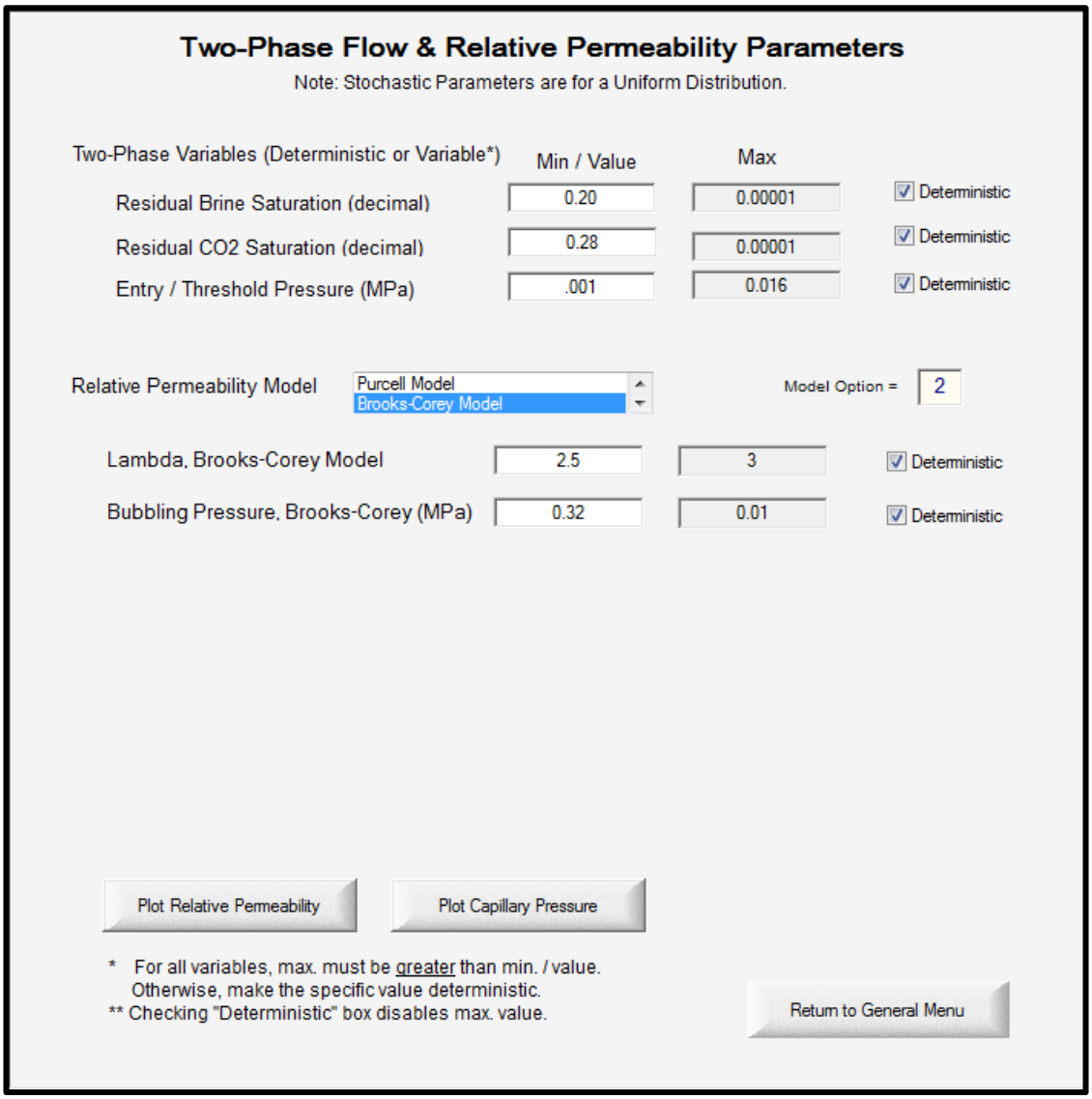

Figure 5A-31 Two-Phase Flow and Relative Permeability Dashboard

1.6.3 Seal Thickness and Reference Parameters

The seal thickness can be defined via three different options: constant value through the formation, probabilistic distribution, or an array of user-defined values input from an external text file. In addition, four reference parameters are defined here: the salinity of the brine in the seal, the brine pressure at a specified depth, the reference depth, and temperature. Other required parameters are shown on **Figure 5A-32**.

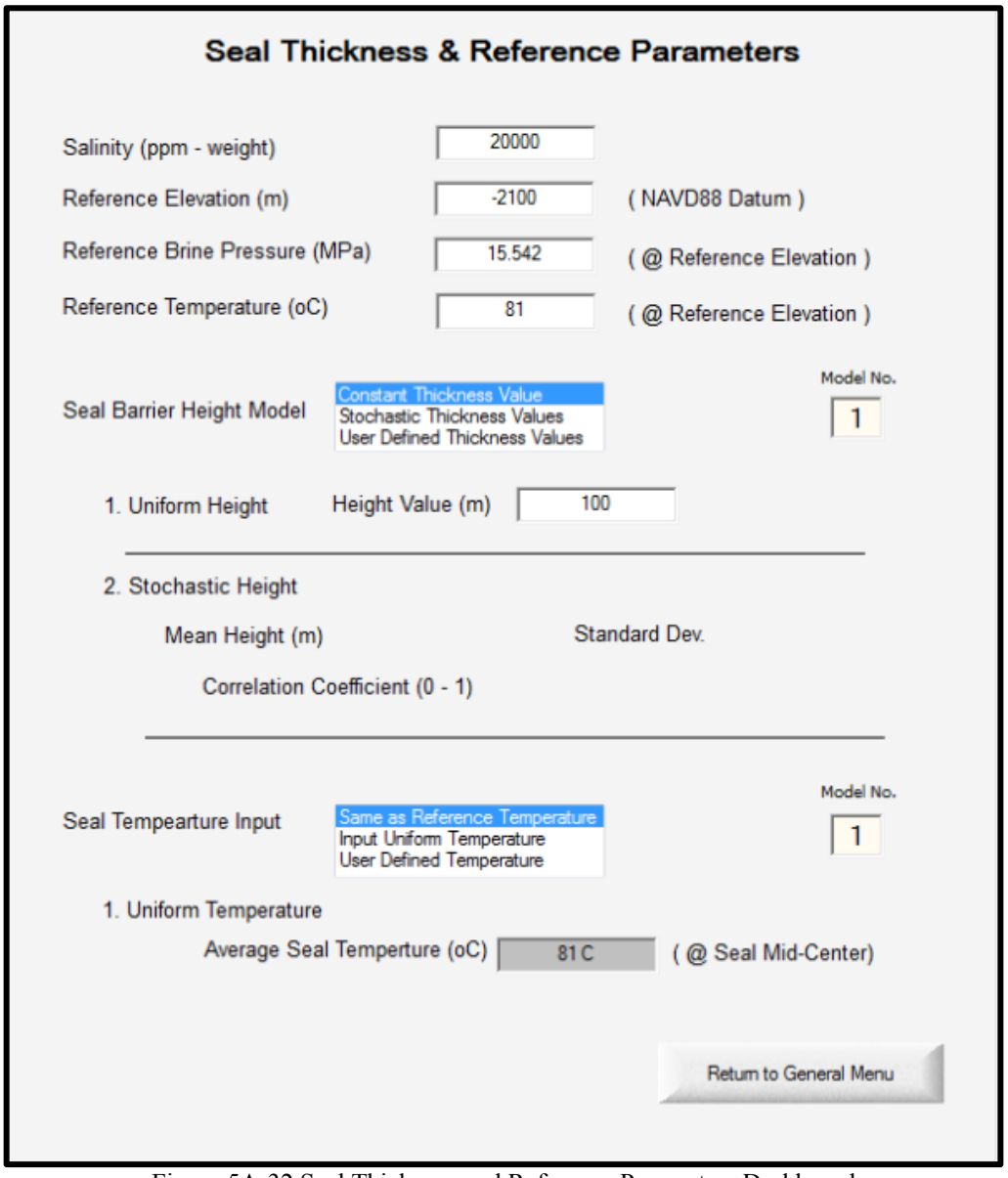

Figure 5A-32 Seal Thickness and Reference Parameters Dashboard

1.6.4 Active Cell Definition and Heterogeneity Controls

The active cell option allows the user to limit the flow to certain areas across the seal horizon, basically generating a sub-model. The required parameters for that option are shown in **Figure 5A-33.**

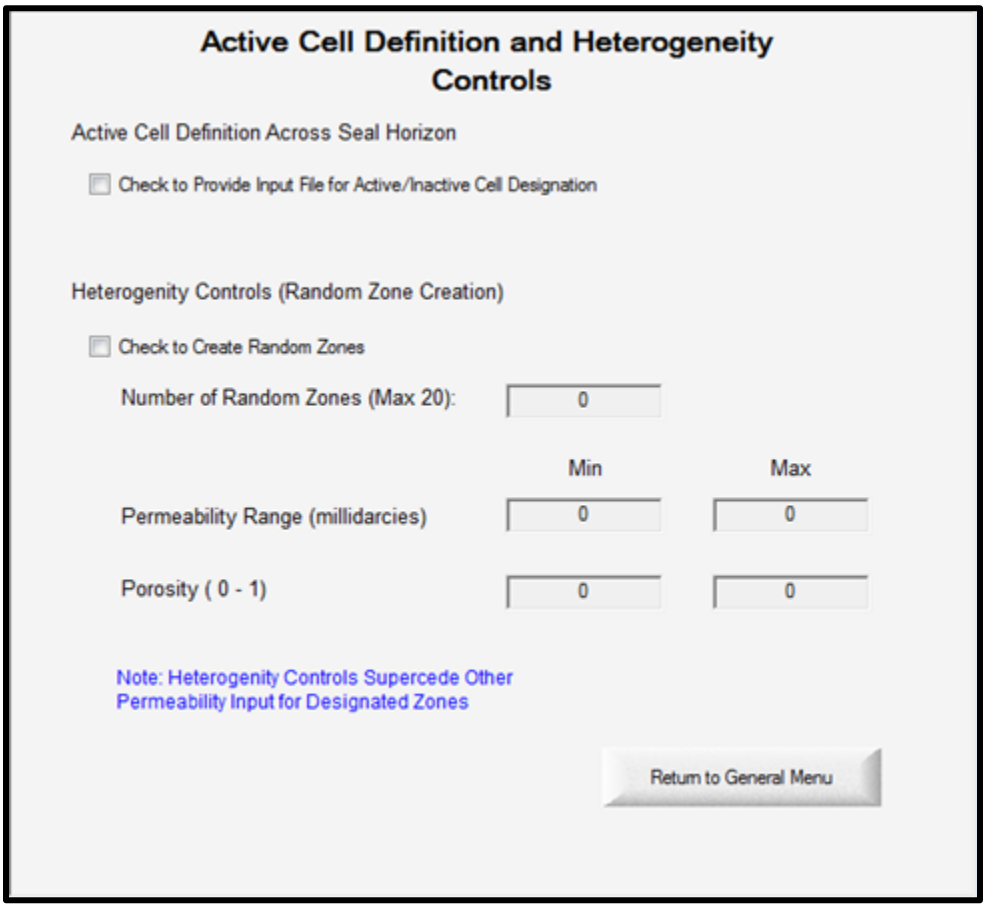

Figure 5A-33 Active Cell Definition and Heterogeneity Controls Dashboard

1.6.5 Upper Seal Boundary Definition

The last form allows the user to define the pressure and saturation conditions at the top of the seal horizon. Three options are available for input:

- static conditions,
- a function that computes the pressure and saturation conditions at the top of the seal as a function of the corresponding values at the bottom,
- and user defined values, which allows values from a text file to be imported.

The required parameters for the upper seal boundary definition are shown on **Figure 5A-34**.

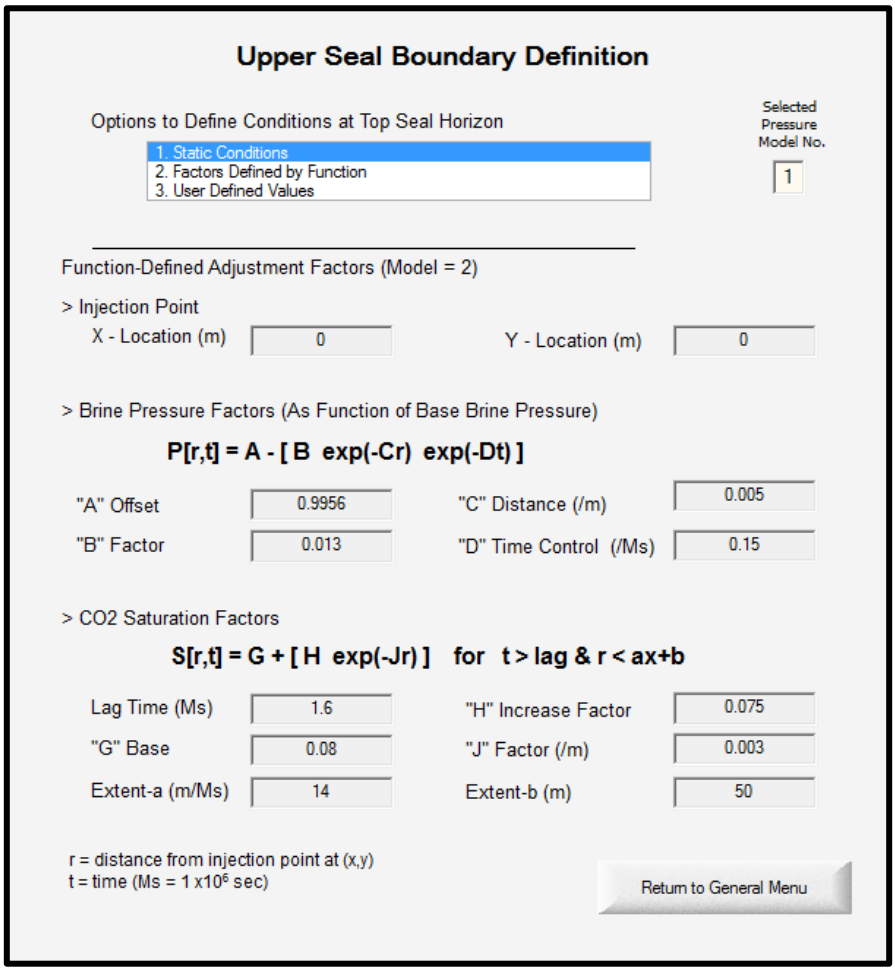

Figure 5A-34 Upper Seal Boundary Definition Dashboard

1.6.6 Ouputs

The results are available in the form of text files and Excel files and are as follows:

- Brine and CO_2 mass flux at specific time intervals
- Brine and CO_2 mass flux for the entire 100*100 grid at a specific time interval

If GoldSim is being used, brine and CO_2 mass flux can be plotted versus time. Additionally, plots of the distribution of the total brine and CO_2 mass flux at the top of the seal horizon at the end of each simulation can be generated. 3D visualization is also available in GoldSim.

1.7 Reservoir Reduced-Order Model Generator RROM-Gen

Introduction. RROM-Gen is a utility program, which uses reservoir simulation parameters (inputs and outputs) from 7 different simulators and converts them to a format acceptable for NRAP-IAM-CS.

1.7.1 RROM-Gen Inputs

RROM-Gen accepts inputs from 7 different simulators:

- TP3D (Two Phase Three-Dimensional model)
- FEHM (Finite Element Heat and Mass model)
- CMG-GEM (Computer Modeling Group, Generalized Equation-of-State Model)
- TOUGH2, (Transport Of Undersaturated Groundwater and Heat 2 model)
- STOMP, (Subsurface Transport Over Multiple Phase model)
- ECLIPSE (Exploration Consultant Limited Implicit Program for Simulation Engineering) and
- PETREL (Schlumberger Exploration and Production software platform).

Depending upon the simulator chosen, one or several files need to be read. The data is manipulated (by using bi-linear interpolation) to be converted to a 100*100 grid size, which is the only grid size accepted by NRAP-IAM-CS, and translated into the appropriate file format. The grid has the option to be regular (meaning all grid blocks have the same size) or linear (the size of the grid blocks can be defined and is especially useful if a grid refinement was applied to the original grid). The units are also converted if needed as NRAP-IAM-CS accepts only meters, MPa, and years. If the original grid is not oriented with the coordinate system, a rotation will be applied to re-orient the grid. The various options for inputs are shown on **Figure 5A-35**.

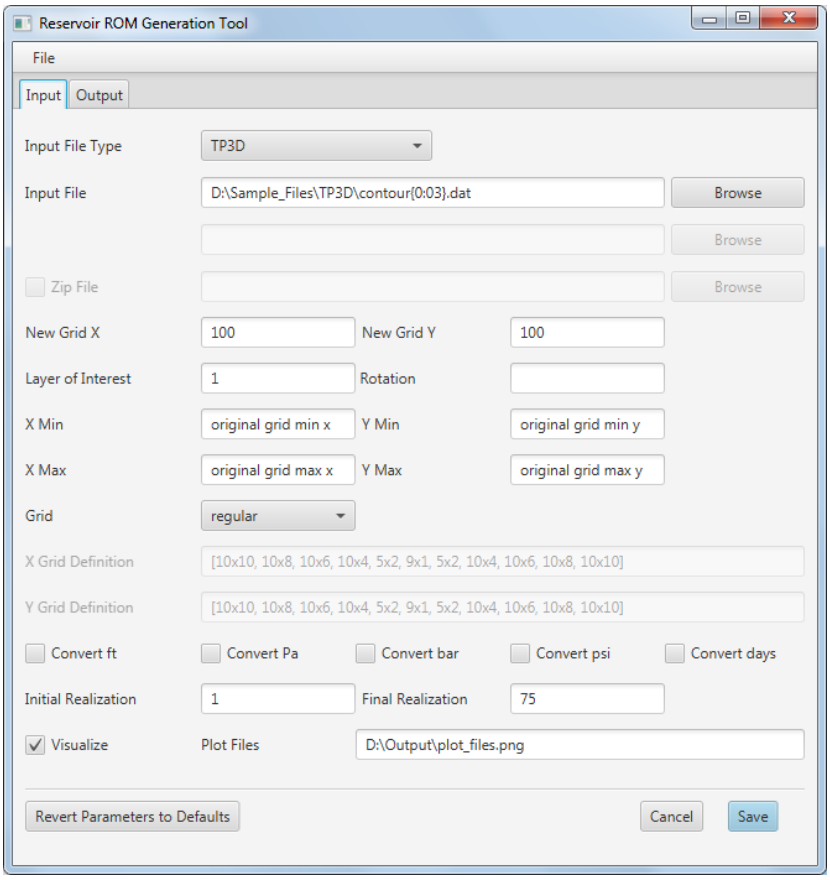

Figure 5A-35 RROM-Gen Inputs Tab

1.7.2 RROM-Gen Outputs

RROM-Gem has 2 required outputs (pressure and saturation) and 4 optional (elevation, dissolved CO_2, temperature, and permeability), **Figure 5A-36**.

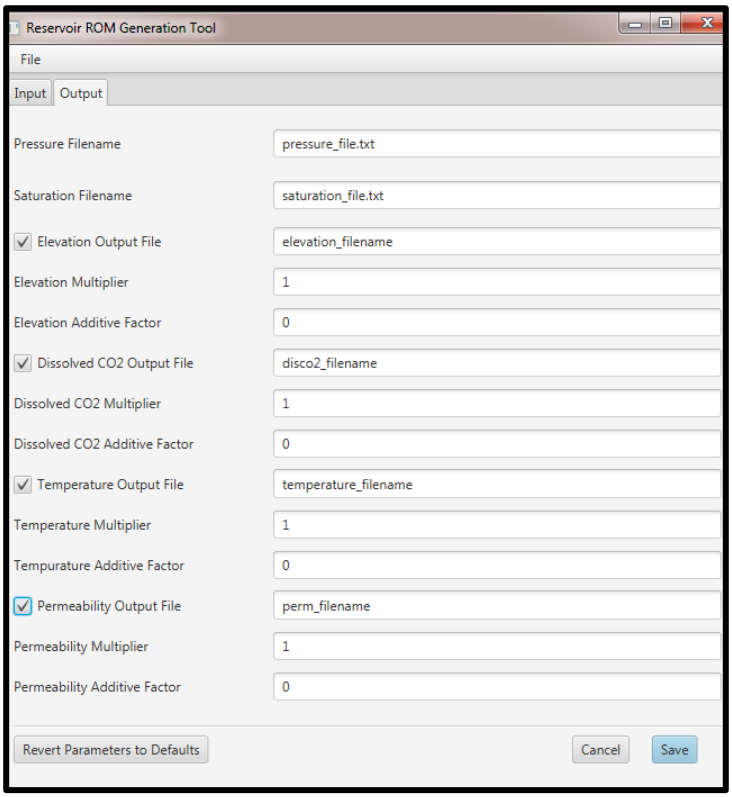

Figure 5A-36 RROM-Gen Outputs Tab

1.8 Short-Term Seismic Forecasting (STSF)

Introduction. The reduced order model was developed to simulate induced seismicity associated with the underground storage of CO_2. The tool is an adaptation of the ETAS (Empirical Type Aftershock Sequence) model (Ogata, 1988)[5] that was originally designed to model the rate of aftershocks after a main large shock. To adapt the model to the behavior of induced seismicity, an additional rate of aftershocks term has been included by Bachman et al. (2011)[6] to account for the external forcing due to the injection.

Input/ Output. The tool only uses two input files, the seismic catalog and the flow file. The seismic catalog contains the recorded magnitude and location of seismic events as a function of time. The user has the option to either use the provided catalogue or create their own. Six different injection parameters can be used as inputs from the flow file to run the simulations: downhole flowrate, surface flowrate, downhole pressure, surface pressure, and flow in, which all vary versus time. The last option, constant, is not time dependent. In addition, event magnitude and Guttenberg-Richter law (relationship between the magnitude and the number of earthquakes of at least that magnitude) parameters are also required. Outputs come in the form of two text files and will forecast the number of seismic events occurring in a specified range of magnitudes during a specified time frame. **Figure 5A-37** shows STSF input tab.

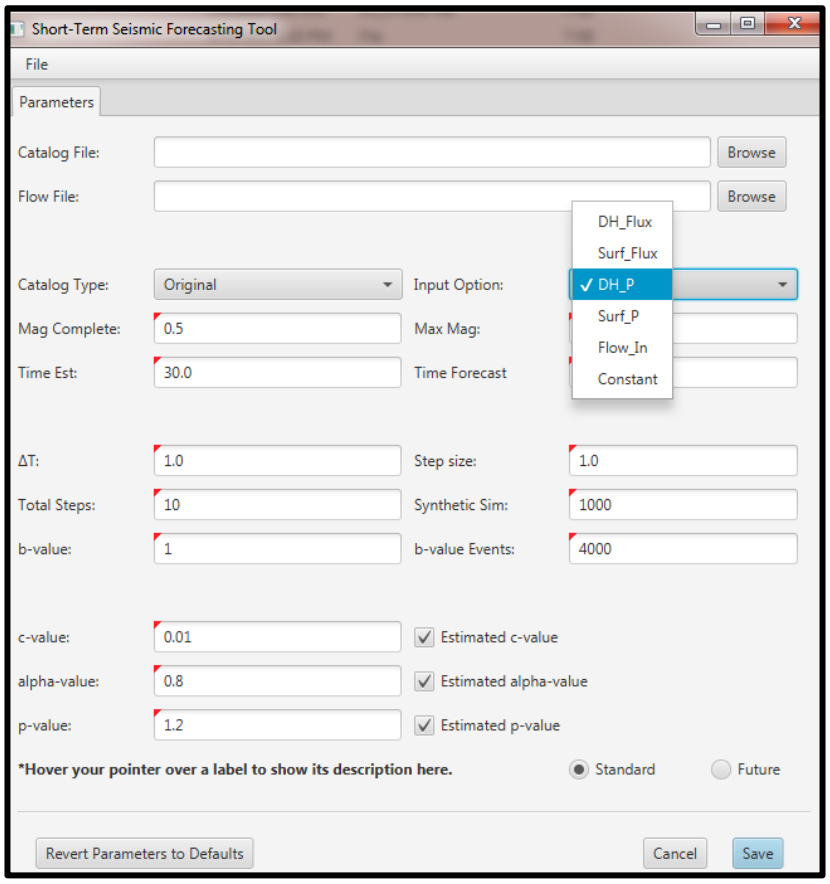

Figure 5A-37 STSF Input Tab

1.9 Well Leakage Analysis Tool (WLAT)

Introduction. This standalone tool contains four Reduced Order Models (ROMs) focused on the analysis of wellbore leakage from geologic CO_2 storage operations: 1) Cemented Wellbore Model 2) Multi-segmented Wellbore Model 3) Brine Leakage Model and 4) Open Wellbore Model. For all models, the outputs consist of plots of leakage rates of CO_2 and brine and can be saved in a text file format for external use. **Figures 5A-38 to 5A-41** show the main input tab for each reduced order model as well as the output plots.

1.9.1 Cemented Wellbore Model

The model treats multiphase flow of CO_2 and brine up a leaky well. It is based on a library of simulations, which were run with detailed full-physics FEHM (Finite Element Heat and Mass) code (Zyvoloski, 2007)[7]. The FEHM transfer simulations are 3D, multiphase solutions and heat and mass transfer of water and supercritical, liquid, and gas CO_2. It assumes that Darcy's flow is applicable to each phase. The model can handle leakage to an overlying aquifer, thief zone, or to the atmosphere. The model has some limitations: geochemical and geomechanical reactions (such as CO_2 dissolution in brine) are not taken into account, and brine density stays constant with pressure and temperature. Some values are currently hard-wired in this version of the tool (such as aquifer and upper layer characteristics).

The input parameters include the field properties (upper shale, shallow aquifer, thief zone, reservoir, and wellbore) and some additional parameters (type of calculation for the leakage and graphic output parameters), **Figure 5A-38**.

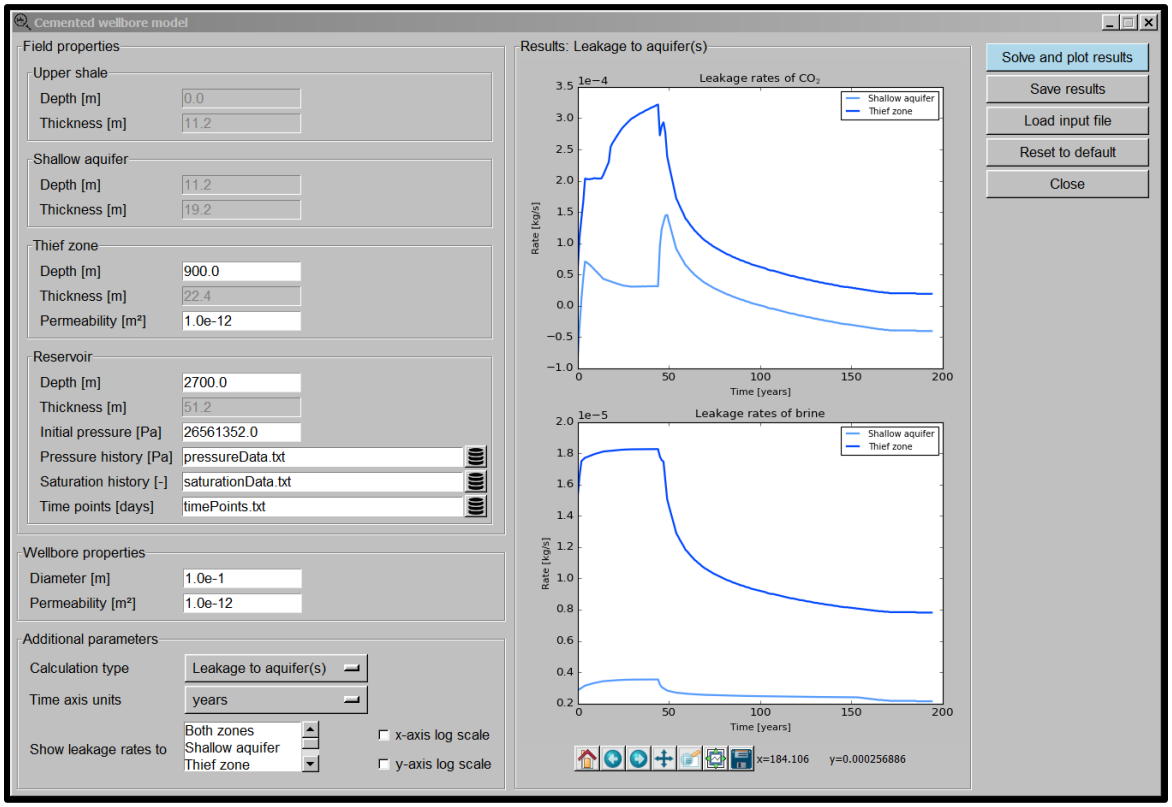

Figure 5A-38 WLAT Main Screen for Cemented Wellbore Model

1.9.2 Multi-Segmented Well Model

Like the Cemented Well Model, this tool treats multiphase flow of CO_2 and brine up a leaky well but in the presence of multiple aquifers and thief zones. The model is based on work by Nordbotten and Celia (2005)[8]. The two main assumptions of the model are vertical equilibrium of the pressure distribution and the existence of a sharp interface between the CO_2 and the brine phase. The model is focused on flow across large distances, and hence, does not account for leakage in flow paths, such as cement fractures, cracks, or annuli. Additionally, it is assumed that leakage occurs in the annulus between the outside of the casing and the borehole. Each individual formation penetrated by the well is assigned an effective permeability. One dimensional multi-phase version of Darcy's law is used to represent flow along the leaky well.

The inputs for the multi-segmented well model are divided into 8 sections, including but not limited to, shale layers (up to 30) characteristics, aquifers' characteristics, reservoir characteristics, leaking well, CO_2, and brine properties, **Figure 5A-39**.

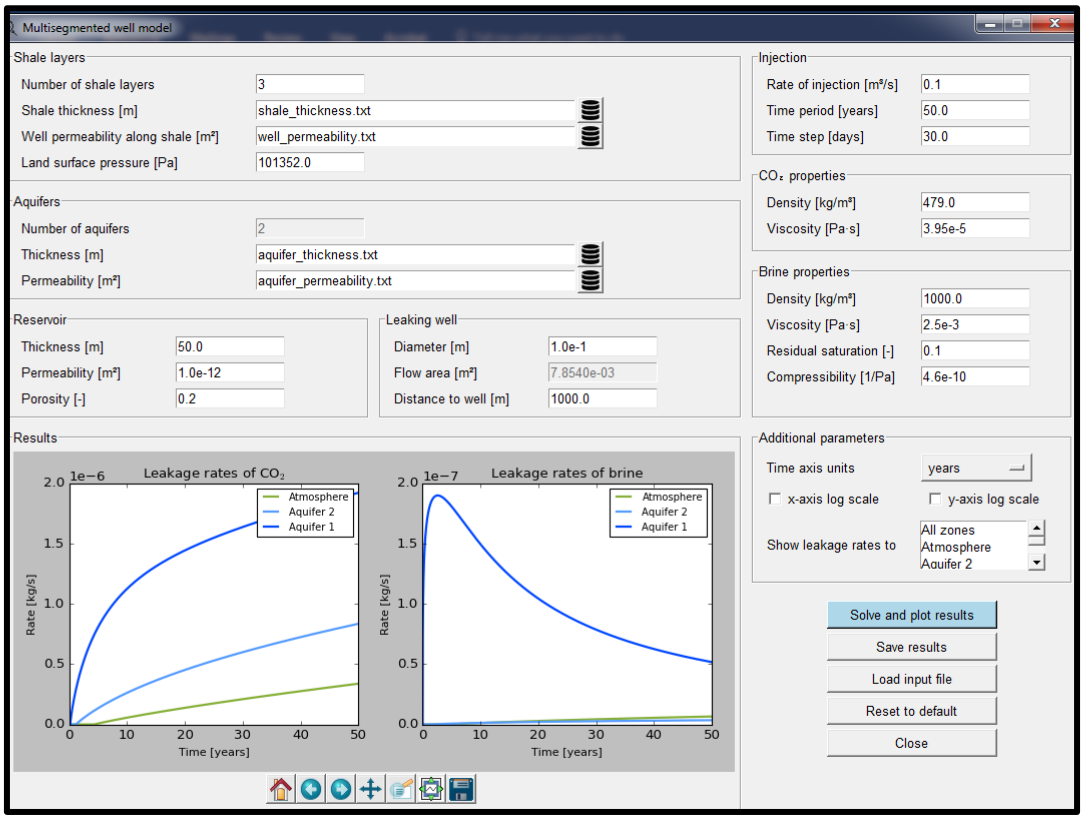

Figure 5A-39 WLAT Main Screen for Multi-Segmented Well Model

1.9.3 Brine Leakage Model

The Brine Leakage Model focuses on the geochemical processes, which are taking place inside the wellbore. It assumes that the fractures inside the cement can seal themselves after being in contact with the acidic brine. The model allows the user to simulate different case scenarios of fracture sealing (permeability decrease due to precipitation) or leaking (permeability increase due to dissolution). An important assumption is flow in series, meaning that the fracture zone contains three different zones of permeability: an unaltered cement zone, followed by a precipitation zone, and a dissolution zone. Some of the model limitations include the fact that the model only takes into account the brine flow but not the CO_2 phase flow and considers the brine properties (such as density and viscosity) to be constant as a function of pressure and temperature.

The main inputs required are well properties, fracture geometry, permeability, and brine properties, **Figure 5A-40**.

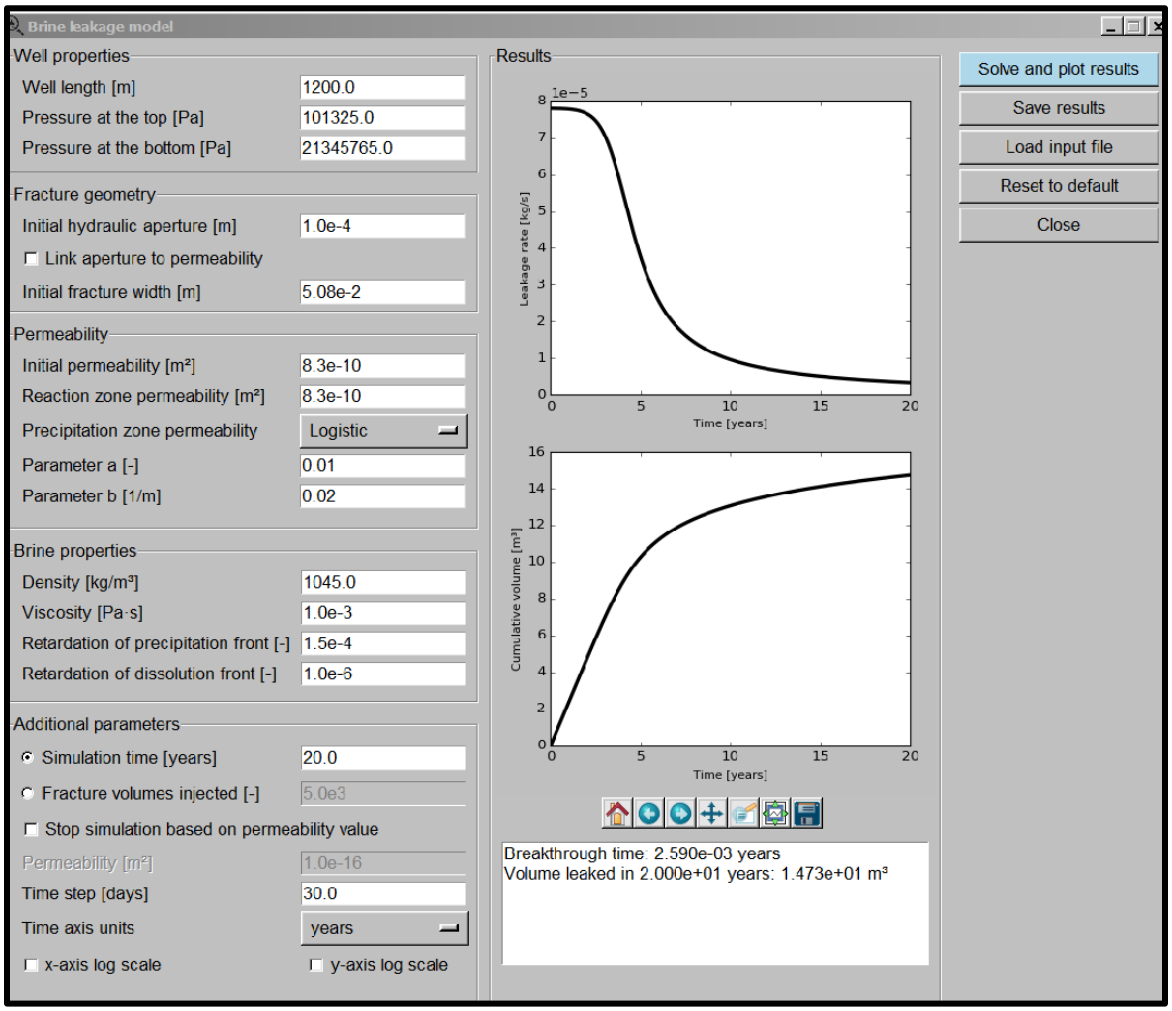

Figure 5A-40 WLAT Main Screen for Brine Leakage Model

1.9.4 Open Wellbore Model

This model treats the non-isothermal flow of CO_2 and brine up an open wellbore using the drift-flux approach (Pan et al., 2011)[9]. The model allows for phase transition of CO_2 from supercritical to gaseous. It is worth noting that the model should only be applied to estimate the leaking rate through an open wellbore for a short initial transient period but should be used with caution for longer period times as it does not consider time dependent reservoir pressure at the bottom of the leaking well. The model is incorporated into NRAP-IAM-CS. The inputs are limited to field properties (aquifer properties are currently hard-wired values and reservoir) and wellbore properties, **Figure 5A-41.**

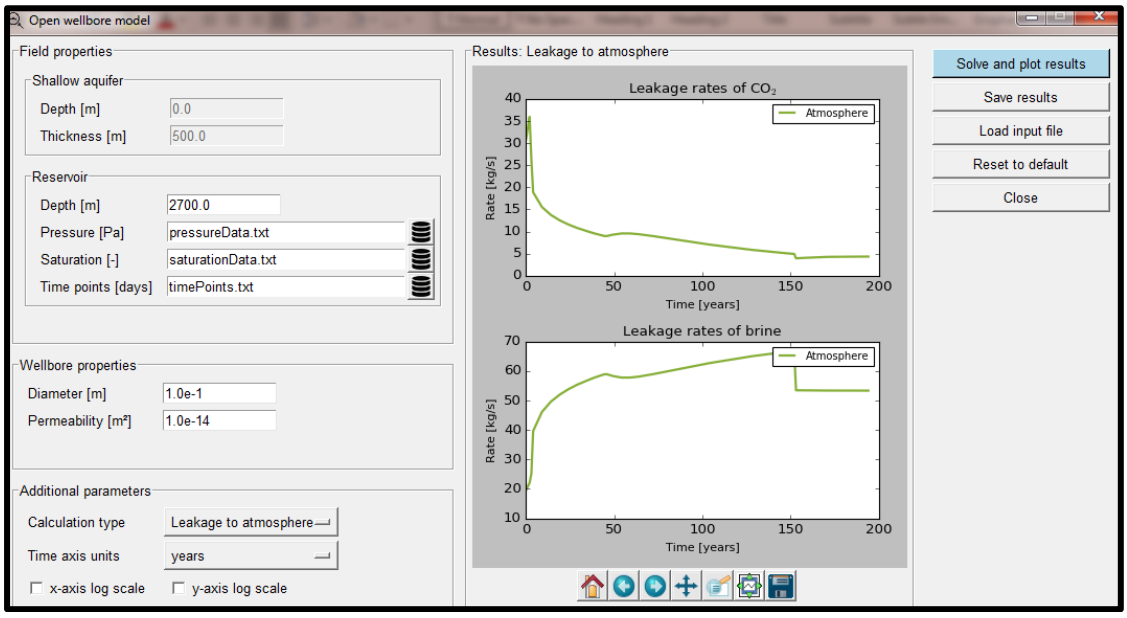

Figure 5A-41 WLAT Main Screen for Open Wellbore Model

Chapter VI: Identification of Future Characterization Activities

Scott Quillinan and Nicholas Bosshart
Director, Center for Economic Geology Research
School of Energy Resources, University of Wyoming
1020 E. Lewis Street, Energy Innovation Center
Laramie, Wyoming 82071

Section 6.1: Site Characterization and testing plan

Goals

The geologic data interpretation, modeling, and simulation efforts of Phase I-Prefeasibility have indicated that the geology at the Dry Fork Study site is suitable for long-term CO_2 injection of at least 2 million tonnes per year for 25 years. This encouraging conclusion was formed primarily from publicly available data in the study area. However, Phase I work is approaching the limits of pre-existing data and will need to collect site-specific subsurface data to resolve remaining uncertainty. The following site characterization efforts are designed to provide site-specific data to build upon Phase I findings and to assess the feasibility of CO_2 storage in Phase II.

This site characterization and testing plan is designed to address technical uncertainties in geologic, geochemical, geomechanical, geophysical, and hydrogeologic characteristics. Collected data will also begin to establish baseline conditions for the study site. Additional data regarding these technical aspects will 1) improve the accuracy of our estimated area of review, CO_2, and pressure plume extents, 2) reduce uncertainty related to the injection program, 3) provide data for a Class VI well permit, and 4) identify technical risks, which may have the potential to affect the project's overall financial feasibility.

Characterization of the target formations

Several potential reservoir and seal pairs lie below the Dry Fork Power Station. In order of decreasing depth these are: (1) the Pennsylvanian Minnelusa Formation reservoir and Permian Goose Egg Formation (Opeche Shale) seal; (2) the Jurassic Hulett-Canyon Spring Sandstones of the Sundance Formation sealed by the Late Jurassic Upper Sundance Member and Morrison Formation and (3) the Early Cretaceous Lakota and Dakota, and Muddy Formation reservoirs sealed by the Mowry Shale. These reservoir and seal combinations will be considered, because they occur within ideal CCS depth constraints and show good reservoir and seal characteristics conducive to commercial-scale storage. The Powder River Basin is a well-known oil and gas basin with substantial subsurface data available in the public domain. However, the highest priority storage targets are in intervals that rarely contain hydrocarbons, and thus, are associated with limited amounts of data. This site characterization plan describes our proposal to decrease the uncertainty in all targeted stratigraphic intervals and especially the least well known intervals to achieve uniform understanding of all targeted intervals. The highest priority, data limited, targets are the D-sand of the Minnelusa Formation and Jurassic Sandstones of the Lower Sundance Formation.

We propose to collect approximately 350 feet of core and fluid samples from the stacked storage complex, deploy a high resolution log suite, and shoot a 3 X 3 mile 3-D seismic survey. Geologic core samples will be used to identify mineralogy, measure porosity, and permeability, measure relative permeability, perform water/rock experiments, and correlate rock properties to the geophysical properties in the well bore. Water samples will allow measure of the fluid salinity, which in the upper stratigraphic targets is the largest remaining unknown parameter. The high resolution log suite will be used to scale-up the measurement from the core analysis to examine the rock and fluid properties over the length of the vertical section. The 3D-seismic will allow interpretation of these properties across the site. Together these activities will provide the necessary data to understand geologic heterogeneity, reservoir properties, and response to commercial-scale CO_2 injection.

In addition to the above collection and analysis of data, we propose modeling and simulation efforts. Predictive simulations using updated models will further reduce uncertainty and allow comparison to the results reported in the prefeasibility study, including expected plume extent (both CO_2 and pressure). The outputs of the modeling and simulation efforts will provide support for the Class VI well permitting process.

Section 6.2 Site Characterization Plan

Baseline characterization includes activities to determine the initial compositions and qualities of the CO_2 injection target formation(s) and the primary sealing formation(s). The proposed well would be a Class V research well proximal to Dry Fork Station and completed to a depth of approximately 9,800 feet. This well will be designed by Schlumberger Carbon Services and permitted through the Wyoming Department of Environmental Quality. We have chosen a Class V well, because it allows us the option of conducting injectivity tests in the formation, if the injectate is of equal or better quality then the formation fluid. After the above activities are complete, we plan to permanently plug and abandon the well, unless it is feasible to upgrade its class and reuse it in later project phases.

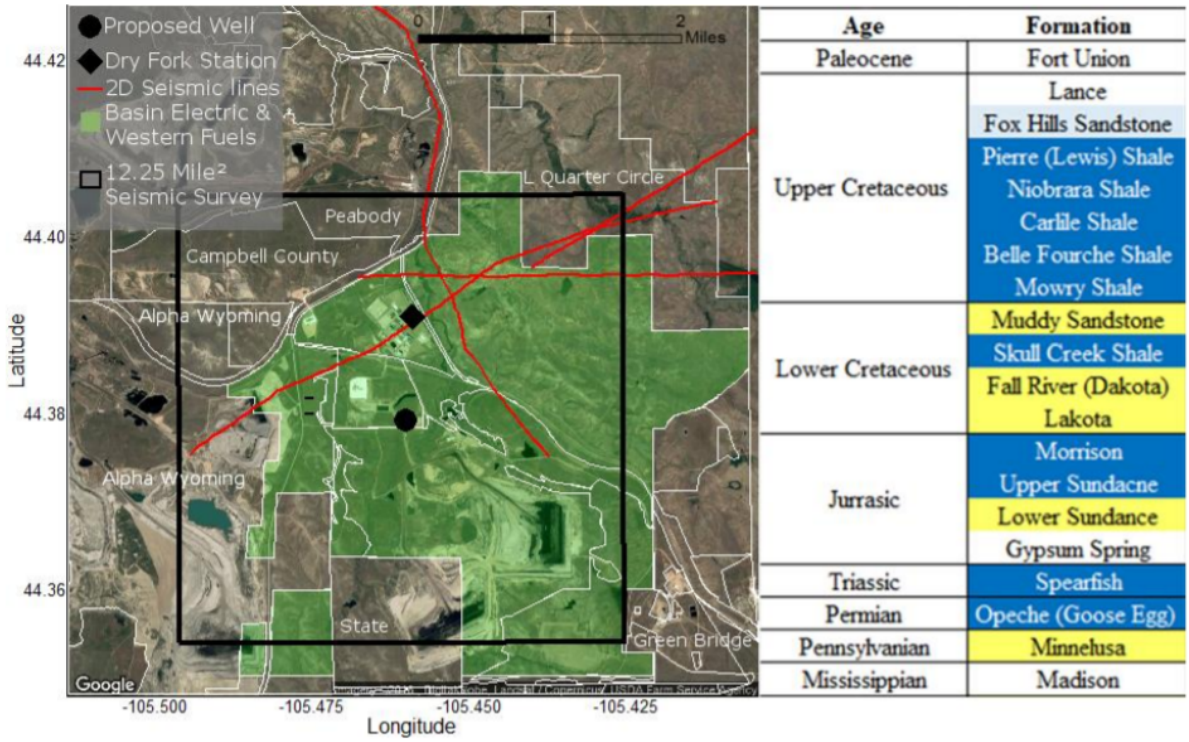

Age	Formation
Paleocene	Fort Union
Upper Cretaceous	Lance
	Fox Hills Sandstone
	Pierre (Lewis) Shale
	Niobrara Shale
	Carlile Shale
	Belle Fourche Shale
	Mowry Shale
Lower Cretaceous	Muddy Sandstone
	Skull Creek Shale
	Fall River (Dakota)
	Lakota
Jurrasic	Morrison
	Upper Sundacne
	Lower Sundance
	Gypsum Spring
Triassic	Spearfish
Permian	Opeche (Goose Egg)
Pennsylvanian	Minnelusa
Mississippian	Madison

The key elements of the for future study include: (1) location of the proposed stratigraphic test well and storage complex; (2) area of coverage for the proposed new 3-D seismic survey; (3) 2-D seismic lines (to be purchased); (4) land ownership; and (5) storage units within the storage complex with reservoirs (yellow) and seals (blue) indicated. The continuous Upper Cretaceous shale package is ~3990 ft. thick and a proven regional seal across the PRB, greatly reducing risk of communication with the overlying USDW, the Fox Hills Sandstone (light blue).

Geologic Core Sample Collection

Geologic core samples will be collected and analyzed from the Minnelusa, Opeche, Sundance, Morrison, Lakota/Dakota, Skull Creek, Muddy, and Mowry Formations. Ideally, ~535 feet of core will be collected. The distribution of core intervals are as follows: Minnelusa Formation reservoir (215 feet minimum top of formation into "E sand") and Opeche Formation seal (20 feet of bottom of seal/contact with reservoir); Lower Sundance Formation reservoir(s) (25 feet of Canyon Springs member, 75 feet of Hullett member) and Morrison Formation seal (20 feet of bottom of seal/contact with reservoir); Lakota/Dakota reservoirs (95 feet of combined reservoir section) and Skull Creek shale seal (20 feet of bottom of seal/contact with reservoir), and Muddy Formation reservoir (45 feet) and Mowry Formation seal (20 feet of bottom of seal/contact with reservoir).

Analysis of this new core will allow for:

1) Development of more robust porosity and permeability correlations to update the geologic model and enable more accurate predictive simulations of fluid flow and pressure response.

2) Investigation of geomechanical strength properties of the sealing formations to determine the formation's competency in acting as a seal.

Petrographic, petrophysical, geomechanical, and geochemical analyses will be performed on core samples from both the target formation(s) and the seal formation(s) to better understand factors that influence the long-term containment of CO_2. These analyses will improve well log correlation and geologic models. The analyses will include:

- Thin section analysis to assess mineralogy, grain size, sorting, morphology and diagenetic effects, and to assist understanding of facies interpretations, rock fabric, depositional trends, and diagenetic history.
- X-ray fluorescence (XRF) to give insight into sample chemistry and dynamics with CO_2/brine/rock interaction.
- X-ray diffraction (XRD) coupled with Rietveld refinement to assess bulk mineralogy and clay mineralogy via clay fraction isolation to understand cap integrity issues and reservoir dynamics in relation to clay types present.
- Field emission scanning electron microscopy (FE SEM) to gain visibility of fine-scale mineralogical and pore space relationships and to serve as a validation technique for XRD.
- Coupling of new FE SEM analysis mineral identification and classification system (AMICS) software to compare with original images acquired with the FE SEM will allow for visual inspection of the AMICS-derived pore and fracture characterization results for comparison to other acquired porosity measurements and also allow for coupled comparison of elemental and mineral content with XRF and XRD, improving reservoir and cap rock characterization.
- Porosity and permeability testing to establish baseline data.
- Geochemical analyses of gas compositions representative of Dry Fork's effluent stream and the formation fluid to investigate chemical reactions, including mineralogical dissolution and precipitation reactions, which may impact injection activities.
- Nuclear magnetic resonance (NMR) to assess total versus effective porosity with representative brine/CO_2 compositions for relative permeability predictions.
- CO_2/brine relative permeability testing to determine the ease with which CO_2 will flow in the presence of the high salinity brine of the reservoir.
- Geomechanical studies to conduct mechanical strength testing and determine the maximum injection integrity of the cap rock.
- Mercury injection capillary pressure (MICP) tests to provide data regarding the pore size distribution available and capillary pressure range in reservoir and cap rock samples.

The results of these analyses will be used to model storage capacity and two phase fluid flow.

Fluid Sampling

Representative fluid samples will be collected from the target formations. Characterization of the formation fluid provides the basis for analytical permitting requirements, allows for investigation of reservoir confinement, and provides the basis for geochemical modeling.
These analyses will include:

- Collections of standard field parameters (pH, ORP, TDS, temperature)
- Major/Minor/Trace geochemistry will be used to calibrate geochemical models to interpret formation response to CO_2 injection, wellbore scaling, and mineral speciation.
- Stable isotope geochemistry, will be used to assign baseline conditions of each formation. Isotopes can be used to differentiate anthropogenic CO_2 from naturally occurring CO_2 in future monitoring programs but requires robust baseline data.
- Mineral speciation and solubility models will be created to predict CO2-brine-rock reactions. Investigation of potential geochemical reactions within formations caused by injection of CO_2. The particular reaction can either increase or reduce injection capacity.
- Assessment of mineral recovery and high value materials. Recent work by the University of Wyoming has shown that rare earth elements and other high value materials occur in deep basin brines. Rare earth character is also specific to lithology, and thus, can be used to determine baseline conditions, and investigate hydrologic connectivity between formations.

Well Logging and Downhole Testing

Well log data will be acquired and downhole formation testing will be conducted in the planned characterization well. The following well logs are planned: spectral gamma ray (GR), triple combination, dipole sonic, nuclear magnetic resonance (NMR), pulsed neutron (PNL/PNX), and cement bond (CBL). Downhole testing will include modular formation dynamics testing (MDT).

- Spectral GR logging will provide passive measurements of natural radioactivity in the subsurface and separate determinations of the contributions of potassium, thorium, and uranium to the overall measured radioactivity. A similar measurement will be made on the entire length of the core acquired, enabling an accurate core-to-log depth correlation. This correlation will be important when integrating core-measured properties in modeling activities.
- The triple combination (“triple combo”) logging will provide a wide variety of physical property measurements of the open hole environment. Data produced from this tool will include GR, neutron porosity, density, photoelectric factor, spontaneous potential, temperature, and resistivity logs. These logs will provide the ability to assess formation top depths (previously estimated from nearby wells), lithology, and petrophysical characteristics (porosity, water resistivity, water saturation, and the presence/absence of gas), which will be important in identifying well test and completion intervals and correlating core data to offset wells. The latest array-induction and array-electrode tools all use some form of inversion (rather than charts) to estimate the invasion parameters — the diameter of invasion (di), the resistivity of invaded zone (Rxo), and

the uninvaded formation resistivity (Rt). The AIT Array Induction Imager tools provide quantitative 2D imaging of formation resistivity with distance away from the borehole. This quantitative information about invasion can be used in permeability modeling or can be converted to a 2D image of water saturation Sw, which finds use in multiple applications (e.g. TDS modeling).

- Dipole sonic logging will provide a means for derivation of sonic porosity (a metric of connected, fluid-filled pore space), which will prove useful in zones characterized with complex lithologies. Dipole sonic logging will provide shear wave data necessary to assess stress anisotropy and investigate the presence of natural fractures. Sonic logging will also provide a means to tie seismic data to the well, should it be collected as part of the baseline characterization in the following proposed/recommended MVA plan, assisting in seismic time-to-depth conversion.
- Nuclear magnetic resonance (NMR) logging, acquired with Schlumberger's combinable magnetic resonance (CMR) tool, will provide estimates of pore size distribution, total porosity, effective porosity, bound fluid (irreducible water saturation), free fluid, and calculated permeability.
- PNL/PNX will provide mineralogic, porosity, and fluid saturations (water, oil, and gas). If the characterization well is completed as an observation/monitoring well, these data may be used in comparison with repeat/monitor PNL/PNX surveys to identify changes in reservoir fluid saturation during injection (monitor CO_2 breakthrough), as well as monitoring of the strata overlying the reservoir for unexpected vertical migration of CO_2.
- Cement bond logs (CBL) and casing collar locator (CCL) logs will provide an assessment of cement quality and identify any associated remedial cementing operations that are required. A measurement of cement top and a depth correlation for perforation and installing downhole equipment in relation to geology will also be provided.
- Modular formation dynamics testing (MDT) technology will be implemented to conduct pressure testing and native formation fluid sampling, as well as injection tests to estimate downhole permeability and formation parting pressure. Formation fluid samples will be used to test for potential fluid and mineralogical reaction with mixtures of the native brine and gas effluent (CO_2 and any impurities present), which could affect injectivity.

Some data redundancy is planned for key parameters, such as porosity and permeability, as these parameters are of utmost importance in reducing the technical risks associated with commercial scale CO_2 injection. Injectivity assessment will rely upon permeabilities calculated from NMR logging, measured from core samples, and measured by MDT. Should inferences of downhole injectivity potential be too low (or simply inconclusive) additional downhole testing (such as a pump test or CO_2 injection test) may be recommended.

Seismic Survey

One of the most important steps in characterizing a geologic CO_2 storage site is the construction of 3-D volumes of seismic attributes. Once these seismic attribute volumes are constructed, key attributes can be correlated to core and well log observations and analytical measurements. These correlations allow standardization and extrapolations of a variety of determinative rock/fluid characteristics from the stratigraphic test well out into the 3-D seismic volume, creating a realistic 3-D heterogeneous property model of storage reservoirs and seals.

This study's new 12.25 mi^2 3-D seismic survey will be centered on the new stratigraphic test well to anchor and ground truth lateral heterogeneity in the subsurface, depths, and thicknesses of storage target formations, and subsurface structures. Seismic interpretations of geologic features can provide location-specific reservoir properties that strongly influence fluid movement. Lineaments identified using volumetric seismic attribute analysis (e.g., seismic coherence and curvature) likely play an important role in confining layer integrity and/or diverting flow through the reservoir.

In addition, several legacy 2-D lines cross the study area. These lines have been subjected to quality control, are of high quality, and will be purchased to guide the final design of the new stratigraphic test well and 3-D seismic survey.